

Enhanced protein degradation by branched ubiquitin chains

Dissertation to obtain the degree “Doctor rerum naturalium” at the University of
Bayreuth in the department of biology, chemistry and geosciences

presented by
Diplom-Biochemiker
Hermann-Josef Meyer

April 2014

für Joel und Maren, just keep going

This doctoral thesis was prepared at the department of molecular and cell biology at the University of California at Berkeley from February 2009 until April 2014 and was supervised by Prof Dr. Michael Rape. Prof. Dr. Olaf Stemmann at the department of genetics was the advisor at the University of Bayreuth.

This is a full reprint of the dissertation submitted to obtain the academic degree of Doctor of Natural Sciences (Dr. rer. nat.) and approved by the Faculty of Biology, Chemistry and Geosciences of the University of Bayreuth.

Date of submission: 22.04.2014

Date of defence: 04.08.2014

Acting dean: Prof. Dr. Rhett Kempe

Doctoral committee:

Prof. Dr. Olaf Stemmann	(1st reviewer)
Prof. Dr. Michael Rape	(2nd reviewer)
Prof. Dr. Franz Xaver Schmid	(chairman)
Prof. Dr. Benedikt Westermann	

This study was performed between February 2009 and April 2014 under the supervision of Dr. Michael Rape in the department of Molecular and Cell biology at the University of California, Berkeley.

Parts of this dissertation are already published or going to be published as follows:

Meyer, H.-J., and Rape, M. (2014). Enhanced protein degradation by branched ubiquitin chains. *Cell. in press*

Meyer, H.-J., and Rape, M. (2011). Processive ubiquitin chain formation by the anaphase-promoting complex. *Semin. Cell Dev. Biol.* 22, 544–550.

Application to obtain the title of “Dr. rer. nat.” was submitted for the session on 30. April 2014.

First referee: Prof. Dr. Olaf Stemmann

Acknowledgments

First of all, I would like to thank my PhD supervisor Dr. Michael Rape for having given me the opportunity to work on a complex and challenging project at UC, Berkeley. He was always very enthusiastic and full of suggestions. Together we were able to overcome several hurdles.

Special thanks go to Prof. Dr. Olaf Stemmann for his kind advice and help in setting up this rather unconventional PhD.

Many thanks go to Anne Fisher for tissue culture related things, Minda Pagtakhan for providing essential lab tasks, Hector Nolla for instructing me in FACS and Lori Kohlstaedt for mass spec analysis.

I want to thank all former and current members of the Rape lab for their team spirit and support, and for all the fun times we had. Especially Kate Wickliffe for fruitful discussions, sharing reagents, establishing protocols together and just being a great bench mate, except when she was wearing her “focus glasses”. I am also very grateful to Annamaria Mocciaro and Adam Williamson for encouragement in various forms and helpful conversations.

I would also like to give a special thanks to the Gussman family, who supported me throughout my studies with encouraging words, wonderful meals and being my American family.

Ich möchte mich an dieser Stelle ganz besonders bei meinen Eltern bedanken, die mich immer unterstützt haben und ohne deren Hilfe diese Arbeit nicht möglich gewesen wäre, sowie zahlreiche Versorgungspakete. Ganz lieben Dank. Dieser gilt auch meinen Geschwistern, Schwagern, Nichten und Neffe.

Outmost gratitude goes to Joel, who kept me sane.

Summary

Posttranslational modification of cell cycle regulators with ubiquitin chains is essential for eukaryotic cell division. Such chains can be connected through seven lysine residues or the amino-terminus of ubiquitin, thereby allowing the assembly of eight homogenous and multiple mixed or branched conjugates. While functions of homogenous chain types have been described, physiological roles of branched structures are unknown. The anaphase-promoting complex (APC/C) catalyzes degradation of key regulators during the cell cycle causing proper transition through the cell cycle.

Here, I report that the APC/C efficiently synthesizes substrate-attached branched conjugates and enhances recognition of ubiquitylated substrates by the proteasome, thereby driving the degradation of cell cycle regulators during early mitosis. I showed several APC/C-substrates require the ubiquitin-conjugating enzyme E2 S (Ube2S) for degradation, e.g. the Never in mitosis A-related kinase 2 (Nek2A). The reconstitution of Nek2A ubiquitylation revealed that Ube2S does not simply extend a conjugate, but instead branches multiple lysine11-linked chains off the ubiquitin chains produced by the ubiquitin-conjugating enzyme E2 C (Ube2C).

Therefore, I identified an enzyme and substrates for modification with branched ubiquitin chains, which points to an important role of these conjugates in providing an improved signal for proteasomal degradation. Compared to homogenous chains, branched conjugates synthesized by the APC/C increase the efficiency of proteasomal substrate recognition, and accordingly, are required for the degradation of cell cycle regulators at times of limited APC/C activity such as prometaphase. Hence, the APC/C is an enzyme that synthesizes branched ubiquitin chains, which provide an improved signal for proteasomal degradation.

Zusammenfassung

Posttranslationale Modifikation von Regulatoren des Zellzyklus mit Ubiquitinketten ist essentiell für Zellteilung. Diese Ketten können durch sieben verschiedene Lysine oder den Amino-Terminus von Ubiquitin verknüpft sein, welches die Formierung von acht homogenen und vielen gemischten oder verzweigten Konjugaten erlaubt. Funktionen für homogene Kettenarten sind bereits beschrieben worden, während die physiologische Bedeutung der verzweigten Strukturen unbekannt ist. Der Anaphase fördernde Komplex (APC/C) katalysiert die Degradierung von wichtigen Regulatoren innerhalb des Zellzyklus, was zu einem geordneten Ablauf des Zellzyklus führt.

Ich berichte hier, dass der APC/C verzweigte, substratgekoppelte Ubiquitinketten effizient synthetisiert, was die Bindung von ubiquitinierten Substraten durch das Proteasom verstärkt und wodurch der Abbau von Zellzyklusregulatoren in früher Mitose vorangetrieben wird. Ich habe aufgedeckt, dass mehrere APC/C-Substrate das ubiquitinkonjugierende Enzym E2 S (Ube2S) für ihre Degradierung benötigen, z.B. die Niemals in Mitose A verwandte Kinase 2 (Nek2A). Die Rekonstitution der Nek2A-Ubiquitinierung zeigt, dass Ube2S nicht nur ein Konjugat verlängert, sondern stattdessen mehrere Lysin11-geknüpfte Ketten verzweigt, welche von Ubiquitinketten ausgehen, die durch das ubiquitinkonjugierende Enzym E2 C (Ube2C) produziert worden sind.

Daher habe ich ein Enzym und Substrate identifiziert, welche mit verzweigten Ketten modifiziert sind, was auf eine wichtige Rolle dieser Konjugate als ein stärkeres Abbausignal hinweist. Verglichen mit homogenen Ketten steigt die Effizienz der vom APC/C-produzierten, verzweigten Ketten im Bezug auf proteasomale Substraterkennung und deshalb sind verzweigte Ubiquitinketten für die Degradierung von Zellzyklusregulatoren zuzeiten limitierter APC/C-Aktivität erforderlich, wie in Prometaphase. Infolgedessen ist der APC/C ein Enzym, das verzweigte Ubiquitinketten synthetisiert, welche ein verstärktes Abbausignal durch das Proteasom darstellen.

Table of content	
Acknowledgements	4
Summary	5
Zusammenfassung	6
Table of content	7
1. Introduction	12
1.1. The posttranslational modification with ubiquitin called ubiquitylation	12
1.1.1. The enzymatic ubiquitylation cascade of E1-E2-E3	16
1.1.2. E2s specify ubiquitin chain linkage and E2-E3 interaction	18
1.1.3. How much information is encoded by the different ubiquitin linkages?	21
1.1.4. The 26S proteasome and other ubiquitin binding proteins	23
1.2. The basics of the cell cycle	25
1.2.1. The anaphase-promoting complex	29
1.2.2. Regulation of the anaphase-promoting complex	31
1.3. Aims	36
2. Materials	37
2.1. Equipment and software	37
2.2. Kits and other lab consumables	39
2.3. Chemicals, reagents and enzymes	40
2.4. Cell lines	40
2.5. DNA oligonucleotides for qRT-PCR	41
2.6. Plasmids	41
2.7. Peptides	44
2.8. Antibodies	44
2.9. RNA oligonucleotide sequences for siRNA	46
3. Methods	47
3.1. Molecular biology techniques	47
3.1.1. Preparation of chemically competent bacteria	47
3.1.2. Transformation of chemically competent <i>E.coli</i>	47

Contents

3.1.3. Isolation of plasmid DNA from bacteria	48
3.1.4. Cloning	48
3.1.5. Real Time quantitative Reverse Transcription PCR	50
3.2. Biochemical techniques	50
3.2.1. Measurement of protein concentration	50
3.2.2. Sodium dodecyl sulfate (SDS) polyacrylamide gel electrophoresis (SDS PAGE)	51
3.2.3. Coomassie staining of gels after SDS PAGE	52
3.2.4. Western blot analysis	52
3.2.5. Autoradiography	53
3.2.6. Isolation of recombinant proteins from bacteria	54
3.2.7. Isolation of recombinant proteins from insect cells	55
3.2.8. <i>In vitro</i> APC/C binding assay	56
3.2.9. <i>In vitro</i> ubiquitylation of recombinant or radiolabeled substrates with immunoprecipitated APC/C	57
3.2.10. <i>In vitro</i> degradation of ubiquitylated Nek2A with human proteasome	57
3.2.11. <i>In vitro</i> reconstitutions of sequential ubiquitylation events by the APC/C	58
3.2.12. Identification of ubiquitin linkages by mass spectrometry	59
3.2.13. Detection of ubiquitin branches with ubiquitin ^{TEV} derivatives	59
3.2.14. <i>In vitro</i> reconstitution of ubiquitylated APC/C substrate binding to ubiquitin receptors	60
3.2.15. HeLa cell extract-based <i>in vitro</i> degradation assay	60
3.2.16. Isolation of ubiquitylated proteins from cells	60
3.2.17. Immunoprecipitations of proteins from cells	62
3.3. Cell biology techniques	62
3.3.1. Cultivation of adherent and suspension cells	62
3.3.2. Transient transfection of human cells with plasmid DNA	63
3.3.3. Transient transfection of human cells with siRNA	63
3.3.4. Generation of stable HeLa or inducible 293 cell lines	64
3.3.5. Cell cycle synchronization of cells	65
3.3.6. Immunofluorescence	65

3.3.7. Analysis of cell cycle progression in cell lines by FACS	66
3.3.8. Determination of cell cycle distribution by automated microscopy and analysis	66
3.3.9. Determination of substrate levels in cells	67
3.3.10. Live cell imaging of Ube2S depleted HeLa cells	68
4. Results	69
4.1. Ube2S enhances ubiquitylation and proteasomal degradation of prometaphase APC/C substrates	69
4.1.1. Nek2A levels are increased upon depletion of Ube2S	69
4.1.2. Ube2S depletion stabilizes prometaphase APC/C substrates	71
4.1.3. Decreased ubiquitylation of prometaphase APC/C substrates caused by reduced Ube2S levels	72
4.1.4. Reduced levels of Ube2S cause a delay in early mitosis	74
4.2. Ube2S synthesizes branched K11-linked ubiquitin chains off non-K11-linkages	77
4.2.1. K11 in ubiquitin is not sufficient for formation of long polyubiquitin chains on Nek2a by Ube2C and Ube2S	77
4.2.2. Ube2S and Ube2C do not form linear mixed ubiquitin chains on Nek2A	78
4.2.3. Ube2S attaches single ubiquitin moieties to N-terminally fused linear ubiquitin chains on cyclin A and Nek2A	79
4.2.4. Ube2S branches off ubiquitin chains on cyclin A preformed by Ube2C	81
4.2.5. Absence of K48 and K63 in ubiquitin leads to decreased ubiquitylation of Ub-cyclin A by Ube2S and Ube2C	82
4.3. The APC/C synthesizes branched ubiquitin chains in cells	83
4.3.1. Mass spectrometry shows the presence of non-K11-linkages within ubiquitin chains on Nek2A made by Ube2S and Ube2C	84
4.3.2. Ube2S modifies Ub-cyclin A with TEV-cleavable ubiquitin derivatives	85
4.3.3. Detection of branched ubiquitin fragments on cyclin A and Nek2A <i>in vitro</i>	87
4.3.4. K11-linked ubiquitin chains co-purify with the APC/C	89
4.3.5. Detection of branched ubiquitin chains co-purifying with the APC/C <i>in vivo</i>	91

4.3.6. Detection of branched ubiquitin chains attached to APC/C substrates <i>in vivo</i>	92
4.4. Altering the linkage-specificity of metazoan APC/C	93
4.4.1. Ube2S without its CTP does not bind APC/C	94
4.4.2. The CTP is sufficient for APC/C-binding	95
4.4.3. Ube2G2 ^{CTP} binds the APC/C <i>in vitro</i> and <i>in vivo</i>	96
4.4.4. Ube2G2 ^{CTP} ubiquitylates APC/C substrates	97
4.4.5. Ube2G2 ^{CTP} requires a functional catalytic E2 domain and APC/C substrate recognition motifs	98
4.4.6. Ube2G2 ^{CTP} synthesizes K48-linked ubiquitin chains on cyclin A	100
4.5. Ube2G2^{CTP} and Ube2S synthesize branched K11/K48-linked chains	102
4.5.1. Ube2S and Ube2G2 ^{CTP} produce ubiquitin chains containing K11 and K48 linkages on cyclin A <i>in vitro</i>	102
4.5.2. Ube2S and Ube2G2 ^{CTP} form K11/K48 branched ubiquitin chains <i>in vitro</i>	104
4.5.3. Presence of Ube2G2 ^{CTP} , Ube2C and Ube2S in extracts and cells leads to formation of high MW ubiquitin chains	105
4.6. Branched ubiquitin chains show improved binding to ubiquitin binding proteins	107
4.6.1. Cyclin A modified with either K11- or K48-linked ubiquitin chains show similar binding to S5a, HHR23A and p97 cofactor complexes	107
4.6.2. Cyclin A modified with either K11- or K48-linked ubiquitin chains does not compete for binding to S5a or p97/SAKS1	109
4.6.3. High MW branched ubiquitin chains show enhanced binding compared to shorter ubiquitin chains	110
4.6.4. Branched ubiquitin chains show better binding than homogenous chains of similar length on cyclin A or Nek2A	111
4.6.5. Branched ubiquitin chains are hydrolyzed by DUBs	113
4.7. Modification of APC/C substrates with branched chains leads to an increase in substrate degradation	114
4.7.1. Branched ubiquitin chains improve Nek2A ubiquitin conjugate turnover by the 26S proteasome <i>in vitro</i>	115
4.7.2. K11- and K48-linked ubiquitin chains lead to APC/C substrate degradation in cell extracts	116

4.7.3. Branched ubiquitin chains enable degradation of weaker binding substrates or under low APC/C activity	117
4.7.4. Decrease of ubiquitin conjugates co-purifying with the APC/C in the presence of Ube2G2 ^{CTP} due to turnover by the proteasome	119
4.7.5. Co-expression of Cdh1 and Ube2G2 ^{CTP} decreases levels of a weakly binding APC/C substrate	120
4.7.6. Depletion of Ube2S leads to stabilization of the proteasomal substrate Nek2A	121
4.8. Presence of Ube2G2^{CTP} causes cell cycle defects	122
4.8.1. Ube2G2 ^{CTP} enables cell cycle progression and degradation of APC/C substrates	123
4.8.2. Ube2G2 ^{CTP} rescues a mitotic arrest induced by depletion of Ube2C and Ube2S	124
4.8.3. Ube2G2 ^{CTP} causes bypass of a taxol induced mitotic arrest	125
4.8.4. Extent of taxol bypass correlates with the expression level of Ube2G2 ^{CTP}	126
4.8.5. Expression of Ube2G2 ^{CTP} leads to aneuploidy in HeLa cells	127
4.9. Branching of ubiquitin chains seems to be applicable to other E2/E3 pairs	128
5. Discussion	130
5.1. The APC/C synthesizes branched ubiquitin chains.	130
5.2. Enhanced protein degradation by branched ubiquitin chains.	134
5.3. Why did branched chains evolve in metazoans?	139
5.4. Concluding remarks and perspectives	140
6. Abbreviations	142
7. References	147
8. (Eidesstattliche) Versicherungen und Erklärungen	165

1. Introduction

Living organisms known to date rely on three kinds of large molecules for basically all their biological functions. These molecules consist of deoxyribonucleic acids (DNA), ribonucleic acids (RNA) and proteins, and are known as biological macromolecules (Berg et al., 2002). Proteins are responsible for vital processes such as metabolism, growth, environmental interaction, morphology and motility. Half the mass of the bacterium *Escherichia coli* consists of proteins, underlying their importance and complexity (Voet and Voet, 2011). An organism needs to be capable of regulating the abundance of myriads of proteins to function properly. Both the synthesis and the destruction of proteins are tightly controlled. On a cellular level the degradation of proteins is mainly carried out by trafficking into lysosome organelles or by degradation through the proteasome, which both can be achieved by a posttranslational modification called ubiquitylation (Ciechanover, 2005). The following will mainly explain how ubiquitylation occurs and what its consequences are during the cell cycle mediated by the enzyme called anaphase-promoting complex/cyclosome (APC/C).

1.1. The posttranslational modification with ubiquitin called ubiquitylation

Ubiquitylation controls critical signaling pathways in eukaryotes and is essential for cell proliferation, differentiation, and survival (Deshaies and Joazeiro, 2009; Schulman and Harper, 2009). It achieves this by targeting proteins to the proteasome for degradation or signaling endocytosis and lysosomal degradation (Figure 1). Furthermore ubiquitylation is not only involved in the degradation of proteins. In several signaling pathways it controls the interactions of key proteins (Komander and Rape, 2012).

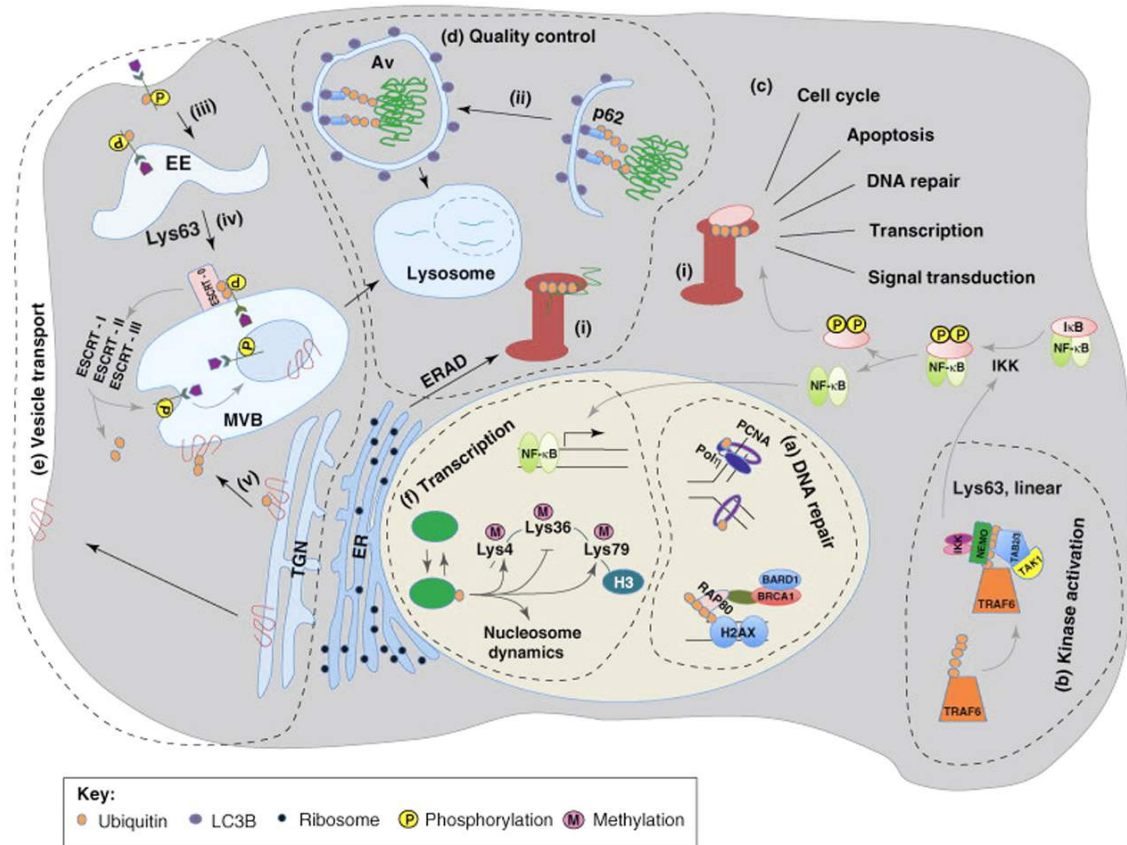


Figure 1: Overview of cellular functions regulated by ubiquitylation. (a) In the nucleus, ubiquitylation signals for proteasome-independent regulation of DNA repair. Histones and Proliferating cell nuclear antigen (PCNA) are examples of nuclear targets of ubiquitylation. (b) Ubiquitylation functions in kinase activation by acting as a scaffold to bring kinases and their substrates together to enable the activation of kinase cascades, as exemplified by the activation of inhibitor of kappa B kinase (IKK) by Transforming growth factor beta activated kinase-1 (TAK1). The E3 Tumor necrosis factor receptor-associated factor 6 (TRAF6) ubiquitylates several proteins including nuclear factor-kappa-B essential modulator (NEMO) and itself upon ligand stimulation. TAK1 and IKK complexes interact with each other upon binding these ubiquitin chains with their ubiquitin-binding subunits (TAB2 and NEMO, respectively). IKK is thus activated by TAK1 and competent to phosphorylate Inhibitor of kappa B (IκB), which leads to its ubiquitylation and proteasomal degradation (i). IκB degradation releases nuclear factor-kappa-B (NF-κB) into the nucleus, thereby activating gene transcription. (c) Proteasome-mediated degradation (i) regulates many cellular processes through targeted degradation of key regulatory proteins. (d) Ubiquitylation signals for protein quality control to degrade misfolded proteins. Protein quality control of endoplasmic reticulum (ER) proteins occurs through the ER-associated protein degradation (ERAD) pathway by proteasomal degradation (i), whereas some large protein aggregates are eliminated through the autophagy (Av, autophagic vesicles)-lysosome route (ii). (e) Vesicle transport

Polyubiquitylation acts as a signal for autophagy targeting. (e) Ubiquitylation signals for vesicular trafficking between membrane compartments. (iii) Ligand-bound plasma membrane proteins internalized into early endosomes (EE). (iv) Proteins are sorted into multivesicular bodies (MVB). (v) Newly synthesized membrane proteins are sorted from the trans-Golgi network (TGN) to the MVB. (f) Ubiquitin signaling regulates gene transcription (BARD1: BRCA1-associated RING domain protein 1; BRCA1: breast cancer type 1 susceptibility protein; ESCRT: endosomal sorting complexes required for transport; H2AX: histone 2 A histone family member, family X; H3: histone 3; Lys: lysine; p62: ; Pol η : DNA polymerase η ; RAP80: receptor-associated protein 80; modified after Liu and Walters, 2010).

Because of its key roles in proteolysis and signaling, misregulated ubiquitylation is involved in a plethora of human diseases and disorders: cancer (Kirkin and Dikic, 2011; Lipkowitz and Weissman, 2011; Micel et al., 2013; Shi and Grossman, 2010; Yerlikaya and Yöntem, 2013), autoimmune diseases (Fierabracci, 2012; Ma and Malynn, 2012; Wang and Maldonado, 2006), cardiac diseases (Carrier et al., 2010; Pagan et al., 2013; Powell et al., 2012), metabolic disorders (Genschik et al., 2013; Vu and Sakamoto, 2000; Zungu et al., 2011), neurodegeneration (Bossy-Wetzel et al., 2004; Ihara et al., 2012; Nijholt et al., 2011), mental disorders (Donohue, 2002; Seelaar et al., 2011) or even pneumonia (Wang et al., 2012a). Because ubiquitylation participates in so many different processes a lot of studies have been conducted to understand the mechanisms behind it.

Ubiquitin itself is a highly conserved 76 amino acid protein, that becomes covalently attached to another protein through the formation of an isopeptide bond between ubiquitin's C terminal carboxyl function and in most studied cases the ϵ -amino group of a lysine residue within the other protein (Figure 2A; Hershko and Ciechanover, 1998). In eukaryotes, ubiquitin is fairly abundant with levels around 0.1-5% of total proteins; it is expressed from two genes as a tetramer or octamer in a head-to-tail configuration and from two other genes as single ubiquitin moiety fusions to ribosomal proteins (Kimura and Tanaka, 2010). These four precursors are processed into the final monomeric ubiquitin molecules by ubiquitin hydrolases. Ubiquitin forms a globular structure and is very stable (Kimura and Tanaka, 2010).

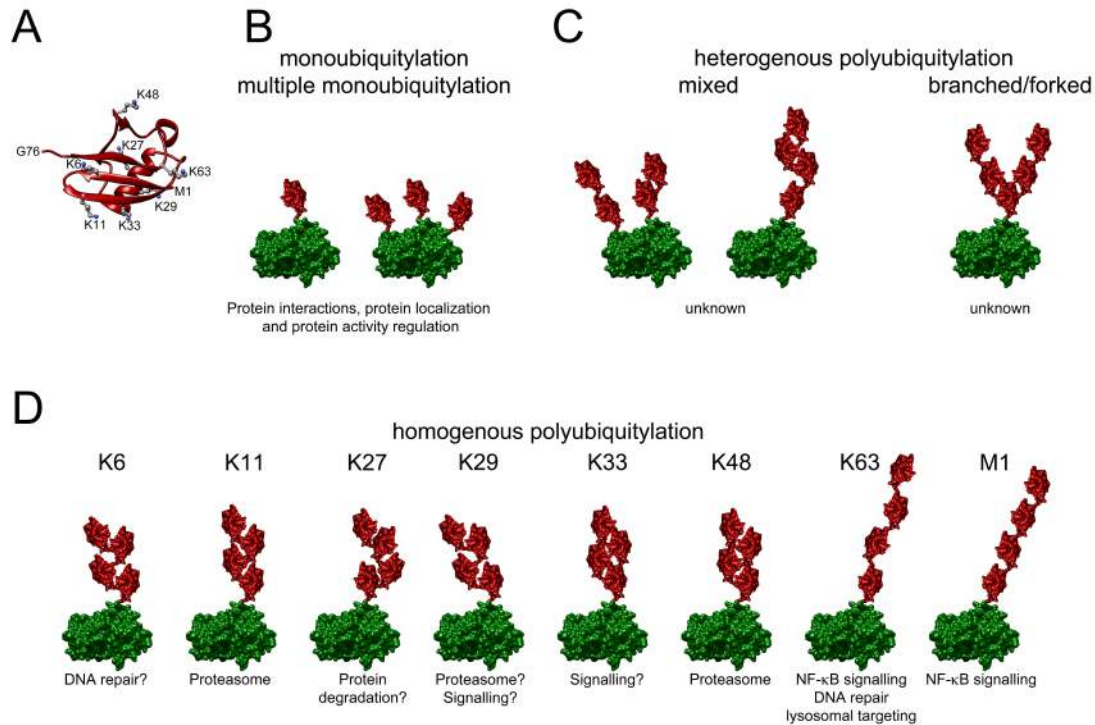


Figure 2: Ubiquitin structure and different ubiquitylation topologies. A. Ubiquitin structure and linkages. Ubiquitin is a globular protein with a flexible C-terminus. Polyubiquitylation can occur through any of the seven lysine residues (blue: ϵ -amino group) and the N-terminus (M1) of ubiquitin (PDB 1UBQ). **B.** Monoubiquitylation and multiple monoubiquitylation. The transfer of a single ubiquitin to one (monoubiquitylation) or multiple (multiple monoubiquitylation) sites can recruit binding partners, inhibit interactions, change protein localizations or modulate protein activities. **C.** Heterogenous polyubiquitylation. A single substrate can get ubiquitylated with chains containing distinct linkages within a single chain or homogenous chains at different sites within the substrate. Branched or forked ubiquitin chains result from the attachment of two ubiquitin molecules to two different lysine residues in a ubiquitin that is already linked to a substrate and are therefore a subtype of mixed ubiquitin chains. If heterogenous chains are responsible for certain cellular functions is unknown. **D.** Homogenous polyubiquitylation. K48- and K11-linked ubiquitin chains target proteins for degradation by the 26S proteasome. K63-linked chains usually mediate the recruitment of binding partners, which can lead to activation of NF- κ B, orchestration of different steps during DNA repair or targeting of the modified protein to the lysosome. All other ubiquitin chains have been detected *in vitro* or *in vivo*, but substrates or enzymes responsible for their assembly are poorly defined (green: substrate (PDB 1VIN), red: ubiquitin (PDB 1UBQ); modified after Ye and Rape, 2009).

The transfer of a single ubiquitin to a substrate, a reaction referred to as monoubiquitylation, typically alters interactions, localization, or activity of the modified protein (Figure 2B; Dikic et al., 2009).

Conversely, the attachment of multiple ubiquitin molecules results in polymeric chains, that depending on their connectivity could have unique functions. Ubiquitin chain formation can occur through seven lysine residues (K6, K11, K27, K29, K33, K48 and K63) or the N-terminus of ubiquitin (M1), leading to the assembly of multiple chains with distinct topology; the use of different lysine residues leads to more complex ubiquitin topologies (Figure 2C,D; Komander and Rape, 2012). All linkages have been detected in cells, and their abundance changes during the cell cycle or cell differentiation (Peng et al., 2003; Xu et al., 2009).

1.1.1. The enzymatic ubiquitylation cascade of E1-E2-E3

Most ubiquitylation reactions occur through the subsequent actions of an adenosine triphosphate (ATP)-dependent enzymatic cascade consisting of ubiquitin activating enzymes (E1), ubiquitin conjugating enzymes (E2) and ubiquitin ligases (E3). Two ubiquitin specific E1s exist in vertebrates called UBA1 and UBA6. While UBA1 is the more extensively investigated E1 working with most E2s, UBA6 was recently discovered and seems to work exclusively with a single E2 named UBA6 specific E2 (USE1) (Jin et al., 2007; Schulman and Harper, 2009). Therefore UBA1 is referred to E1 from here on. The human genome contains about 40 E2s; some of them do not interact with ubiquitin or show no catalytic activity on their own (Deshaies and Joazeiro, 2009). More than 600 distinct E3s ensure the regulated modification of specific substrates within human cells (Deshaies and Joazeiro, 2009). About 85 deubiquitinating enzymes (DUBs) can reverse ubiquitylation making it a highly dynamic process, which can be regulated on multiple levels (Komander et al., 2009).

The initial step in the ubiquitylation cascade is the binding of Mg•ATP and ubiquitin to E1. Next, ubiquitin is adenylated by E1 under release of

pyrophosphate (PP_i) at its C-terminus (Figure 3A; Haas and Rose, 1982; Haas et al., 1982, 1983). E1's catalytic cysteine sulfhydryl group attacks the ubiquitin adenylate bond leading to discharge of adenosine monophosphate (AMP) and the formation of a thioester between E1 and ubiquitin's C terminal carboxyl group (Ciechanover et al., 1981, 1982; Haas and Rose, 1982; Haas et al., 1982). Another round of ubiquitin adenylation leads to a complex of E1 bound to the activated ubiquitin adenylate and the thioester ubiquitin intermediates (Haas and Rose, 1982; Haas et al., 1982). This single E1 bound to two activated ubiquitin species binds E2s with nanomolar affinities (Haas et al., 1988). Ubiquitin is then transferred to the catalytic site cysteine residue of the respective E2 in a transthioesterification reaction (Figure 3B; Haas and Bright, 1988; Haas et al., 1982, 1988; Hershko et al., 1983; Pickart and Rose, 1985).

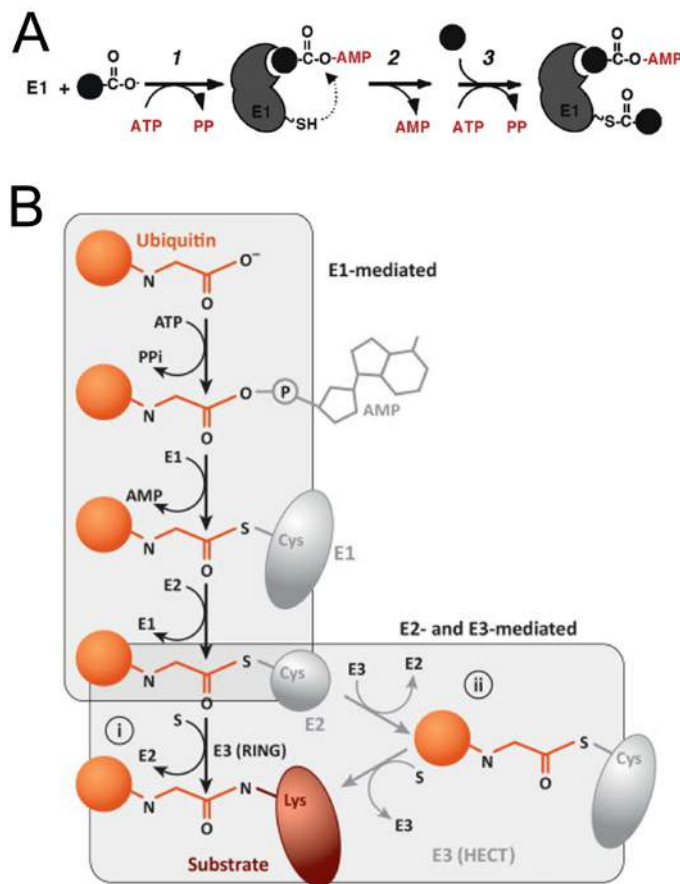


Figure 3: The enzymatic cascade responsible for ubiquitin transfer.

A. E1-catalyzed reaction. Step 1, ubiquitin adenylate formation; step 2, transfer of ubiquitin from adenylate to cysteine (product not shown); step 3, second round of adenylate formation to yield fully loaded enzyme, modified after (Pickart, 2004). **B.** Schematic representation of the different modifications occurring at the carboxyl end of ubiquitin during ubiquitylation. (i) RING (really interesting new gene) mediate the direct transfer of ubiquitin from the E2 onto the substrate; (ii) an additional transthioesterification step is mediated by HECT (homologous to E6-AP carboxyl

terminus) before substrate ubiquitylation, modified after (Kleiger and Mayor, 2014).

The ubiquitin charged E2 dissociates from E1, which now can undergo another cycle of ubiquitin thioester and subsequent ubiquitin adenylate formation. An E3 will bind an E2 loaded with ubiquitin and catalyze ubiquitin transfer from the E2's active site onto the substrate forming a stable isopeptide bond between ubiquitin's C terminal carboxyl group and an ϵ -amino group of a lysine residue of the respective substrate (Ye and Rape, 2009). This process can be repeated multiple times resulting in the formation of polyubiquitin chains on a substrate; engagement of the substrate already modified with ubiquitin by an E3 causes the addition of another ubiquitin moiety from an E2 leading to formation of a covalent bond between the C-terminus of E2 bound ubiquitin and a lysine residue of the substrate attached ubiquitin (Hochstrasser, 2006). E3 binding sites in substrates are called degrons, if the E3 causes substrate degradation. The determinants of E2/E3 pairs are further elaborated below. E3s can be divided in two major classes: really interesting new gene (RING) and homologous to E6-AP carboxy terminus (HECT) ligases. While RING E3s permit transfer of ubiquitin from E2 directly to the substrate, HECT E3s have a catalytic side cysteine residue within their HECT domain. Due to transthioesterification ubiquitin becomes transferred from the E2 on to the HECT E3. Binding of a substrate to a charged HECT E3 results in modification of the substrate with ubiquitin. If E3s are mentioned here generally RING E3s are meant. Ubiquitin ligases that further ubiquitylate oligoubiquitylated substrates are called E4s (Hoppe, 2005; Koegl et al., 1999).

1.1.2. E2s specify ubiquitin chain linkage and E2-E3 interaction

An increasing number of studies show that E2s are often the deciding force behind ubiquitin topology specificity of E3s (Komander and Rape, 2012; Wenzel et al., 2011a). HECT E3s are the exception as the C-terminal lobe of the HECT domain decides linkage specificity (Wang et al., 2006). In general the last enzyme in the ubiquitylation cascade carrying ubiquitin via a thioester bond seems to determine what kind of chain is constructed.

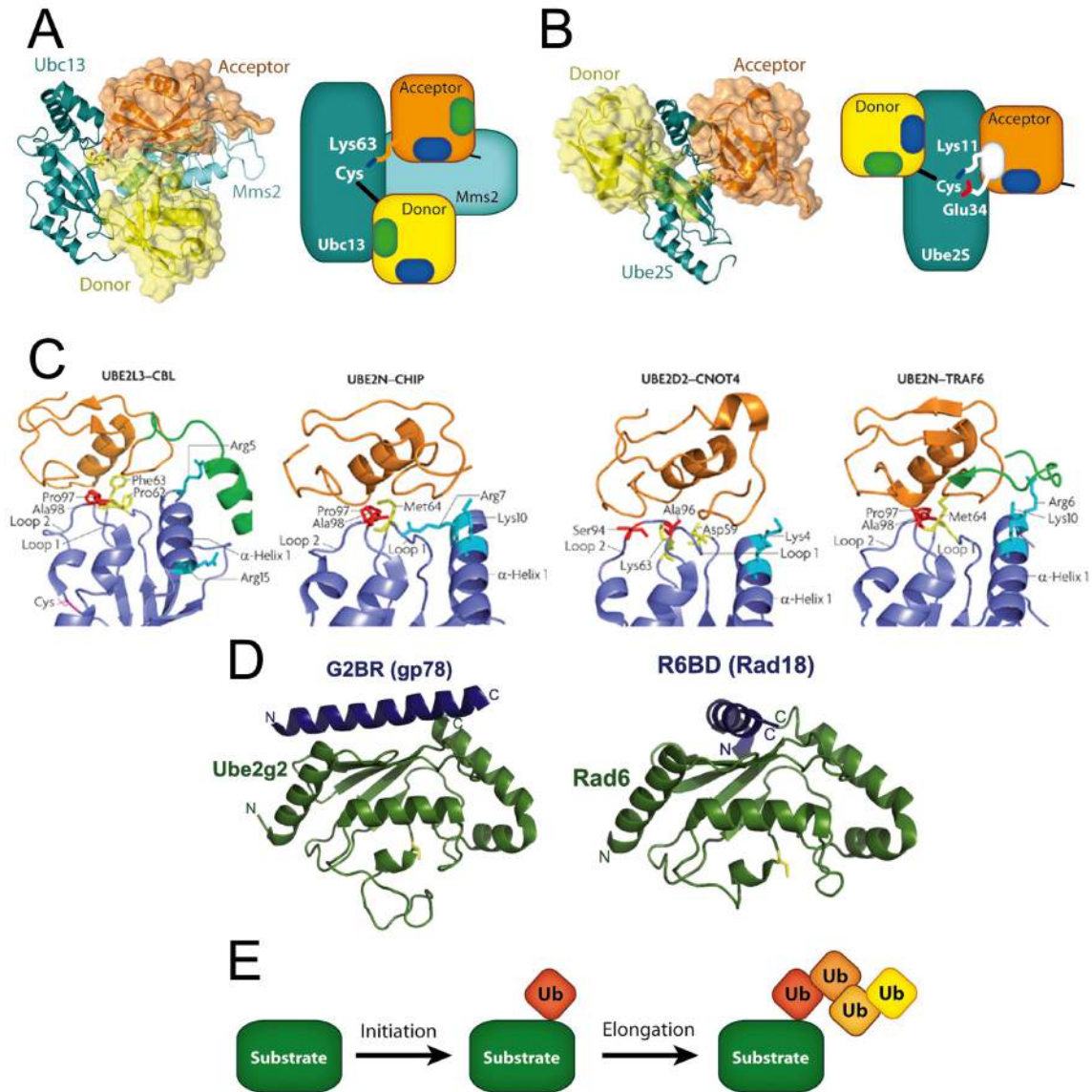


Figure 4: Mechanism of linkage-specific ubiquitin chain assembly and RING interaction by E2s. **A.** Heterodimeric Ube2N-Ube2V2 (Ubc13-Mms2 in *S.cerevisiae*) recognizes acceptor ubiquitin through the UBC-variant domain of Ube2V2. This positions the acceptor K63 to the active site of charged Ube2N. **B.** Monomeric Ube2S catalyzes linkage formation through substrate-assisted catalysis. Ube2S recognizes the so-called TEK-box (Jin et al., 2008) of acceptor ubiquitin. Activation of the acceptor K11 requires a ubiquitin residue, E34. Thus, the correct surface of the acceptor ubiquitin, which includes K11 and E34, must be exposed to the catalytic cysteine of charged Ube2S in order for the active site to be completed and for linkage formation to occur. **C.** Comparison of different E2-E3 interactions: UBE2L3-casitas B-lineage lymphoma (CBL) (PDB 1FBV44), UBE2N-carboxy terminus of HSC70 interacting protein (CHIP; also known as STUB1) (PDB 2C2V46), UBE2D2-CNOT4 (CCR4-NOT transcription complex, subunit 4) (PDB 1UR645) and UBE2N-TNF receptor associated factor 6 (TRAF6) (PDB

Introduction

3HCT47). All E2s use loop 1, loop 2 and α -helix 1 to interact with E3s. The side chains of the residues involved in E3 recognition are colour-coded (residues in loop 1 are yellow, in loop 2 are red and in α -helix 1 are cyan). Note that for CBL and TRAF6, E3 elements outside the RING domain (shown in green) participate in E2 binding. The CNOT4–UBE2D2 structure is an NMR model, whereas the others were solved by crystallography. The RING finger (or the U-Box for CHIP) is in orange, and the cognate E2s are in blue. **D.** E2 binding domains other than the RING modulate ubiquitylation by binding to the ‘backside’ of E2s. Structures of the Postreplication repair protein Rad18 (R6BD, 2YBF); Autocrine motility factor receptor, called gp78 (G2BR, PDB 3H8K); binding to the ‘backside’ of their respective E2s (labeled and shown in green). The catalytic cysteine of each E2 is highlighted in yellow. **E.** Ubiquitin chain formation proceeds through an initiation step, during which a substrate lysine residue is modified, and elongation, during which ubiquitin molecules are added to the growing chain. (Modified after Komander and Rape, 2012; Metzger et al., 2014; Ye and Rape, 2009)

In the case of RING E3s this is achieved by proper orientation of E2 active site and target ubiquitin lysine residue. Two major orientation mechanisms have been observed, as either an E2 binding protein helps to orient the acceptor ubiquitin or surfaces on the E2 itself that are distinct from the catalytic site bind and orient acceptor ubiquitin. Donor ubiquitin is the ubiquitin molecule, which is attached to the E2 via its C-terminus, while the ubiquitin molecule, which becomes modified via its lysine residue, is called acceptor ubiquitin (Figure 4A,B). In the resulting polyubiquitin chain donor ubiquitin would be the proximal ubiquitin moiety, while the acceptor ubiquitin would be the distal ubiquitin. The E2 Ube2N is able to use Ube2V1/2 for acceptor ubiquitin orientation (Figure 4A; Eddins et al., 2006). Ube2K possesses a ubiquitin-associated domain (UBA), binding and orienting the acceptor ubiquitin (Wilson et al., 2011). On the other hand Ube2S, Ube2G2 and Ube2R1 can orient acceptor ubiquitin via binding to the core E2 itself (Figure 4B; Liu et al., 2014; Suryadinata et al., 2013; Wickliffe et al., 2011a). Domains within an E3 like the RING itself might contribute to orientation of acceptor ubiquitin, which needs to be further determined.

While it is important to know what kind of linkage-specificity is encoded by an E2, it is equally important to understand which E3s and E2s are able to interact in a productive manner. All E2s have an evolutionary conserved ubiquitin conjugating

domain (UBC) of about 150 amino acids with extensions N- or C-terminal of the UBC and within the UBC (Wenzel et al., 2011a). Generally every E2 interacts with an E3 through its UBC. Certain loops have been identified in the UBC as essential for productive RING or HECT interaction (Figure 4C). Replacement of residues in these loops tested in combination with different E3s indicate a certain degree of E3 specificity encoded in these loop regions (Wenzel et al., 2011a; Xu et al., 2008). As only few functional E2/E3 pairs are known and have been tested this way, generalizations regarding E2/E3 compatibility should be met with caution. The N-or C-terminal extensions of the UBC can provide specific interaction with their E3s (Kleiger et al., 2009; Summers et al., 2008). Additionally, elements outside the RING domain in E3s seem to be involved in binding to their cognate E2s via the UBC (Figure 4C,D; Bailly et al., 1997; Das et al., 2009; Li et al., 2009). Moreover, productive interaction of an E2 with an E3 can be based on the class of the E3 (Wenzel et al., 2011b).

Furthermore different E2s are able to work sequentially with a given E3. One E2 initiates chain formation by monoubiquitylation and subsequently another E2 elongates the single ubiquitin moiety with more ubiquitin molecules in form of chains (Figure 4E; Rodrigo-Brenni and Morgan, 2007).

1.1.3. How much information is encoded by the different ubiquitin linkages?

The first chain types to be discovered, termed canonical ubiquitin chains, have distinct consequences for the modified protein: while chains connected through K48 of ubiquitin promoted proteasomal degradation (Chau et al., 1989; Johnson et al., 1995), K63 linked chains regulated the assembly of oligomeric complexes (Figure 2D; Spence et al., 2000; Wang et al., 2001). Based on these observations, it was hypothesized that diverse ubiquitylation marks might trigger unique biological outcomes, reminiscent of a code. Since then many more physiological ubiquitylation events have been characterized in terms of K48 or K63 linkages. Just to name a few, K48-linked chains are used for degradation of proteins involved in the cell cycle (Mocciaro and Rape, 2012; Petroski and

Deshai, 2005), tumor suppression (Chen et al., 2013a; Wang et al., 2013, 2012b), tumorigenesis (Chandra et al., 2013; Lin et al., 2013; Narisawa-Saito and Kiyono, 2007; Wang and Pickart, 2005), development (Latres et al., 1999; Ro and Dawid, 2009; Wodarz and Nusse, 1998), apoptosis (Gonzalvez et al., 2012; Guicciardi et al., 2014; van de Kooij et al., 2013; Yeh and Bratton, 2013), transcription (Chang et al., 2011; Chen et al., 2013b; Lei et al., 2013; Liu et al., 2012; Yuan et al., 2012) or in clearance of misfolded proteins at the endoplasmic reticulum (ER) (Bagola et al., 2013; Li et al., 2007b; Smith et al., 2011). On the other hand more examples have been found, where K63-linked chains modulate composition of protein complexes with functions such as DNA repair (Doil et al., 2009; Al-Hakim et al., 2010; Huang et al., 2009; Sobhian et al., 2007; Stewart et al., 2009), cell proliferation (Davies et al., 2013; Linares et al., 2013; Peschiaroli et al., 2010; Tauriello et al., 2010), immune response (Conze et al., 2008; Hou et al., 2011; Xia et al., 2009; Zeng et al., 2010) protein trafficking (Hao et al., 2013; Huang et al., 2013; Kramer et al., 2010; Stawiecka-Mirota et al., 2007), splicing (Bellare et al., 2008; Song et al., 2010) and translation (Spence et al., 2000). At this point it should be mentioned that trafficking of proteins regulated by K63-linked chains often leads to their degradation in lysosomes (Figure 1; Barriere et al., 2007; Tofaris et al., 2011; Varghese et al., 2008).

Other ubiquitin linkages have been detected in cells and some of them are attributed to E2/E3 pairs and their biological functions (Komander and Rape, 2012). Several of these linkages can mediate proteasomal degradation, but the reason for this redundancy is unclear (Jin et al., 2008; Johnson et al., 1995; Koegl et al., 1999; Xu et al., 2009).

Linear ubiquitin chains or M1-linked chains have been reported to function similarly to K63-linked chains in regulating formation of protein complexes often even in the same pathway as K63 chains (Rieser et al., 2013; Walczak et al., 2012). Again the redundancy for different chain types fulfilling very similar functions remains elusive.

Conjugates of more complex topology, such as mixed chains, are formed during endocytosis or immune signaling (Figure 2C; Boname et al., 2010; Emmerich et

al., 2013). Furthermore, *in vitro* reconstitution of several E2/E3 pairs showed that a single ubiquitin molecule embedded within a chain can be modified at two lysine residues, a process that leads to the assembly of branched conjugates (Figure 2C; Kim et al., 2007). These branched conjugates were also found in cells (Peng et al., 2003; Tagwerker et al., 2006).

Many of the identified E3/substrate pairs still have to be investigated regarding their linkage specificity especially *in vivo*. Another way to determine linkage specificity is *in vitro* reconstitution of the respective reaction. Unfortunately only few physiological E2/E3 pairs have been identified. Studies that address ubiquitin linkages generally report the linkage used by a certain E3 and what function this linkage specific substrate ubiquitylation has. Hence these studies pair a certain linkage and its impact on substrates in a purely correlative way. Future studies are needed to show the outcomes of changing linkage specificity to gain further insights into the ubiquitin code.

1.1.4. The 26S proteasome and other ubiquitin binding proteins

The human 2.5 MDa 26S proteasome is responsible for ubiquitin dependent protein degradation in the ubiquitin proteasome system (UPS; Figure 5; Finley, 2009). It consists of the proteolytic 20S core particle (CP) and a 19S regulatory particle (RP). The CP consists of 28 subunits encoded by 14 different genes and is shaped like a barrel in a symmetrical manner (Borissenko and Groll, 2007; Groll et al., 1997). The interior of the barrel is coated with six peptidase active sites, which together are able to hydrolyze a wide range of proteins into oligopeptides (Borissenko and Groll, 2007). Entry into the inner chamber of the CP is regulated by the RP (Finley, 2009). The RP consists of 19 subunits in yeast and can be further subdivided into base and lid. Six different ATPases responsible for CP-RP complex formation, two scaffold proteins and two ubiquitin binding proteins, the 26S proteasome regulatory subunits Rpn10/S5a and Rpn13, also called ubiquitin receptors, make up the base. ATP binding to the ATPases is necessary for proper assembly of the proteasome (Smith et al.,

2005). ATP hydrolysis is required for protein unfolding and translocation of the unfolded polypeptide via a channel into the proteolytic chamber of the CP (Finley, 2009).

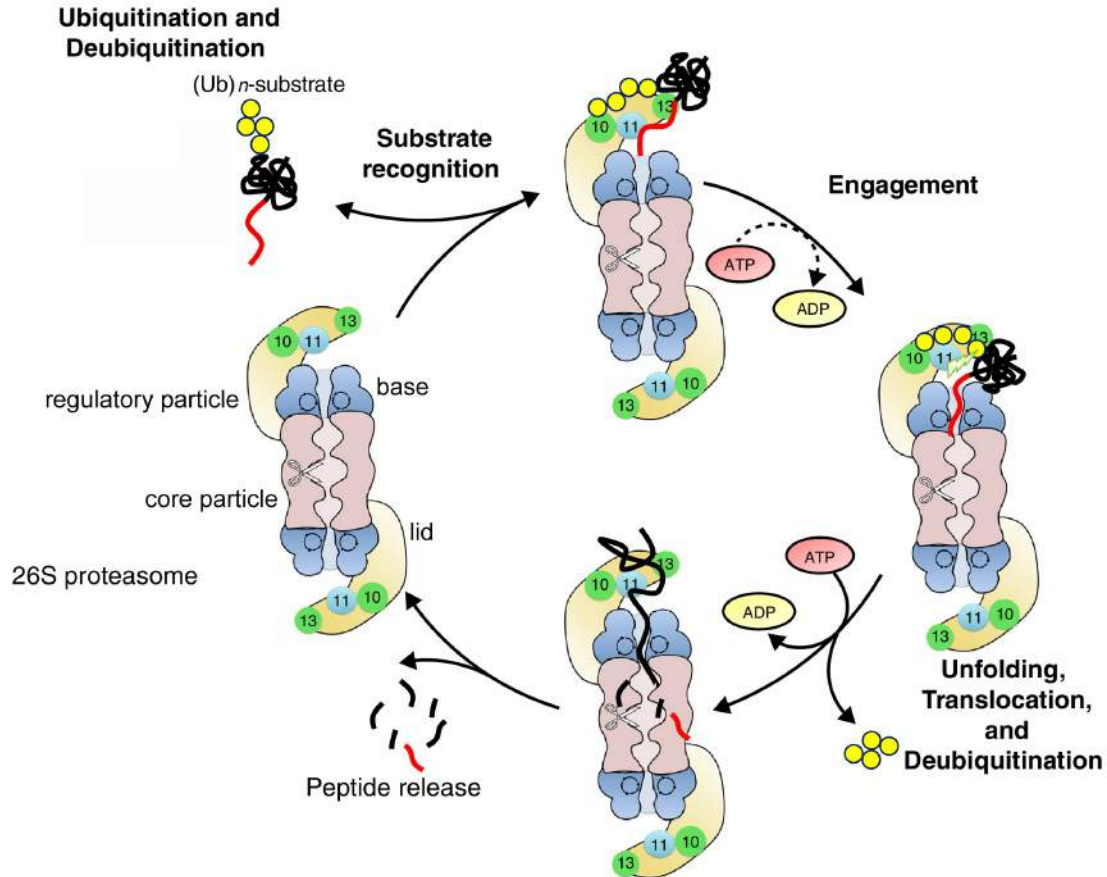


Figure 5: Schematic representation of the degradation cycle of the ubiquitin proteasome system. Proteins are targeted to the proteasome by a two-part degradation signal or degron. It consists of a disordered region within the substrate and a reversibly attached polyubiquitin tag (Ub_n). The proteasome recognizes its substrates at the ubiquitin tag through ubiquitin receptors (Rpn10/S5A and Rpn13; green) (top) and initiates degradation at the unstructured region (right). Once the proteasome has engaged its substrate, it unravels the protein by translocating it into a central cavity in the core particle, where the protein is proteolysed (bottom). The polyubiquitin tag is cleaved off by the intrinsic DUB Rpn11 (skyblue) as unfolding and degradation begins (modified after Inobe and Matouschek, 2014).

The only assigned function for one of the nine lid subunits is the deubiquitinating activity of Rpn11, which is important for proteasome activity cleaving off a ubiquitin chain in one step at the proximal ubiquitin (Gallery et al., 2007; Maytal-

Kivity et al., 2002; Verma et al., 2002; Yao and Cohen, 2002). Consequently the concerted actions of CP and RP enable the 26S proteasome to bind a ubiquitylated protein via its ubiquitin receptors, to unfold the protein with its ATPases, to cleave off ubiquitin with its DUB and to translocate the unfolded protein into the inside of the CP, where its peptidases hydrolyze the proteins.

Several other proteins bind the proteasome, regulating its function. Most relevant here are the so-called proteasomal shuttle or delivery factors that bind and protect ubiquitylated proteins from DUBs, while supposedly recruiting them to the proteasome by direct binding (Finley, 2009). The homologues of S5A/Rpn10 and human UV excision repair protein RAD23 homolog A (HHR23A), one of the proteasomal delivery factors, are both crucial in mice (Hamazaki et al., 2007; Ng et al., 2003) and were therefore mostly used as a readout for proteasomal ubiquitin binding in this study.

The ATP-driven chaperone valosin-containing protein/p97 (p97) has been implicated in targeting ubiquitylated proteins to the proteasome as well (Kim et al., 2004; Richly et al., 2005). In complex with its cofactors, which have ubiquitin binding domains, p97 is able to interact with ubiquitylated proteins (Alexandru et al., 2008; Richly et al., 2005). Using its so-called “segregase” activity, p97 can extract proteins from the ER or the mitochondrial membrane as well as chromatin for proteasomal degradation; it has also been shown to be involved in the clearance of intracellular protein aggregates, in autophagy and in endosomal trafficking (Meyer et al., 2012). Hence, p97 is an important hub in the cell for ubiquitin dependent processes and was used as another readout for ubiquitin binding experiments.

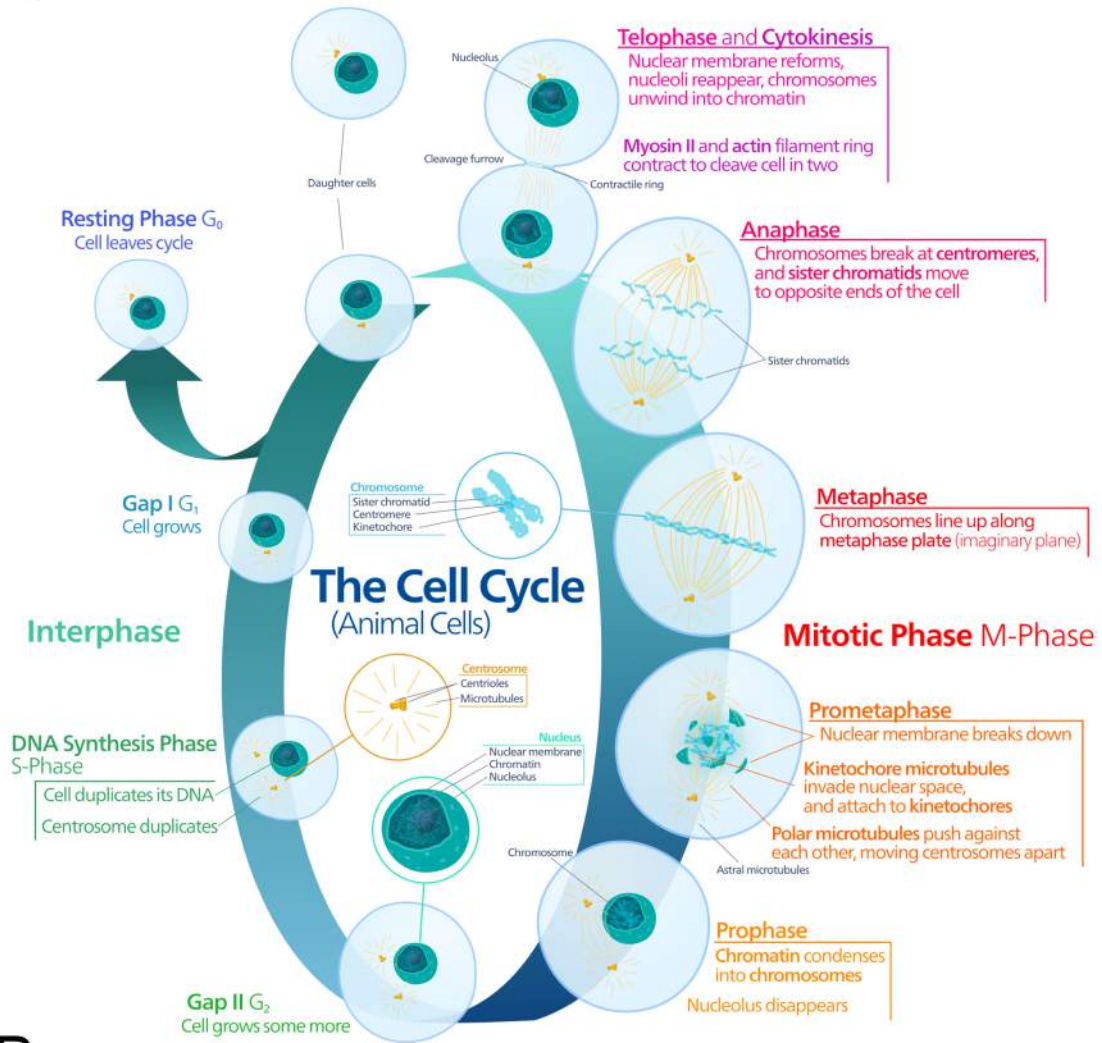
1.2. The basics of the cell cycle

For the human organism to survive, grow and reproduce its cells have to undergo cell division. The separation of a single cell into two cells and the simultaneous distribution of its content into the daughter cells is called cell division. Proteins, RNA, ribosomes and organelles such as mitochondria, peroxisomes or

lysosomes are constantly synthesized and present in multiple copies in a cell; therefore division of a cell can simply distribute them into daughter cells. Other cellular compartments like the Golgi apparatus, the ER and the nuclear membrane disintegrate into fragments, which can be separated into daughter cells and are able to reform the mature structures in the progeny. Most importantly, the DNA of a cell needs to be duplicated before cells undergo division. Also the centrosome, the organelle responsible for microtubule-organization and for the establishment of the DNA separating machinery, is another component, which needs to be duplicated before cell division (Figure 6A; Morgan, 2007).

To ensure proper separation into daughter cells, distribution of cell components and ability for further cell divisions, a program was established during evolution called the cell cycle. In general the cell cycle consists of four different phases. The replication of the genome occurs in the synthesis or S phase. Chromatin is replicated and the resulting copies, called sister chromatids are held together by cohesin protein complexes (Nasmyth et al., 2000). The separation of the DNA duplicates, known as nuclear division, and separation of daughter cells, known as cytokinesis, occur in mitosis (M phase). Mitosis is further subdivided into other phases (Figure 6A). In metaphase sister chromatids are aligned in the middle of a bipolar microtubule array emanating from centrosomes (Bailly and Bornens, 1992; Bornens, 2002). Transition from metaphase into anaphase leads to cleavage of cohesin and transport of the separated sister chromatids towards the spindle poles. The period from the end of one M phase until the start of another M phase is referred to as interphase. In between M and S phases are so-called gap or G1 and G2 phases. Cells progress through G1 phase, before they enter S phase. They can also exit the cell cycle from G1 and enter the G0 phase. Cells in G0 are often called quiescent cells, which do not proliferate until certain conditions signal them to start dividing again. Three major checkpoints are in place to ensure error free division (Hartwell and Weinert, 1989; Murray and Kirschner, 1989). Enough resources and proliferation signals have to be present to pass the G1/S checkpoint.

A



B

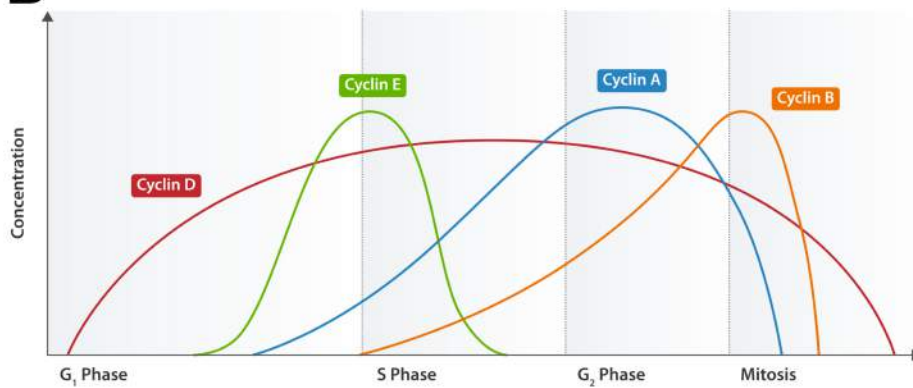


Figure 6: Major events of the cell cycle are connected to changes in cyclin levels. A. Diagram of the cell cycle in metazoans (2014a). **B.** Changes of cyclin levels during the cell cycle (2014b).

Cells progress through the G2/M checkpoint, if the genome was accurately copied during S phase. Otherwise cells persist in G2 until inhibitory signals such as DNA damage are successfully eliminated. The last checkpoint before final division is at the metaphase-to-anaphase transition and is also known as mitotic checkpoint, metaphase checkpoint, spindle checkpoint or spindle assembly checkpoint. Only if every sister chromatid pair is attached to opposing centrosomes via microtubules and consequently under bipolar tension, will the APC/C become active and cause the cleavage of cohesin and progression through mitosis (Morgan, 2007; Musacchio and Salmon, 2007).

Cyclin dependent kinases (Cdks) are of utmost importance to catalyze biochemical reactions, which drive accurate progression through the cell cycle. Cdks become active upon binding to cyclins. While the amount of a certain cyclin oscillates during the cell cycle dependent on the kind of cyclin, Cdk levels stay constant throughout the cell cycle (Figure 6B; Morgan, 1997). Cdk4/6 and cyclin D trigger entry into the cell cycle in G1 (Lucibello et al., 1993; Matsuoka et al., 1994). Cdk2 together with cyclin E is mainly responsible for transition through the G1/S checkpoint, but also for duplication of centrosomes and formation of DNA pre-replication complexes. Cdk2/1 and cyclin A initiate DNA replication and early mitotic events e.g. upregulation of cyclin B levels starting in S phase and enhancement of Cdk1/cyclin B activity. Active Cdk1 and cyclin B cause condensation of DNA, nuclear envelope breakdown (NEBD), and subsequently the formation of the mitotic spindle and alignment of sister chromatids at the spindle midzone (Hunt, 1989; Nigg, 2001; Takizawa and Morgan, 2000). Therefore cyclin B has to be destroyed in order to progress through mitosis and for cells to ultimately divide. Thus the rise and fall of cyclin levels in the cell regulates accurate progression through the cell cycle (Morgan, 2007).

1.2.1. The anaphase-promoting complex

The APC/C is a conserved RING E3 ubiquitin ligase of about 1.5 MDa with more than a dozen core subunits (Peters, 2006). Most of these subunits, like Cell division control protein 27 (Cdc27; name of Anaphase-promoting complex subunit APC3 in *S.cerevisiae*), APC5, Cdc16/APC6, APC7 or APC8, are responsible for scaffolding using tetratricopeptide repeat (TPR) motifs for protein-protein interactions (Figure 7A; Barford, 2011). The Cullin-like subunit APC2 and the RING subunit APC11 build similar to the modular Skp1-Cul1-F-box (SCF) ligases the catalytic center of the APC/C (Tang et al., 2001). The core APC/C is expressed at constant levels throughout the cell cycle, but depending on the cell cycle stage it interacts with two different coactivators, Cdc20 and Cdh1, for substrate recognition comparable to F-box proteins (Zhang et al., 2014). The core subunit APC10 binds substrates cooperatively with Cdh1 (Figure 7B; da Fonseca et al., 2011; Matyskiela and Morgan, 2009). Another subunit APC15 seems to be important for inactivating Cdc20 to control APC/C activity in mitosis (Primorac and Musacchio, 2013). The APC/C is mainly studied for its essential functions in mitosis, but has also been reported to be important in meiosis; additionally it has been implicated in post-mitotic neurobiology and metabolism (Barford, 2011). APC/C-mediated polyubiquitylation of its substrates leads to their proteasomal degradation (King et al., 1995; Sudakin et al., 1995). Securin, cyclin A, cyclin B and geminin are some of the most prominent APC/C substrates (Peters, 2006). Securin has to be degraded in order to release active separase, which then cleaves cohesin and allows for separation of sister chromatids (Nasmyth, 2001). Cdt1 is kept inactive by geminin binding; once geminin is removed free Cdt1 is available as a replication factor necessary in S phase (McGarry and Kirschner, 1998; Quinn et al., 2001; Tada et al., 2001; Wohlschlegel et al., 2000). Degradation of the cyclins renders Cdks inactive allowing for timely progression through the cell cycle.

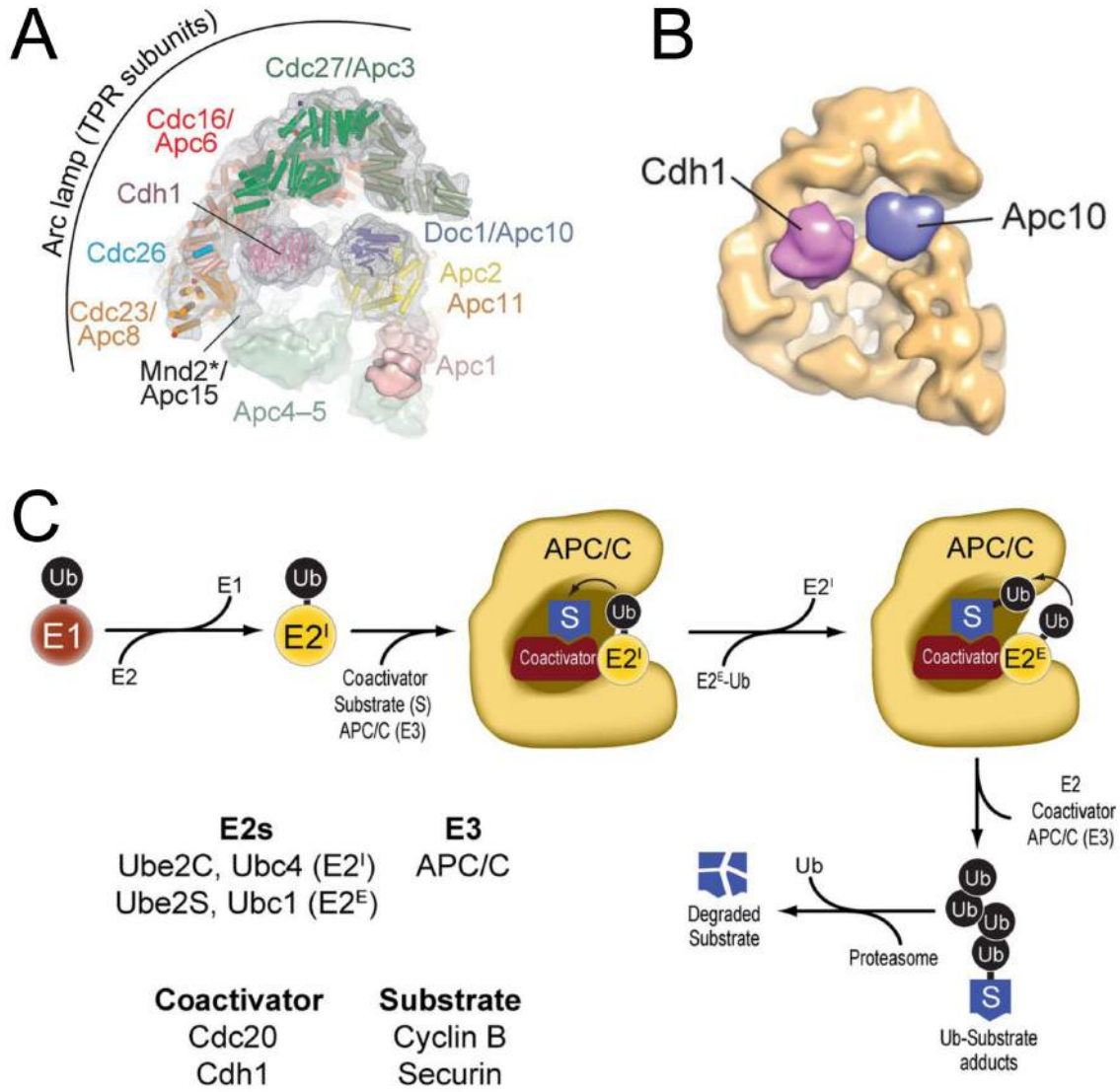


Figure 7: Structure and functional mechanism of the APC/C. **A.** Schematic representation of the APC/C. A pseudoatomic model was generated by fitting known high-resolution structures (currently available only for a subset of the APC/C subunits or for closely related sequences) into an ~ 10 -Å cryo-EM map of the APC/C^{Cdh1}-D box ternary complex from *S. cerevisiae* (Schreiber et al., 2011). The subunits are labeled with both the yeast and vertebrate names. The approximate expected position of Mnd2/Apc15, for which a molecular model is currently missing, is indicated (marked therefore with an asterisk). PDB accession numbers for deposited high-resolution models are as follows: Apc10/Doc1, 1JHJ; APC7 N-terminal domain, 3FFL; Cdc26-Apc6 complex, 3HYM; Apc10/Doc1, 1GQP; Cdc16/Cut9-Cdc26/Hcn1 complex, 2XPI; Apc8/Cdc23, 3ZN3; and Cdc27, 3KAE. **B.** Negative stain EM reconstruction of APC/C^{Cdh1} from *S. cerevisiae* (da Fonseca et al., 2011) with densities assigned to Cdh1 and Apc10. **C.** Ubiquitin (Ub) is first

activated by an E1 enzyme, transferred to a chain-initiating E2 (E2I; Ube2C in *H.sapiens*; Ubc4 in *S.cerevisiae*), and transferred to a substrate (S; cyclin B or securin). The creation of poly-Ub chains by the APC/C requires an elongating E2 (E2E; Ube2S in *H.sapiens*; Ubc1 in *S.cerevisiae*). The substrate is presented to the RING-E3 ligase APC/C by a coactivator (Cdc20 or Cdh1); modified after Primorac and Musacchio, 2013); (EM: electron microscopy).

But many more APC/C substrates have been identified so far, such as the spindle assembly factors HURP, NuSAP and Tpx2, the mitotic kinases Nek2A, Aurora A and Plk1, or the Cdk inhibitor p21 (Meyer and Rape, 2011; Zhang et al., 2014). The best-understood APC/C degrons are the so-called destruction box or D box (RxxL; Glotzer et al., 1991) and the KEN box (Pfleger and Kirschner, 2000). Other binding motifs have been described as well. In metazoans (with exception to organisms such as *Caenorhabditis elegans*) the best-characterized E2s for the APC/C are Ube2C and Ube2S (Meyer and Rape, 2011). E2s of the Ube2D family have also been reported to work with the APC/C *in vitro* (Aristarkhov et al., 1996; Yu et al., 1996). Ube2C catalyzes the initiation of polyubiquitin chain formation by modifying the substrate with single ubiquitin moieties or short ubiquitin chains (Figure 7C; Kirkpatrick et al., 2006). The K11 specific Ube2S elongates these chains rapidly allowing processive polyubiquitylation of APC/C substrates by concerted action of Ube2C and Ube2S (Garnett et al., 2009; Williamson et al., 2009a; Wu et al., 2010). Ube2C requires the presence of an interaction motif (IM) besides the canonical degron within a substrate for processive ubiquitylation (Williamson et al., 2011). As the functions of the APC/C during the cell cycle are of such great importance it is not surprising that its temporal activity is controlled by several intertwined mechanisms.

1.2.2. Regulation of the anaphase-promoting complex

The orderly destruction of substrates is crucial for accurate cell division. Therefore, inherent attributes of APC/C substrates differ and cause their sequential degradation, based on how processively they are ubiquitylated by the APC/C (Rape et al., 2006; Williamson et al., 2011). APC/C's coactivators and E2s are simultaneously substrates of the APC/C, which leads to changes of their

levels and autonomous regulation of APC/C activity (Peters, 2006; Williamson et al., 2009a).

Besides this intrinsic regulation, APC/C is controlled by many other cell cycle components. While the APC/C limits cyclin levels, Cdk activity itself influences APC/C activity. Cdk1 promotes formation of APC/C^{Cdc20} by phosphorylation of Cdc20 and other APC/C subunits (Barford, 2011). Cdk2/cyclin A phosphorylates Cdh1, which inhibits Cdh1 binding to the APC/C and creates a Cdh1 phosphodegron leading to its destruction by SCF^{Skp2} (Peters, 2006). The F-box protein Emi1 inhibits the APC/C by binding and altering its conformation; it can interact with both APC/C^{Cdc20} in S and G2 phases and APC/C^{Cdh1} at the G1/S transition (Zhang et al., 2014). Inhibition of APC/C^{Cdc20} in G2 by Emi1 is necessary for an increase in cyclin B levels and prevention of premature mitotic division. Inactivation of APC/C^{Cdh1} in G1 by Emi1 allows for accumulation of geminin and cyclin A to start and finish DNA replication. Emi1 is phosphorylated by Plk1 and subsequently degraded by SCF ^{β -TrCP} (Hansen et al., 2004; Moshe et al., 2004). Plk1 is at the same time a substrate of the APC/C and thereby closing the cycle (Lindon and Pines, 2004).

The most complex and probably most important inhibitor of the APC/C is the spindle assembly checkpoint (SAC), which ensures that transition into anaphase does not occur, until biorientation of chromosomes on the spindle is complete (Foley and Kapoor, 2013; Lara-Gonzalez et al., 2012). Hence, improperly attached kinetochores and a lack of tension activate the SAC. Kinetochores are large protein structures assembled on chromosomes at their centromeres, where microtubules emanating from the centrosomes attach to chromatids. The SAC is conserved in eukaryotes and includes budding uninhibited by benomyl 1 (Bub1), the serine/threonine kinases monopolar spindle protein 1 (Mps1) as well as the non-kinase components mitotic arrest deficient 1 (Mad1), Mad2, Bub3 and the probably pseudo-kinase Bub1-related 1 (BubR1; the human orthologue of yeast Mad3) (Figure 8A; Foley and Kapoor, 2013). Mps1-dependent phosphorylation leads to recruitment of Mad1 and Bub1 to unattached kinetochores (Figure 8B; Lara-Gonzalez et al., 2012).

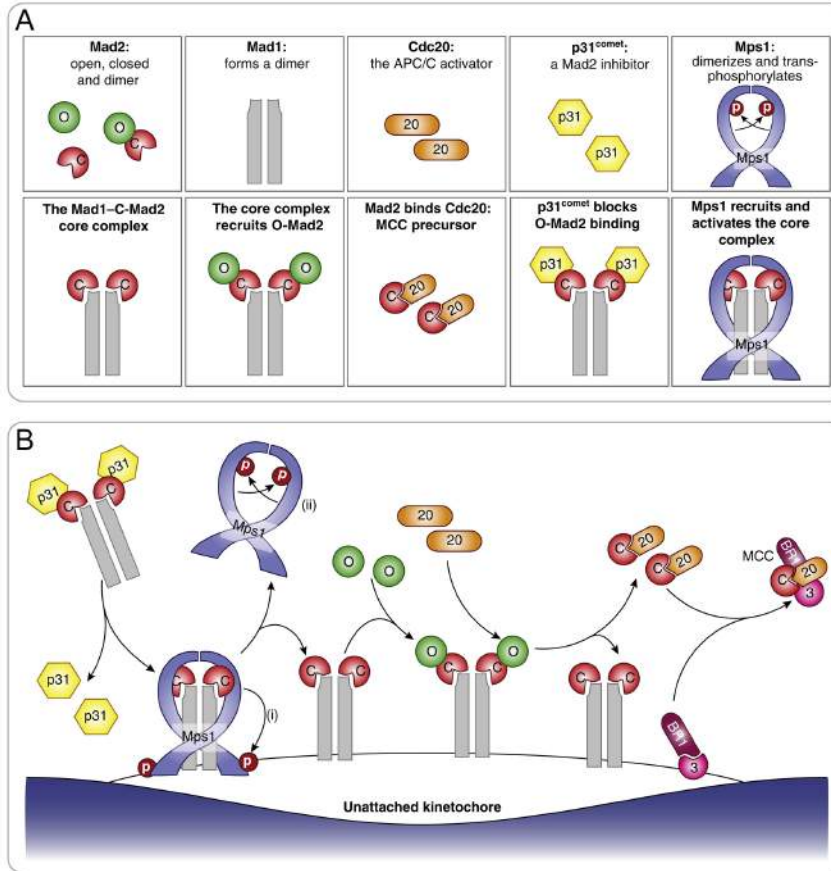


Figure 8: Regulation of the Mad2 template mechanism. A.

The key components, including Mad2 in the open (O) and closed (C) conformations, which can dimerise; Mad1, the kinetochore receptor for Mad2, is a ligand for C-Mad2; the APC/C activator Cdc20 is also a ligand for C-Mad2; p31^{comet} which binds C-Mad2 at the dimerisation interface; and Mps1, a protein kinase which can dimerise and transphosphorylate.

B. Mad2 binds Mad1 to form the Mad1–C-Mad2 core complex. In interphase, and when not bound to kinetochores, this core complex is ‘capped’ by p31^{comet}. Upon kinetochore binding, p31^{comet} is somehow released, allowing recruitment of O-Mad2 via Mad2 dimerisation. O-Mad2 is then ‘handed over’ to Cdc20, and in doing so closes to form a C-Mad2-Cdc20 subcomplex, which then binds BubR1-Bub3, thereby forming the MCC. Mps1 plays a two-step role: (i) upon mitotic entry, Mps1 activity is required to recruit Mad1–C-Mad2 to the kinetochore; (ii) Mps1 activity is also required continuously during mitosis to promote its own release from kinetochores and in doing so allow recruitment of O-Mad2 to Mad1–C-Mad2 (Lara-Gonzalez et al., 2012).

According to the “Mad2 template” model, Mad2 converts from an open cytosolic conformation to a closed conformation upon interaction with kinetochore-bound Mad1/Mad2 heterodimers (Mapelli and Musacchio, 2007). Cdc20 subsequently is bound by closed Mad2, which serves as a template for further conversion of open Mad2 into its closed state. Therefore closed Mad2/Cdc20 complexes would pose a diffuse signal explaining how a single unattached kinetochore can prolong metaphase until proper orientation is achieved.

Mad2/Cdc20 together with BubR1 and Bub3 build the mitotic checkpoint complex (MCC), which inhibits APC/C activity (Figure 9A; Primorac and Musacchio, 2013). Cdc20 still interacts with the APC/C, when it is sequestered into the MCC. But Cdc20 is not able to engage substrates, as its substrate binding site is shielded by BubR1 (Figure 9A) and it gets displaced from its usual position within the active APC/C^{Cdc20} complex (Figure 9B; Chao et al., 2012). Binding of MCC to Cdc20 also triggers autoubiquitylation of Cdc20 by the APC/C leading to Cdc20 degradation and further inactivation of the APC/C (Foley and Kapoor, 2013).

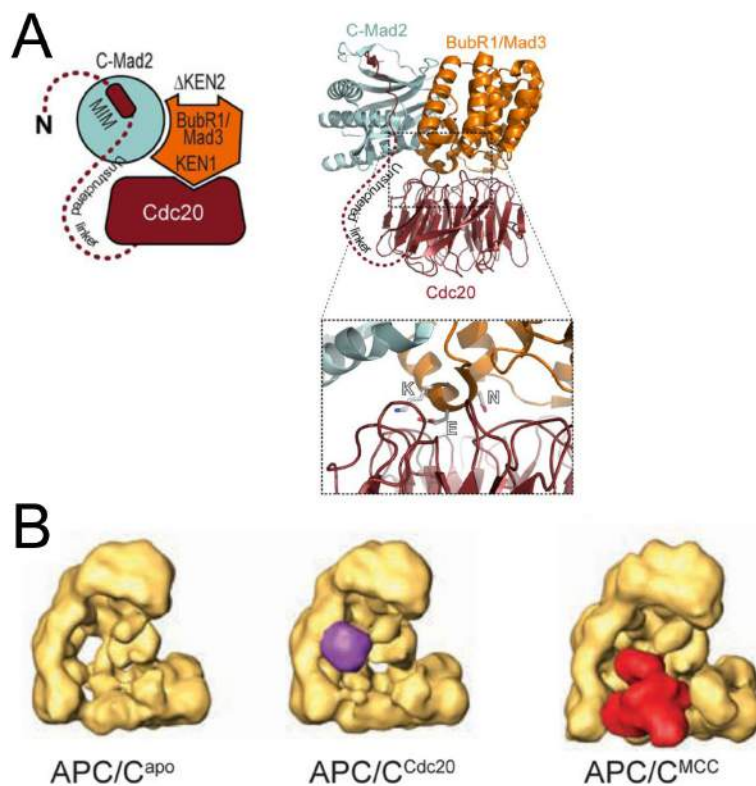


Figure 9: Organization of the MCC. **A.** Schematic organization and cartoon model of the Mad2–BubR1/Mad3–Cdc20 complex.

The KEN1 motif of BubR1/Mad3 binds on the Cdc20 propeller. Mad2 binds to the MIM motif and makes extensive contacts with BubR1/Mad3. The Cdc20 linker between the MIM and the entry point in the propeller was disordered in the crystal structure (Chao et al., 2012). The KEN2 motif of BubR1/Mad3 was not included in the crystallized construct. Cartoon model of the MCC

(PDB 4AEZ). An enlargement of the area boxed in C and showing the interaction of the KEN1 motif with Cdc20. The KEN motif lies within a folded region. **B.** A series of EM reconstructions showing APC/C devoid of coactivator or MCC subunits (APC/C^{apo}), APC/C^{Cdc20}, and APC/C^{MCC} (Herzog et al., 2009). The position and orientation of Cdc20 varies significantly in the presence of the MCC (Primorac and Musacchio, 2013).

After bi-oriented microtubule attachment to kinetochores is achieved, and proper tension is established, SAC components lose their kinetochore-localization and no longer propagate MCC formation. Cdc20 is released from MCC by APC/C-dependent autoubiquitylation or by p31^{comet} binding (Lara-Gonzalez et al., 2012). Some APC/C substrates, such as Nek2A, Cdc20, cyclin A and p21 seem to bind the APC/C even in the presence of SAC (Amador et al., 2007; den Elzen and Pines, 2001; Foley and Kapoor, 2013; Geley et al., 2001; Hames et al., 2001; Hayes et al., 2006). They therefore get targeted for proteasomal degradation in prometaphase. Nek2A and cyclin A bind to APC/C^{MCC} through motifs distinct from the canonical degrons. Nek2A binds through its C terminal MR residues similar to Cdc20, Cdh1 and APC10 with their C terminal IR tail (Hayes et al., 2006). Cyclin A interacts with APC/C^{MCC} via another binding partner (Wolthuis et al., 2008; van Zon et al., 2010). Other APC/C substrate such as HOXC10, E2F1 and RASSF1A seem to be degraded before transition into anaphase in the presence of an active SAC (Chow et al., 2012; Gabellini et al., 2003; Peart et al., 2010).

The best understood function of Nek2 activity is separation of centrosomes; the duplicated centrosomes are held together by a proteinaceous structure (O'Regan et al., 2007). Nek2 localizes to the centrosome and causes the dissolution of this proteinaceous structure in late G2, thus allowing separation of the centrosomes. Centrosome disjunction is necessary for the formation of the bipolar spindle apparatus. However, Nek2 has also been implicated in the SAC, chromatin condensation and NEBD (Fry et al., 2012). Why these substrates are degraded, before APC/C inhibition by the SAC is relieved, is not very well understood.

1.3. Aims

The APC/C provides a powerful model to test for functions of atypical chains. While yeast APC/C modifies its substrates with canonical K48-linked chains (Rodrigo-Brenni and Morgan, 2007), the metazoan APC/C assembles atypical K11-linked conjugates to drive proteasomal degradation and mitotic exit (Jin et al., 2008). The abundance of K11 linkages rises dramatically during mitosis, when the APC/C is active, and this boost in K11-linked chain formation is dependent on Ube2S (Matsumoto et al., 2010; Wickliffe et al., 2011a). This study aims to determine the physiological meaning of K11-linked chains. Therefore substrates only degraded in the presence of Ube2S and cellular processes relying on Ube2S activity are to be identified. The ubiquitylation of the identified substrates needs to be reconstituted and the reaction products are to be investigated in terms of binding to ubiquitin receptors and degradation by the proteasome regarding their ubiquitin topologies. For further characterization of the ubiquitylated substrates, tools need to be developed and implemented to compare the influence of different ubiquitin topologies on identical substrates.

2. Materials

2.1. Equipment and software

<i>Equipment</i>	<i>Provider</i>
Autoclave Consolidate MK II	Stills&Sterilizers
Automated fluorescence microscope ImageXpress Micro	Molecular Dynamics
Automatic film processor Konica SRX-101	Diagnostic Imaging Inc
Biosafety cabinet Logic	Labconco
Biosafety cabinet SterilGARD	The Baker Company
Blotting apparatus Mini Trans-Blot cell	Bio-Rad
Centrifuge Allegra X-30R	Beckman-Coulter
Centrifuge CL10	Thermo Scientific
Centrifuge RC-3B	Sorvall Instruments
Centrifuge Sorvall Legend Micro 21R	Thermo Electron Corp.
Centrifuge Sorvall Legend RT+, RC 3BP+, RC 6+	Thermo Scientific
Centrifuges 5415C, 5417C, 5415R, 5424	Eppendorf
Charged-couple device camera	Andor technology
Confocal microscope Revolution XD spinning disk	Olympus, Yokogawa
Customized electrophoresis apparatus Midi Maxi sized gels	R. Shadel Inc.
Epifluorescence microscope IX71	Olympus
Flow Cytometer EPICS XL	Beckman-Coulter
Gel dryer model 583	Bio-Rad
Heating block Dry bath	Fisher Scientific
Incubator AutoFlow Nu-5510	NuAire
Incubator innova 42	New Brunswick scientific
Incubator Isotemp	Fisher Scientific
Incubator NAPCO 8000 DH	Thermo Electron Corp.
Laser imaging device Pharos FX Plus	Bio-Rad
Laser imaging device Typhoon 9400	GE Healthcare
Microscope Invertoskop 40 C	Zeiss
Mini Protean II electrophoresis appartus	Bio-Rad
PCR machine MyCycler	Bio-Rad

Materials

PCR machine PTC-200	MJ Research
Power supple Power Pac HC	Bio-Rad
Power supply FisherBiotech™ Electrophoresis 1000V	Fisher Scientific
Power supply Model 494	Isco
qRT-PCR machine Mx3000P	Stratagene
Scanner V700 Photo	Epson
Sonicator Q700	Qsonica
Sonicator W185D	Ultrasonics Inc.
Spectrometer Ultraspec III	Pharmacia
Spectrophotometer NanoDrop 2000c	Thermo Scientific
Tank Blotting Unit TE62 Hoefer	Fisher Scientific
Thermomixer	Eppendorf
Vacuum pump FisherBiotech™ Vacuum System	Fisher Scientific
Vacuum pump HydroTech	Bio-Rad
Water bath Isotemp 220 and 202	Fisher Scientific
Water purifier Milli Q Synthesis A10	Millipore

<i>Software</i>	<i>Provider</i>
CellProfiler	Broad Institute
CellProfiler Analyst	Broad Institute
Epson Scan	Epson
ImageJ	National Institutes of Health
MetaMorph	Molecular Devices
MxPro	Stratagene
NanoDrop 2000	Thermo Scientific
Oligo Perfect Designer	Invitrogen
Photoshop	Adobe
Prism6	GraphPad Software
Protparam	expasy.org
PyMol	DeLano Scientific
Quantity One	Bio-Rad
QuickChange Primer Design	Agilent Technologies

Materials

Translate	expasy.org
Typhoon control	GE Healthcare
Word, PowerPoint, Excel	Microsoft
Zotero	zotero.org

2.2. Kits and other lab consumables

<i>Name</i>	<i>Provider</i>
10-MWCO columns	Millipore
30 MWCO Microcon filters	Millipore
Black polystyrene 384-Well Clear-Bottom Plates	Corning
Chromatography paper 0.35mm	Fisher Scientific
Dialysis cassettes	Thermo Scientific
Disposable chromatography columns 10 ml	Bio-Rad
Maxima SYBR Green qPCR Master Mixes	Fermentas
Nitrocellulose membrane 0.45 μ m	Bio-Rad or Fisher Scientific
QIAGEN Plasmid Plus Midi	Qiagen
QIAprep Spin Maxiprep	Qiagen
QIAprep Spin Miniprep	Qiagen
QIAquick Gel Extraction	Qiagen
RevertAid First Strand cDNA Synthesis	Fermentas
RNeasy Mini	Qiagen
Sterile filters 0.22-0.45 μ m	Millipore
Tissue culture dishes	VWR
TnT-Quick Coupled translation/transcription Systems	Promega
X-ray film	Kodak or PhenixResearch Products

2.3. Chemicals, reagents and enzymes

All chemicals, reagents and enzymes were purchased from Sigma-Aldrich, Fisher Scientific, National Diagnostics, BD Biosciences, Invitrogen, New England Biolabs (NEB), Pierce, Gibco, Gold Shield Chemical Corporation, HyClone, MP Biomedicals, Fermentas, Millipore, Apex, Roche, BostonBiochem, Boehringer, Qiagen, Agilent, Bio-Rad, Alfa Aesar and Ubiquitin-Proteasome Biotechnologies unless marked otherwise.

2.4. Cell lines

<i>Name</i>	<i>Provider</i>
Flp-In™ T-REx™ 293	Invitrogen
Flp-In™ T-REx™ 293-Ube2G2 ^{CTP}	this work
HEK 293T	Ann Fisher
HeLa	Michael Rape
HeLa S3	Michael Rape
HeLa-HR	this work
HeLa- ^{mcherry} H2B- ^{GFP} tubulin	Rebecca Heald
HeLa-Ube2G2 ^{CTP}	this work
HeLa-Ube2G2 ^{CTP}	this work
HeLa-Ube2S	(Wickliffe et al., 2011)
T98G	Ann Fisher
ES SF9, SF9	Ann Fisher
BL21(DE3) pRIL	Michael Rape
DH5 α	Michael Rape
XL1blue	Michael Rape

Michael Rape and Rebecca Heald – MCB, UC Berkeley

Ann Fisher – Manager of the tissue culture facility at UC Berkeley

2.5. DNA oligonucleotides for qRT-PCR

<i>Target gene</i>	<i>Right</i>	<i>Left</i>
actin	GCCGCCAGCTCACCATGGAT	CACCATCACGCCCTGGTGCC
ANAPC2	GTGTGCTTCCAAGTGGGGT	CCTTCAAGGACGAGAAGCTG
Cdc16	CCCACGGAGGTGAAATAATG	CATTGGTGATTCTGAAGCTTATATTG
Cdc20	TGTAATGGGGAGACCAGAGG	ATTCGCATCTGGAATGTGTG
cyclin B1	CAGATGTTTCCATTGGGCTT	GAACCTGAGCCAGAACCTGA
Nek2A	TCCCCACTGAAATGAACTTTCT	CAGCTTGCTAAAGGAACGGA
Pkn1	AGCTGCTGCTGTACCCCG	AGGACATGGCCAGCGAC
securin	GAGAGGCACTCCACTCAAGG	AAAGCTCTGTTCTGCCTCA
Ube2C	GCTGGTGACCTGCTTTGAGT	AGCAGGAGCTGATGACCCTC
Ube2S	GCCGCATACTCCTCGTAGTT	GTGCTCAAGAGGGACTGGAC

2.6. Plasmids

The human coding sequence of the listed genes was cloned into the respective vector backbone. If not otherwise specified the construct was made by the author.

Ube2G2 - NM_003343; OTU7B - BC072681; Nek2A - NM_002497; p97 - BC110913; FAF1 - BC004970; FAF2 - BC014001; p47 - BC002801; UBXD7 - NP_056377.1; SAKS1 - BC000902; S5A - BC002365; Usp37 - AM392929, TRAF6 - BC031052; gp78 - BC069197

<i>Vector</i>	<i>Insert</i>	<i>Restriction sites</i>	<i>Details</i>
pCDNA3.1(+) gro empty	no Insert	see vector map (Invitrogen)	
pCDNA3.1(+) gro empty	Ube2G2 ^{CTP}	BamHI/NotI	untagged, as tagged version is supposedly less active, generated by fusing full-length human Ube2G2 to residues 186-222 of Ube2S
pCDNA3.1(+) gro empty	Ube2G2 ^{CTP} -C89S	BamHI/NotI	see above and mutation of active site C89 to S
pCDNA3.1(+) gro empty	Ube2S	BamHI/NotI	untagged, as tagged version is supposedly less active (Wickliffe et al., 2011)
pCS2	Ub ^{K29R,K48R} -cyclin A	FseI/AscI	K29R, K48R mutations in ubiquitin inhibit UFD activity in reticulocyte lysate, ubiquitin is missing the C-terminal GG to inhibit DUB activity, ubiquitin is fused to cyclin A by the linker GSLVPRGSG (thrombin cleavage site)
pCS2	no Insert	originally Marc Kirschner lab, Harvard, MA	
pCS2	6xHis-ubiquitin ^{64TEV/Flag}	FseI/AscI	NLYFQGS DYKDDDDKKG was inserted after after E64

Materials

pCS2	6xHis ubiquitin ^{64TEV/Flag} -K11R,K48R,K63R	Fsel/Ascl	see above and mutation of K11, K48 and K63 to R
pCS2	6xHis ubiquitin-KO	Fsel/Ascl	all K in ubiquitin are mutated to R (Lingyan Jin)
pCS2	6xHis ubiquitin-K11	Fsel/Ascl	all K in ubiquitin are mutated to R except K11 (Jin et al., 2008)
pCS2	6xHis ubiquitin- K6,K11	Fsel/Ascl	all K in ubiquitin are mutated to R except K6 and K11
pCS2	cyclinA2	Fsel/Ascl	(Rape and Kirschner, 2004)
pCS2	Flag ubiquitin ^{53TEV}	Fsel/Ascl	SENLVYFQGS was inserted after G53
pCS2	Flag ubiquitin ^{53TEV} - K11R,K48R,K63R	Fsel/Ascl	see above and mutation of K11, K48 and K63 to R
pCS2	geminin	Fsel/Ascl	(Rape and Kirschner, 2004)
pCS2	geminin ^{ΔDBOX}	Fsel/Ascl	(Williamson et al., 2011)
pCS2	geminin ^{ΔIM}	Fsel/Ascl	(Williamson et al., 2011)
pCS2-HA	Cdh1	Fsel/Ascl	(Rape and Kirschner, 2004)
pCS2-HA	Nek2A ²⁷²⁻⁴⁴⁵	Fsel/Ascl	aa 272-445 were used meaning kinase domain is missing
pCS2	6xHis ubiquitin	Fsel/Ascl	(Jin et al., 2008)
pCS2	NuSAP	Fsel/Ascl	(Song and Rape, 2010)
pCS2	securin	Fsel/Ascl	(Rape and Kirschner, 2004)
pCS2	securin ^{ΔDBOX}	Fsel/Ascl	Olaf Stemmann
pCS2	Ube2C-C114S	Fsel/Ascl	(Rape and Kirschner, 2004)
pCS2	Ube2G2 ^{CTP}	Fsel/Ascl	see above
pCS2	Ube2G2 ^{CTP} -C89S	Fsel/Ascl	see above
pCS2	Ube2S-C95S	Fsel/Ascl	Katherine Wickliffe
pEGFP-C1	no Insert	see vector map (Clontech Laboratories)	
pET28a	6xHis ubiquitin	Ncol/Ascl	(Jin et al., 2008)
pET28a	6xHis ubiquitin ^{53TEV}	Ncol/Ascl	see above
pET28a	6xHis ubiquitin ^{53TEV} - K11R,K48R,K63R	Ncol/Ascl	see above
pET28a	6xHis ubiquitin ^{64TEV/Flag}	Ncol/Ascl	see above
pET28a	6xHis ubiquitin ^{64TEV/Flag} -K11R,K48R,K63R	Ncol/Ascl	see above
pET28a	6xHis ubiquitin ^{71TEV}	Ncol/Ascl	GSENLVYFQGS was inserted after L71
pET28a	6xHis ubiquitin-KO	Ncol/Ascl	Lingyan Jin
pET28a	6xHis ubiquitin-K11	Ncol/Ascl	see above
pET28a	6xHis ubiquitin-K11R	Ncol/Ascl	Lingyan Jin
pET28a	6xHis ubiquitin-K48	Ncol/Ascl	all K in ubiquitin are mutated to R except K48
pET28a	6xHis ubiquitin- K6,K11	Ncol/Ascl	see above
pET28a	6xHis ubiquitin-K6	Ncol/Ascl	all K in ubiquitin are mutated to R except K6
pET28a-His	Cezanne (OTU7B)	Fsel/Ascl	
pET28a-His	cyclin A2	Fsel/Ascl	(Rape et al., 2006)
pET28a-His	Emi1 ²⁹⁹⁻⁴⁴⁷	Fsel/Ascl	(Rape et al., 2006)
pET28a-His	FAF1	Fsel/Ascl	
pET28a-His	FAF2	Fsel/Ascl	
pET28a-His	Nek2A ²⁷²⁻⁴⁴⁵	Fsel/Ascl	see above
pET28a-His	p47	Fsel/Ascl	
pET28a-His	SAKS1	Fsel/Ascl	
pET28a-His	securin	Fsel/Ascl	(Rape and Kirschner, 2004)
pET28a-His	Ube2V1	Fsel/Ascl	Lingyan Jin
pET28a-His	UBXD7	Fsel/Ascl	
pET28a	Ub-cyclin A ^{6xHis}	Ncol/Ascl	see above
pET28a	Ub-cyclin A ^{HA/6xHis}	Ncol/Ascl	see above

Materials

pET28a	Ub-Ub-cyclin A ^{HA/6xHis}	NcoI/Ascl	ubiquitin is missing C-terminal GG to inhibit DUB activity, Ub is fused by the linker GSLVPRGSG (thrombin cleavage site) to cyclin A, ubiquitin is fused to ubiquitin via the linker GSEDLYFQSG (TEV cleavage site)
pET28a	Ub-K0-cyclin A ^{HA/6xHis}	NcoI/Ascl	all K in ubiquitin are mutated to R, otherwise see above
pET28a	Ub-K11R-cyclin A ^{HA/6xHis}	NcoI/Ascl	K11 in ubiquitin is mutated to R, otherwise see above
pET28a	Ub-K11R-Ub-cyclin A ^{HA/6xHis}	NcoI/Ascl	K11 in the distal ubiquitin is mutated to R, otherwise see above
pET28a	Ube2C ^{6xHis}	NcoI/Ascl	(Jin et al., 2008)
pET28a	Ube2C ^{6xHis} -C114S	NcoI/Ascl	(Jin et al., 2008)
pET28a	Ube2G2 ^{6xHis}	NcoI/Ascl	
pET28a	Ube2G2 ^{CTP-6xHis}	NcoI/Ascl	see above
pET28a	Ube2G2 ^{CTP-6xHis} - C89S	NcoI/Ascl	see above
pET28a	Ube2G2 ^{CTP-6xHis} - Δacidic loop	NcoI/Ascl	aa A95-A107 of Ube2G2 are deleted, otherwise see above
pET28a	Ube2G2 ^{CTP-6xHis} - I92E	NcoI/Ascl	see above and mutation of catalytic site I92E
pET28a	Ube2G2 ^{CTP-6xHis} - K118A	NcoI/Ascl	see above and mutation of RING interacting network residue K118 to A
pET28a	Ube2G2 ^{CTP-6xHis} - L66D	NcoI/Ascl	see above and RING interaction site L66 to D
pET28a	Ube2G2 ^{CTP-6xHis} - Q114A	NcoI/Ascl	see above and mutation of RING interacting network residue Q114 to A
pET28a	Ube2G2 ^{CTP-6xHis} - V113E	NcoI/Ascl	see above and mutation of RING interacting network residue V113 to E
pET28a	Ube2N ^{6xHis}	NcoI/Ascl	cut and paste from pET28a-His-F/A Michael Rape
pET28a	Ube2S ^{6xHis}	NcoI/Ascl	(Wickliffe et al., 2011)
pET30a(+)	no Insert	see vector map invitrogen	
pET30a(+)	Ub-Ub-Ub- CycA ^{HA/6xHis}	NdeI/NotI	synthetically made Ub-Ub-Ub sequence is listed below (Life Technologies)
pET30a(+)	Ub-Ub-Ub- Nek2A ^{272-445-HA/6xHis}	NdeI/NotI	see above
pFastBac	Ube1	Sall/HindIII	(Wickliffe et al., 2011)
pFastBac	Usp37	BamHI/KpnI	
pFastBac	TRAF6	Sall/NotI	
pGEX	gp78C ^{6xHis}	FseI/Ascl	cytosolic domain of gp78, residues 309–643
pGEX	HHR23A; UBA domains		(Raasi et al., 2004)
pMAL-TEV	CTP ^{6xHis}	FseI/Ascl	residues 186-222 of Ube2S
pMAL-TEV	HHR23A ^{6xHis}	FseI/Ascl	Michael Rape
pMAL-TEV	p97 ^{6xHis}	FseI/Ascl	
pMAL-TEV	S5a	FseI/Ascl	
pMAL-TEV	Ube2G2	FseI/Ascl	
pMAL-TEV	Ube2G2 ^{CTP}	FseI/Ascl	see above
pMAL-TEV	TEV ^{6xHis}	FseI/Ascl	Katherine Wickliffe

Michael Rape – MCB, UC Berkeley

Olaf Stemmann – Department of Genetics, University of Bayreuth

Katherine Wickliffe and Lingyan Jin – former member of the Rape Lab

Materials

Ubiquitin sequence:

```
ATGCAGATTTTCGTGAAAACCCTTACGGGGAAGACCATCACCTCGAGGTTGAACCCTCGGATACGATA
GAAAATGTAAAGGCCAAAGATCCAGGATAAGGAAGGAATTCCTCCTGATCAGCAGAGACTGATCTTTGCT
GGCAAGCAGCTGGAAGATGGACGTACTTTGTCTGACTACAATATTCAAAAGGAGTCTACTCTTCATCTT
GTGTTGAGACTTCGTGGTGGTTAA
```

Triple ubiquitin sequence with restriction sites underlined:

```
ATGCAGATCTTTGTTAAAACCCTGACCGGTAACCATTACCCTGGAAGTTGAACCGAGCGATACCATT
GAAAATGTGAAAGCCAAAATCCAGGACAAAAGAAGGTATTCGCCTGATCAGCAGCGTCTGATTTTTGCA
GGTAAACAGCTGGAAGATGGTCGTACCCTGAGCGATTATAACATTCAGAAAGAAAAGCACCTGCATCTG
GTTCTGCGTCTGCGTGGTACCGCACAGATTTTTGTGAAAACACTGACAGGCAAAAACAATCACACTGGAA
GTAGAGCCGTGAGATAACAATCGAAAACGTCAAAGCGAAAATTCAAGATAAAGAGGGCATCCCTCCGGA
TCAGCAACGCCTGATCTTTGCTGGCAAACAACCTGGAAGATGGACGCACACTGTCAGATTACAATATCCA
GAAAGAATCAACACTGCACCTGGTGCTGCGCCTGCGGGTCGACGCCAGATTTTCGTAAAACGCTGA
CGGGAAAAACGATTACACTGGAAGTGAACCTCCGATACGATTGAGAACGTTAAAGCAAAAATCCAGG
ATAAAGAGGGAATTCACCGGACCAACAGCGGCTGATCTTTGCCGAAAACAGCTGGAAGATGGCCGT
ACGCTGTCTGACTATAACATCCAAAAAGAGTCTACGCTGCATCTGGTACTGCGCCTGCGTGGATCC
```

2.7. Peptides

<i>Name</i>	<i>Sequence</i>	<i>Provider</i>
3xFLAG	(MDYKDHDGDYKDHDIDYKDDDDK) ₃	Sigma
3xHA	(YPYDVPDYA) ₃	Biosynthesis Inc
biotin-CTP	biotin-KKHAGERDKKLAAKKKTDKKRALRRL	Elim Biopharmaceuticals
G2BR	SADERQRMLVQRKDELLQQARKRFLNKS	Elim Biopharmaceuticals

2.8. Antibodies

Antibody dilutions are provided for western blot analysis unless marked for immunofluorescence (IF).

<i>Target</i>	<i>Species</i>	<i>Dilution</i>	<i>Source</i>	<i>ID</i>
α -tubulin	mouse	1:5000 (WB)/1:200 (IF)	Calbiochem	DM1A
APC4	rabbit	1:2000	Santa Cruz	H-298
APC5	rabbit	1:3000	Santa Cruz	H-300
APC7	rabbit	1:4000	Santa Cruz	H-300
Aurora A	rabbit	1:2000	Abcam	ab12875
β -actin	mouse	1:10000	MP Biomedicals	3G4-F9

Materials

BubR1	mouse	1:5000	Millipore	8G1
CD3	mouse	IP only	Santa Cruz	C415.9A
Cdc16/APC6	rabbit	1:1000	Santa Cruz	H-175
Cdc20	rabbit	1:2000	Santa Cruz	H-300
Cdc27/APC3	mouse	1:2000	Santa Cruz	AF3.1
cyclin A2	rabbit	1:2000	Santa Cruz	C-19
cyclin B1	rabbit	1:2000	Santa Cruz	H-20
FLAG	rabbit	1:3000	Sigma	F7425
geminin	rabbit	1:2000	Santa Cruz	FL-209
GFP	rabbit	1:1000	Achim Werner	
human influenza hemagglutinin (HA)	rabbit	1:3000	Cell Signalling	C29F4
HURP	rabbit	1:3000	Bethyl Laboratories	A300-853A
IgG	mouse	IP only	Santa Cruz	2027
K11	human	1:1000	(Matsumoto et al., 2010)	
K48	human	1:4000	(Newton et al., 2008)	
Kif18A	rabbit	1:2000	Abcam	ab72417
Mad2	mouse	1:2000	BD Biosciences	48/Mad2
Nek2A	mouse	1:3000	BD Biosciences	20/Nek2
NuSAP	rabbit	1:3000	Proteintech	12024-1-AP
p21	rabbit	1:1000	Santa Cruz	C-19
phospho-Histone H3 (Ser10)	rabbit	1:2000	Millipore	06-570
Tpx2	rabbit	1:300 (IF)	Novus Biologicals	NB500-179
Ube2G2	mouse	1:1000	BostonBiochem	AB-230
Ube2S	rabbit	1:5000	Novus Biologicals	22570002
ubiquitin	rabbit	1:50	Santa Cruz	P4D1
<i>HRP-coupled secondary</i>				
human	goat	1:10000	Jackson ImmunoResearch	109-486-098
mouse	goat	1:5000	Sigma	A5906
rabbit	goat	1:5000	Sigma	A6154
<i>Fluorophore-coupled secondary</i>				
mouse (Alexa 568)	goat	1:500 (IF)	Invitrogen	A-11004
rabbit (Alexa 488)	goat	1:500 (IF)	Invitrogen	A-11034

2.9. RNA oligonucleotide sequences for siRNA

Custom-made small interfering RNAs were ordered with UU overhangs as duplexes in lyophilized form. They were resuspended in RNase-free water according to the manufacturer's guidelines and stored in small aliquots at 20 μ M at -80°C.

<i>Target gene</i>	<i>Antisense (5'→3')</i>
Control (Dharmacon)	UAGCGACUAAACACAUCAA
Ube2C (Dharmacon)	GUAUAGGACUCUUUAUCUU
Ube2S (Dharmacon)	GGCACUGGGACCUGGAUUU
Ube2S (Qiagen)	CCCGAUGGCAUCAAGGUCU
	GAAGAUUGGUUUCGACCCA
p31 ^{comet} smartpool (Dharmacon)	UUUAAAGGCUUCCGCGAGU
	GGUAUGAGAAGUCCGAAGA
	GGACACUAGUACCGCGAGU

3. Methods

3.1. Molecular biology techniques

3.1.1. Preparation of chemically competent bacteria

Chemically competent *E.coli* were prepared using a rubidium chloride based protocol from a 3L growing culture in LB (1% (w/v) tryptone, 1% (w/v) NaCl, 0.5% yeast extract) with an optical density of 0.3 at 600nm. Bacteria were incubated on ice for 10min and harvested by centrifugation at 5000g and 4°C. The cell pellet was resuspended in 90ml ice-cold sterile TFB-I buffer (30mM potassium acetate, 100mM RbCl₂, 10mM CaCl₂, 50mM MnCl₂, 15% (v/v) glycerol, pH6.5) followed by incubation on ice for 2 h. Cells were again collected at 5000g and 4°C, resuspended in 18ml of sterile, cold TFB-II buffer (10mM 3-(N-morpholino)propanesulfonic acid (MOPS), 75mM CaCl₂, 10mM RbCl₂, 15% (v/v) glycerol, pH6.5), flash frozen as 200µl aliquots in liquid nitrogen, and stored at -80°C.

3.1.2. Transformation of chemically competent *E.coli*

Chemically competent *E.coli* were thawed on ice and incubated with 0.1-1µg plasmid DNA for 30min on ice. Incorporation of the DNA was achieved by heat-shock at 42°C for 60s, followed by brief incubation on ice. To recover the transformed bacteria, they were supplemented with 250µl LB and incubated in a thermomixer (Eppendorf) at 37°C for 1h in case of ampicillin- and 2h in case of kanamycin- or chloramphenicol-resistance. Transformed cells were plated on LB agar plates (1% (w/v) tryptone, 1% (w/v) NaCl, 0.5% yeast extract, 1.5% (w/v) agar) supplemented with the respective antibiotic for the transformed plasmid. Final concentrations of antibiotics in plates or in liquid cultures were 34µg/ml chloramphenicol, 0.1mg/ml ampicillin or 25µg/ml kanamycin.

3.1.3. Isolation of plasmid DNA from bacteria

Single colonies or suspensions of transformed cells were used to inoculate LB overnight cultures (5ml for Mini, 50ml for Midi, 500ml for Maxi). The next day cells were harvested by centrifugation at 4000g for 10min. The DNA was isolated from the cells using kits according to the manufacturer's instructions (Qiagen). If sterile DNA was required for tissue culture, the DNA containing solution was sterile filtered with 0.22 μ m filters (Millipore). To assess the DNA's concentration and purity, its optical density (OD) was measured at 260nm and 280nm using a NanoDrop spectrophotometer (Thermo Scientific). Elution occurred in 50 μ l, 200 μ l or 600 μ l for Mini, Midi or Maxi preparations.

3.1.4. Cloning

The enzymes and buffer systems of New England Biolabs (NEB) were used for DNA restrictions. Reaction conditions were chosen according to the manufacturer's instructions (NEB). To create linearized vector for cloning, 5 μ g DNA was digested in a volume of 20 μ L with 2-10 units of enzyme at 37°C for 1-2h; to test for successful cloning 0.5-1 μ g DNA in a volume of 10 μ L was digested with 1-5 units of enzyme for 1h.

FastAP alkaline phosphatase (Fisher) catalyzes the removal of 5'phosphate from DNA to reduce the amount of linearized vector religating without annealing to the PCR fragment, as the phosphate group is required by T4 ligase for successful ligation. The cut DNA was incubated with the phosphatase (1 U/ μ g DNA) for 30min at 37°C and the phosphatase was subsequently heat inactivated by an incubation at 75°C for 5min.

DNA fragments of different sizes were separated by agarose gel electrophoresis. Depending on the fragment size, 0.5-2% (w/v) agarose, 0.005% (v/v) ethidiumbromide (Fisher), TAE (40mM Tris, 20mM acetic acid, and 1mM EDTA pH8.0) gels were used to separate DNA samples supplemented with 6x DNA loading dye (NEB) at 120V and visualized with UV light of 365nm. Desired DNA

was extracted from gel pieces using the QIAquick Gel Extraction (Qiagen) according to the manufacturer's instructions. DNA was typically eluted in 30 μ L. Ligations were performed using 50-100ng of vector in a molar vector to insert ratio ranging from 1:3 to 1:9. Reactions were performed in a total volume of 10 μ L containing 400 units T4 DNA ligase (NEB) and 1x ligation buffer (NEB). The ligation reaction was typically performed at 23°C for 1h and half the reaction was transformed into DH5 α cells.

Amplification of specific DNA fragments using 5'- and 3'-flanking primers was performed by polymerase chain reaction (PCR) according to Mullis et al., 1986. Reactions were set up in a final volume of 50 μ L with 100ng template, 25 pmol of each forward and reverse primer, 1x Pfu buffer (Agilent), 500 μ M dNTP-mix (Fermentas), 2 units Taq polymerase (NEB) and 1 unit PfuUltra polymerase (Agilent). Addition of up to 10% DMSO (Sigma) for GC-rich regions in the DNA was optional. Primers were designed using Oligo Perfect Designer (Invitrogen). An elongation time of 30s/kb was generally assumed. PCR reactions were carried out by denaturing the DNA template at 94°C for 2min, going through 25-30 cycles of 94°C for 30s, 42-55°C for 30s and 68°C for 30s/kb, and final elongation at 68°C for 10min.

To fuse two DNA fragments by PCR, reactions were performed to first amplify the two fragments individually and purify them subsequently. Overlapping sequences were introduced in the first round of PCR via the respective primers. In a second PCR the two synthesized fragments with overlapping sequences are mixed and amplified using only the two distal primers of the fused construct.

Site-directed mutagenesis of plasmids was performed according to the QuickChange Site-Directed Mutagenesis Protocol from Stratagene. QuickChange Primer Design (Agilent) was used to design mutagenesis primers. Mutagenesis PCR reactions were normally performed in 25 μ L final volume containing 50ng plasmid DNA, 7.5 pmol of forward and reverse primer, 0.4mM dNTP-mix (Fermentas), 1x Pfu buffer (Agilent) and 2 units PfuUltra DNA polymerase (Agilent). Mutagenesis PCR reactions were carried out by denaturing the DNA template at 94°C for 2min, going through 18 cycles of 94°C for 30s, 53°C for

1min and 68°C for 12min. The reaction products are incubated with 5 units DpnI (NEB) for 1h at 37°C afterwards to cleave parental DNA. 5 μ L of the product is transformed into XL1blue cells.

All plasmids constructed via these PCR reactions were verified by DNA sequencing carried out at the sequencing facility in the Department of Molecular and Cell Biology, University of California, Berkeley or at Quintara Biosciences in Richmond, CA.

3.1.5. Real Time quantitative Reverse Transcription PCR

Real Time quantitative Reverse Transcription PCR (qRT-PCR) measures PCR product accumulation through a dual-labeled fluorogenic probe to quantify gene copies (Heid et al., 1996). The reaction was carried out using total RNA as template to assess the quantities of certain genes in HeLa cells. Total RNA was isolated using a RNeasy Mini kit (Qiagen) according to the manufacturer's instructions. For the synthesis of first strand cDNA, 2 μ g isolated RNA was used with the RevertAid First Strand cDNA Synthesis kit (Fermentas) following the manufacturer's instructions. Then, 0.5 μ l of the reaction product were used with Maxima SYBR Green qPCR Master Mix according to the manufacturer's instructions (Thermo). Reactions were carried out using a qRT-PCR machine Mx3000P (Stratagene) with a 95°C-10min initial denaturation step, 40 cycles of 30s-95°C, 60s-55°C, 60s-72°C followed by 1min of 95°C, 30s of 55°C and 30s of 95°C. Analysis was carried out relative to actin mRNA copies in the cell.

3.2. Biochemical techniques

3.2.1. Measurement of protein concentration

Protein concentrations of solutions were determined via measurement of absorption at 280nm using a NanoDrop. The aromatic amino acids phenylalanine, tyrosine, and disulfide bonds lead to absorption of energy at 280nm. Proteins were kept under reducing conditions using 2mM dithiothreitol

(DTT) supposedly preventing the formation of disulfide bonds under these conditions. Extinction coefficient and MW of a protein based on its amino acid sequence were determined using an algorithm (<http://web.expasy.org/protparam>) for calculation of protein concentration based on the absorption at 280nm. Absorption at 280nm was also used for normalization of cell extracts to equalize cell lysate samples for western blot analysis.

3.2.2. Sodium dodecyl sulfate (SDS) polyacrylamide gel electrophoresis (SDS PAGE)

Separation of proteins was performed by SDS PAGE (Laemmli, 1970). Different gels with a range of 8% to 20% acrylamide were used in a Mini, Midi or Maxi format. Acrylamide solutions with distinct acrylamide to bisacrylamide ratios were used, as a ratio of 29:1 was beneficial for resolution of small proteins like ubiquitin compared to a 37.5:1 ratio generally used for larger protein separation. For resolving gels the desired percentage (w/v) of polyacrylamide solutions in 0.2M Tris-HCl pH8.8, 0.05% (w/v) SDS were prepared. Polymerization was started by adding 0.1% (w/v) ammonium persulfate (APS) and 0.02% (v/v) tetramethylethylenediamine (TEMED). The solutions were filled into the casting chambers and overlaid with 2-propanol to even the surface. After polymerization of the separating gel, 2-propanol was removed and the stacking gel consisting of 5% (w/v) polyacrylamide, 125mM Tris-HCl pH6.8, 0.1% (w/v) SDS, 0.1% (w/v) APS and 0.1% (v/v) TEMED was poured on top of the separation gel. After insertion of combs gels were allowed to polymerize. The gels were run with SDS-glycine (25mM Tris Base, 192 mM glycine, 0.1% (w/v) SDS) or SDS-tricine (100mM Tris Base, 100mM tricine, 0.1% (w/v) SDS) running buffer at 150V for Mini, 250V for Midi or 300V for Maxi gels at room temperature. Tricine running buffer was used for separation of small ubiquitin fragments. Before loading, samples were supplemented with SDS-loading buffer (62.5mM Tris-HCl pH6.8, 2% (w/v) SDS, 0.1% (w/v) bromophenol blue, 25% glycerol, 5% (v/v) β -

mercaptoethanol) and boiled at 95 °C for a few minutes. Prestained molecular markers (Bio-Rad) were used as standards. Separated proteins were stained by Coomassie, transferred onto a nitrocellulose membrane or dried onto chromatography paper (Fisher) for autoradiography (see below).

3.2.3. Coomassie staining of gels after SDS PAGE

Separated proteins were visualized by their binding to the Coomassie Brilliant Blue R-250, short Coomassie. After SDS PAGE the disassembled gel was incubated in Coomassie staining solution for 1-24 hours (10% (v/v) ethanol, 10% (v/v) acetic acid, 0.25% (w/v) Coomassie). Next the gel was washed with destaining solution (10% (v/v) acetic acid) until excess dye was removed. Last the gel was scanned for documentation. If higher detection sensitivity was needed, gels were stained with a different method, as described previously (Neuhoff et al., 1985). In short, gels were incubated in a fixing solution (40% (v/v) ethanol, 10% (v/v) acetic acid) for 20 minutes, rehydrated in water and stained with another Coomassie solution (1.6% (v/v) ortho-phosphoric acid, 8% (w/v) ammonium sulfate, 4% (v/v) methanol and 0.08% Coomassie G-250). Excess dye was washed off with water and the gel was scanned subsequently.

3.2.4. Western blot analysis

Proteins separated by SDS PAGE were transferred onto a nitrocellulose membrane (Bio-Rad or Fisher) according to Stott et al., 1985. After SDS-PAGE, the separating gel, the membrane and two chromatography papers were immersed in blotting buffer (25mM Tris, 192mM glycine, 20% (v/v) methanol). A sandwich, consisting of a chromatography paper, a nitrocellulose membrane, a gel and another chromatography paper was assembled between the two electrodes of a tank transfer blotting apparatus with the gel facing the negative and the membrane the positive electrode and submerged in blotting buffer. The

standard blotting conditions were 75V for two hours at 4°C regarding Mini and 80V for four hours regarding Midi or Maxi gels at 4°C. For ubiquitin linkage specific western blots the conditions were 30V for 2h at 23°C. Transferred proteins were visualized by staining with ATX Ponceau S (Sigma) for one minute before excess dye was removed by washing with water. The stained membrane was optionally scanned for documentation.

Membranes were transferred into 5% (w/v) dry milk (Safeway, Alco) in PBST or TBST (PBS (137mM NaCl, 2.7mM KCl, 10mM Na₂HPO₄, 1.8mM KH₂PO₄, pH7.4) or TBS (50mM Tris-HCl, pH 7.5, 150mM NaCl) with 0.1% (v/v) Triton X-100). PBST was only used for ubiquitin linkage antibodies. The primary antibodies were added and incubated with the membranes at 4°C for 18 hours. Membranes were washed in PBST or TBST three times and incubated with secondary antibody coupled to horseradish peroxidase (HRP) in 5% (w/v) dry milk in PBST or TBST. After incubation at 23°C for one hour the membranes were washed three times with PBST or TBST. The western blots were coated with chemiluminescent HRP substrate solution (Millipore) for one minute and the resulting chemiluminescent signal was detected with X-ray films (Kodak or PhenixResearch Products), which were developed in an automatic film processor (Diagnostic Imaging Inc).

3.2.5. Autoradiography

To detect proteins by autoradiography they were labeled with a radioactive isotope. Master mix of the SP6 quick coupled transcription/translation system (IVT/T, Promega) supplemented with about 0.1mCi/ml L-Methionine, [³⁵S] and L-Cysteine, [³⁵S] (MP Biomedicals) was added to 2μg plasmid DNA encoding for the desired protein under control of a SP6 promotor with a final volume of about 27μl. After incubation for 1.5-2h at 30°C the ³⁵S-radiolabeled protein was used for binding or ubiquitylation experiments *in vitro*. The samples were analyzed by SDS PAGE and the resulting gel was placed in fixing solution (20% (v/v) ethanol,

6% (v/v) acetic acid) for 0.5-18h or stained with Coomassie. The fixed gel was subsequently placed between a wet chromatography paper and plastic wrap, and placed in a vacuum dryer (Bio-Rad). The gel was dried for 0.5-2h at 72°C using a vacuum pump (Bio-Rad or Fisher). After exposing the gel to a phosphorimager screen (Bio-Rad or Molecular Dynamics) for 2-96h the signal was scanned with a laser imaging device (Typhoon scanner from GE Healthcare or Pharos from Bio-Rad). Stained gels were also documented with a regular scanner.

3.2.6. Isolation of recombinant proteins from bacteria

For protein expression BL21(DE3) pRIL *E.coli* cells were transformed with the plasmid encoding the desired protein by heat shock. The resulting cells were grown for 18h at 37°C in LB in the presence of 34µg/ml chloramphenicol and 0.1mg/ml ampicillin (pMAL, pGEX) or 25µg/ml kanamycin (pET28a, pET30a) depending on the used plasmid. These initial cultures were diluted 1:150 into LB containing appropriate antibiotics and incubated at 37°C until an OD of 0.5 at 600nm was reached. In the presence of 0.5mM isopropyl β-D-1-thiogalactopyranoside (IPTG) further incubation was performed at 23°C for 18h. The consequent steps were performed at 4°C and all used solution were cooled to a temperature of 4°C. Bacterial cultures expressing His-tagged proteins were centrifuged at 4000g for 10min and pellets were resuspended in lysis buffer (50mM NaH₂PO₄, 500mM NaCl, 10mM imidazole, pH8.0). 200mg/ml lysozyme (Sigma) was added and cells were incubated for 20min. Resuspensions were sonicated twice for 2min. The resulting lysates were supplemented with 0.1% (v/v) Triton X-100 and cleared by centrifugation at 12500rpm for 30min. In general for a 1.5l culture 0.5-1ml NiNTA slurry was used. The slurry was washed twice with lysis buffer by centrifugation at 3000rpm. Beads were added to cleared lysates and incubated for 3-4h. NiNTA agarose was pelleted at 3000rpm and washed twice with 20-fold bead volume of lysis buffer plus 0.1% (v/v) Triton X-100 and placed in 10ml column. After two more washes with lysis buffer, proteins

were eluted in 200mM imidazole, 50mM NaH₂PO₄, 500mM NaCl, pH8.0 and dialyzed overnight into PBS with 2mM DTT. The protein solution was aliquoted and shock frozen in liquid nitrogen.

Maltose binding protein (MBP) tagged proteins were isolated according to the steps above with a different lysis buffer (20mM Tris, pH 7.5, 500mM NaCl), amylose resin (NEB) instead of NiNTA agarose and elution into 20mM maltose, 20mM Tris, pH 7.5, 500mM NaCl.

Following the steps above Glutathione-S-transferase (GST) tagged proteins were purified with Glutathione Sepharose 4B (GE Healthcare) instead of NiNTA agarose with lysis in 50mM Tris, pH7.4, 250mM NaCl, 5mM EDTA. GST-tagged proteins were eluted with 20mM glutathione, 50mM Tris, pH7.4, 250mM NaCl, 5mM EDTA.

3.2.7. Isolation of recombinant proteins from insect cells

To introduce the DNA encoding the recombinant protein of interest into insect cells baculoviruses were used. Generation of baculoviruses followed the instructions of the Bac-to-Bac Baculovirus Expression system (Invitrogen, (Luckow et al., 1993)). In short, the pFastBac donor plasmid was transformed into DH10Bac *E.coli* cells, which contain the bacmid with a mini *attTn7* target site and the helper plasmid. The mini Tn7 element (containing the sequence of the recombinant protein) on the pFastBac donor plasmid transposes to the mini-*attTn7* site on the bacmid in the presence of transposition proteins provided by the helper plasmid. Colonies positive for the introduced DNA were distinguished from those containing unaltered bacmids by blue-white screening (insertion of the mini Tn7 element into the bacmid disrupts the *lacZ* gene). High molecular weight DNA was then isolated from positive clones via the mini prep kit. The bacmid DNA was transfected into ES SF9 (Expression Systems) cells with CellfectinII (Invitrogen) according to the manufacturer's guidelines. After 72 h cells showed signs of late viral infection, indicating virus budding and release into the media.

The medium of the infected cells (P1 viral stock) was harvested and cleared from cell debris via centrifugation. For virus titer amplification, P2 and P3 viral stocks were generated by using the P1 (or P2) viral stock in a 1:10 dilution for infection of ES SF9 cells for 72 h followed by collection of the medium as described above. Viral stocks (in general P2) were stored protected from light at 4°C (for short term storage) or flash frozen in liquid nitrogen and stored at -80°C (for long term storage). For isolation of protein from ES SF9 cells generally 1-2l of ES SF9 cells were infected with fresh P3 for 72h and harvested at 1500rpm for 5min. After resuspension in NP40 lysis buffer (20mM Tris-HCl pH7.5, 150mM NaCl, 1% (v/v) Nonident P-40 (NP40)) cells were further broken apart with a dounce homogenizer. The lysate was cleared at 12500rpm for 30min and incubated with NiNTA agarose for 3-4h. The resin was washed with 20mM Tris-HCl pH7.5, 500mM NaCl, 20mM imidazole, 10% (v/v) glycerol first with, and later without 0.5% (v/v) NP40. Protein was eluted with 20mM Tris-HCl pH7.5, 10% (v/v) glycerol and 250mM imidazole, and dialyzed into PBS, 2mM DTT, 10% (v/v) glycerol.

3.2.8. *In vitro* APC/C binding assay

Binding of radiolabeled APC/C-subunits to MBP-tagged proteins was performed as published (Wickliffe et al., 2011a). For binding of APC/C-subunits to biotinylated CTP, ³⁵S-labeled APC/C-subunits were synthesized by IVT/T. 1mg biotin-CTP was immobilized on streptavidin-agarose (Thermo) in 50mM HEPES, pH 7.5, 1.5mM MgCl₂, 5mM KCl, 150mM NaCl, 0.1% Triton, and 100mg/ml BSA for 2h at 4°C. ³⁵S-labeled subunits were added to the beads and incubated for 3h at 4°C. After extensive washes, bound proteins were eluted with SDS sample buffer, separated by SDS-PAGE, and analyzed by autoradiography.

3.2.9. *In vitro* ubiquitylation of recombinant or radiolabeled substrates with immunoprecipitated APC/C

³⁵S-labeled substrates were synthesized by IVT/T as described above. Ub^{K29R,K48R}-cyclin A was synthesized to inhibit the UFD-pathway, which is active in reticulocyte lysate as part of the IVT/T system. To purify ³⁵S-Ub^{K29R,K48R}-cyclin A, HisCdk2 was bound to NiNTA. IVT/T was added to beads for 3h at 4°C. Beads were eluted with PBS, 200mM imidazole, and Ub^{K29R,K48R}-cyclin A/HisCdk2-complexes were concentrated with 30 MWCO Microcon filters.

Human APC/C was purified from extracts of HeLa S3 cells synchronized in M (APC/C^{Cdc20}) or G1 (APC/C^{Cdh1}), as described (Rape et al., 2006; Williamson et al., 2009b), using αCdc27 antibodies and Protein G agarose (Roche). 500mM NaCl and 0.1% (v/v) Triton X-100 were added during the immunoprecipitation to wash off endogenous Ube2S. Washed beads were incubated with 100nM HisE1, 60μM wt-ubiquitin or mutants, 3mM ATP, 22.5mM creatine phosphate, 10mM DTT, and substrate. Ube2S, Ube2G2, Ube2G2^{CTP} and its mutants were used at 10μM. Ube2C in combination with Ube2S or Ube2G2^{CTP} was used at a concentration of 150nM; when used by itself, Ube2C was at 1μM. Recombinant substrate was used at about 1μM. Ubiquitylation assays were usually incubated for 30-60min at 25, 30 or 37°C at 800rpm in a Thermomixer depending on the respective experiment.

3.2.10. *In vitro* degradation of ubiquitylated Nek2A with human proteasome

³⁵S-labeled HA²⁷²⁻⁴⁴⁵Nek2A was purified after IVT/T by binding to HA-affinity matrix (Sigma) and elution with 3xHA-peptide (Biosynthesis Inc). The concentrated radiolabeled protein was ubiquitylated as described above at 30°C for 30 minutes with APC/C^{Cdc20}. The ubiquitylation reactions were supplemented with reagents to stabilize 26S proteasome (10% (v/v) glycerol, 0.5mM EDTA, 5mM ATP, 20mM creatine phosphate and ~0.08mg/ml bovine creatine kinase (Sigma)). Human 26S proteasome (BostonBiochem) was diluted to achieve

noted concentrations in 60mM HEPES pH7.5, 50mM KCl, 50mM NaCl, 10% (v/v) glycerol, 5mM MgCl₂, 0.5mM EDTA, 1mM DTT, 0.5mM ATP and added to the ubiquitylation reactions. After an additional 45 minutes the reactions were stopped by boiling in SDS-loading buffer, resolved by SDS PAGE, detected by autoradiography and quantified with ImageJ.

3.2.11. *In vitro* reconstitutions of sequential ubiquitylation events by the APC/C

To separate Ube2G2^{CTP}- from Ube2S-dependent ubiquitylation, recombinant Ub-cyclin A^{HAHis} was incubated with APC/C^{Cdh1}, Ube2G2^{CTP}, and 10μM ubiquitin for 4min at 25°C. An excess of 400μM ubi^{R48} was added and incubated at 25°C for 10min. After addition of Ube2S, the reaction was incubated for 50min at 30°C. Reactions were stopped in SDS-loading buffer and analyzed by SDS PAGE and αK11 or αK48 western blot.

To purify conjugates synthesized by both Ube2G2^{CTP} and Ube2S, Ub-cyclin A^{HAHis} was incubated with APC/C^{Cdh1}, Ube2G2^{CTP}, 8μM ubiquitin, and 2μM FLAG^{ubiquitin} for 4min at 25°C. An excess of 400μM ubi^{R48} was added and reactions were incubated at 25°C for 10min. Next, Ube2S was added and reactions were incubated for further 50min at 30°C. The supernatant containing reaction products was incubated with FLAG-M2-affinity resin (Sigma) for 2hr at 4°C. FLAG-beads were extensively washed and eluted three times with 100μg/mL 3xFLAG-peptide (Sigma). Eluates were pooled and concentrated by centrifugation through 10-MWCO columns (Millipore). Samples were boiled in SDS-loading buffer and analyzed by SDS PAGE and αK11 western blot.

To separate Ube2C- from Ube2S-dependent ubiquitylation, Ub-cyclin A^{HAHis} was incubated with APC/C^{Cdh1}, 1μM Ube2C, 20μM ubiquitin for 20min at 30°C. An excess of 50μM Ube2C^{C114S} and 600μM methylubiquitin was added. The reaction was either stopped in SDS-loading buffer or continued for 30min at 30°C with either PBS or 5μM Ube2S. Reactions were stopped in SDS-loading buffer and analyzed by αHA western blot.

3.2.12. Identification of ubiquitin linkages by mass spectrometry

For analysis of ubiquitin conjugates on Nek2A by mass spectrometry 5 μ M recombinant His²⁷²⁻⁴⁴⁵Nek2A was incubated with immunopurified APC/C^{Cdc20}, 100nM E1, 3mM ATP, 22.5mM creatine phosphate, 10mM DTT, various Ube2C- and Ube2S-concentrations, 50 μ M ubiquitin for variable times at 30°C or 37°C. After SDS PAGE gel slices in the MW range of 37-250 kDA were excised. Tryptic digest of samples occurred in 25mM NH₄HCO₃ after 45mM DTT- and 100 mM iodoacetamide-treatment. Peptides were extracted with acetonitrile, exposed to formic acid and dried. Samples were analyzed by the Vincent J. Coates Proteomics/Mass Spectrometry Laboratory at UC Berkeley.

3.2.13. Detection of ubiquitin branches with ubiquitin^{TEV} derivatives

To detect branched ubiquitin signatures *in vitro* on Nek2A, 5 μ M recombinant His²⁷²⁻⁴⁴⁵Nek2A was incubated with APC/C^{Cdc20}, 100nM E1, 3mM ATP, 22.5mM creatine phosphate, 10mM DTT, 10 μ M Ube2C, 10 μ M Ube2S, 60 μ M ubiquitin^{53TEV} and 60 μ M ubiquitin^{64TEV/Flag} for 30min at 37°C. 4 μ g Tobacco Etch Virus nuclear inclusion a endopeptidase (TEV) protease was added in excess over substrate and incubated for 1h at 34°C. After removal of the supernatant reactions were resolved by tricine SDS PAGE on a 20% gel and ubiquitin branches were detected by α Flag western blot analysis.

To detect branched ubiquitin signatures on endogenous APC/C-substrates or HA-Nek2A *in vivo*, Flag^{53TEV} ubiquitin and His^{64TEV/Flag} ubiquitin were expressed in 293T cells using calcium phosphate in the presence or absence of HA²⁷²⁻⁴⁴⁵Nek2A. After 48h, cells were harvested, and lysates were subjected to immunoprecipitation by protein G-coupled α Cdc27 antibody or α HA-resin. After several washes, TEV protease was added in excess and incubated for 1h at 34°C. Reactions were resolved by tricine SDS PAGE on a 20% gel and ubiquitin branches were detected by α Flag western blot analysis.

3.2.14. *In vitro* reconstitution of ubiquitylated APC/C substrate binding to ubiquitin receptors

MBP-tagged proteins were coupled to amylose resin (NEB) in 50mM HEPES pH7.5, 1.5mM MgCl₂, 5mM KCl, 150mM NaCl, 0.1% (v/v) Triton X-100, 100μg/ml BSA for 2h at 4°C. ³⁵S-labeled or recombinant cyclin A or Ub-cyclin A were ubiquitylated as described. Bait proteins and ubiquitylated cyclin A were incubated for 2h at 4°C. After washes, bound proteins were eluted by boiling in SDS-loading buffer and analyzed by autoradiography or western blot. Equal coupling of ubiquitin binding proteins was detected by Ponceau or Coomassie staining.

3.2.15. HeLa cell extract-based *in vitro* degradation assay

Extracts of HeLa S3 cells synchronized in mitosis by thymidine and nocodazole treatment, in early G1 phase by 2h release from thymidine and nocodazole treatment or extracts of serum starved T98G cells were prepared as described (Jin et al., 2008; Reddy et al., 2007). Radiolabeled substrates were incubated in extracts supplemented with ATP, creatine phosphate and ubiquitin as described (Jin et al., 2008). Reactions were incubated for indicated times at 23°C or 30°C and for endpoint assays containing GST-UBA and/or 200μM MG132 (Boston Biochem) for 2h at 23°C. Reactions were stopped in SDS-loading buffer and analyzed by autoradiography or western blot.

3.2.16. Isolation of ubiquitylated proteins from cells

To purify endogenous ubiquitylated proteins from cells in prometaphase dependent on the presence of Ube2S, HeLa cells were transfected with 5nM Ube2S siRNA using Lipofectamine RNAimax (Invitrogen) according to the manufacturer's protocol and 18h later with His-tagged ubiquitin or empty vector

using calcium phosphate as described below. After 21h cells were treated with 100ng/mL nocodazole for 16h and 15 μ M MG132 for the last 2h of the nocodazole treatment. Cells were harvested, washed with PBS, resuspended in 8M Urea, 300mM NaCl, 0.5% (v/v) NP40, 50mM Na₂HPO₄, 50mM Tris-HCl pH8.0 and lysed by sonication. Inputs were removed and ^{His}ubiquitin-conjugates were purified with NiNTA agarose (Qiagen). Bound proteins were eluted by boiling in SDS-loading buffer. Ubiquitylated endogenous APC/C substrates were detected by western blot analysis using the respective antibodies against the substrate.

To purify ubiquitylated proteins from cells, 293T cells were transiently transfected with APC/C-substrates and His-tagged wt- or mutant ubiquitin using calcium phosphate or TransIT-293 Transfection Reagent (Mirus). Cells were harvested and washed with PBS. 10% of cells were lysed for direct sample processing as described. The remaining cells were resuspended in 6M guanidine hydrochloride (GdHCl), 0.1M Na₂HPO₄/NaH₂PO₄, 10mM imidazole pH8.0 and lysed by sonication. ^{His}ubiquitin-conjugates were purified by NiNTA agarose (Qiagen), washed with 25mM Tris-HCl, 20mM imidazole pH6.8 and eluted by boiling in SDS-loading buffer. Ubiquitylated APC/C substrates were detected by western blot using the respective antibodies against the substrate or against the tag of the transfected APC/C substrate.

To detect ubiquitin conjugates in cells expressing Ube2G2^{CTP}, HeLa cells were transfected with geminin, ^{His}ubiquitin, Ube2G2^{CTP} and the dominant negative versions of Ube2G2^{CTP}, Ube2C and Ube2S by calcium phosphate. 6h post transfection, 2mM thymidine was added for 24h. After a 3h release, cells were treated with 100ng/ml nocodazole for 11h. Mitotic cells were harvested by shake-off, washed, released for 30min into fresh medium, and then incubated in the presence of 15 μ M MG132 for 2h. Cell lysates were analyzed by α K11 western blot.

3.2.17. Immunoprecipitations of proteins from cells

293T or HeLa cells were either grown without synchronization or synchronized in mitosis by a thymidine and nocodazole treatment as described above. Cells were lysed in 50mM HEPES pH7.5, 1.5mM MgCl₂, 5mM KCl by double freeze/thaw in liquid nitrogen and multiple passages through a 25G5/8 needle. Cell debris was pelleted by centrifugation at 20000g and the remaining lysates were normalized according to their absorption at 280nm. Inputs were removed from the lysates and boiled in SDS-loading buffer. Lysates were incubated with mouse IgG, α CD3- or α Cdc27-antibody coupled to protein G agarose for 4h at 4°C. Beads were washed and eluted in SDS-loading buffer. Samples were analyzed by western blot using the relevant antibodies.

3.3. Cell biology techniques

3.3.1. Cultivation of adherent and suspension cells

Adherent HeLa, HeLa S3 and 293T cells were propagated in Dulbecco's Modified Eagle Medium (DMEM; Gibco) supplemented with 10% (v/v) fetal bovine serum (FBS; HyClone) at 37°C and 5% CO₂ in incubators (NuAire, Thermo). Flp-In 293 T-REx cell lines were supplemented with certified tetracycline-negative FBS (HyClone) instead of regular FBS. Usually cells were split at a 1/10 ratio just before reaching confluency, when cells were washed with sterile PBS, detached from the culture dishes with 0.25% trypsin/1mM EDTA (Gibco) and diluted with fresh medium. To grow HeLa S3 cells in large quantities spinner flasks (Bellco) were used adding antibiotics/antimycotics (Gibco) and rotating at about 60rpm at 37°C and 5% CO₂.

ES SF9 cells were propagated in ESF-921 medium (Expression Systems) supplemented with 1% (v/v, HyClone) and 1x antibiotic/antimycotic (Gibco) at 26°C and shaking at 140rpm.

To freeze cells exponentially growing cells were trypsinized, diluted in serum-containing medium, and collected by centrifugation at 100g for 5 min. Cells were then resuspended in DMEM, 20% (v/v) FBS supplemented with 10 % DMSO (v/v, Sigma), aliquoted and slowly frozen enclosed in a 2-propanol insulation chamber at -80°C. For long-term storage, cells were transferred to -150°C.

3.3.2. Transient transfection of human cells with plasmid DNA

HEK 293T or HeLa cells were transfected with plasmid DNA using calcium phosphate DNA precipitates (Graham and van der Eb, 1973). Up to 77µg plasmid DNA was dissolved in 1.3ml of HBS (21mM HEPES, 136mM NaCl, 0.1% (m/v) dextrose, 50mM KCl, 0.7mM Na₂HPO₄, pH7.1, sterile filtered by 0.22 µm membrane) per 15cm dish of cells. 0.06ml of a sterile 2.5M CaCl₂ solutions was added and mixed. After 20min the mixture was added drop-wise to the cells. The medium was replaced 24h later in most cases. Cells were generally harvested after 48h.

HeLa cells were transfected with Lipofectamine 2000 (Invitrogen) according to the manufacturer's instructions.

HEK 293T cells were transfected with TransIT-293 Transfection Reagent (Mirus) according to the manufacturer's instructions.

3.3.3. Transient transfection of human cells with siRNA

To downregulate different genes (e.g. Ube2S or Ube2C) in HeLa cells, siRNA-mediated gene silencing was employed (Elbashir et al., 2001). HeLa cells were transfected using Lipofectamine RNAiMax (Invitrogen), according to the manufacturer's instructions. Briefly, HeLa cells in a 15cm dish (40-50 % confluent if synchronized afterwards) were transfected with 5-10nM siRNA and 25µL Lipofectamine RNAiMax reagent per dish. Cells were analyzed for protein depletion generally 48h later by western blot.

For some early experiments Oligofectamine (Invitrogen) was used according to the manufacturer's instructions. The amount of siRNA used with this transfection reagent was 100-200nM siRNA.

3.3.4. Generation of stable HeLa or inducible 293 cell lines

To generate HeLa cell lines stably expressing Ube2G2^{CTP}, Ube2G2^{CTP}-C89S, or Ube2S, transfection and selection occurred as described (Wickliffe et al., 2011a). Briefly untagged Ube2G2^{CTP}, Ube2G2^{CTP}-C89S or Ube2S was cloned into a vector (pCDNA3.1(+)) hygro) under a CMV promoter containing the gene for hygromycin B phosphotransferase. After transfection of the generated plasmid with Lipofectamine 2000 HeLa cells were selected for expression of the hygromycin resistance gene and supposedly co-expression of the introduced sequence by treatment with 300µg/ml hygromycin B, which kills organisms by stabilizing the ribosomal acceptor site for tRNA, thereby inhibiting translocation and translation. HeLa cells expressing the introduced gene were identified by western blot analysis for Ube2S levels higher than present in control cells to identify Ube2S positive clones or appearance of a lower MW form to identify Ube2G2^{CTP} positive clones using antibodies against the CTP of Ube2S (Bethyl). A Ube2G2^{CTP} inducible 293 cell line was created using the Flp-In™ T-REx™ system according to the manufacturer's instructions (Invitrogen). In short, untagged Ube2G2^{CTP} was cloned into a vector (pCDNA5/FRT/TO) under a hybrid human cytomegalovirus (CMV)/TetO₂ promoter for high-level, tetracycline-regulated expression of the gene of interest. The vector also contained FLP Recombination Target (FRT) sites for Flp recombinase-mediated integration into the Flp-In™ T-REx™ 293 host cell line and a gene encoding for hygromycin B resistance for selection. After transfection of the generated plasmid and another plasmid allowing expression of Flp recombinase (pOG44) with Lipofectamine 2000, 293 cells were selected for expression of the hygromycin resistance gene. 293 cells were tested for expression of Ube2G2^{CTP} upon treatment with tetracycline by western blot analysis.

3.3.5. Cell cycle synchronization of cells

The presence of thymidine in excess leads to arrest in S phase, which can be alleviated by removal of the excess thymidine (Bootsma et al., 1964). Treatment with nocodazole leads to arrest of HeLa cells at the onset of mitosis (Zieve et al., 1980) in a prometaphase like state as microtubule depolymerize in the presence of nocodazole. To enrich HeLa or HeLa S3 cells in prometaphase, dividing cells were treated with 2mM thymidine (Sigma) for 24h. Cells were washed and incubated in medium without thymidine for 3h. Nocodazole (Sigma) was added to a final concentration of 100ng/ml for 11h, if the cells were to be released from a nocodazole induced arrest for 2-4h to let them enter G1, or for 12h, if cells arrested in mitosis were wanted.

Thymidine in combination with nocodazole led to reduced expression of exogenous proteins after transfection. Therefore cells transfected with DNA and to be enriched in certain phases were only treated with either 2mM thymidine for 24h to moderately enrich for cells in S phase or with 100ng/ml nocodazole for 16h to moderately enrich for cells in M phase.

3.3.6. Immunofluorescence

For immunofluorescence analysis of constitutively expressing Ube2S- and Ube2G2^{CTP}-HeLa cells, they were grown to confluency on glass coverslips. Cells were fixed with 4% (w/v) formaldehyde/TBST for 10min, permeabilized with TBS, 0.4% (v/v) Triton X-100, 2% BSA for 10min and blocked with blocking solution, 2% (w/v) BSA in TBS, for 30min prior to application of primary antibody. Cells were incubated with the primary antibody diluted appropriately in blocking solution for 1-2h in a humid chamber, then washed three times for 5min with TBS, 2% (w/v) BSA. Then, cells were incubated for 0.5-1h in a humid chamber with Alexa488- or Alexa569-conjugated secondary antibodies (Molecular Probes) diluted 1:500 and Hoechst 33342 (VWR) diluted 1:1000 in blocking solution.

Cells were then washed three times for 5min in PBS before mounting with ProLong Gold (Invitrogen) on slides.

3.3.7. Analysis of cell cycle progression in cell lines by FACS

To determine the DNA content and hence the cell cycle stage of cells with propidium iodide (PI) staining and fluorescence-activated cell sorting (FACS), cells were plated in 6-well plates and transfected with 100nM siRNA against the 3'-UTRs of *p31*, *UBE2C* and *UBE2S* and oligofectamine, as described (Williamson et al., 2009), or with 5nM siRNA against the 3'UTR of *UBE2S*, as described here. 40h post transfection untreated or thymidine and nocodazole treated cells were harvested, washed and resuspended in PBS containing 2% (v/v) FBS. Cells were fixed by adding 75% ethanol at -20°C, washed, and stained in 50µg/ml propidium iodide in 3.8mM sodium citrate containing RNase A for 30min at 37°C. Excess dye was washed away and the cell cycle profile was determined using a Beckman-Coulter EPICS XL Flow Cytometer (575nm band pass filter).

3.3.8. Determination of cell cycle distribution by automated microscopy and analysis

For measuring the taxol or nocodazole response, HeLa cells or cells constitutively expressing Ube2S, Ube2G2^{CTP}, Ube2G2^{CTP}-C89S or empty vector were plated in a 384 well plate (Corning) at 30% confluency. The next day, taxol (Sigma) was diluted in medium and added in increasing concentrations. Cells were incubated for 14-16h, before staining with 20µM Hoechst 33342 (VWR) for 30min at 37°C. Cells were fixed with formaldehyde at a final concentration of 3.7% (v/v). I imaged eight sites per well with an average of 400 cells using an automated microscope ImageXpress Micro (Molecular Devices) and MetaMorph. Images were analyzed in terms of their mitotic index with CellProfiler and

CellProfilerAnalyst (Broad Institute) after training the software by visual input of at least 200 cells per mitotic or interphase morphology. When done in combination with siRNAs against Ube2C and Ube2S, cells were treated with siRNA using oligofectamine as described above and treated with 100nM taxol after 20h. In case of nocodazole titrations, cells were transfected using LipofectamineRNAimax and 10nM control or Ube2S siRNA, treated with the indicated nocodazole concentrations after 24h and fixed 16h later.

3.3.9. Determination of substrate levels in cells

HeLa cells stably expressing Ube2S, Ube2G2^{CTP}, Ube2G2^{CTP}-C89S or empty vector were plated in 6-well plates and transfected with 100nM siRNA against the 3'-UTR of *UBE2C* and *UBE2S*, as described (Williamson et al., 2009b). To exclude off-target effects, I used a previously characterized siRNA against the 3'-UTR of *UBE2S* (Dharmacon; GGCACUGGGACCUGGAUUU) (Wickliffe et al., 2011a; Williamson et al., 2009b) and another siRNA obtained from a different vendor against the open reading frame (ORF) of *UBE2S* (Qiagen; CCCGAUGGCAUCAAGGUCUUU). Cells were treated with 2mM thymidine for 24h. After a 3h release, cells were treated with 100ng/ml nocodazole (Sigma) for 11h. Mitotic cells were harvested by shake-off and plated into fresh medium. Samples were taken after the indicated times post release for analysis by western blot. For cycloheximide (CHX) chases thymidine and nocodazole treated cells were left in nocodazole and treated with 50 μ g/mL cycloheximide (Sigma) for the indicated time points.

Tet-inducible Ube2G2^{CTP} 293T cells were plated in a 6-well plate and transfected with TransIT-293 (Mirus) to express 3xHA-Cdh1 and securin ^{Δ DBOX}. 24h post transfection, expression of Ube2G2^{CTP} was induced with 1 μ g/mL doxycyclin (Sigma) for 24h. Cells were harvested and analyzed by western blot.

3.3.10. Live cell imaging of Ube2S depleted HeLa cells

For live cell imaging, HeLa cells that constitutively express mCherry-H2B and GFP-tubulin (gift from Rebecca Heald) were maintained in DMEM (no phenol red, Gibco) containing 10% (v/v) FBS at 37 °C with 5% CO₂ using 4-well chambered coverglass (Fisher), and imaged at a single focal plane every 3min for 12h beginning 36h after transfection with 15nM RNA-oligos using Lipofectamine RNAimax (Invitrogen). Images were taken with a 0.95 NA 40x objective on an Olympus Revolution XD spinning disk confocal microscope equipped with a charged-couple device camera (Andor technology) and a Yokogawa spinning disk. Image analysis was performed using MetaMorph. The time between NEBD and sister chromatid separation was determined by counting the frames between the first frame showing the beginning of chromosome condensation plus GFP-staining in former nucleus location and the first frame showing recognizable separation of sister chromatids after formation of a metaphase plate. Cumulative percentages were plotted using Prism6.

4. Results

4.1. Ube2S enhances ubiquitylation and proteasomal degradation of prometaphase APC/C substrates

The metazoan APC/C cooperates with Ube2S to assemble K11-linked chains that drive the degradation of cell cycle regulators during mitosis and G1. However as depletion of Ube2S showed few defects during mitosis, it is not fully understood whether K11-linked chains have essential roles for cell division (Garnett et al., 2009; Williamson et al., 2009a; Wu et al., 2010). To address this issue cells were tested, that expressed Ube2S at lower levels due to siRNA against Ube2S.

4.1.1. Nek2A levels are increased upon depletion of Ube2S

Using siRNA targeted against Ube2S with the transfection reagent Lipofectamine RNAimax the mRNA levels of Ube2S were reduced to less than 2% of its normal abundance in HeLa cells.

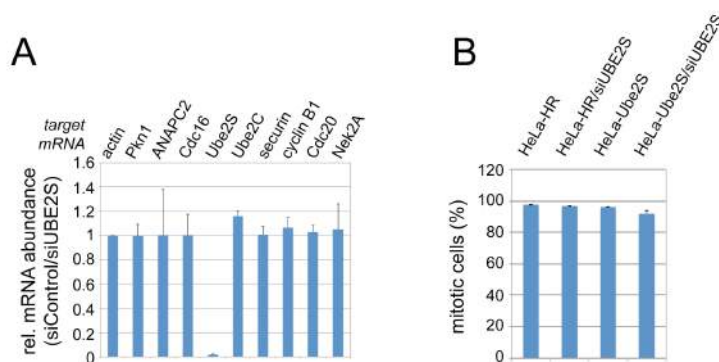


Figure 10: Depletion of Ube2S by siRNA only changes the mRNA levels of Ube2S in HeLa cells.

A. Depletion of Ube2S does not change Nek2A mRNA levels. HeLa cells treated with control or Ube2S siRNAs were synchronized with thymidine and nocodazole, and mRNA abundance was determined by qRT-PCR. Depicted is the abundance relative to actin mRNA levels in control versus siUBE2S treated cells. Note that siRNA against Ube2S led to a reduction in Ube2S mRNA to less than ~2% of its normal levels (n=3; data are represented as average + standard deviation (SD)). **B.** Depletion of Ube2S does not change the cell cycle stage of synchronized cells. HeLa cells were treated with control or Ube2S siRNA, synchronized by thymidine and nocodazole and analyzed by FACS after propidium iodide staining (n=3; data are average + SD).

Results

These cells were synchronized in prometaphase using thymidine and nocodazole (Figure 10A). Furthermore the depletion of Ube2S by RNAi in HeLa cells did not change the overall synchronization in prometaphase (Figure 10B). Strikingly, a decrease of Ube2S levels caused a strong increase in the abundance of Nek2A during prometaphase, a cell cycle stage in which the APC/C is mostly inhibited by the spindle checkpoint (Figure 11A). An even stronger stabilization of Nek2A can be achieved by inhibition of the 26S proteasome with the compound MG132 during prometaphase (Figure 11A) leading to the conclusion that Ube2S, as a ubiquitin conjugating enzyme, contributes to the ubiquitylation and consequently degradation of Nek2A as a substrate of the proteasome. The accumulation of Nek2A was seen with two different siRNAs against Ube2S (Figure 11B) negating the possibility of an off-target effect caused by the Ube2S Dharmacon RNA oligo used in this study.

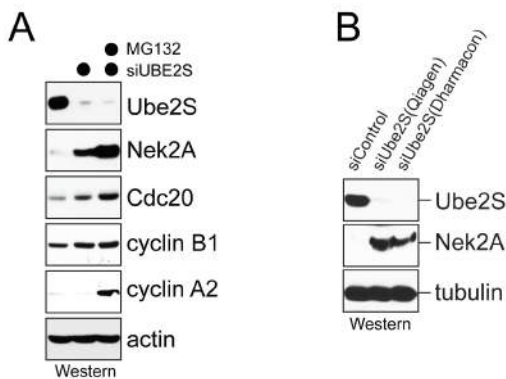


Figure 11: Depletion of Ube2S by siRNA leads to stabilization of Nek2A in prometaphase. **A.** Depletion of Ube2S increases the levels of Nek2A during prometaphase. HeLa cells transfected with control or Ube2S siRNA using Lipofectamine RNAimax were synchronized in prometaphase using thymidine and nocodazole. If indicated, cells were treated with 20 μ M MG132 for an

additional two hours in nocodazole containing media after the initial 11-hour nocodazole treatment. The abundance of endogenous proteins was measured by western blot analysis. **B.** Different RNA oligos targeting Ube2S lead to similar increases in Nek2A levels during prometaphase. Two siRNA oligos with different target sequences were obtained from distinct vendors and tested for effects on Nek2A levels after thymidine and nocodazole arrest. Nek2A levels were determined by western blot analysis.

To rule out any other secondary effects caused by Ube2S mRNA depletion, HeLa cells constitutively expressing Ube2S were created. The introduced sequence of Ube2S was insensitive to the used siRNA, because the Ube2S RNA oligo targets a region of the gene encoding for Ube2S downstream of the stop codon. While control cells resistant to hygromycin B still showed stabilization of

Nek2A upon Ube2S depletion the effect was not observed with the stable expression of siRNA-resistant Ube2S (Figure 12). The slight overexpression of Ube2S seemed to have led to a decrease in Nek2A levels arguing a high sensitivity of Nek2A levels towards the amount of Ube2S present (Figure 12). In summary the levels of Ube2S and Nek2A are anticorrelated in prometaphase HeLa cells.

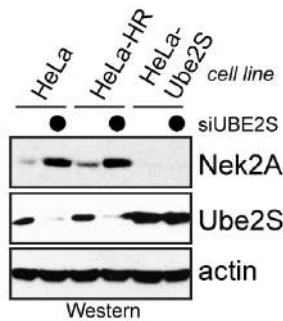


Figure 12: Stabilization of Nek2A caused by Ube2S depletion is rescued by ectopic expression of Ube2S. Ube2S was depleted by siRNA from prometaphase HeLa cells that are resistant to hygromycin B (HeLa-HR) or that are resistant and constitutively expressing siRNA-resistant Ube2S (HeLa-Ube2S). Cells were transfected with Lipofectamine RNAimax, synchronized in prometaphase using thymidine and nocodazole, and analyzed for Nek2A levels by western blot analysis.

4.1.2. Ube2S depletion stabilizes prometaphase APC/C substrates

Based on these findings I used cycloheximide chase experiments to test, whether Ube2S was required for APC/C substrate degradation during prometaphase. Cycloheximide inhibits protein synthesis by inhibiting elongation of the polypeptide during translation through binding of the exit site of the 60S ribosomal unit and interfering with deacetylated tRNA (Klinge et al., 2011; Pestova and Hellen, 2003; Schneider-Poetsch et al., 2010). By inhibiting *de novo* protein synthesis with cycloheximide, the half-life of a protein can be determined giving a more sensitive readout for protein stability in the cell. Indeed the depletion of Ube2S resulted in a pronounced increase in the half-life of Nek2A, as well as the CDK inhibitor p21, another APC/C-substrate (Figure 13; Amador et al., 2007). At the same time levels of phospho-histone H3 (Ser10), Mad2 and Kif18A showed no change, leading to the assumption that the cells were not progressing within the cell cycle (Johansen and Johansen, 2006) and did not experience a general change in levels of APC/C-inhibiting MCC components

Results

(Chao et al., 2012; Herzog et al., 2009; Schreiber et al., 2011) or of anaphase APC/C substrates (Sedgwick et al., 2013). Therefore, Ube2S is important for the timely degradation of APC/C substrates during prometaphase.

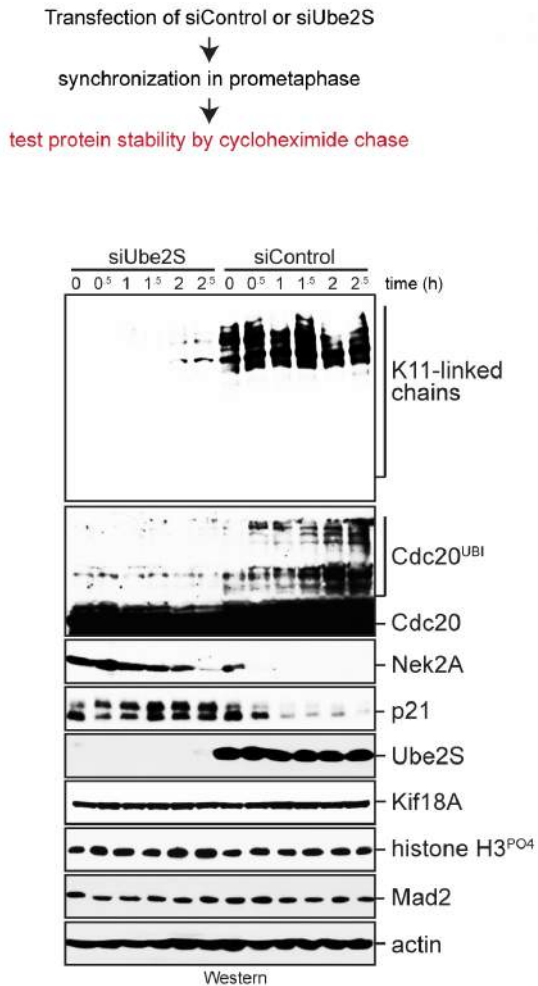


Figure 13: The half-lives of the APC/C prometaphase substrates Nek2A and p21 are increased upon Ube2S depletion. HeLa cells transfected with control or Ube2S siRNA using Lipofectamine RNAiMax were synchronized in prometaphase by thymidine and nocodazole, treated with 50µg/ml cycloheximide while still in nocodazole for the indicated time points, and analyzed for protein abundance by western blot analysis. The top shows an outline of the experimental workflow.

4.1.3. Decreased ubiquitylation of prometaphase APC/C substrates caused by reduced Ube2S levels

To further corroborate the effect of Ube2S depletion on the stability of prometaphase APC substrates, it was directly tested if the loss of the ubiquitin conjugating enzyme Ube2S led to a decrease of ubiquitylated APC/C substrates in prometaphase. HeLa cells were transfected with control or Ube2S RNA oligos using Lipofectamine RNAiMax. After 18 hours, these cells were again transfected

Results

with control or His ubiquitin encoding expression vectors using calcium phosphate, synchronized with nocodazole, treated with 15 μ M MG132 for two hours while still arrested with nocodazole and lysed. His-tagged protein complexes were purified with NiNTA under denaturing conditions in 8 M Urea to inhibit DUB activity and co-purification of other proteins leading to false-positive detection of ubiquitylated proteins. The purification of these ubiquitin conjugates from prometaphase cells revealed that Ube2S was required for the attachment of high molecular weight (MW) chains to endogenous Nek2A and p21 (Figure 14A,B). Ube2S also mediated the ubiquitylation of Cdc20 (Figure 14A, Figure 13), a reaction that disassembles spindle checkpoint complexes (Foster and Morgan, 2012; Reddy et al., 2007; Uzunova et al., 2012; Williamson et al., 2009a).

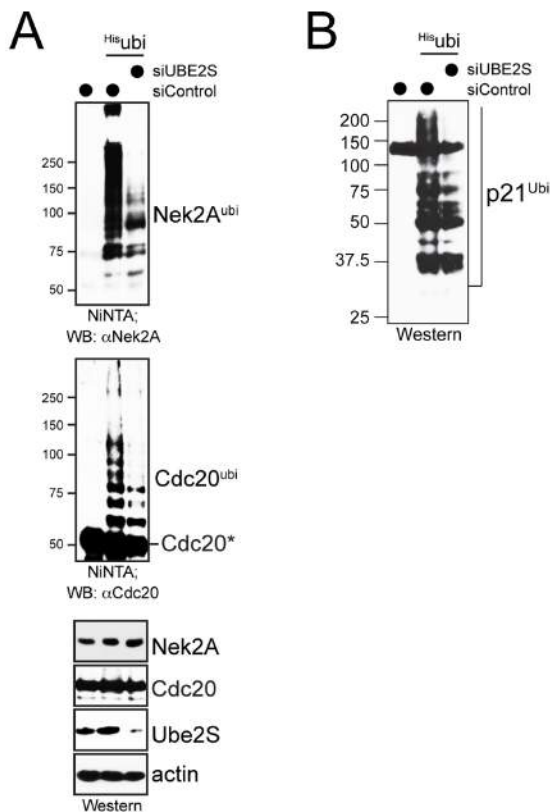


Figure 14: Ube2S siRNA leads to loss of APC/C prometaphase substrate ubiquitylation of Nek2A, Cdc20 and p21. A. HeLa cells expressing His ubiquitin were transfected with control or Ube2S siRNA using Lipofectamine RNAimax, synchronized in prometaphase by 100ng/ml nocodazole and treated with 15 μ M MG132 for two hours while remaining in nocodazole. Purified ubiquitin conjugates were analyzed by α Nek2A or α Cdc20 western blot. **B.** HeLa cells expressing His ubiquitin and transfected with control or Ube2S siRNA using Lipofectamine RNAimax were synchronized in prometaphase by nocodazole and treated with 15 μ M MG132 for two hours while remaining in nocodazole. Purified ubiquitin conjugates were analyzed by α p21 western blot.

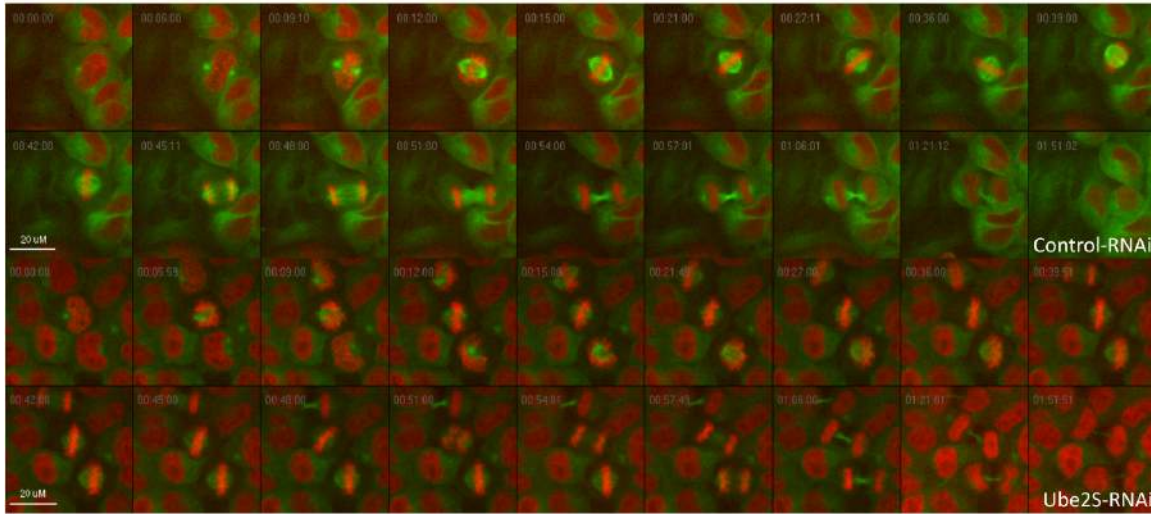
In contrast, another prometaphase substrate, cyclin A, was not stabilized (Figure 11A), which might be due to incomplete Ube2S depletion or redundant mechanisms governing degradation of this cell cycle regulator (Kikuchi et al.,

2014). These experiments therefore show that Ube2S is important during prometaphase, a time in the cell cycle when the spindle checkpoint reduces the overall APC/C-activity.

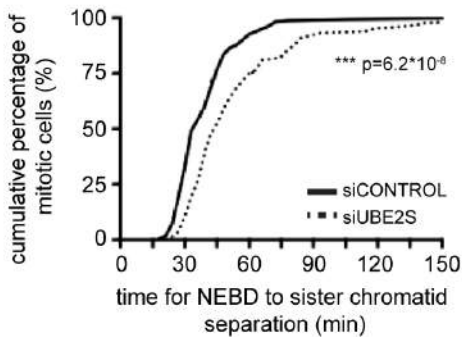
4.1.4. Reduced levels of Ube2S cause a delay in early mitosis

After detecting the loss of APC/C prometaphase substrate ubiquitylation and the increase in their protein levels upon Ube2S depletion, the overall effects of Ube2S siRNA on progression through early mitosis were determined. HeLa cells constitutively expressing ^{GFP}tubulin and ^{mCherry}histone H2B (gift from Rebecca Heald's lab) were transfected with control or Ube2S siRNA using Lipofectamine RNAimax for 32 hours and stills were taken every three minutes for 16 hours. Over 130 cells for each condition were used in analysis if they contained fluorescent markers, no apparent multi-nucleation and an intact bipolar spindle. In these cells, the time between nuclear envelope breakdown and sister chromatid separation was quantified. The time of nuclear envelope breakdown was taken at the first frame of DNA condensation based on ^{mCherry}histone H2B morphology plus NEBD based on ^{GFP}tubulin localization at the position of the formerly intact nucleus (seen at 9 minutes in control and at 6 minutes in Ube2S siRNA treated cells; Figure 15A). The time of sister chromatid separation was taken at the first frame of apparent spatial separation of sister chromatids determined by ^{mCherry}histone H2B morphology (seen at 45 minutes in control and 51 minutes in Ube2S siRNA treated cells; Figure 15A). A significant number of cells was quantified showing an increase in time needed by HeLa cells depleted of Ube2S to progress through early mitosis (Figure 15B). On average Ube2S depleted cells needed 15 minutes longer to achieve sister chromatid separation after NEBD, while the median time increased by nine minutes. This delay in mitosis becomes even more obvious if HeLa cells treated with control or Ube2S siRNA and arrested in prometaphase by thymidine and nocodazole, are released from the nocodazole arrest and harvested every 30 minutes for western blot analysis of APC/C substrates.

A



B



C

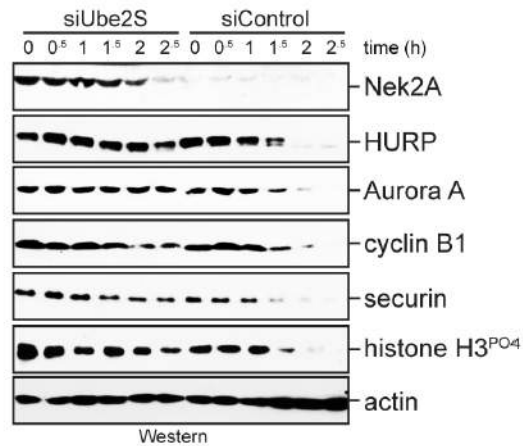


Figure 15: Ube2S siRNA delays progression through early mitosis. A. Depletion of Ube2S delays anaphase initiation. HeLa cells constitutively expressing ^{GFP}tubulin and ^{mCherry}histone H2B were transfected with control or Ube2S siRNA using Lipofectamine RNAimax and monitored by live cell imaging. The time from nuclear envelope breakdown to initiation of sister chromatid separation was determined. **B.** Quantification of live cell imaging depicted above for >130 cells per condition. **C.** HeLa cells were treated with control or Ube2S siRNA and synchronized with thymidine and nocodazole. After an arrest in nocodazole, cells were released into drug-free medium and protein levels were analyzed by western blot at the indicated time points.

While the degradation of Nek2A can only be observed in this experiment due to Ube2S depletion other substrates like HURP, Aurora A, cyclin B1 and securin are degraded within about two hours after release from the nocodazole-induced

arrest in control cells. Depletion of Ube2S however causes stabilization of these APC/C substrates, which correlates with a general delay of mitosis seen by the steady levels of phospho-histone H3 (Ser10) in these cells. The delaying effect of Ube2S siRNA in prometaphase was also seen in asynchronous cells treated with increasing concentrations of the microtubule poison nocodazole. In a 384 well format cells were treated with control or Ube2S siRNA. Twenty-four hours after transfection, cells were treated with different amounts of nocodazole for another 16 hours. The cells were stained with Hoechst and fixed with formaldehyde. After automated acquisition, Hoechst-stained DNA intensity and morphology was determined using a software-based approach, allowing for the quantification of mitotic cells for more than 1000 cells per condition. Cells depleted of Ube2S and treated with low concentrations of nocodazole showed an increased in the percentage of mitotic cells by up to 2.5-fold (Figure 16). This is consistent with the previous observation that HeLa cells depleted of Ube2S show a delay throughout early mitosis. Ube2S depleted cells are more prone towards stress in mitosis based on the increased sensitivity towards nocodazole. Ube2S is therefore important for proper progression of HeLa cells through mitosis.

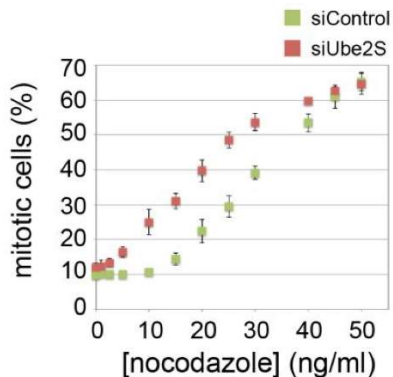


Figure 16: Depletion of Ube2S sensitizes cells to a nocodazole-dependent prometaphase arrest. HeLa cells transfected with control or Ube2S siRNA using Lipofectamine RNAimax were treated with increasing concentrations of nocodazole and analyzed for mitotic status measured by Hoechst staining and automated image analysis of >1000 cells/condition (n=3; data are represented as average +/- SD).

4.2. Ube2S synthesizes branched K11-linked ubiquitin chains off non-K11-linkages

Previous work had shown that Ube2S elongates single ubiquitin moieties or ubiquitin chains that were initiated by Ube2C or Ube2D with K11-linked ubiquitin chains (Garnett et al., 2009; Wickliffe et al., 2011a; Williamson et al., 2009a; Wu et al., 2010). To gain further insight into this reaction driven by Ube2S during prometaphase, the ubiquitylation of Nek2A and of linear ubiquitin fusion substrates (Ub)_{n=1,2,3}-cyclin A or Ub₃-Nek2A was reconstituted *in vitro*.

4.2.1. K11 in ubiquitin is not sufficient for formation of long polyubiquitin chains on Nek2a by Ube2C and Ube2S

As Nek2A shows autophosphorylation due to the presence of its N-terminal kinase domain, a truncation consisting of residues 272-445 was created; this truncation includes all necessary APC/C recognition and modification sites (Sedgwick et al., 2013) and did not show a phosphorylation pattern in SDS-PAGE simplifying the visualization of Nek2A ubiquitin conjugates (data not shown). Using ³⁵S-radiolabeled ^{HA}Nek2A²⁷²⁻⁴⁴⁵ with immunoprecipitated APC/C, recombinant Ube2C and Ube2S, the modification of Nek2A with high MW conjugates in the presence of wild type ubiquitin, but not a K11R-mutant of ubiquitin (ubi^{R11}), was observed (Figure 17A). Chains derived with ubi^{R11}, which cannot be used by Ube2S for chain formation, closely mirrored those seen in cells lacking Ube2S (Figure 14B), recapitulating the *in vivo* modification of endogenous Nek2A. Surprisingly, the abundance of high MW of Nek2A conjugates was strongly reduced in reactions that contained ubiquitin mutant with K11 as the only site for chain formation (ubi^{K11}; Figure 17A). This was in contrast to the radiolabeled model substrate Ub^{K29,48R}-cyclin A modified by Ube2S alone (Figure 17B) and suggested that formation of high MW chains on Nek2A by Ube2C and Ube2S was dependent on multiple linkages. Instead of using Ube2C as the initiating enzyme, Ube2D3 was used to further validate the requirement of

multiple linkages. While Ube2C is limited in the variety of ubiquitin linkages formed, mainly K11 but also K48 and K63 (Kirkpatrick et al., 2006), E2s of the Ube2D family show little linkage preference (Kim et al., 2007). Ubiquitylation of recombinant Nek2A²⁷²⁻⁴⁴⁵ using wt-ubiquitin with Ube2D3 and Ube2S showed formation of high MW species, while using ubi^{K11} or ubi^{R11} restricted the formation of long ubiquitin conjugates on Nek2A (Figure 17C).

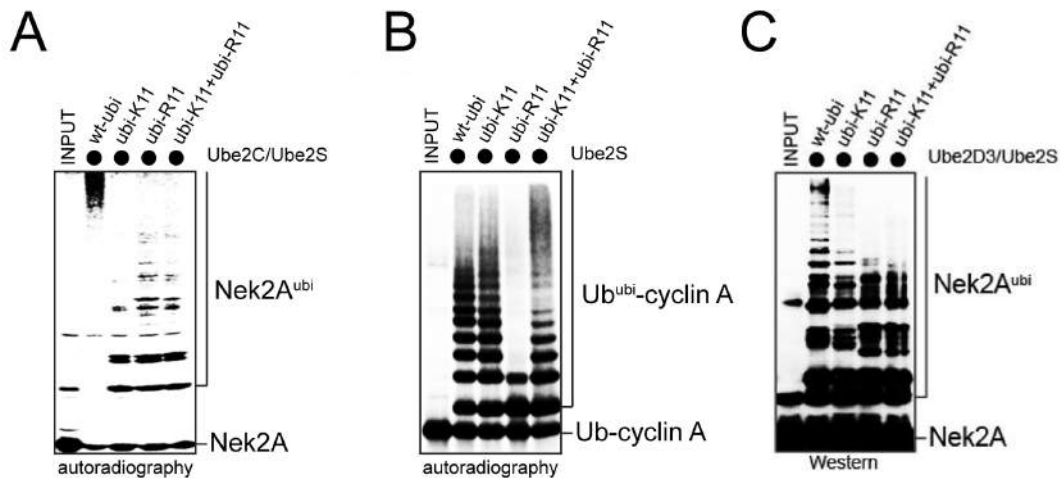


Figure 17: K11 in ubiquitin is not sufficient for high MW ubiquitin conjugate formation on Nek2A. **A.** Nek2A is modified with branched chains *in vitro*. ³⁵S-labeled HA-Nek2A²⁷²⁻⁴⁴⁵ was incubated with APC/C^{Cdc20}, Ube2C, Ube2S, and ubiquitin mutants at 30°C for 30 minutes. Reactions were analyzed by autoradiography. **B.** Ube2S elongates Ub-cyclin A efficiently with homogenous K11-linked chains. His-Cdk2 affinity purified ³⁵S-labeled Ub^{K29,48R}-cyclin A was incubated with APC/C^{Cdc20}, Ube2S, and ubiquitin mutants at 30°C for 20 minutes. Reactions were analyzed by autoradiography. **C.** Ube2D3 supports formation of branched chains. Reactions were performed with APC/C^{Cdc20}, Ube2D3 and Ube2S, ubiquitin mutants and recombinant Nek2A²⁷²⁻⁴⁴⁵ at 30°C for 30 minutes. Reactions were analyzed by αNek2A western blot.

4.2.2. Ube2S and Ube2C do not form linear mixed ubiquitin chains on Nek2A

Conjugates with multiple linkages could be mixed chains, in which distinct connections are used within a single conjugate (linear mixed chain), or branched structures, in which at least one moiety received two or more ubiquitin molecules. To distinguish between these possibilities, Nek2A was incubated with mixtures of ubi^{R11} and ubi^{K11}. If the APC/C assembled linear mixed chains, it could

Results

sequentially use ubi^{R11} and ubi^{K11} to build conjugates of similar MW as seen with wt-ubiquitin. In contrast, branched conjugates that result from concurrent modification of K11 and another ubiquitin lysine could not be assembled; thus, if the APC/C were a branching enzyme, chains formed with ubi^{K11} and ubi^{R11} should be of lower MW than with wt-ubiquitin. Nek2A was modified with low MW conjugates in the presence of ubi^{R11} and ubi^{K11} , suggesting that the APC/C decorated this substrate with branched chains (Figure 17A,C).

4.2.3. Ube2S attaches single ubiquitin moieties to N-terminally fused linear ubiquitin chains on cyclin A and Nek2A

As physiological enzymes for the assembly of branched chains were unknown, the notion that the APC/C could produce such conjugates was tested.

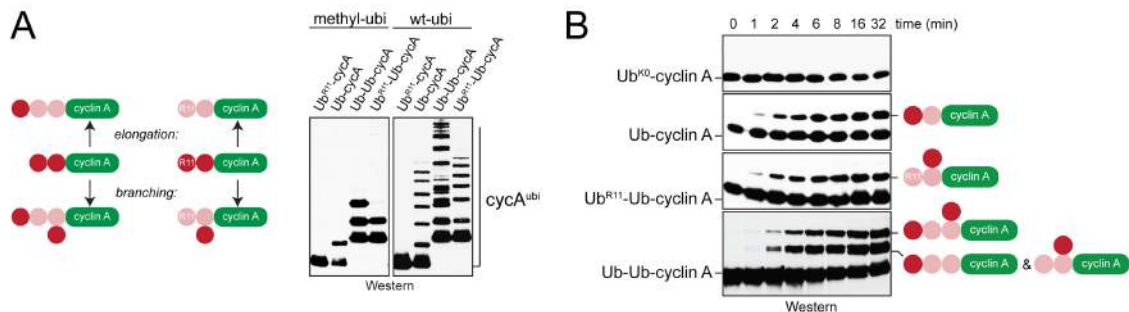


Figure 18: Ube2S introduces ubiquitin branches by modifying internal ubiquitin moieties of Ub-Ub-cyclin A. **A.** Ub-cyclin A, Ub^{R11} -cyclinA, Ub-Ub-cyclin A and Ub^{R11} -Ub-cyclin A were incubated with APC/C, Ube2S, and methyl-ubiquitin or wt-ubiquitin. Left: reaction products if Ube2S would elongate or branch chains. Pink: fused substrate-ubiquitin; red: ubiquitin added by Ube2S. Right: Reactions were analyzed by αHA western blot. **B.** Ube2S synthesizes branched linkages with similar efficiency as it promotes chain elongation. Ub^{K0} -cyclin A^{HA}, Ub-cyclin A^{HA}, Ub^{R11} -Ub-cyclin A^{HA}, and Ub-Ub-cyclin A^{HA} were incubated with APC/C, Ube2S, and methyl-ubiquitin. Reactions were analyzed by αHA western blot. Pink ball: fused ubiquitin; red ball: ubiquitin added by Ube2S.

The initiation step was circumvented to detect introduction of branches in a simplified manner. By PCR the C-terminus of ubiquitin was fused to the N-terminus of the respective APC/C substrate, while G75 and G76 of ubiquitin were

Results

omitted to inhibit accessibility by DUBs or E1. More ubiquitin moieties were added by fusing the C-terminus of ubiquitin again without G75 and G76 to the N-terminus of the already substrate fused ubiquitin. Two prometaphase APC/C-substrates were fused to these quasi-linear ubiquitin moieties: Nek2A, which requires Ube2S for degradation, and cyclin A, which can be robustly ubiquitylated *in vitro* (Rape et al., 2006).

To test for branching in ubiquitylation reactions of these model substrates, methyl-ubiquitin was added, which allows transfer of the first ubiquitin by Ube2S, but interferes with further chain extension, as lysine residues are methylated. If Ube2S elongates preexisting chains, only the distal ubiquitin of these substrates should be modified, yet if it assembles branched conjugates, internal moieties could be ubiquitylated as well. Demonstrating the formation of branched chains, Ube2S added two methyl-ubiquitin molecules to Ub-Ub-cyclin A, and it attached one ubiquitin to a substrate variant that lacked K11 in its distal moiety (Ub^{R11}-Ub-cyclin A; Figure 18A). Ube2S synthesized the branched linkage on Ub^{R11}-Ub-cyclin A with the same specificity and efficiency as seen for elongation (Figure 18A,B).

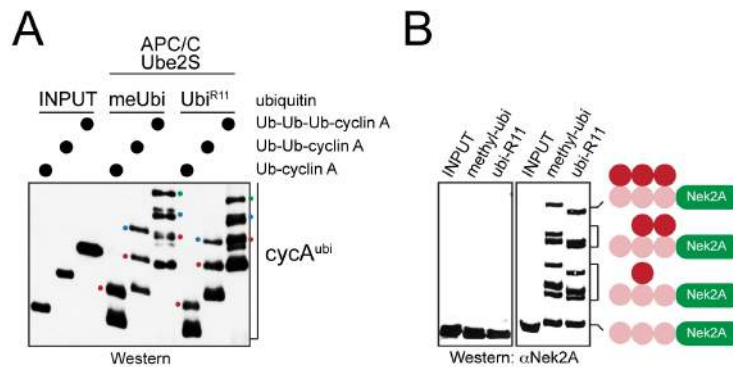


Figure 19: Ube2S is able to branch ubiquitin molecules off Ub₃-cyclin A and Ub₃-Nek2A. A. Ub-cyclin A^{HA}, Ub-Ub-cyclin A^{HA}, or Ub-Ub-Ub-cyclin A^{HA} was incubated with APC/C^{Cdh1}, Ube2S and methyl-ubiquitin or ubi^{R11}. Reaction products were analyzed by αHA western blot. Red dot: first added ubiquitin; blue dot: second added ubiquitin; green dot: third added ubiquitin. **B.** Ube2S efficiently modifies Nek2A with branched chains *in vitro*. Ub₃-Nek2A was incubated with APC/C^{Cdc20}, Ube2S, and methyl-ubiquitin or ubi^{R11}, and analyzed by αNek2A western blot.

Furthermore, Ube2S was able to branch ubiquitin molecules off substrates with longer chains, such as Ub₃-cyclin A and Ub₃-Nek2A, while retaining K11-specificity shown by single modification of each present ubiquitin moiety with ubi^{R11} (Figure 19). As shown for Ub₃-cyclin A and Ub₃-Nek2A the ability of Ube2S to introduce branches within ubiquitin chains seems not be limited to an individual substrate (compare Figure 19 A and B). If these assays were performed with wt-ubiquitin, Ube2S branched a block of ~6 K11-linked molecules off each ubiquitin containing a free K11, thereby effectively modifying Ub-Ub-cyclin A with chains that had twice the MW as those on Ub-cyclin A or Ub^{R11}-Ub-cyclin A (Figure 18A). By using model substrates Ube2S was therefore shown to introduce branches within ubiquitin chains.

4.2.4. Ube2S branches off ubiquitin chains on cyclin A preformed by Ube2C

Next, I determined if Ube2S could also introduce these branches within short ubiquitin chains synthesized by the physiological initiating E2 Ube2C. Ube2C decorates APC/C-substrates with short chains containing ~50% K11-, but also K48- and K63-linkages (Kirkpatrick et al., 2006). If Ube2C produced the latter two linkages, Ube2S could use an internal ubiquitin to branch off a K11-linked chain. To test this hypothesis, Ub-cyclin A was incubated with Ube2C at concentrations that led to formation of short chains (Ub₃-cyclin A; Figure 20).

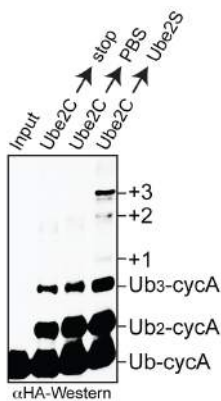


Figure 20: Ube2S synthesizes branched conjugates off chains initiated by Ube2C. 1μM Ub-cyclin A^{HA} was incubated with an estimated 10nM APC/C^{Cdh1} and 1μM Ube2C, which led to selective modification of ubiquitin in Ub-cyclin A (data not shown). After 5min reactions were stopped (stop); or 50μM Ube2C^{C114S}, PBS and methyl-ubiquitin were added to inhibit further initiation (PBS); or 50μM Ube2C^{C114S}, 10μM Ube2S and methyl-ubiquitin were added (Ube2S). Reactions were analyzed by αHA western blot.

The initiation step was stopped with an excess of Ube2C^{C114S}, which does not affect Ube2S activity (Wickliffe et al., 2011a), and then added methyl-ubiquitin and Ube2S. Ube2S attached up to three ubiquitin molecules to Ub₃-cyclin A produced by Ube2C (Figure 20). Consequently Ube2S introduces branches, when Ube2C is used to synthesize the template ubiquitin chain.

4.2.5. Absence of K48 and K63 in ubiquitin leads to decreased ubiquitylation of Ub-cyclin A by Ube2S and Ube2C

In addition to show that Ube2C and Ube2S work together to form branched K11-linked ubiquitin chains, single substrate-turnover reactions (Rape et al., 2006) with ubi^{R48/63} or ubi^{K6/K11} were performed. These mutants support formation of K11-linked chains, but prevent the synthesis of K48 and K63 linkages by Ube2C (Kirkpatrick et al., 2006), that are required for branching by Ube2S. Importantly, Ube2S decorated APC/C substrates with high MW chains in the presence of Ube2C and wt-ubiquitin, but not if Ube2C was omitted or ubi^{R48/63} or ubi^{K6/K11} were used (Figure 21). Less Ube2S activity is seen comparing ubi^{K11} and ubi^{K6/K11} revealing a small caveat in the analysis of ubiquitylations performed with ubi^{K11} (Figure 21B left panel). Thus, the APC/C modifies substrates with branched chains *in vitro*.

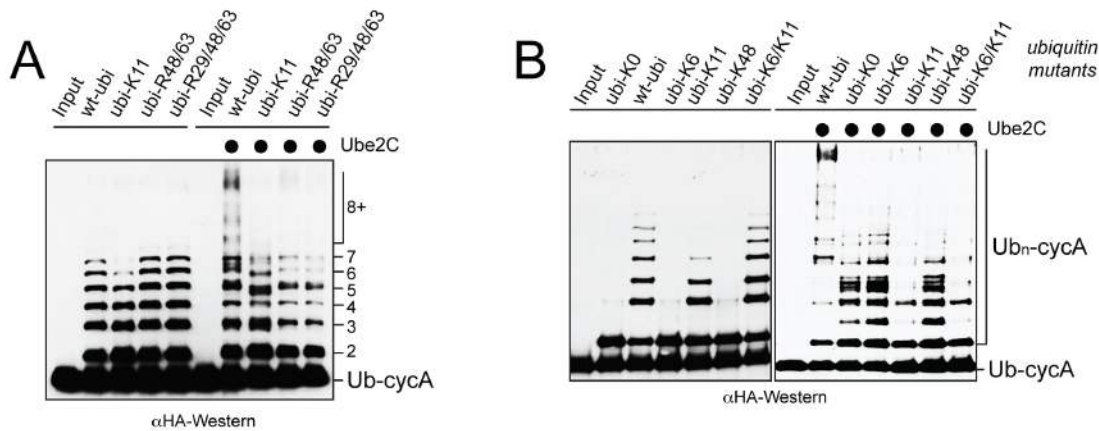


Figure 21: Mutation of K48 and K63 in ubiquitin inhibit formation of longer, branched ubiquitin chains by Ube2S and Ube2C. **A.** APC/C synthesizes branched conjugates with Ube2C and Ube2S. Ub-cyclin A^{HA} was incubated with APC/C^{Cdh1}, Ube2S, or Ube2C and Ube2S, and ubiquitin mutants. The concentrations of Ube2C used for this assay allowed modification of ubiquitin in Ub-cyclin A, but not lysine residues in cyclin A. Reactions were analyzed by western blot against HA. **B.** The APC/C synthesizes branched conjugates with its physiological E2s. Left panel: 1 μ M Ub-cyclin A^{HA} was incubated with an estimated 10nM APC/C^{Cdh1}, Ube2S, and ubiquitin mutants. Ubi^{K6/K11} acts as efficiently as wt-ubiquitin, as it provides residues required for chain formation (K11) and acceptor recognition (K6) (Wickliffe et al., 2011a). The excess of substrate over APC/C guarantees single turnover conditions (Rape et al., 2006). Right panel: Ub-cyclin A^{HA} was incubated with APC/C^{Cdh1}, Ube2C, Ube2S, and ubiquitin mutants. High MW conjugates indicative of branched chains were only observed with wt-ubiquitin, but not with any ubiquitin mutant that inhibited Ube2S (i.e. ubi^{K48}) or branching (i.e. ubi^{K6/K11}). Reactions were analyzed by α HA western blot.

4.3. The APC/C synthesizes branched ubiquitin chains in cells

To further validate these findings I established an assay that directly shows the existing branches within a ubiquitin chain without mutating lysine residues on ubiquitin, which could lead to artifacts by forcing E2s to use other lysine residues than the naturally preferred residues. Mass spectrometry can be used to detect the general kind of ubiquitin linkages (Nishikawa et al., 2004; Peng et al., 2003; Wang et al., 2006; Xu et al., 2009) and even to detect K6/11, K27/29 and K29/33 branches (Kim et al., 2007). Unfortunately several trypsin digestion sites

separated K11/48 and K11/63 branches. Hence, mass spectrometry was only useful for detecting the presence of ubiquitin linkages individually. Because of this, ubiquitin variants with protease cleavage sites were created allowing the detection of K11/48 and K11/63 branches.

4.3.1. Mass spectrometry shows the presence of non-K11-linkages within ubiquitin chains on Nek2A made by Ube2S and Ube2C

I determined by mass spectrometry, which ubiquitin linkages are present, when Nek2a is ubiquitylated by APC/C, Ube2C and Ube2S. Consequently recombinant Nek2A²⁷²⁻⁴⁴⁵ was incubated with APC/C^{Cdc20}, Ube2C and Ube2S, and resolved by SDS-PAGE. The separating gel area between 37 and 250 kDa was excised. Proteins were extracted and digested with trypsin. The QB3/Chemistry Mass Spectrometry Facility at UC Berkeley performed mass spectrometry and analysis. Several independent experiments showed that the APC/C decorated Nek2A with chains containing K11, K48, and K63 linkages (Figure 22). Based on the linkage specificities of Ube2C and Ube2S (Kirkpatrick et al., 2006; Williamson et al., 2009), Ube2S seemed to assemble K11/K48 and K11/K63 branches, which - due to the multiple lysine and arginine residues separating the two attachment sites in the branched ubiquitin - cannot be detected by trypsin-based mass spectrometry. The apparent, higher amount of K11 is in line with Ube2S being able to efficiently synthesize long K11-linked chains using only few K48 or K63 linkages to add a large amount of K11 linkages.

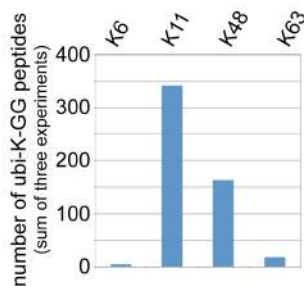


Figure 22: Mass spectrometry detects K11, K48 and K63 linkages within Nek2A ubiquitin conjugates *in vitro*. APC/C^{Cdc20}, Ube2C and Ube2S modify Nek2A with chains containing K11, K48 and K63 linkages. Recombinant Nek2A²⁷²⁻⁴⁴⁵ was incubated with APC/C, Ube2C, Ube2S, and ubiquitin, and reaction products were subjected to mass spectrometry. The sum of ubiquitin linkages from three independent reactions is shown.

Thus, agreeing with previous reports Ube2S and Ube2C build K11 and non-K11-linkages on an APC/C substrate (Kirkpatrick et al., 2006; Williamson et al., 2009a).

4.3.2. Ube2S modifies Ub-cyclin A with TEV-cleavable ubiquitin derivatives

Because of the shortcomings of mass spectrometry an alternative method was developed to monitor formation of branched chains to track the synthesis of such conjugates in cells (Figure 23A). To directly identify the attachments of the C-termini of several donor ubiquitin moieties to one acceptor ubiquitin molecule, I decided to take a similar approach to the mass spectrometry method. Instead of using trypsin, which creates fragments that are too small to detect K11/48 or K11/63 branches, a single protease cleavage site was placed within ubiquitin, C-terminal of K48 to detect K11/48 branches or C-terminal of K63 to detect both K11/48 and K11/63 branches. Once the fragments are created by protease cleavage, the branches will be detected based on an increase in their apparent mass observed by SDS-PAGE. As ubiquitin is fragmented in the process, western blot analysis with ubiquitin antibodies is not feasible and a tag was placed C-terminal of the protease cleavage site. This allows for detection of N-terminal ubiquitin fragments modified with tagged C-terminal ubiquitin fragments. C-terminal of two ubiquitin residues, G53 and E64, located in loop regions of ubiquitin, insertion of a TEV-cleavage site (ubi^{53TEV}) plus a FLAG-epitope in the case of E64 (ubi^{64TEV/FLAG}) was successful. The resulting derivatives were still recognized by E1, Ube2S and APC/C (Figure 23B). Ub-cyclin A was modified with ubi^{53TEV} or ubi^{64TEV/FLAG} and treated with TEV protease. Almost complete cleavage was observed for ubi^{53TEV} and complete cleavage for ubi^{64TEV/FLAG}. A mixture of ubi^{53TEV} and ubi^{64TEV/FLAG} seemed to give the most turnover of Ub-cyclin A and highest amount of ubi^{53TEV} or ubi^{64TEV/FLAG} cleaved fragments on Ub-cyclin A (Figure 23B). Addition of a TEV cleavage site C-terminal of L71 was detrimental towards ubiquitylation activity (Figure 23B) likely due to blocked recognition of the ubiquitin C-terminus by E1 (Olsen and Lima, 2013).

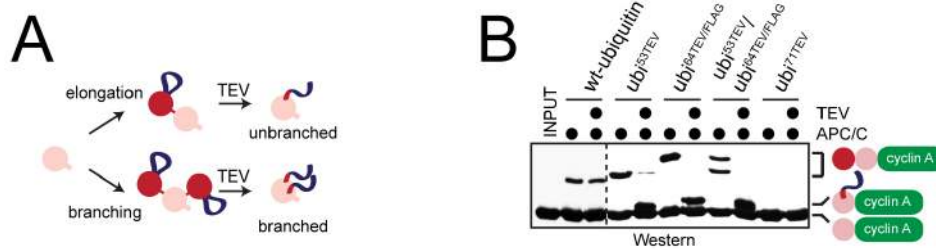


Figure 23: APC/C and Ube2S can use ubiquitin with an internal cleavage site and FLAG epitope. **A.** Outline of a method to monitor synthesis of branched chains. A TEV-site and FLAG-epitope ($\text{ubi}^{\text{TEV/FLAG}}$) were introduced into ubiquitin. Cleavage of $\text{ubi}^{\text{TEV/FLAG}}$ -conjugates reveals a ~2kDa stamp for elongation or multiple stamps for branching. **B.** $\text{Ubi}^{\text{TEV/FLAG}}$ is recognized by Ube2S and APC/C, and sensitive to TEV cleavage. Ub-cyclin A^{HA} was incubated with APC/C^{Cdh1}, Ube2S, and wt-ubiquitin or ubi^{TEV} mutants. Reactions were treated with TEV and analyzed by α HA-Western.

To further validate this new system ³⁵S-radiolabeled cyclin A was modified with $\text{ubi}^{53\text{TEV}}$ or $\text{ubi}^{64\text{TEV/FLAG}}$ and subsequently the reaction products were treated with TEV-protease. This led to the collapse of long chains and the emergence of supposedly diagnostic FLAG-reactive peptides, when $\text{ubi}^{64\text{TEV/FLAG}}$ was present: while modification of a distal moiety produced a small cleavage product (Figure 23B), ubiquitin branches or multiple ubiquitylation sites on cyclin A were detected as additional species of higher MW (Figure 24A). Use of both $\text{ubi}^{53\text{TEV}}$ and $\text{ubi}^{64\text{TEV/FLAG}}$ proved to be most efficient for detecting ubiquitin branches (data not shown). A time course showed that the addition of $\text{ubi}^{53\text{TEV}}$ or $\text{ubi}^{64\text{TEV/FLAG}}$ to an already present ubiquitin moiety does not impede the transfer of ubiquitin by Ube2S compared to addition of wt-ubiquitin (Figure 24B).

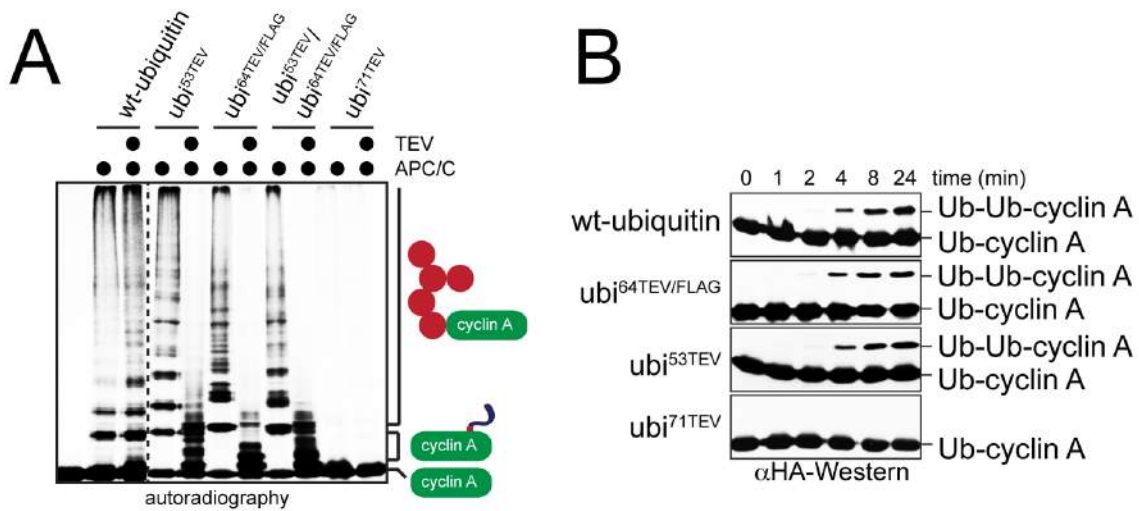


Figure 24: APC/C, Ube2C and Ube2S can use ubi^{53TEV} or ubi^{64TEV/FLAG} to modify cyclin A with polyubiquitin chains. **A.** ³⁵S-cyclin A was incubated with APC/C^{Cdh1}, Ube2C, Ube2S, and wt-ubiquitin, ubi^{53TEV} or ubi^{64TEV/FLAG} proteins. Reactions were treated with TEV and analyzed by autoradiography. **B.** The APC/C and Ube2S are able to use ubi^{53TEV} or ubi^{64TEV/FLAG}. Ub-cyclin A^{HA} was incubated with APC/C^{Cdh1}, Ube2S, and ubiquitin mutants, and reaction products were analyzed by α HA western blot.

4.3.3. Detection of branched ubiquitin fragments on cyclin A and Nek2A *in vitro*

Next I determined if the developed assay was suitable to detect branches within ubiquitin chains. To exclude the detection of artifacts the formation of homogenous chains with Ube2S and ubiquitin fusions of cyclin A and Nek2A²⁷²⁻⁴⁴⁵ were monitored at the same time (Figure 25A). Additionally a control reaction was performed without addition of TEV after ubiquitylation, checking for the occurrence of artifacts when using ubi^{53TEV} and ubi^{64TEV/FLAG}. Mixing recombinant cyclin A, APC/C^{Cdh1}, Ube2S, Ube2C, ubi^{53TEV} and ubi^{64TEV/FLAG} led to the formation of branched ubiquitin conjugates, which were detected by FLAG western blot analysis after TEV treatment (Figure 25B). The same was observed when Nek2A²⁷²⁻⁴⁴⁵ was tested (Figure 25C). In both cases the lanes not containing TEV show the presence of free intact ubi^{64TEV/FLAG} at the bottom.

Results

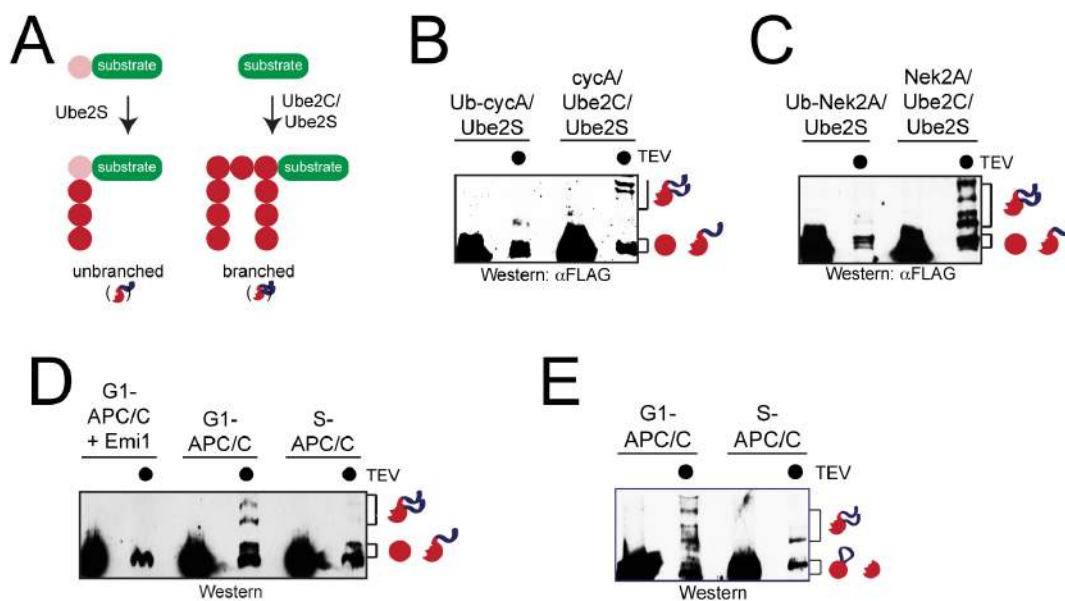


Figure 25: Detection of branched ubiquitin fragments on cyclin A and Nek2A *in vitro*. **A.** Cartoon depicting the outcome compared between control reaction of Ube2S with ubiquitin fusion of a substrate producing homogenous chains and test reaction of Ube2C and Ube2S with substrate producing branched chains. **B.** Ub-cyclin A^{HA} was incubated with APC/C^{Cdh1}, Ube2S, ubi^{53TEV} and ubi^{64TEV/FLAG} to add homogenous K11-linked chains; alternatively, cyclin A was modified by APC/C^{Cdh1}, Ube2C, Ube2S, ubi^{53TEV} and ubi^{64TEV/FLAG} with branched chains. Reactions were treated with TEV and analyzed by 20% tricine gels and α FLAG western blot. **C.** Ub₃-Nek2A²⁷²⁻⁴⁴⁵ was incubated with APC/C^{Cdh1}, Ube2S, ubi^{53TEV} and ubi^{64TEV/FLAG} to add homogenous K11-linked chains; alternatively, Nek2A²⁷²⁻⁴⁴⁵ was modified by APC/C^{Cdh1}, Ube2C, Ube2S, ubi^{53TEV} and ubi^{64TEV/FLAG} with branched chains. Reactions were treated with TEV and analyzed by 20% tricine gels and α FLAG western blot. **D.** Nek2A²⁷²⁻⁴⁴⁵ was incubated with APC/C, Ube2C, Ube2S, ubi^{53TEV} and ubi^{64TEV/FLAG}. APC/C was purified from G1 phase, when it is active, or S phase, when APC/C-activity is low. APC/C^{Cdh1} was also inhibited by Emi1. Reactions were treated with TEV and analyzed by 20% tricine gels and α FLAG western blot. **E.** Branching is impeded by a ubiquitin mutant that does not have lysine residues used by Ube2C and Ube2S. Nek2A²⁷²⁻⁴⁴⁵ was incubated with APC/C^{Cdh1}, Ube2C, Ube2S, ubi^{53TEV} and ubi^{64TEV/FLAG}. In the right reaction, ubiquitin with mutant K11R, K48R, and K63R was utilized. Reaction products were treated with TEV and analyzed by 20% tricine gels and α FLAG western blot.

The lanes containing TEV show a band at similar MW to intact ubi^{64TEV/FLAG} either because of modification of one ubiquitin moiety by another single moiety or incomplete cleavage of free ubi^{64TEV/FLAG}, which is unlikely due to the high excess of used TEV. Any band at a slightly higher MW represents the introduction of

branches in the former ubiquitin conjugates. The combinatorial possibilities of multiple branches and presence of ubi^{53TEV} and ubi^{64TEV/FLAG} led to multiple higher MW species (Figure 25C). The formation of ubiquitin branches on Nek2A were only observed if active APC/C was present, as inhibition by the APC/C-inhibitor Emi1 (Reimann et al., 2001) or usage of inactive APC/C immunoprecipitated from HeLa cell extract synchronized in S-phase by a double thymidine arrest (Rape and Kirschner, 2004) ablated formation of ubiquitin branches (Figure 25D). The majority of detected fragments were K11/48, K11/63 or theoretically K48/K63, because the mutation of K11, K48 and K63 to arginine in the used ubiquitin variants inhibited the detection of these branched ubiquitin fragments (Figure 25E). Therefore the here-described assay detects the presence of K11/48 and K11/63 branched ubiquitin conjugates on APC/C substrates.

4.3.4. K11-linked ubiquitin chains co-purify with the APC/C

To determine whether the APC/C synthesizes branched chains *in vivo*, significant amounts of ubiquitin conjugates that were made in prometaphase by APC/C had to be purified. Strikingly α K11 western blot analysis revealed the co-purification of enriched K11-linked ubiquitin conjugates in APC/C immunoprecipitations from thymidine and nocodazole arrested HeLa cells (Figure 26A; Matsumoto et al., 2010). Immunoprecipitations were performed with an antibody against Cdc27, which is an integral subunit of the APC/C (Barford, 2011). The presence of these ubiquitin conjugates was dependent on Ube2S as depletion of Ube2S by siRNA decreased the amount of ubiquitin conjugates in APC/C immunoprecipitations (Figure 26A). To confirm the existence of K11-linked ubiquitin conjugates co-purifying with the APC/C and to exclude the detection of artifacts by the K11 antibody, APC/C immunoprecipitations were treated with the K11-specific DUB Cezanne (Bremm et al., 2010). The disappearance of signal in the α K11 western blot over time due to Cezanne, corroborates the isolation of K11-linked ubiquitin conjugates from HeLa cells in prometaphase (Figure 26B).

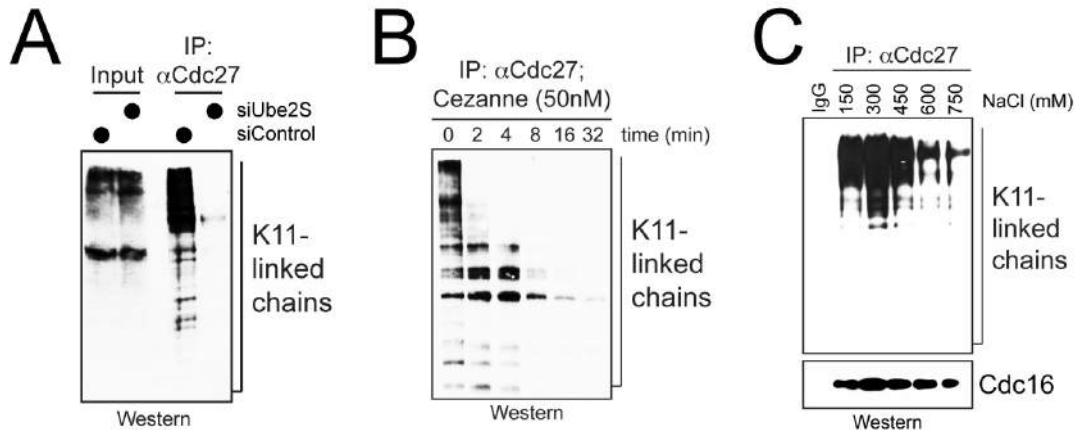


Figure 26: APC/C substrate K11 ubiquitin conjugates can be co-purified by APC/C immunoprecipitation. **A.** APC/C was purified from nocodazole arrested HeLa cells transfected with control or Ube2S siRNA and analyzed for co-purifying K11-linked chains using α K11 western blot analysis. **B.** Chains co-purifying with mitotic APC/C are disassembled by the K11-specific DUB Cezanne. Immunoprecipitated APC/C from nocodazole arrested HeLa cells was treated with 50nM Cezanne and binding of K11-modified proteins was determined by α K11-western blot analysis. **C.** Chains co-purifying with mitotic APC/C can be washed off by high-salt buffers. Immunoprecipitated APC/C from nocodazole arrested HeLa cells was treated with buffers containing increasing concentrations of sodium chloride and binding of K11-modified proteins was determined by α K11 western blot analysis.

The purified ubiquitin conjugates could either be attached to APC/C subunits itself due to autoubiquitylation or to APC/C substrates. Sodium chloride at increasing concentrations should be able to inhibit the interaction of APC/C substrates with the APC/C, as this interaction is relatively weak and mainly electrostatic (da Fonseca et al., 2011). Indeed, the amount of K11-linked ubiquitin conjugates is drastically lowered at 600 or 750mM salt, while the APC/C stays intact based on the Cdc16 levels in a Cdc27 immunoprecipitation (Figure 26C). APC/C cofactors and E2s could technically be washed off as well, but are considered substrates of the APC/C as well (Ge et al., 2009; Listovsky et al., 2004; Rape and Kirschner, 2004; Williamson et al., 2009a). Consequently K11-linked ubiquitin conjugates were attached to endogenous substrates that remained bound to the APC/C following their modification. Hence mitotic APC/C co-purifies with its K11 modified substrates.

4.3.5. Detection of branched ubiquitin chains co-purifying with the APC/C *in vivo*

I developed an approach to detect ubiquitin branches directly *in vitro* and showed that the isolation of ubiquitin conjugates on APC/C substrates in cells was possible. These two methods were therefore combined to show if ubiquitin branching on APC/C substrates would occur in cells. Consequently FLAG-ubi^{53TEV} and His-ubi^{64TEV/FLAG} were expressed in 293T cells, which did not change general ubiquitin levels (Figure 27A). Asynchronous 293T cells were used instead of synchronized HeLa cells, as 293T cells allow higher expression of exogenous proteins in general.

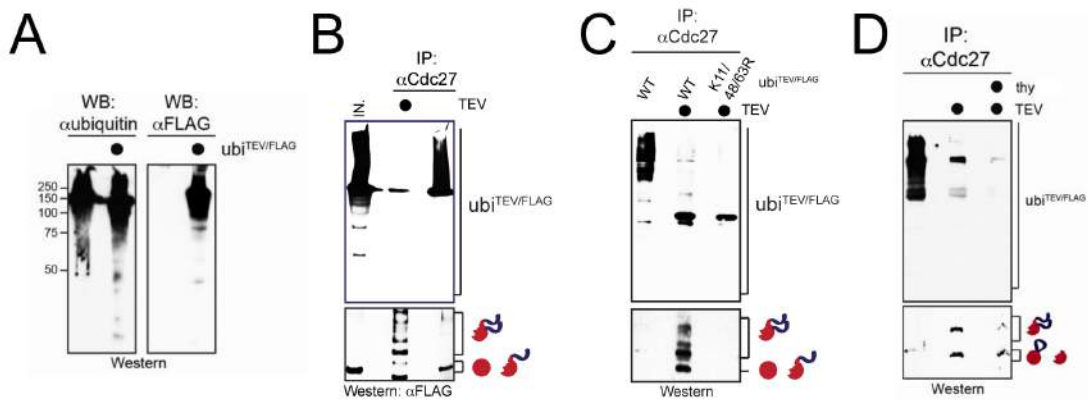


Figure 27: Detection of branched ubiquitin chains co-purifying with the APC/C *in vivo* **A.** Expression of ubi^{TEV/FLAG} does not change ubiquitin levels in cells. Lysates of 293T cells transfected with FLAG-ubi^{53TEV} and His-ubi^{64TEV/FLAG} were probed for ubiquitin and the FLAG epitope by western blot. **B.** APC/C synthesizes branched chains *in vivo*. APC/C was purified from 293T cells expressing FLAG-ubi^{53TEV} and His-ubi^{64TEV/FLAG}, treated with TEV, and analyzed by α FLAG western blot. Upper panel: conjugates co-purifying with APC/C. Lower panel: MW range for diagnostic peptides (longer exposure). Ubiquitin detected in reactions without TEV is produced by DUBs that co-precipitate with APC/C. **C.** APC/C was purified from 293T cells expressing wt- or Lys-mutant FLAG-ubi^{53TEV} and His-ubi^{64TEV/FLAG}, treated with TEV, and analyzed for co-purifying conjugates (upper panel) or diagnostic peptides (lower panel). **D.** APC/C was precipitated from 293T cells expressing FLAG-ubi^{53TEV} and His-ubi^{64TEV/FLAG}, treated with TEV as shown and analyzed by α FLAG western blot. As indicated, APC/C was purified from cells enriched in S phase by thymidine treatment (thy).

Results

The APC/C was purified from 293T cells expressing $^{FLAG}ubi^{53TEV}$ and $^{His}ubi^{64TEV/FLAG}$ with co-precipitating substrates, and the samples were treated with TEV. These experiments showed that endogenous APC/C-substrates were modified with branched chains, while the branching pattern reflecting that of the *in vitro* analyses (Figure 27B). The formation of branched linkages was severely reduced upon expression of $ubi^{R11/48/63}$ in the $^{FLAG}ubi^{53TEV}$ and $^{His}ubi^{64TEV/FLAG}$ background (Figure 27C), a mutant that obliterated branching *in vitro* (Figure 25E), showing that also *in vivo* mainly K11/48 and K11/63 ubiquitin branches are formed. Furthermore was APC/C activity needed *in vivo*, as 293T cells overexpressing $^{FLAG}ubi^{53TEV}$ and $^{His}ubi^{64TEV/FLAG}$ showed reduced levels of the predominant branching fragment, when arrested in S phase by thymidine treatment (Figure 27D). In summary APC/C introduces ubiquitin branches in cells, which were detected in APC/C co-purifying ubiquitin conjugates of endogenous substrates.

4.3.6. Detection of branched ubiquitin chains attached to APC/C substrates *in vivo*

To test whether the APC/C modifies Nek2A with branched chains in cells, the newly developed approach was used in combination with exogenously expressed $^{HA}Nek2A$ and a classical approach with expressing ubiquitin mutants was used with other APC/C substrates, namely geminin and NuSAP (Li et al., 2007a; McGarry and Kirschner, 1998). First, 293T cells were transfected with $^{HA}Nek2A$, $^{FLAG}ubi^{53TEV}$ and $^{His}ubi^{64TEV/FLAG}$ and treated for six hours with 20 μ M MG132. Treatment of HA-immunoprecipitations with TEV revealed a fraction of branched chains, similar to the modification of Nek2A with such conjugates *in vitro* (Figure 28A). These findings were supported by the second approach showing that expression of $^{His}ubi^{K6/11}$ and similarly $^{His}ubi^{K11}$, a mutant that allows formation of K11-linked chains, but prevents branched conjugates, strongly impaired the modification of APC/C-substrates in cells (Figure 28B). Expression

of GFP was used to control for equal transfection efficiency. Hence, the APC/C assembles branched chains in cells and Nek2A is a substrate for this modification.

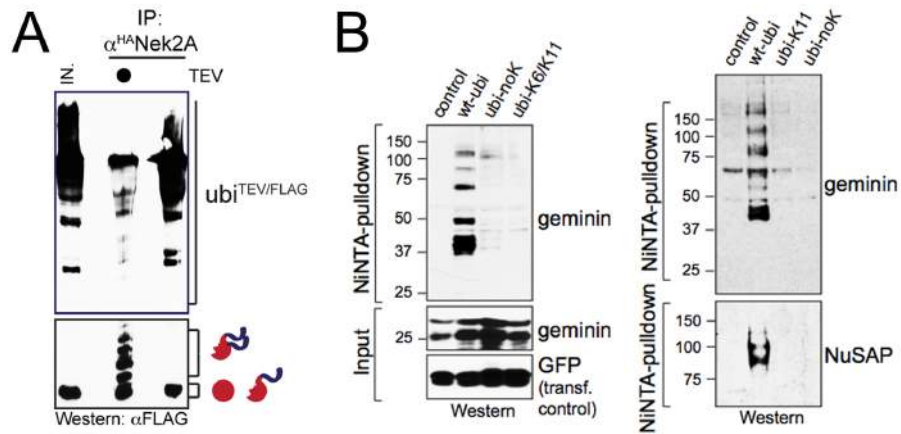


Figure 28: Detection of branched ubiquitin chains attached to APC/C substrates *in vivo*. **A.** Nek2A is modified with branched chains in cells. ^{HA}Nek2A was purified from cells expressing FLAG_{ubi^{53TEV}} and His_{ubi^{64TEV/FLAG}} and treated with TEV. Reactions were analyzed by αFLAG western blot. **B.** APC/C requires multiple ubiquitin lysine residues for efficient substrate modification *in vivo*. 293T cells were transfected with geminin or NuSAP, His-tagged wt- or mutant ubiquitin, and GFP as control. Ubiquitylated proteins were purified under denaturing conditions and detected by western blotting. Probably due to high activity of DUBs monoubiquitylation or short chains cannot be detected under these conditions (see the ubi-noK control).

4.4. Altering the linkage-specificity of metazoan APC/C

To determine specific functions of branched chains, another experimental system was required, which allowed me to compare the fate of a substrate decorated with different distinct homogenous chains or branched conjugates that resulted from a combination of these distinct chain types respectively. Such experiments are difficult to perform with Ube2C, as this E2 produces chains of mixed topology. To overcome this limitation, a K48-specific APC/C-E2 was engineered, which together with the physiological E2s enabled me to modify substrates either with K11-, K48-linked, or K11/K48 branched chains.

4.4.1. Ube2S without its CTP does not bind APC/C

To generate an APC/C E2 with new linkage specificity, Ube2S was imitated, in the way it stably binds to APC/C (Williamson et al., 2009a). Ube2S consists of a catalytic N-terminal ubiquitin conjugating (UBC) domain connected to a stretch of positively charged residues at the C-terminus (CTP) via a linker region (Figure 29A).

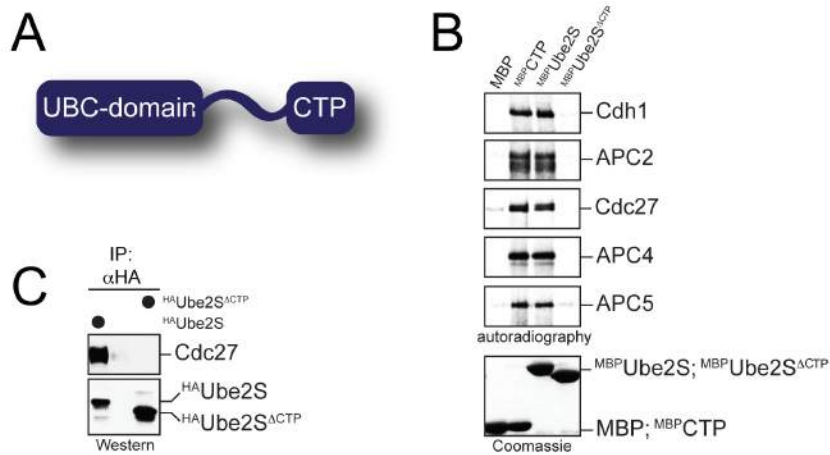


Figure 29: The CTP of Ube2S is essential for binding to the APC/C. **A.** Ube2S consists of a catalytic UBC domain and a C-terminal peptide (CTP) connected by a linker region. **B.** The CTP is required and sufficient for APC/C-binding of Ube2S *in vitro*. ^{35}S -labeled APC/C-subunits were incubated with immobilized MBP, $^{\text{MBP}}\text{CTP}$, $^{\text{MBP}}\text{Ube2S}$, or $^{\text{MBP}}\text{Ube2S}^{\Delta\text{CTP}}$. Binding reactions were analyzed by autoradiography. **C.** The CTP is required for APC/C-binding of Ube2S in cells. $^{\text{HA}}\text{Ube2S}$ or $^{\text{HA}}\text{Ube2S}^{\Delta\text{CTP}}$ were precipitated from HeLa cells, and co-purifying APC/C was detected by αCdc27 western blot analysis.

To determine the main binding surface on Ube2S, MBP as a control, $^{\text{MBP}}\text{Ube2S}$ or $^{\text{MBP}}\text{Ube2S}^{\Delta\text{CTP}}$ were immobilized on amylose-resin, as shown in the Coomassie stained gel (Figure 29B), and incubated with ^{35}S -radiolabeled APC/C subunits (APC2, Cdc27, APC4 and APC5) or an APC/C coactivator Cdh1. Autoradiography showed that $^{\text{MBP}}\text{Ube2S}$ was able to bind all APC/C components, which is likely due to incorporation of radiolabeled proteins into APC/C complexes present in the reticulocyte lysate (Figure 29B). On the other hand binding of all APC/C components was lost if the region C-terminal of the UBC

domain in Ube2S was deleted (Figure 29B) showing that the main binding motif of Ube2S for the APC/C lies within its C-terminus. To further validate this finding in cells, 293T cells were transfected with either full-length (FL) ^{HA}Ube2S or a C-terminal deletion ^{HA}Ube2S^{ΔCTP}. HA-immunoprecipitations showed that only the FL version pulled down endogenous Cdc27 (Figure 29C). Consequently the CTP of Ube2S is essential for binding to APC/C in cells.

4.4.2. The CTP is sufficient for APC/C-binding

The next step to generate an APC/C E2 with new linkage specificity was to test, if the CTP was not only essential for binding to the APC/C, but if it was also sufficient for targeting to the APC/C. To determine this *in vitro* the CTP was coupled to biotin (Williamson et al., 2009a), immobilized on streptavidin agarose and incubated with ³⁵S-radiolabeled APC/C components.

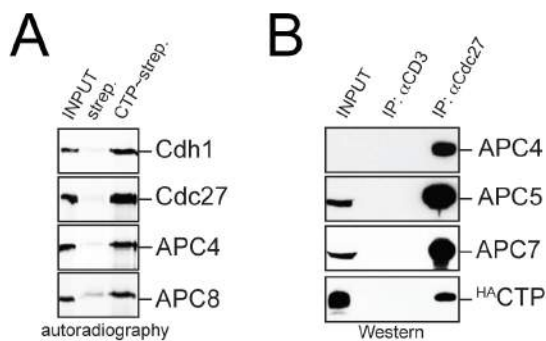


Figure 30: The CTP is sufficient for APC/C binding **A.** The CTP is sufficient for APC/C binding *in vitro*. Biotinylated CTP was immobilized on streptavidin agarose, incubated with ³⁵S-labeled APC/C subunits and analyzed by autoradiography. **B.** The CTP is sufficient for APC/C-binding in cells. APC/C was purified from 293T cells

expressing ^{HA}CTP and binding reactions were analyzed by western blot against the respective APC/C component or HA.

Autoradiography revealed enrichment of APC/C components on CTP coupled beads compared to the streptavidin resin control, showing the CTP is sufficient for binding to the APC/C *in vitro* (Figure 30A). This was further validated by using ^{MBP}CTP (Figure 29B). To determine if the CTP is also enough for binding to endogenous APC/C in cells, ^{HA}CTP was expressed in 293T cells. By western blot analysis the presence of ^{HA}CTP was only observed in APC/C immunoprecipitations showing the capability of the CTP for binding to the APC/C

in vivo (Figure 30B). Thus the CTP is sufficient for APC/C targeting *in vitro* and *in vivo*.

4.4.3. Ube2G2^{CTP} binds the APC/C *in vitro* and *in vivo*

Several UBC domains of E2s were tested to engineer a novel APC/C E2 with a ubiquitin linkage specificity distinct from the K11 specificity of Ube2S (data not shown). In the end it was decided respectively to fuse FL Ube2G2 to the CTP (Ube2G2^{CTP}). Ube2G2 is a K48 specific E2 normally working with the E3 gp78 to degrade substrates of the endoplasmic-reticulum-associated protein degradation (ERAD) pathway (Fang et al., 2001; Li et al., 2007b). First it had to be determined, if Ube2G2^{CTP} can actually bind the APC/C. MBP, ^{MBP}Ube2S, ^{MBP}Ube2G2^{CTP}, ^{MBP}Ube2S^{ΔCTP} and ^{MBP}Ube2G2 were bound to amylose-resin (Figure 31A: Coomassie stained gel) and incubated with ³⁵S-radiolabeled APC/C components Cdc27 or Cdh1. Autoradiography revealed that only ^{MBP}Ube2S and ^{MBP}Ube2G2^{CTP} bind the APC/C (Figure 31A), showing that Ube2G2 by itself does not interact with the APC/C, while Ube2G2^{CTP} is able to bind the APC/C *in vitro*. To test if Ube2G2^{CTP} is targeted to the APC/C *in vivo* as well, HeLa cells constitutively expressing untagged Ube2G2^{CTP} were generated. The predicted MW of Ube2S is 23.8kDa, but the apparent MW of Ube2S in SDS PAGE seems to be slightly above 25kDa. The predicted MW of Ube2G2^{CTP} is 22.5kDa, which seems to be in line with its apparent MW in SDS PAGE allowing clear separation and detection of both Ube2S and Ube2G2^{CTP} by Ube2S western blot analysis (Figure 31B). An extract of a generated Ube2G2^{CTP} cell line was used for immunoprecipitation of APC/C. Ube2S and Ube2G2^{CTP} both co-purified with precipitated APC/C, while a control immunoprecipitation (CD3) excluded unspecific binding (Figure 31B). Taken together, this indicates that Ube2G2^{CTP} binds APC/C *in vitro* and in cells.

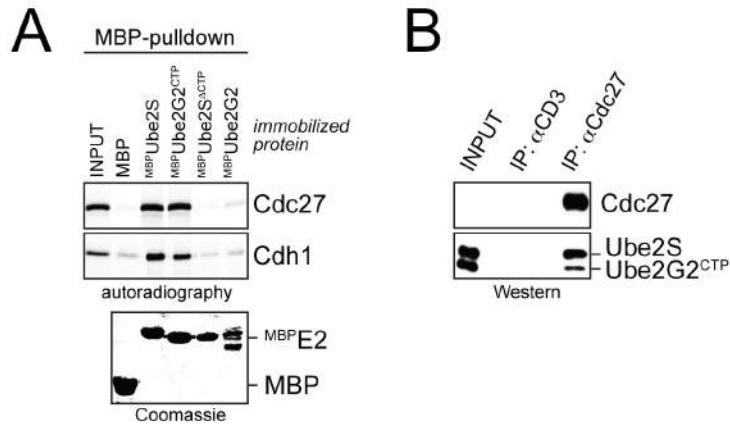


Figure 31: Ube2G2^{CTP} binds the APC/C *in vitro* and *in vivo*. **A.** Ube2G2^{CTP} binds APC/C *in vitro*. Binding of ³⁵S-labeled Cdc27 or Cdh1 to immobilized MBP, MBP Ube2S, MBP Ube2G2, MBP Ube2G2^{CTP}, or MBP Ube2S^{ΔCTP} was analyzed by autoradiography. **B.** Ube2G2^{CTP} binds APC/C in cells. APC/C was immunoprecipitated from extracts of HeLa cells constitutively expressing Ube2G2^{CTP} with αCD3- or αCdc27-antibodies, and co-purifying Ube2S and Ube2G2^{CTP} were detected by the Ube2S antibodies recognizing the CTP.

4.4.4. Ube2G2^{CTP} ubiquitylates APC/C substrates

After confirming the ability of Ube2G2^{CTP} to interact with APC/C, I tested, if the newly engineered E2 was able to modify APC/C substrates with ubiquitin. ³⁵S-labeled cyclin A, APC/C^{Cdh1}, and either no E2, Ube2G2 or Ube2G2^{CTP} with the other necessary ubiquitylation components were incubated. Autoradiography visualized the outcome of the reaction. The presence of an E2 was necessary for ubiquitylation of cyclin A (Figure 32A). Luckily the designed Ube2G2^{CTP} was able to polyubiquitylate cyclin A. Ubiquitylation activity of Ube2G2^{CTP} was dependent on the CTP, as Ube2G2 did not modify cyclin A (Figure 32A). Furthermore catalyzed Ube2G2^{CTP} the formation of ubiquitin chains on geminin at a rate similar to Ube2S (Figure 32B). Ube2C had to be added to these reactions at 100nM, as Ube2G2^{CTP} shows slower ubiquitylation of substrate lysine residues than Ube2C (data not shown). Ubiquitylation reactions of cyclin A with Ube2G2^{CTP} were sensitive to inhibition by Emi1 or excess of another APC/C

Results

substrate (Rape et al., 2006), here securin, the same way Ube2S is inhibited under these conditions (Figure 32C). Respectively, Ube2G2^{CTP} ubiquitylates APC/C substrates similar to Ube2S *in vitro*.

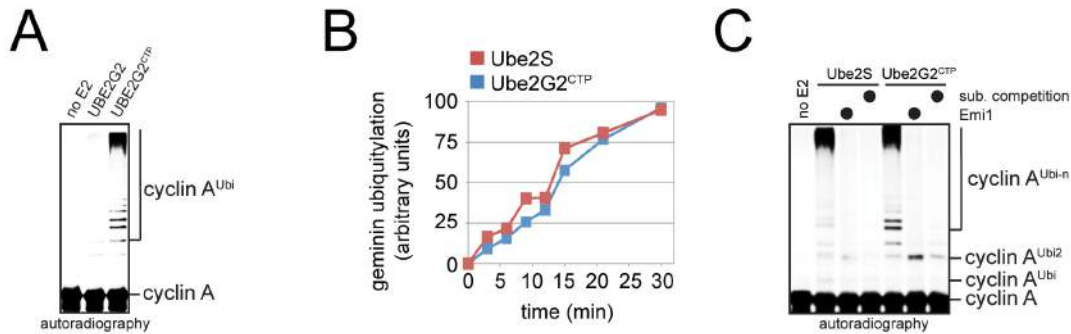


Figure 32: Ube2G2^{CTP} ubiquitylates APC/C substrates. **A.** Ube2G2^{CTP} ubiquitylates cyclin A. ³⁵S-cyclin A was incubated with APC/C^{Cdh1} and no E2, Ube2G2, or Ube2G2^{CTP} for 30min at 30°C. Reactions were analyzed by autoradiography. **B.** Ube2G2^{CTP} catalyzes ubiquitylation of geminin with similar efficiency as Ube2S. ³⁵S-labeled geminin was incubated with APC/C^{Cdh1}, low levels of Ube2C for initiation, and either Ube2G2^{CTP} or Ube2S for the indicated time points at 25°C. Reactions were analyzed by autoradiography and quantified using ImageJ. **C.** ³⁵S-labeled cyclin A was incubated with APC/C^{Cdh1}, low levels of Ube2C, and Ube2G2^{CTP} or Ube2S. APC/C was inhibited by Emi1 or an excess of recombinant securin, an APC/C-substrate. Reactions were analyzed by autoradiography.

4.4.5. Ube2G2^{CTP} requires a functional catalytic E2 domain and APC/C substrate recognition motifs

Next I investigated if engineered Ube2G2^{CTP} still catalyzed ubiquitin transfer in the same way Ube2G2 and other E2s do regarding its catalytic site. The most obvious requirement for ubiquitin transfer within an E2 is its active site cysteine residue. Mutation of the active site cysteine C89 to serine (C89S) led to the abrogation of Ub-cyclin A ubiquitylation activity of Ube2G2^{CTP} detected by K48 western blot analysis (Figure 33A). Mutating the catalytic domain of Ube2G2^{CTP} further corroborated this. Deletion of the acidic loop (A95-A107) close to the active site of Ube2G2^{CTP} inhibited ubiquitin transfer (Figure 33B) as reported for Ube2G2 (Li et al., 2007b).

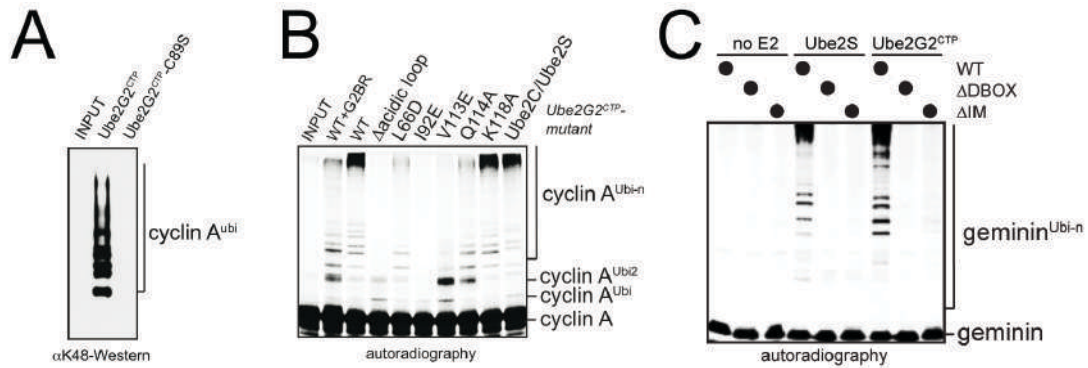


Figure 33: Ube2G2^{CTP} requires a functional catalytic E2 domain and APC/C substrate recognition motifs for ubiquitylation. **A.** The catalytic cysteine is required for Ube2G2^{CTP}-activity towards APC/C-substrates. Ub-cyclin A was incubated with APC/C^{Cdh1} and Ube2G2^{CTP} or Ube2G2^{CTP}-C89S, and reactions were analyzed by αK48-linkage specific western blot. **B.** Ube2G2^{CTP} requires its RING-domain interaction loop for activity with APC/C. ³⁵S-labeled cyclin A was incubated with APC/C^{Cdh1} and indicated Ube2G2^{CTP}-mutants. Reactions were analyzed by autoradiography. **C.** ³⁵S-geminin or mutants in its D-box (DBOX) or initiation motif (IM) were incubated with APC/C^{Cdh1}, low levels of Ube2C, and Ube2G2^{CTP} or Ube2S. Reactions were analyzed by autoradiography.

Mutation of the surface responsible for interaction with the RING finger also inhibited Ube2G2^{CTP} activity (Figure 33B) as published (Das et al., 2009). Therefore, Ube2G2^{CTP} supposedly interacts with the APC/C RING finger to ubiquitylate APC/C substrates. Addition of a peptide representing the portion of gp78 that interacts with Ube2G2 (Das et al., 2009) reduced ubiquitylation by Ube2G2^{CTP} indicating that this allosterically activated conformation of Ube2G2^{CTP} is reduced in its ability to bind the APC/C RING domain or that the peptide is competing with the APC/C RING for binding to Ube2G2^{CTP}. Additionally Ube2G2^{CTP} needed the same APC/C substrate recognition motifs as the physiological APC/C E2s. Geminin with mutations in its destruction box (DBOX) or initiation motif (IM) was used for this purpose (Williamson et al., 2011). Wt-geminin or its mutants were incubated with no E2s as a control, Ube2S as the physiological E2 or Ube2G2^{CTP}. Autoradiography showed that Ube2G2^{CTP} relies on the same APC/C substrate interactions as Ube2S (Figure 33C). In summary

Ube2G2^{CTP} requires an active site cysteine, RING finger interaction and APC/C substrate recognition motifs to ubiquitylate APC/C substrates.

4.4.6. Ube2G2^{CTP} synthesizes K48-linked ubiquitin chains on cyclin A

As Ube2G2^{CTP} was shown to be active with the APC/C, it was determined if it retained the K48 linkage specificity of the original Ube2G2 or if the APC/C could change its linkage specificity. Radiolabeled cyclin A was incubated with APC/C, the respective ubiquitin mutants and Ube2S or Ube2G2^{CTP}. The use of wt-ubiquitin or ubiquitin mutants with only a single lysine residue (all other lysine residues were mutated to arginine) revealed that the linkage specificity of the APC/C switched from K11 to K48 using Ube2G2^{CTP} instead of Ube2S, as Ube2S supported formation of ubiquitin chains using ubi^{K11}, while Ube2G2^{CTP} ubiquitylated cyclin A using ubi^{K48} (Figure 34A). Remarkably the linkage specificity of the 1.5MDa large APC/C is consequently determined by the 15kDa large UBC domain of its E2. At this point it should be mentioned, that APC/C immunoprecipitations as the source in these reactions had to be washed with 500mM sodium chloride to isolate almost Ube2S free APC/C (data not shown). A small amount of Ube2S possibly still remained bound explaining negligible amounts of K11-linked chains in the ubi^{K11} lane of Ube2G2^{CTP} (Figure 34A). The same result is achieved, if the experiment is done with the reverse ubiquitin mutants. Instead of using mutants with a single lysine residue, ubiquitin mutants with a single lysine to arginine substitution were employed. Again Ube2S synthesized K11 chains on cyclin A shown by the inhibition of ubiquitylation in the presence of ubi^{R11}, while Ube2G2^{CTP} ubiquitylated cyclin A with K48 chains based on inhibition by ubi^{R48} (Figure 34B). Ubiquitin linkage specific antibodies (Matsumoto et al., 2010; Newton et al., 2008) allow to determine the linkage of wt-ubiquitin conjugates. This approach becomes important as E2s can change their linkage specificity if used in combination with ubiquitin mutants (Wickliffe et al., 2011a). Hence, recombinant Ub-cyclin A was incubated with either Ube2S or Ube2G2^{CTP} and the resulting reaction products were analyzed by α K11, α K48 or

Results

α cyclin A western blot. In the presence of APC/C, both Ube2S and Ube2G2^{CTP} form substrate attached ubiquitin conjugates linked through K11 or K48 (Figure 34C). Use of ubiquitin mutants or linkage specific antibodies demonstrated that Ube2G2^{CTP} modified APC/C-substrates with K48-linked chains switching the linkage specificity of the APC/C from K11 to K48.

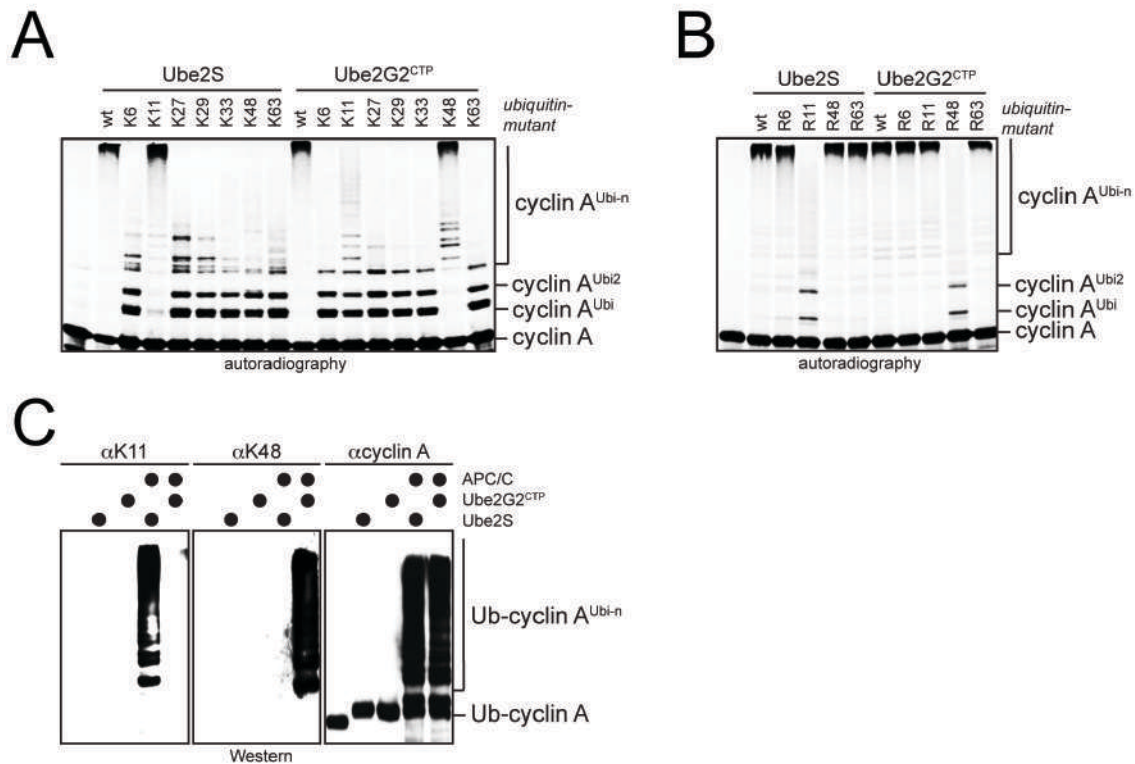


Figure 34: Ube2G2^{CTP} synthesizes K48-linked ubiquitin chains on cyclin A. **A.** Ube2G2^{CTP} catalyzes chain formation with ubi^{K48}. ³⁵S-cyclin A was incubated with APC/C^{Cdh1}, low levels of Ube2C, Ube2S or Ube2G2^{CTP}, and ubiquitin mutants. Reactions were analyzed by autoradiography. **B.** Ube2G2^{CTP} requires K48 of ubiquitin for chain formation. ³⁵S-cyclin A was incubated with APC/C^{Cdh1}, low levels of Ube2C, Ube2S or Ube2G2^{CTP}, and ubiquitin variants. Reactions were analyzed by autoradiography. **C.** Ube2G2^{CTP} catalyzes K48-linked chain formation with APC/C. Ub-cyclin A was incubated with APC/C^{Cdh1}, either Ube2S or Ube2G2^{CTP}, and ubiquitin. Reaction products were analyzed by western blot.

4.5. Ube2G2^{CTP} and Ube2S synthesize branched K11/K48-linked chains

I created a novel E2 producing K48 ubiquitin conjugates on APC/C substrates. Using this tool it was tested if the combination of both K11 and K48 linkages would lead to the attachment of larger ubiquitin conjugates to APC/C substrates as an additional and elegant proof of principle for ubiquitin chain branching. It was carefully analyzed, if K11 and K48 linkages could be detected within the same APC/C substrate ubiquitin conjugates, if it was due to mixing or branching of different ubiquitin linkages and if it would also occur in cells and not only in an *in vitro* system.

4.5.1. Ube2S and Ube2G2^{CTP} produce ubiquitin chains containing K11 and K48 linkages on cyclin A *in vitro*

First I tested, what happens when K11 and K48 producing enzymes, here Ube2S and Ube2G2^{CTP}, would both be present in APC/C ubiquitylation reactions. Recombinant Ub-cyclin A was used as a substrate for Ube2S and Ube2G2^{CTP}. Furthermore was Ub-cyclin A in excess over immunoprecipitated APC/C for single substrate turnover (Rape et al., 2006) to ensure that the outcome of the reaction could potentially take place in cells and is not a result of overcrowding *in vitro*. While Ube2S alone transferred about six ubiquitin moieties, a combination of Ube2S and Ube2G2^{CTP} added K11 polyubiquitin chains of a drastically higher MW (Figure 35A). The combination of Ube2G2^{CTP}-C89S and Ube2S did not recapitulate the formation of these long ubiquitin chains excluding activation of Ube2S by the presence of Ube2G2^{CTP}. Next it was checked, if the high MW polyubiquitin chains made by Ube2S and Ube2G2^{CTP} were comprised of K11 and K48 linkages within the same ubiquitin conjugates or if they were a mixture of substrates modified with either K11 or K48 chains. Ub-cyclin A and ^{FLAG}ubiquitin were incubated with or without Ube2G2^{CTP} allowing the formation of K48-linked chains on Ub-cyclin A (Figure 35B).

Results

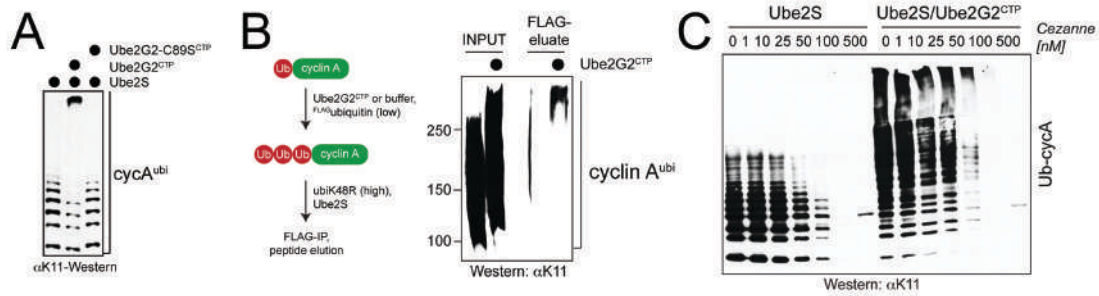


Figure 35: Ube2S and Ube2G2^{CTP} produce ubiquitin chains containing K11 and K48 linkages on cyclin A *in vitro*. **A.** High MW chains are seen in single substrate turnover assays. An excess of Ub-cyclin A (1 μ M) over APC/C^{Cdh1} (~10nM) was incubated with Ube2S, Ube2S/Ube2G2^{CTP}, or Ube2S and Ube2G2^{CTP}-C89S. Reactions were analyzed by western blot. **B.** Ube2S and Ube2G2^{CTP} catalyze formation of high MW conjugates that contain K11 and K48 linkages. Ub-cyclin A was incubated under single turnover conditions with APC/C, Ube2G2^{CTP} and a low concentration of ^{FLAG}ubiquitin. After 5min, reactions were supplemented with an excess of ubi^{R48}, which blocks Ube2G2^{CTP}-activity, but does not affect Ube2S. Then, Ube2S was added to allow formation of K11-linkages. To purify conjugates that contained both K48 and K11 linkages, the final reactions were subjected to affinity purification on FLAG-agarose, and peptide-eluates were analyzed with α K11 specific western blotting. **C.** Long chains formed by Ube2G2^{CTP} and Ube2S contain K11 linkages. Chains produced by APC/C^{Cdh1}, Ube2S and Ube2G2^{CTP} were incubated with the K11 specific DUB Cezanne and analyzed by α K11 specific western blot.

Adding excessive amounts of ubi^{R48} stopped the incorporation of ^{FLAG}ubiquitin. At the same time Ube2S was added allowing the modification of Ube2S with K11-linked chains. Detection of ubiquitin species after FLAG immunoprecipitation, elution with FLAG peptide and α K11 western blot analysis meant that these ubiquitin conjugates were created by incorporation of ^{FLAG}ubiquitin through Ube2G2^{CTP} in form of K48 linkages and sequential attachment of K11-linked chains by Ube2S in the presence of ubi^{R48}. Indeed only high MW polyubiquitin chains gave a strong signal for this analysis and therefore consist of K11 and K48 ubiquitin linkages (Figure 35B). The combination of the two linkages made by Ube2S and Ube2G2^{CTP} was validated by another approach. High MW species synthesized by Ube2S and Ube2G2^{CTP} were treated with the K11 specific DUB Cezanne. If these species existed because of the modification with long homogenous K48 chains introduced by the engineered Ube2G2^{CTP}, incubation

with Cezanne should show no change in the abundance of K11-linked chains. The contrary was the case, as Cezanne hydrolyzed the high MW ubiquitin chains made by Ube2S and Ube2G2^{CTP} in a similar manner to homogenous K11 chains made by Ube2S alone (Figure 35C). Together these data show that combination of K11 and K48 linkages leads to the formation of high MW polyubiquitin chains on an APC/C substrate.

4.5.2. Ube2S and Ube2G2^{CTP} form K11/K48-branched ubiquitin chains *in vitro*

Next, I determined if the ubiquitin species by Ube2S and Ube2G2^{CTP} contained K11- and K48-linked chains due to mixing or branching of K11 and K48 linkages. Ub-cyclin A incubated with wt-ubiquitin, Ube2S and Ube2G2^{CTP} produced high MW ubiquitin conjugates positive for K11 and K48 linkages based on α K11 and α K48 western blot analysis (Figure 36A).

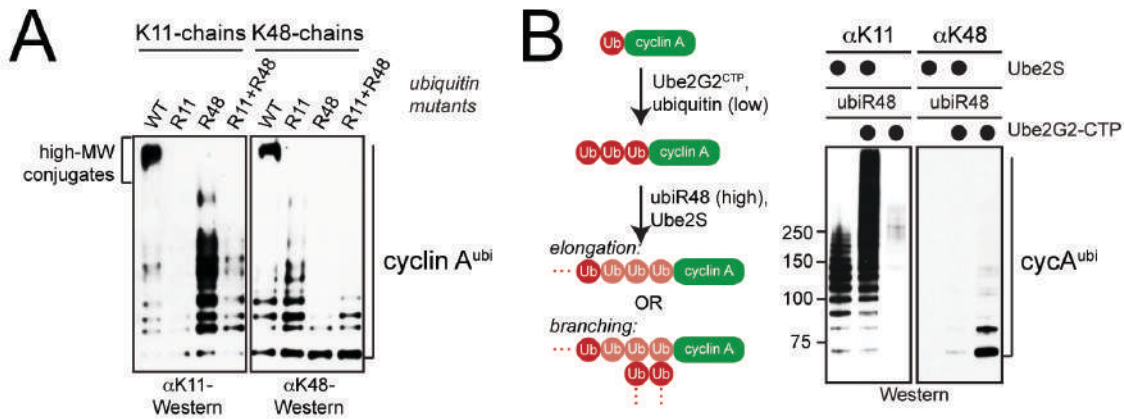


Figure 36: Ube2S and Ube2G2^{CTP} modify cyclin A with K11/K48-branched ubiquitin chains.

A. High MW conjugates assembled by Ube2S and Ube2G2^{CTP} are branched chains. Ub-cyclin A was incubated with APC/C^{Cdh1}, Ube2S, Ube2G2^{CTP}, and ubiquitin mutants under single substrate-turnover conditions and analyzed by Western. Mixtures of ubi^{R11} and ubi^{R48} allow Ube2S and Ube2G2^{CTP} to synthesize mixed chains, yet prevent introduction of branches. **B.** Ube2S elongates K48-linked chains by Ube2G2^{CTP} with K11-linked chains. Ub-cyclin A was mixed with APC/C^{Cdh1}, Ube2G2^{CTP} and low levels of ubiquitin, which leads to addition of two K48-linked ubiquitin molecules (Ub₃-cyclin A). Next, an excess of ubi^{R48} and Ube2S were added. Ub-cyclin A was also directly incubated with Ube2S and ubi^{R48}. Reactions were analyzed by western blot.

Using ubi^{R11} or ubi^{R48} inhibited the formation of these conjugates showing that both K11 and K48 linkages are needed. Even more importantly Ube2S and Ube2G2^{CTP} did not produce high MW chains, if incubated with mixtures of ubi^{R11} and ubi^{R48} (Figure 36A). Under these conditions mixed chains with K11 and K48 linkages can be synthesized, but K11/K48-branched chains cannot be produced, as no ubiquitin contains K11 and K48 at the same time. To further test whether the engineered E2 could be used to produce branched chains, Ub-cyclin A was incubated with APC/C^{Cdh1}, Ube2G2^{CTP}, and wt-ubiquitin at a low concentration for a short time, which led to attachment of two K48-linked ubiquitin molecules (Ub₃-cyclin A). An excess of ubi^{R48} then inactivated Ube2G2^{CTP}, before Ube2S was added. As expected for the assembly of branched chains Ube2S decorated Ub₃-cyclin A with conjugates of much higher MW than those formed on Ub-cyclin A, a substrate that can only be modified with a single K11-linked chain (Figure 36B). Thus, these experiments show that Ube2S and Ube2G2^{CTP} produce K11/K48-branched chains on APC/C-substrates.

4.5.3. Presence of Ube2G2^{CTP}, Ube2C and Ube2S in extracts and cells leads to formation of high MW ubiquitin chains

To check if the physiological E2s and the engineered E2 would also form K11/K48-branched high MW ubiquitin conjugates in cells two different experiments were performed. First the ubiquitylation of geminin, as a model APC/C substrate, by the physiological E2s, Ube2C and Ube2S and the engineered E2, Ube2G2^{CTP} was analyzed separately in extracts made from HeLa cells synchronized in prometaphase by thymidine and nocodazole. Endogenous Ube2S is present and further addition of Ube2S does not lead to improved ubiquitylation (data not shown). The concentration of active APC/C in these extracts is limiting and the substrate ubiquitin transfer activity of Ube2G2^{CTP} is weak compared to Ube2C (data not shown). Therefore addition of Ube2G2^{CTP} to these extracts did not result in significant ubiquitylation of geminin compared to the control (Figure 37A). Addition of a high concentration of Ube2C on top of low

Results

levels of endogenous Ube2C already present in the control, led to ubiquitylation of geminin, which became detectable in the presence of high amounts of GST tagged UBA domains (Hjerpe et al., 2009; Raasi et al., 2004). When Ube2C and Ube2G2^{CTP} were added together the formation of high MW ubiquitin species was detected (Figure 37A).

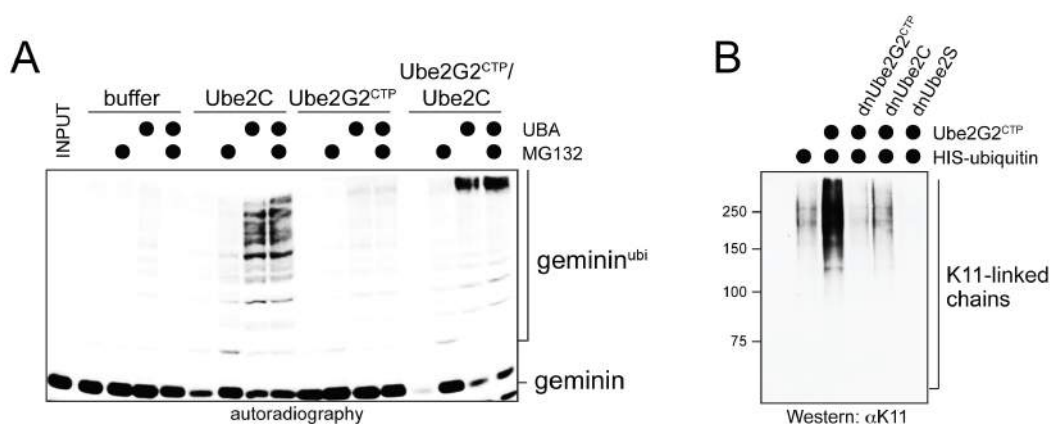


Figure 37: Ube2G2^{CTP}, Ube2C and Ube2S cooperate in extracts and cells. **A.** Cooperation of K11 and K48 specific APC/C E2s results in high MW conjugates. Extracts of prometaphase HeLa cells synchronized with thymidine and nocodazole were supplemented with ³⁵S-labeled geminin and 200μM MG132, or recombinant GST tagged UBA domains of HHR23A (to capture ubiquitylated substrates and thereby inhibiting deubiquitylation). Reactions were incubated for two hours and analyzed by autoradiography. **B.** Ube2S and Ube2G2^{CTP} cooperate *in vivo*. Prometaphase HeLa cells synchronized with thymidine and nocodazole expressing His-ubiquitin, Ube2G2^{CTP}, or dominant-negative E2s (Ube2G2^{CTP}-C89S, Ube2C-C114S and Ube2S-C95S) were released into anaphase, and treated with 15μM MG132 for 2 hours to enrich for ubiquitin conjugates. Conjugates were purified under denaturing conditions with NiNTA, and K11-linked chain formation was monitored by αK11 western blot analysis.

To determine if Ube2G2^{CTP}, Ube2C and Ube2S also cooperate in cells to form K11/K48-branched chains, HeLa cells were transfected with His-ubiquitin, synchronized in anaphase after release from thymidine and nocodazole into MG132 containing medium and enriched for ubiquitin conjugates by NiNTA pull down under denaturing conditions. As revealed by αK11 western blot analysis co-expression of Ube2G2^{CTP} increased the amount and MW of ubiquitin conjugates (Figure 37B). This increase relied on the presence of active Ube2G2^{CTP}, Ube2C or Ube2S, as co-expression of dominant negative

Ube2G2^{CTP}, Ube2C or Ube2S abolished significant detection of high MW species (Figure 37B). Hence Ube2G2^{CTP}, Ube2C and Ube2S collaborate in the formation of K11/K48 branched high MW ubiquitin conjugates in extracts and cells.

4.6. Branched ubiquitin chains show improved binding to ubiquitin binding proteins

After establishing that the physiological E2s Ube2C and Ube2S and the engineered E2 Ube2G2^{CTP} and Ube2S were able to produce branched chains, it was now possible to investigate the effects of homogenous versus branched ubiquitin chains in terms of interaction with ubiquitin binding proteins. Furthermore Ube2G2^{CTP} making specifically K48-linked chains gives the opportunity to test for differences in K11 versus K48 ubiquitin linked chains for binding to ubiquitin receptors.

4.6.1. Cyclin A modified with either K11- or K48-linked ubiquitin chains shows similar binding to S5a, HHR23A and p97 cofactor complexes

To compare chains of certain linkages versus branched chains resulting from a combination of these linkages in terms of ubiquitin receptor affinities, I tested first to what extent the different linkages bind individually. Chains made by Ube2C and Ube2S were considered mainly K11 chains and chains made by Ube2C and Ube2G2^{CTP} were considered mainly K48 chains. The proteasomal delivery factor HHR23A, the major ubiquitin receptor within the 26S proteasome S5a and complexes of p97 with its ubiquitin binding cofactors involved in ubiquitin dependent processes were analyzed for binding to K11- and K48-linked chains. Radiolabeled cyclin A was modified using Ube2C for efficient chain initiation and either Ube2S or Ube2G2^{CTP} for efficient attachment of K11- or K48-linked chains. The modified cyclin A was incubated with HHR23A, S5a or p97, which were immobilized on amylose resin via their N-terminal MBP tags. In the case of MBP^{p97} the His tagged cofactors were indirectly bound to amylose resin through

4.6.2. Cyclin A modified with either K11- or K48-linked ubiquitin chains does not compete for binding to S5a or p97/SAKS1

Additionally it was investigated, if in the presence of both chain types, K11 or K48 ubiquitin chains might show enhanced binding over the other.

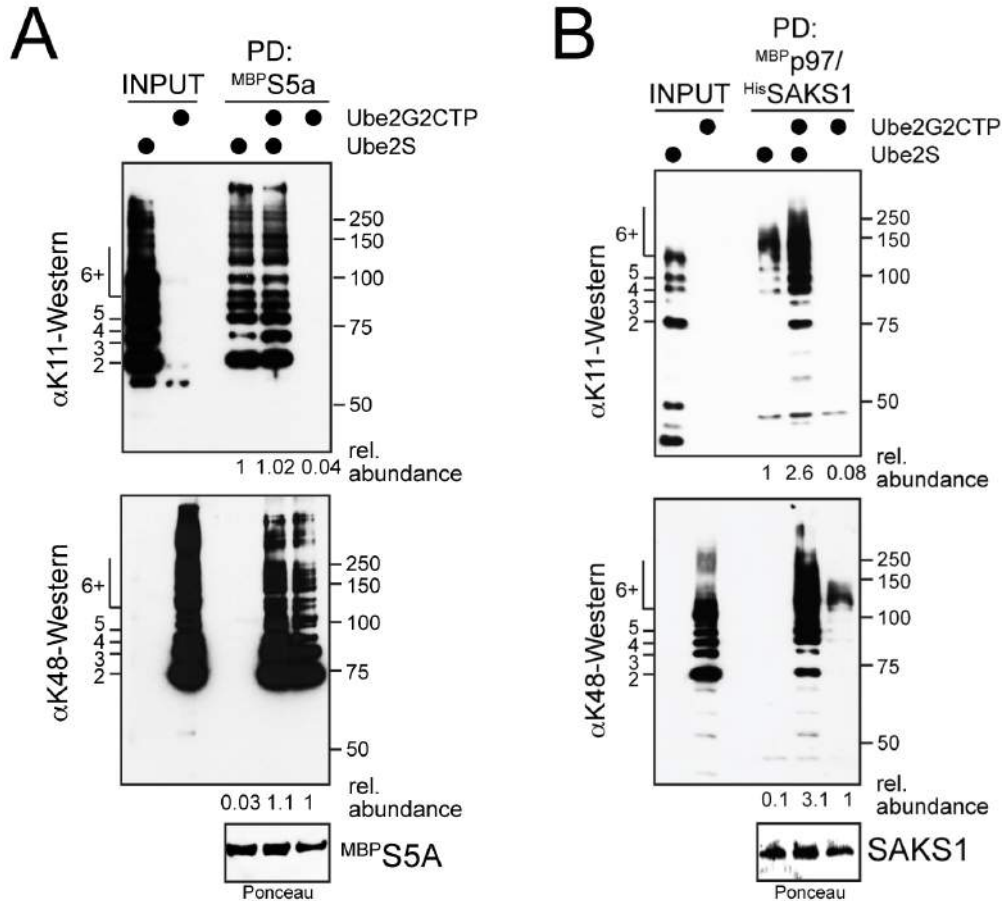


Figure 39: K11- or K48-linked ubiquitin chains do not compete for binding to ubiquitin binding proteins. A. Ub-cyclin A was modified by the APC/C^{Cdh1} and Ube2S or Ube2G2^{CTP} with either K11- or K48-linked chains. Reaction products were incubated with immobilized MBP S5a either alone or together, and analyzed by western blot. **B.** K11- and K48-linked chains mediate substrate binding to p97/SAKS1. Ub-cyclin A was modified with K11- or K48-linked chains. Products were added to immobilized MBP p97/His SAKS1-complexes, and binding was analyzed by western blot using K11 or K48 specific antibodies.

Therefore, recombinant Ub-cyclin A was modified with either homogenous K11 chains by Ube2S or homogenous K48 chains by Ube2G2^{CTP}. Reaction products either individually or in combination were incubated with immobilized MBP S5a or

^{MBP}p97/^{His}SAKS1. Binding of ubiquitylated cyclin A was determined by α K11 or α K48 western blot analysis and quantified with ImageJ. While K11- and K48-linked ubiquitin chains similarly bind to S5a, the presence of both chain types seems not to negatively interfere with binding of the respective chain type (Figure 39A).

Competition for interaction with p97/SAKS1 was observed neither (Figure 39B). To the contrary a significant enhancement of binding was detected in the presence of cyclin A modified with K11 chains and cyclin A modified with K48 chains. This was not further investigated. Consequently K11- or K48-linked ubiquitin chains on an APC/C substrate do not compete for binding to S5a or p97/SAKS1.

4.6.3. High MW branched ubiquitin chains show enhanced binding compared to shorter ubiquitin chains

After determining that K48- and K11-linked chains show similar binding I determined if K11/K48-branched chains would enhance binding to S5a or p97/SAKS1 compared to shorter K11-linked chain. Ub-cyclin A was either modified with about six K11-linked ubiquitin moieties by Ube2S or with a mixture of similar shorter chains possibly either K11 or K48 and high MW K11/K48-branched chains by combining Ube2S and Ube2G2^{CTP}. The reaction products were incubated with ^{MBP}S5a immobilized on amylose resin and binding was visualized by α K11 western blot. While short K11 chains interact weakly with S5a, large K11/K48 branched chains bind relatively strong (Figure 40A). The same was observed when ³⁵S-radiolabeled cyclin A was modified with Ube2S, Ube2G2^{CTP} and low levels of Ube2C. Detecting all ubiquitin conjugates by autoradiography a mixture of shorter chains and long K11/K48-branched chains were seen on cyclin A. A preference for the branched chains was determined when ubiquitin conjugates were incubated with ^{MBP}p97/^{His}SAKS1 and ^{MBP}S5a (Figure 40B). Thus, these experiments show the enhanced binding of K11/K48-branched chains to ubiquitin receptors.

Results

or homogenous K48-linked chains using ubi^{K48}. Cyclin A attached to branched or homogenous K48 chains appeared to be of similar MW (Figure 41A).

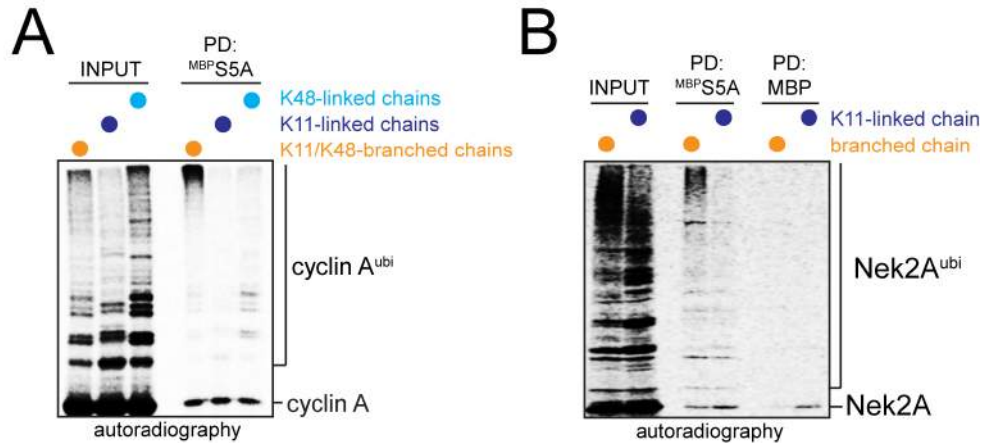


Figure 41: Enhanced binding of branched ubiquitin chains. A. Preferential binding of branched chains is independent of chain length. ³⁵S-labeled cyclin A was modified by APC/C^{Cdc20}, low levels of Ube2C, Ube2S and/or Ube2G2^{CTP}, and wt-ubiquitin, ubi^{K11}, or ubi^{K48} to assemble K11-, K48-linked, or K11/K48-branched chains, and incubated with MBP^{S5a}. Reactions were analyzed by autoradiography. **B.** Branched chains increase the affinity of Nek2A for the proteasomal receptor S5a. ³⁵S-labeled Nek2A²⁷²⁻⁴⁴⁵ was modified by APC/C^{Cdc20}, Ube2C and Ube2S with homogenous or branched chains (using ubi^{K11} or wt-ubiquitin) and incubated with MBP^{S5a}. Reactions were analyzed by autoradiography.

When tested for binding to immobilized MBP^{S5a} though, branched chains seemed to be more effective. Subsequently it was determined if modification of the prometaphase substrate Nek2A by APC/C^{Cdc20}, Ube2C and Ube2S with branched chains results in stronger binding to ubiquitin receptors. ³⁵S-radiolabeled Nek2A²⁷²⁻⁴⁴⁵ was attached to branched chains using wt-ubiquitin or homogenous K11-linked chains using ubi^{K11}. The reaction products were incubated with MBP^{S5a} and analyzed by autoradiography. Only Nek2A modified with high MW branched chains showed significant binding to the proteasomal ubiquitin receptor (Figure 41B). The difference between ubiquitylation of Nek2A with wt-ubiquitin or ubi^{K11} compared to earlier experiments is not as pronounced (Figure 17A), as the reaction was incubated longer to increase product formation, more substrate was used to create more product and the gel was contrasted differently to see binding of Nek2A ubiquitin conjugates to S5a. In summary

enhanced binding of branched ubiquitin chains was not a mere function of the number of ubiquitin molecules attached to the respective APC/C substrates.

4.6.5. Branched ubiquitin chains are hydrolyzed by DUBs

To exclude that branched ubiquitin chains were an *in vitro* artifact, which could interact with ubiquitin binding domains but not be hydrolyzed by DUBs, the turnover of branched chains by DUBs was tested. Ub-cyclin A^{HA} or Ub^{R11}-Ub-cyclin A^{HA} was modified with APC/C^{Cdh1}, Ube2S and methyl-ubiquitin, creating K11 linkages in an either linear or branched fashion.

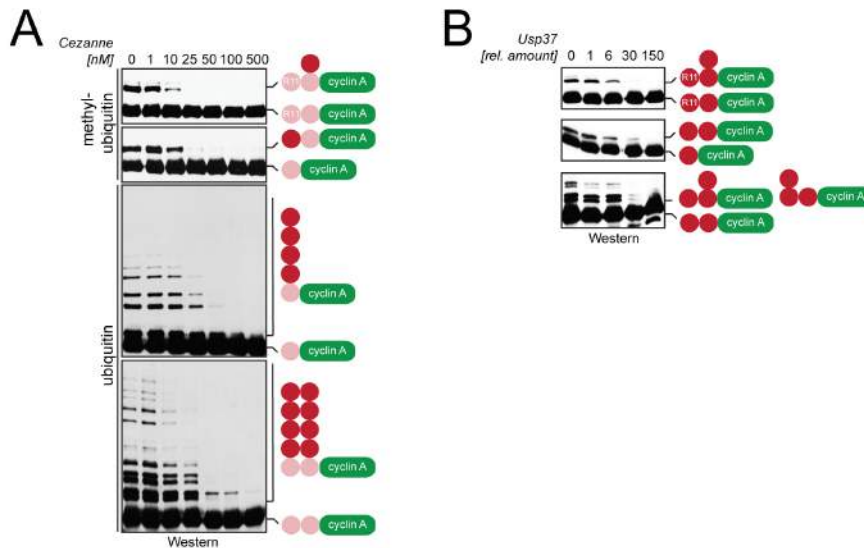


Figure 42: DUBs hydrolyze branched and homogenous chains similarly. **A.** Deubiquitinases recognize branched conjugates. Ub-cyclin A^{HA} or Ub^{R11}-Ub-cyclin A^{HA} was modified with APC/C^{Cdh1}, Ube2S, and methyl-ubiquitin to generate linear or branched substrates, before incubation with the K11-specific DUB Cezanne. In the bottom panel, Ub-cyclin A^{HA} or Ub-Ub-cyclin A^{HA} was modified by APC/C^{Cdh1}, Ube2S, and wt-ubiquitin with one or two ubiquitin chains. Reactions were analyzed by α HA western blot. **B.** Usp37 deubiquitylates substrates modified with linear or branched conjugates with similar efficiency. As described above, Ub-cyclin A^{HA}, Ub^{R11}-Ub-cyclin A^{HA}, or Ub-Ub-cyclin A^{HA} were modified by APC/C, Ube2S, and methyl-ubiquitin. Deubiquitylation by Usp37 was analyzed by α HA western blot.

Both substrates are hydrolyzed similarly in a titration of Cezanne, as detected by disappearance of higher MW species in α HA western blot (Figure 42A). Titrations with Ub-cyclin A^{HA} or Ub-Ub-cyclin A^{HA} modified by wt-ubiquitin and Ube2S showed similar hydrolysis of single homogenous K11-linked chain and two branched K11-linked by Cezanne (Figure 42A). Besides the K11 specific Cezanne, which contains an ovarian tumor (OTU) domain as its catalytic domain, hydrolysis of branched chains was tested with Usp37, a DUB containing a ubiquitin specific protease (USP) domain and supposedly being an APC/C DUB (Huang et al., 2011). Ub-cyclin A^{HA}, Ub^{R11}-Ub-cyclin A^{HA} or Ub-Ub-cyclin A^{HA} was modified by APC/C^{Cdh1}, Ube2S and methyl-ubiquitin, and used as substrates in titrations with Usp37. Hydrolysis of linear or branched ubiquitin chains occurred at similar Usp37 concentrations (Figure 42B). Concomitantly the DUBs similarly process homogenous or branched linkages.

4.7. Modification of APC/C substrates with branched chains leads to an increase in substrate degradation

As branched chains on APC/C substrates allow an enhanced binding to proteasomal delivery factors, I tested whether proteasomal degradation was enhanced as well. While branched chains could enhance degradation based on the higher proteasomal retention times *in vitro*, it could be possible that branches do not allow for proper processing of the ubiquitylated substrate in the context of the full proteasome. With the different ubiquitin mutants and the different APC/C E2s at my disposal I compared the *in vitro* degradation efficiencies of APC/C substrates modified with ubiquitin chains of different topologies in the presence of purified human 26S proteasome. In HeLa cell extracts stability of APC/C substrates was observed upon addition of the different ubiquitin variants and E2s. Furthermore the formation of ubiquitin aggregates might occur in cells due to high local ubiquitin concentrations. The presence of cellular DUBs might negate the enhanced binding of branched ubiquitin chains; consequently the levels of APC/C substrates were detected in HeLa cells, upon increased ubiquitin

chain branching due to expression of Ube2G2^{CTP}. The inhibition of branching was investigated by depletion of Ube2S. A caveat of Ube2S siRNA was the simultaneous inhibition of elongation; this was fully addressed with the *in vitro* characterization above and can be neglected.

4.7.1. Branched ubiquitin chains improve Nek2A ubiquitin conjugate turnover by the 26S proteasome *in vitro*

I tested first if branched chains on Nek2A lead to differences in degradation by purified 26S proteasomes compared to homogenous chains on Nek2A. ³⁵S-radiolabeled HA-Nek2A²⁷²⁻⁴⁴⁵ was modified with branched chains by APC/C^{Cdc20}, Ube2C, Ube2S and wt-ubiquitin or with homogenous K11-linked chains using ubi^{K11}. The reaction products were supplemented with glycerol and ATP to prevent the added proteasomes from dissociating into CP and RP (Beckwith et al., 2013).

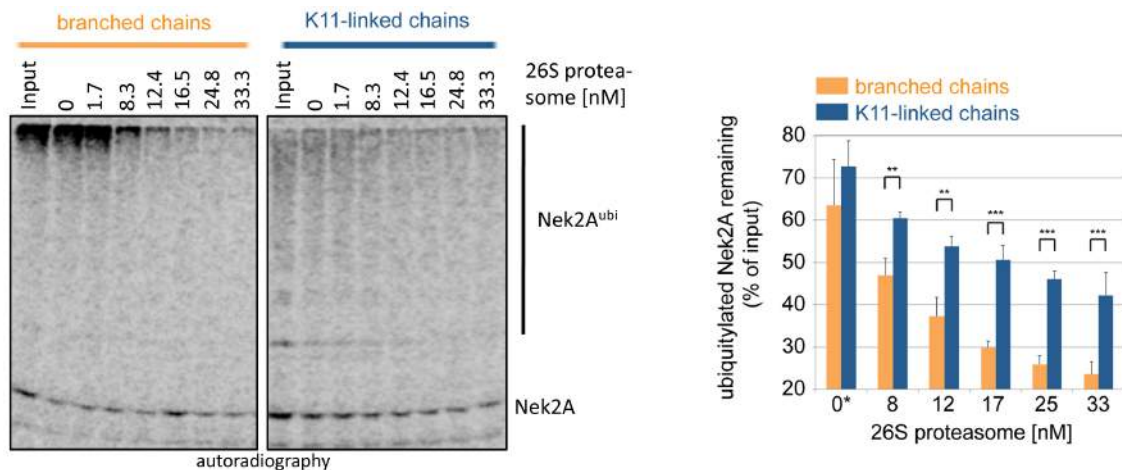


Figure 43. Branched chains improve the efficiency of proteasomal degradation *in vitro*.

³⁵S-HA-Nek2A²⁷²⁻⁴⁴⁵ was modified with branched or homogenous K11-linked chains and added to increasing concentrations of 26S proteasomes. A representative gel is shown. Five independent titrations were monitored by autoradiography and quantified using ImageJ (n=5; data are average +/- SD; ** p<0.002 in paired t-test; *** p<0.001). The asterisk marks background degradation by proteasomes that co-purify with APC/C.

After incubation with different amounts of 26S proteasomes, abundance of ubiquitin conjugates on Nek2A were determined by autoradiography and quantified with ImageJ. Homogenous K11-linked chains on Nek2A were shorter and less abundant than the high MW branched chains and the degradation of conjugates was measured relative to the initial products. This analysis showed that branched chains led to faster degradation than homogenous chains (Figure 43). While at the highest proteasome concentration only about 25% branched chains were left over, K11-linked chains were still at levels of slightly more than 40%. In agreement with the previous binding experiments branched chains were more efficient than linear K11-linked conjugates in driving the degradation of Nek2A by purified proteasomes.

4.7.2. K11- and K48-linked ubiquitin chains lead to APC/C substrate degradation in cell extracts

Subsequently the distinct chain types were compared in cell extracts. To understand differences between degradation of K11-linked and K11/K48-branched chains, it was first tested how K11- and K48-linked ubiquitin chains compare in extracts. Extracts of HeLa cells synchronized in early G1 by thymidine and nocodazole arrest and release from nocodazole for two hours, were used to show degradation of a standard APC/C substrate, geminin, by K11-linked chains (Figure 44A) in line with previous publication (Jin et al., 2008). Ube2G2^{CTP} was used to modify APC/C substrates with K48-linked chains and it was investigated, whether this would lead to degradation at a similar rate. As it was shown above Ube2C, Ube2S and Ube2G2^{CTP} together modify APC/C substrates. Therefore a cell extract free of Ube2C and Ube2S was used. Extract prepared from serum starved T98G cells does not contain Ube2C or Ube2S (Jin et al., 2008; Williamson et al., 2009a). Supplementing this extract with Ube2G2^{CTP} led to degradation of another standard APC/C substrate, securin (Figure 44B). K48- and not K11-linked ubiquitin chains drove securin degradation

Results

as ubi^{R48} inhibited degradation while ubi^{R11} had no effect. Therefore K11 and K48 chains individually mediate degradation of APC/C substrates.

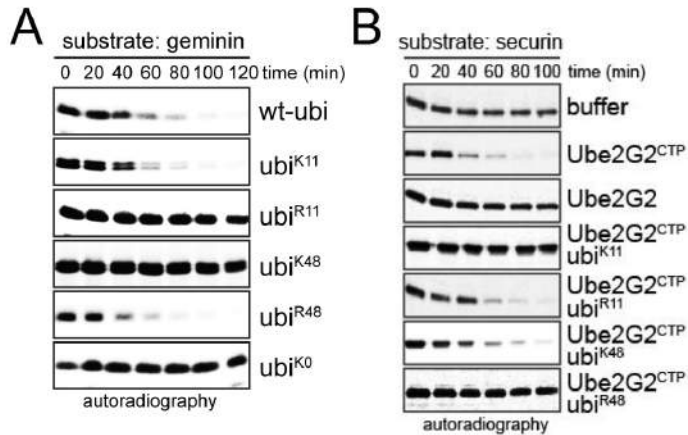


Figure 44: Degradation of APC/C substrates is mediated by K11 or K48 chains individually **A.** The physiological APC/C E2s drive K11 specific degradation.

³⁵S-geminin was incubated in endogenous Ube2S containing G1 extracts that were supplemented with Ube2C and the indicated ubiquitin mutants. Reactions were analyzed by autoradiography. **B.** K48-linked chains drive APC/C-substrate degradation in extracts.

³⁵S-labeled securin was added to extracts of serum starved T98G cells, which do not contain endogenous K11-specific APC/C-E2s. Extracts were supplemented with Ube2G2^{CTP} or Ube2G2, respectively, and wt-ubiquitin or ubiquitin mutants. Reactions were analyzed by autoradiography.

4.7.3. Branched ubiquitin chains enable degradation of weaker binding substrates or under low APC/C activity

APC/C substrates therefore are degraded due to K11 or K48 chains individually. I determined next, if the combination of K11 and K48 to form K11/K48-branched chains would lead to enhanced degradation. Degradation was measured in prometaphase synchronized HeLa cell extracts, in which APC/C activity should be fairly low due to the presence of MCC. Indeed, even though Ube2S and Ube2C are present in these extracts (Williamson et al., 2009a), no degradation of endogenous geminin is observed (Figure 45A). Addition of Ube2G2^{CTP} allowed degradation that was APC/C specific based on the inhibition by Emi1 and Ube2C^{C114S}, and RING finger dependent based on inhibition by Ube2C^{C114S}. The degradation of geminin in the presence of active APC/C and Ube2G2^{CTP} was therefore dependent on K48-linked ubiquitylation.

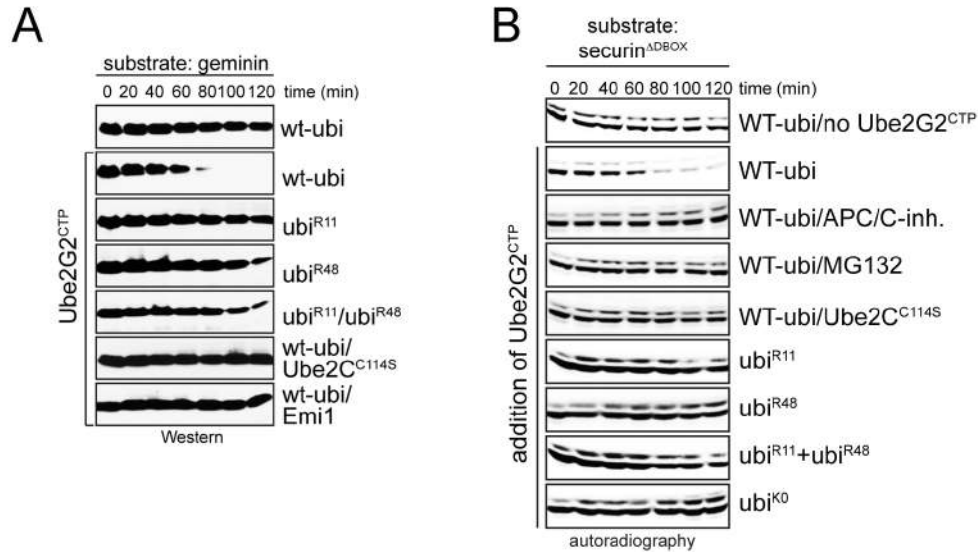


Figure 45: Enhanced APC/C substrate degradation by branched ubiquitin chains in HeLa cell extracts. **A.** Branched chains promote degradation more efficiently. Prometaphase extracts with endogenous Ube2S and Ube2C were treated with Ube2G2^{CTP} in the presence of ubiquitin mutants. The stability of geminin was monitored by α geminin western blot analysis. Geminin was stable in extracts containing mixtures of ubi^{R11} or ubi^{R48}, a condition that allows Ube2S and Ube2G2^{CTP} to assemble mixed, but not branched chains. **B.** Branched chains accelerate substrate degradation. Extracts of early G1 HeLa cells containing endogenous Ube2S and Ube2C were supplemented with ³⁵S-securin ^{Δ DBOX}, Ube2G2^{CTP} as indicated on the left, and various ubiquitin mutants or degradation controls, shown on the right. The stability of securin ^{Δ DBOX} was analyzed by autoradiography. Presence of ubi^{R11} or ubi^{R48} allows Ube2S and Ube2G2^{CTP} to form homogenous or mixed chains but prevent branching, and securin ^{Δ DBOX} was stable under these conditions.

Ubi^{R11} inhibited degradation though, which means that Ube2S must be needed under these conditions. Combination of ubi^{R11} and ubi^{R48} did not rescue geminin turnover. Consequently only branched chains permitted degradation of an APC/C substrate in prometaphase cell extracts. I additionally checked if branched chains enhance protein degradation by measuring the degradation of an APC/C substrate that only weakly interacts with the APC/C, securin ^{Δ DBOX}. This allowed the use of G1 HeLa cell extract instead of prometaphase cell extract excluding secondary effects caused by the presence of MCC. Radiolabeled securin ^{Δ DBOX} was not degraded in the presence of endogenous Ube2C and Ube2S, but the addition of Ube2G2^{CTP} led to its degradation (Figure 45B). The different controls

showed that degradation is dependent on APC/C and proteasome. Degradation only took place, when branching was possible according to the use of ubiquitin mutants. Together, these experiments show that artificial ubiquitin chain branching allows APC/C substrate degradation, even though APC/C activity is low due to presence of MCC or due to weakened interaction with its substrate. Therefore branched ubiquitin chains enhance protein degradation in cell extracts.

4.7.4. Decrease of ubiquitin conjugates co-purifying with the APC/C in the presence of Ube2G2^{CTP} due to turnover by the proteasome

I investigated whether Ube2G2^{CTP} expressed in cells could achieve a similar increase in protein degradation. The constitutively Ube2G2^{CTP} expressing HeLa cell line, described above, was used to look at general levels of APC/C ubiquitin conjugates upon enhanced ubiquitin chain branching. Substrate ubiquitin conjugates co-purify with APC/C immunoprecipitations (Figure 26), which was considered as readout for the overall presence of ubiquitylated APC/C substrates. HeLa cells were enriched in the presence of ubiquitylated APC/C substrates by release from thymidine and nocodazole into MG132 containing medium. In control cells ubiquitylated substrates were detected in APC/C immunoprecipitations based on α K11 western blot analysis (Figure 46).

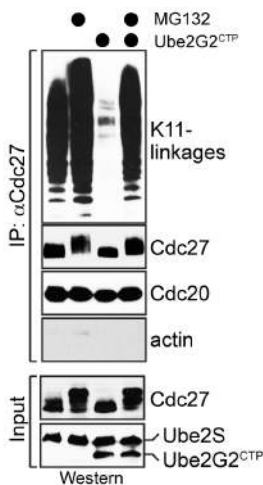


Figure 46: Decrease of ubiquitin conjugates co-purifying with the APC/C in the presence of Ube2G2^{CTP} due to turnover by the proteasome. HeLa cells constitutively expressing Ube2G2^{CTP} were released from thymidine and nocodazole induced mitotic arrest and treated with 20 μ M proteasome inhibitor MG132 for two hours as indicated. Co-purifying K11-conjugates were monitored by western blot analysis.

By contrast, in cells expressing Ube2G2^{CTP} and therefore assembling K11/K48-branched chains relatively little conjugates were observed. The absence of ubiquitin conjugates was rescued by MG132 treatment, suggesting that an increased formation of branched chains facilitated substrate degradation by the proteasome (Figure 46). Inhibition of the APC/C by Ube2G2^{CTP} could explain this result but the *in vitro* experiments above showed enhanced ubiquitylation and no significant growth defect was observed in this cell line, which would be expected upon APC/C inhibition.

4.7.5. Co-expression of Cdh1 and Ube2G2^{CTP} decreases levels of a weakly binding APC/C substrate

Instead of measuring the level of all ubiquitylated APC/C substrates at once, it was tested if expression of Ube2G2^{CTP} would augment degradation of a specific APC/C substrate by enabling enhanced K11/K48-branching.

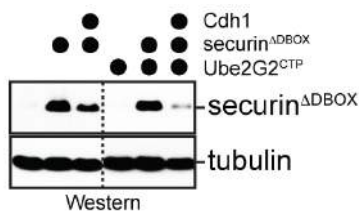


Figure 47: Ube2G2^{CTP} enhances substrate degradation in 293T cells. Securin^{ΔDBOX} was expressed with Cdh1 in 293T cells or in 293T cells stably expressing Ube2G2^{CTP} under a Tet-inducible promoter. Levels of securin^{ΔDBOX} were measured by western blot.

A Ube2G2^{CTP} inducible 293 cell line was created using the Flp-InTM T-RExTM system. The model substrate securin^{ΔDBOX} was used as degradation readout under weakened APC/C activity, as securin^{ΔDBOX} has only little affinity towards APC/C. Degradation was triggered by co-expression of Cdh1 (Jin et al., 2008). While co-expression of Cdh1 lowered the levels of securin^{ΔDBOX} in not induced cells as expected, additional induction of Ube2G2^{CTP} led to enhanced degradation. Thus the augmented formation of branched chains on a model APC/C substrate enhances protein destruction in cells.

4.7.6. Depletion of Ube2S leads to stabilization of the proteasomal substrate Nek2A

HeLa cells were depleted of Ube2S to inhibit branching, which is normally catalyzed by Ube2C and Ube2S. It was tested if this inhibition of branching had an effect on the stability of certain APC/C substrates in cells. As depletion of Ube2S seemed to have a pronounced effect on Nek2A levels in prometaphase, HeLa cells were depleted of Ube2S and synchronized by thymidine and nocodazole arrest. Arrested cells were treated for the indicated times with 50µg/ml cycloheximide. Nek2A levels were determined in cell extract and in APC/C immunoprecipitations. The cycloheximide chase showed that Ube2S depletion leads to slower turnover of Nek2A in prometaphase HeLa cells (Figure 48A).

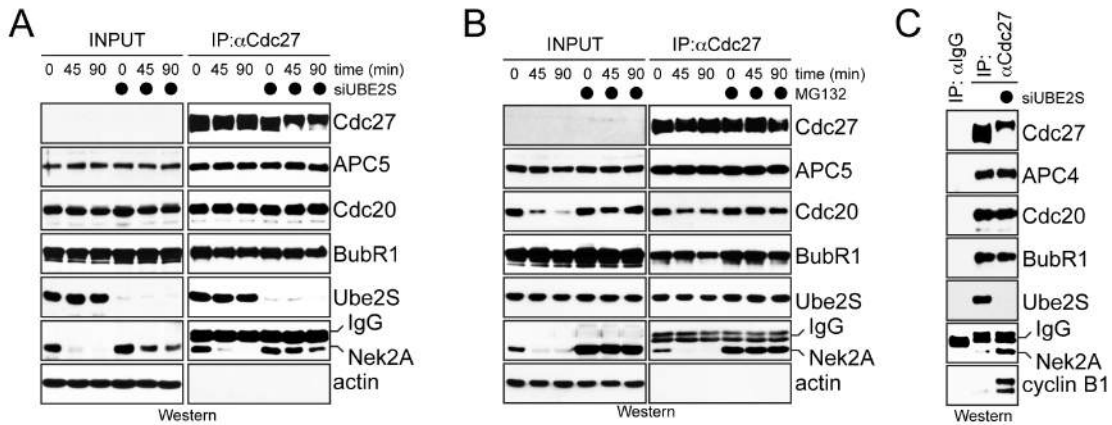


Figure 48: Ube2S depletion or proteasome inhibition increase APC/C bound Nek2A levels.

A. Ube2S RNAi increases APC/C bound Nek2A levels. HeLa cells transfected with control or Ube2S siRNA using Lipofectamine RNAimax were synchronized in prometaphase by thymidine and nocodazole, and treated with 50µg/ml cycloheximide. APC/C was purified at indicated times after cycloheximide addition, and co-purifying proteins were analyzed by western blot. **B.** MG132 treatment increases APC/C bound Nek2A levels. The levels of Nek2A bound to the APC/C were analyzed in prometaphase HeLa cells treated with 50µg/ml cycloheximide and 20µM MG132 proteasome inhibitor by western blot. **C.** Ube2S RNAi increases APC/C bound Nek2A and cyclin B1 levels coinciding with hyperphosphorylation of Cdc27. APC/C was purified from prometaphase HeLa cells treated with control or Ube2S siRNA and Lipofectamine RNAimax, and levels of co-purifying proteins were determined by western blot analysis.

Nek2A was only detected on the APC/C if cells were depleted of Ube2S, while the overall level of MCC components seemed unaffected. The increase of Nek2A on the APC/C might be due to higher Nek2A levels or based on reduced active removal of Nek2A from the APC/C by UPS components. Nek2A stabilization and binding to the APC/C caused by inhibition of branching, seemed to be proteasome dependent, as treatment with 15 μ M MG132 led to similar increases of Nek2A levels within prometaphase cells and on the APC/C (Figure 48B). Furthermore I showed that binding of Nek2A is APC/C specific compared to an control immunoprecipitation. The increased levels of Nek2A on the APC/C caused by Ube2S depletion coincided with higher amounts of cyclin B1 on prometaphase APC/C (van Zon et al., 2010). An upward shift in MW of the APC/C subunit Cdc27 was seen upon Ube2S depletion (Figure 48C), probably related to its phosphorylation status, which is important for regulation of the cell cycle and proliferation (Huang et al., 2007; Kraft et al., 2003; Zhang et al., 2011). Importantly presence of Ube2S, a mediator for branching, is detrimental for APC/C bound prometaphase substrate levels and phosphorylation status of Cdc27.

4.8. Presence of Ube2G2^{CTP} causes cell cycle defects

Decoration of APC/C substrates with branched ubiquitin chains by the physiological E2s is important for substrate stability. Inhibition of ubiquitin chain branching caused by Ube2S depletion also delays cell cycle progression. The introduction of Ube2G2^{CTP} in cells leads to enhanced branching and increased APC/C substrate degradation. Hence, I investigated whether the presence of Ube2G2^{CTP} and consequently constitutive K11/K48-branching interfered with proper cell cycle regulation. It was tested first, if Ube2G2^{CTP} alone would support APC/C activity in cells based on APC/C substrate levels in anaphase and mitotic indices of RNAi treated cells. HeLa cells were treated with taxol and analyzed for aberrant cell divisions to check for proper cell cycle regulation in the presence of enhanced K11/K48-branching by Ube2S and Ube2G2^{CTP}.

Results

4.8.1. Ube2G2^{CTP} enables cell cycle progression and degradation of APC/C substrates

Depletion of Ube2C, Ube2S and p31^{Comet} was performed in HeLa cells to test whether Ube2G2^{CTP} contributes to APC/C activity in cells. This depletion leads to a significant increase in the number of mitotic cells due to APC/C inactivation (Reddy et al., 2007; Summers et al., 2008; Williamson et al., 2009a). Control hygromycin resistant HeLa cells or constitutively Ube2S or Ube2G2^{CTP} expressing HeLa cells were transfected with a combination of siRNAs against Ube2C, Ube2S and p31^{Comet} and Oligofectamine. After 48 hours the cells were fixed in ethanol and stained with fluorescent propidium iodide, which intercalates into DNA. FACS analysis revealed the DNA content of single cells and consequently the cell cycle stage of the treated cells. Control cells showed an increase of cells in G2/M by about 30% upon triple depletion (Figure 49A).

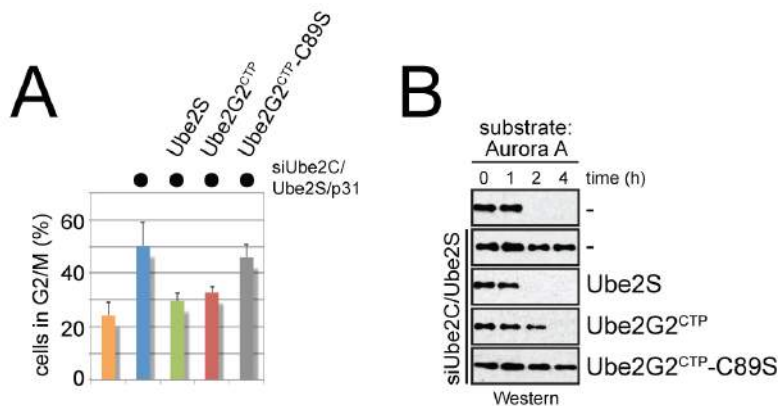


Figure 49: Ube2G2^{CTP} rescues APC/C activity in cells. **A.** Ube2G2^{CTP} rescues a cell cycle defect caused by depletion of APC/C-E2s and p31^{Comet}. HeLa cells were treated with Ube2C, Ube2S and p31^{Comet} siRNA at the same time using Oligofectamine

for 48 hours, stained with propidium iodide and analyzed by FACS (n=3; data are average + SD).

B. K48-linked chains support APC/C substrate degradation *in vivo*. APC/C E2s Ube2C and Ube2S were depleted from HeLa cells by Ube2C and Ube2S siRNA with Oligofectamine. HeLa cells were constitutively expressing siRNA resistant Ube2S, Ube2G2^{CTP}, or Ube2G2^{CTP}-C89S as indicated. Degradation of the APC/C-substrate Aurora A in anaphase was monitored by western blot analysis.

Presence of RNAi resistant Ube2S mostly rescued this phenotype showing that reintroduction of a physiological APC/C E2 is restoring APC/C activity to sufficient levels. Strikingly, active Ube2G2^{CTP} was able to greatly rescue G2/M

enrichment by contributing to APC/C activity in cells, while inactive Ube2G2^{CTP}-C89S showed no significant difference.

The stable cell lines were also treated with a combination of Ube2C and Ube2S RNAi using Oligofectamine. They were arrested in prometaphase by thymidine and nocodazole treatment and released into nocodazole free medium. Cells were analyzed by western blot at the indicated times after nocodazole release. The anaphase APC/C substrate Aurora A is stabilized upon Ube2S/Ube2C RNAi treatment (Williamson et al., 2009a). This phenotype seemed to be completely rescued in a Ube2S stable cell line and reduced in a Ube2G2^{CTP} cell line, while inactive Ube2G2^{CTP}-C89S showed no effect (Figure 49B). Together these two experiments show that K11 or K48 specific E2s promote substrate degradation and cell cycle progression during mitosis.

4.8.2. Ube2G2^{CTP} rescues a mitotic arrest induced by depletion of Ube2C and Ube2S

Additionally I tested if Ube2G2^{CTP} could rescue the synergistic increase of mitotic cells upon Ube2C and Ube2S depletion (Williamson et al., 2009a). This experiment is more direct, as only Ube2C and Ube2S need to be depleted to detect a raise in the number of mitotic cells. Using software-based analysis of Hoechst stained cells, it was possible to differentiate between G2 and mitotic cells.

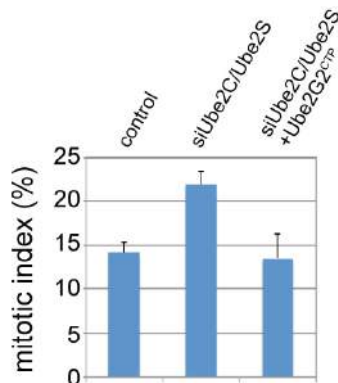


Figure 50: Ube2G2^{CTP} rescues a cell cycle delay caused by depletion of APC/C-E2s. HeLa cells or HeLa cell lines constitutively expressing Ube2G2^{CTP} were treated with control or Ube2C/Ube2S siRNAs. Mitotic index was determined by automated image capture and analysis (n=3; >1000 cells per n; data are average + SD).

To determine the mitotic index for different treatments, control or Ube2G2^{CTP} constitutively expressing HeLa cells were seeded in a 384-well format and transfected with control or Ube2C and Ube2S siRNA using Oligofectamine. Analysis in this format was described above. A significantly higher percentage of cells were in mitosis due to synergy between reduced levels of Ube2C and Ube2S, while presence of Ube2G2^{CTP} negated this effect (Figure 50). Therefore Ube2G2^{CTP} seems to show E2 activity with the APC/C in mitosis.

4.8.3. Ube2G2^{CTP} causes bypass of a taxol induced mitotic arrest

Taxol treatment and the subsequent mitotic arrest of HeLa cells, is established as a sensitive readout for properly regulated APC/C activity by the spindle assembly checkpoint (Ikui et al., 2005; Stegmeier et al., 2007). Thus, HeLa cells constitutively expressing Ube2G2^{CTP} were tested for their response upon treatment with taxol to determine if enhanced ubiquitin chain branching in the presence of Ube2C, Ube2S and Ube2G2^{CTP} interferes with a taxol induced arrest indicating a change in APC/C activity. Therefore hygromycin resistant HeLa cells, HeLa cells constitutively expressing Ube2G2^{CTP} or Ube2G2^{CTP}-C89S were plated in a 384-well format and treated with different taxol concentrations of 0 to 100nM the next day. After 18 hours the cells were fixed, stained with Hoechst and the percentage of mitotic cells was determined by software based image analysis. While control cells showed more than 80% enrichment in mitotic cells at 100nM taxol, the Ube2G2^{CTP} expressing cells would only arrest to about 40% (Figure 51A). Cells expressing Ube2G2^{CTP} were less sensitive to taxol over the whole range of concentrations used. This effect was only observed in the presence of active Ube2G2^{CTP} and not with catalytically inactive Ube2G2^{CTP}-C89S. The multilobed morphology of the Hoechst stained DNA, indicated spindle assembly checkpoint bypass (Figure 51A). The extent of Ube2G2^{CTP} dependent taxol bypass was reduced upon depletion of Ube2S and Ube2C by siRNA using Oligofectamine (Figure 51B), showing that bypass only occurs in the presence of increased ubiquitin branching.

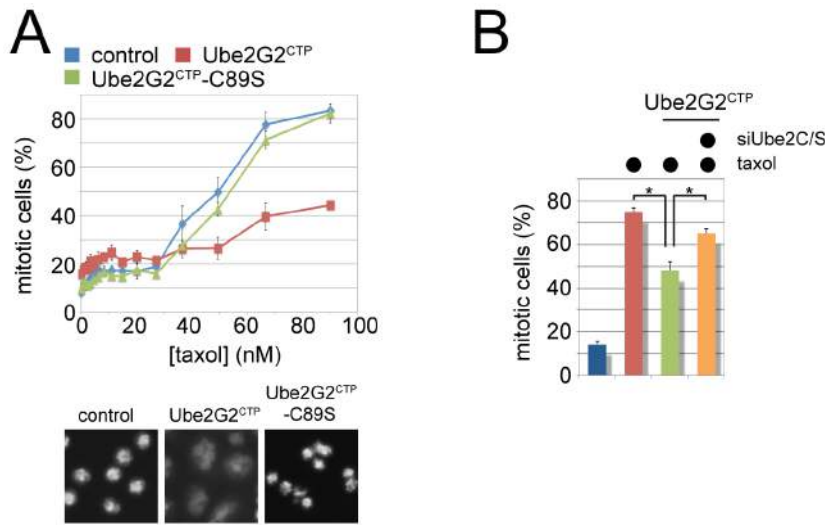


Figure 51: Ube2G2^{CTP} causes bypass of a taxol induced mitotic arrest. **A.** Stable expression of Ube2G2^{CTP}, but not Ube2G2^{CTP}-C89S, causes spindle checkpoint bypass. Upper panel: HeLa cells constitutively expressing indicated

proteins were treated with taxol at concentrations from 0-100 nM for 18 hours. Mitotic arrest was scored by automated microscopy (n=3; >1000 cells/condition; data are average +/- SD; unpaired t- tests p<0.0005). Lower panel: Images of representative cells stained with Hoechst. **B.** Checkpoint bypass requires Ube2G2^{CTP} and Ube2C/Ube2S. HeLa cells or stable cell lines expressing Ube2G2^{CTP} were treated with siRNAs against Ube2C and Ube2S as well as 100 nM taxol, and the mitotic index was determined by automated microscopy (n=3; 1000 cells/condition; data are average +SD; paired t-test p<0.02).

4.8.4. Extent of taxol bypass correlates with the expression level of Ube2G2^{CTP}

To further corroborate that the observed taxol bypass depends on the degree of ubiquitin chain branching, HeLa cells expressing Ube2G2^{CTP} at different levels were tested for taxol bypass assuming that expression levels correlate with ubiquitin branching. Hence, cell lines with varying concentrations of Ube2G2^{CTP} were analyzed after taxol treatment (Figure 52A). The higher the expression level of Ube2G2^{CTP} was the weaker was the response to taxol. This was not due to overall increased levels of E2s working with the APC/C, as raised levels of Ube2S in HeLa cells did not lead to taxol bypass (Figure 52B). Consequently the amount of K11/K48-branched chain formation determined the degree of spindle checkpoint bypass, which is a known consequence of increased APC/C activity.

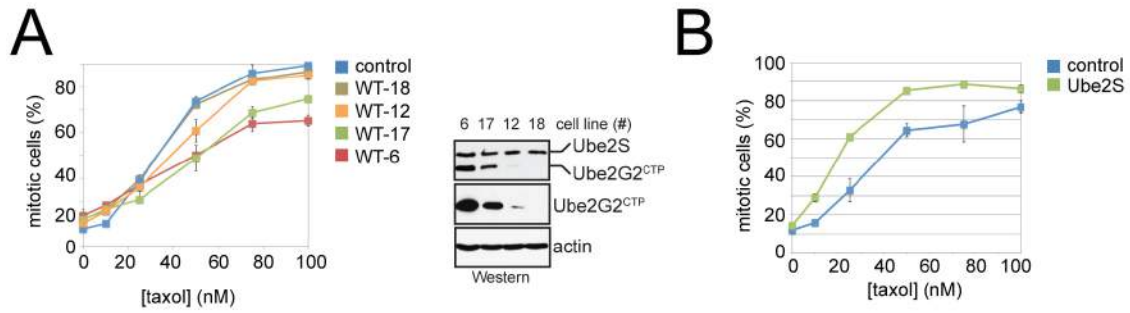


Figure 52: Correlation between taxol bypass and Ube2G2^{CTP} levels. **A.** Stable expression of Ube2G2^{CTP} along with endogenous Ube2S and Ube2C results in concentration dependent spindle checkpoint bypass. Different clones of Ube2G2^{CTP} expressing stable cell lines were analyzed for cell cycle arrest by taxol, as measured by Hoechst staining and automated image analysis (n=3; >1000 cells/n; data are average +/- SD). Protein expression was monitored by western blot analysis. **B.** Constitutive expression of Ube2S does not cause spindle checkpoint bypass. HeLa cells constitutively expressing additional exogenous Ube2S were subjected to increasing concentrations of taxol, and the number of mitotic cells was determined as described above (n=3, >1000 cells per n; data are average +/- SD).

4.8.5. Expression of Ube2G2^{CTP} leads to aneuploidy in HeLa cells

Enabling the APC/C to form K11/K48-branched increases APC/C activity and desensitizes the APC/C towards inhibition by the spindle assembly checkpoint, which was determined in taxol bypass assays. The inability of the SAC to regulate the APC/C leads to aneuploidy, as cells are not able to halt progression into anaphase before chromosomes are properly aligned. Expression of high levels of Ube2G2^{CTP} in HeLa cells caused extensive multinucleation after extensive periods of time in culture, as was seen in cells stained by immunofluorescence, while expression of additional Ube2S did not show multinucleation (Figure 53). To quantify aneuploidy in these cells the relative amount of DNA based on propidium iodide fluorescence was measured. FACS detected a significant, more than twofold increase of cells beyond the G2/M population. Accordingly aberrant ubiquitin chain branching leads to aneuploidy.

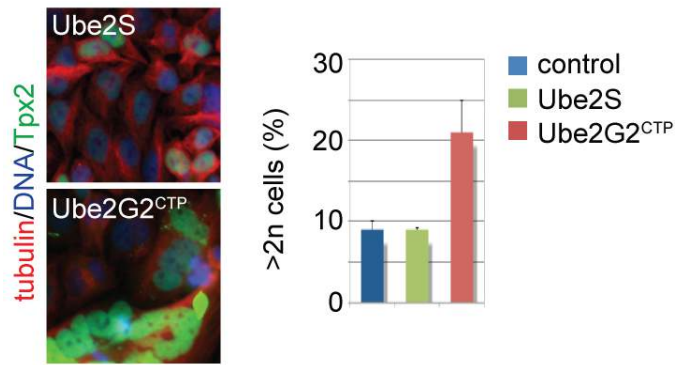


Figure 53: Ube2G2^{CTP} causes aneuploidy. Left: Expression of Ube2G2^{CTP} with endogenous Ube2S results in multinucleation. HeLa cells constitutively expressing an extra copy of Ube2S or Ube2G2^{CTP} were imaged for tubulin (red), Tpx2 (green), and DNA (blue). Right: The stable cell lines described above

were subjected to propidium iodide staining and FACS (n=3; 30000 cells per n; data are average + SD).

4.9. Branching of ubiquitin chains seems to be applicable to other E2/E3 pairs

At last it was tested if the formation of K11-branched chains by Ube2S on short chains made by Ube2C was unique to the way K11 chains are built by the APC/C. The ability of other lysine specific E2s to introduce ubiquitin branches was investigated, to determine if these could extend chains of a different linkage type. Ube2G2 activated by the cytosolic domain of the ERAD E3 ligase gp78 and the heterodimeric E2 complex of Ube2N and Ube2V1 activated by the E3 TRAF6 (Deng et al., 2000) are known to specifically synthesize K48- or K63-linked ubiquitin chains (Eddins et al., 2006; Li et al., 2009). The linear ubiquitin fusions of cyclin A were used as a template for branching. Modification of these fusions with the respective E3 activated E2s using methyl-ubiquitin, showed the introduction of branches (Figure 54A). The introduction of branches was linkage specific as the respective ubiquitin mutants, ubi^{R48} or ubi^{R63}, led to attachment of single ubiquitin moieties (Figure 54A). The rate for elongating a distal or a proximal ubiquitin moiety seemed to be similar for K48 and K63 ubiquitylation enzymes (Figure 54B), which was shown to be the case for the K11 specific Ube2S above. Theoretically the branching of ubiquitin chains could therefore be a general cellular mechanism for other kinds of ubiquitin linkages.

Results

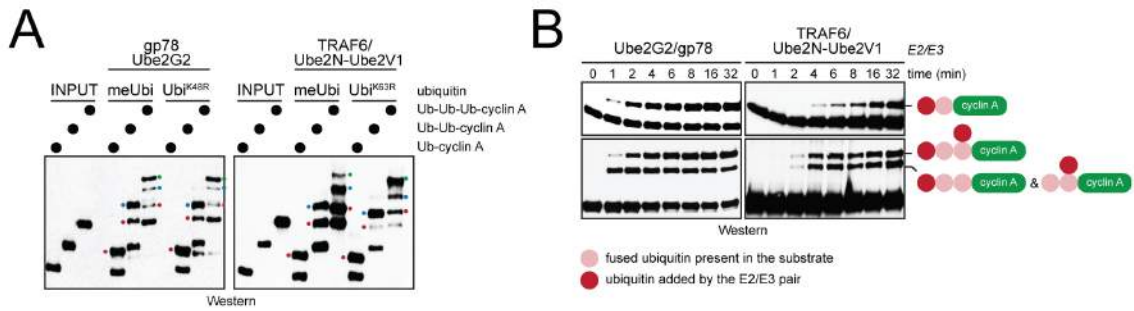


Figure 54: K48 and K63 specific ubiquitylation enzymes are able to branch ubiquitin chains. **A.** Ube2G2-gp78 and Ube2N/Ube2V1-TRAF6 catalyze branching, and branched chains have K48 or K63 linkage specificity. Ub-cyclin A^{HA}, Ub₂-cyclin A^{HA} or Ub₃-cyclin A^{HA} was incubated with Ube2G2 and gp78 in the presence of methyl-ubiquitin or ubi^{R48}. Reactions were analyzed by α HA western blots. The E2s Ube2N/Ube2V1 and its E3 TRAF6 catalyze branching, and branched chains have K63 specificity. Ub-cyclin A^{HA}, Ub₂-cyclin A^{HA}, or Ub₃-cyclin A^{HA} was incubated with Ube2N/Ube2V1 and TRAF6 in the presence of methyl-ubiquitin or ubi^{R63}. Reactions were analyzed by α HA western blots. **B.** Ube2G2-gp78 and Ube2N/Ube2V1-TRAF6 catalyze branching as efficiently as chain elongation. Ub-cyclin A^{HA}, Ub₂-cyclin A^{HA} or Ub₃-cyclin A^{HA} was incubated with Ube2G2-gp78 or Ube2N/Ube2V1-TRAF6 and methyl-ubiquitin for the indicated time points and the reaction products were analyzed by α HA western blot.

5. Discussion

The posttranslational modification of proteins with ubiquitin is a powerful tool for the cell to modulate crucial processes in eukaryotes and is therefore essential for signaling, proliferation, differentiation and survival of cells (Deshaies and Joazeiro, 2009; Schulman and Harper, 2009). Besides attachment of a single ubiquitin molecule to a substrate, ubiquitin chain formation can occur through seven lysine residues (K6, K11, K27, K29, K33, K48, K63) or the N-terminus of ubiquitin (M1), leading to the assembly of multiple chains with distinct topology (Komander and Rape, 2012). While all different topologies exist within cells (Peng et al., 2003; Xu et al., 2009) it is not completely understood how much the modification of a certain protein with a specific ubiquitin chain topology actually matters. Much progress had recently been made in the characterization of K11-linked ubiquitin chains synthesized by the APC/C, sometimes still referred to as an atypical or non-canonical chain type (Meyer and Rape, 2011; Wickliffe et al., 2011b). In this study the formation of ubiquitin chains by the APC/C on its substrates and the outcome of changing the topology of ubiquitin chains was closely investigated. The reported findings above are further discussed regarding the current literature and remaining open questions.

5.1. The APC/C synthesizes branched ubiquitin chains.

Branched chains were detected for the first time in yeast about ten years ago (Peng et al., 2003). In this case, K29/K33 branched ubiquitin peptides were detected by mass spectrometry of a NiNTA pull down of untreated yeast cells expressing ^{His}ubiquitin. The same branch and two others, K11/K27 and K27/K29, were reported three years later, again using mass spectrometry and this time tandem purification with NiNTA and streptavidin of ^{His/Biotin}ubiquitin from yeast (Tagwerker et al., 2006). Further evidence for the existence of branched chains was given *in vitro* four years later (Kim et al., 2007), when denatured luciferase was modified by the E3 carboxy terminus of Hsp70-interacting protein (CHIP)

and Ube2D or in autoubiquitylation of the E3s Muscle-specific RING finger protein 1 (MuRF1) or Double minute 2 protein (Mdm2). Branches of K6/K11, K27/K29 and K29/K33 were detected by mass spectrometry. Ube2D in combination with different RING E3 ubiquitin ligases seems to be mainly unspecific regarding the linkage of ubiquitin chains (Komander and Rape, 2012). Therefore, branches could occur randomly involving any of the seven lysine residues on ubiquitin. Due to methods-based limitations, only K6/K11, K27/K29 and K29/K33 ubiquitin branches might have been detected. Four years later a combination of linkage specific immunoprecipitation and mass spectrometry of samples from human cells was used for quantitative analysis of ubiquitin linkages, which indicated branched chains mainly consisting of K11, K48 and K63 linkages (Phu et al., 2011).

Furthermore, the presence of S5a *in vitro* was shown to inhibit the formation of branched chains by Ube2D (Kim et al., 2009); this has not been tested in the case of the APC/C *in vitro* and in general *in vivo*. Hence it is unclear if free S5a is changing the abundance of branched chains in the cell. If this were the case, it would be an example of how the formation of branched chains might be regulated in cells.

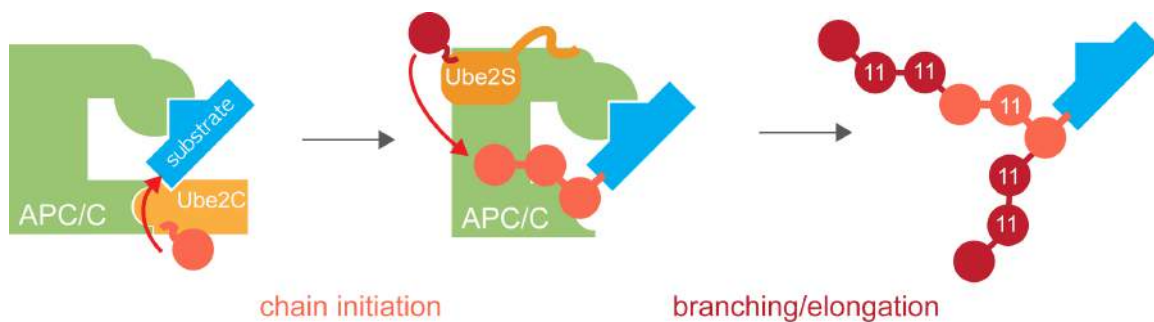


Figure 55: Enhanced protein degradation by branched ubiquitin chains. Ube2C initially modifies APC/C substrates with short chains containing mainly K11, K48 and K63 linkages. Ube2S adds blocks of about six K11-linked ubiquitin molecules to each chain moiety with an unmodified K11. This process leads to the formation of branched ubiquitin chains that increase the proteolytic capacity of the initial ubiquitylation mark.

The synthesis of branched chains by the APC/C seems to be different from the Ube2D/E3 pairs discussed above. The assembly of branched chains in this study

depends upon the cooperation of ubiquitylation enzymes with different linkage specificities, a condition fulfilled by the E2s of metazoan APC/C. Ube2C initiates chain formation by modifying substrates with short conjugates containing 50% K11-, but also K48- and K63-linkages (Kirkpatrick et al., 2006). At least *in vitro*, the APC/C is also able to nucleate chains with E2s of the Ube2D-family, which synthesize ubiquitin chains with little linkage preference (Kirkpatrick et al., 2006). The collaboration of APC/C and Ube2C versus Ube2D is still controversial, but it seems Ube2C is the main E2 specifically working with the APC/C (Summers et al., 2008). If the initiating E2s use K48- or K63-linkages, K11 of an internal ubiquitin remains unmodified and provides a site for Ube2S to branch off a K11-linked chain (Figure 55). Ube2S is also able to modify ubiquitin molecules embedded in linear or completely K48-linked chains. This is in line with published structures of K48, K63 or M1 polyubiquitin. K11 is surface exposed in these chain types and should be accessible by Ube2S (Figure 56). Ube2S might additionally be able to induce changes in the conformation of a present ubiquitin chain. It has been shown that ubiquitin dimers undergo conformational transitions (Ye et al., 2012). Binding to Ube2S could lead to a polyubiquitin conformation favorable for K11-linked ubiquitin chain modification. It seems the presence of a free K11, but not overall chain linkage or structure, determines formation of a branch point. Consistent with this notion, Ube2S synthesized a branch with the same efficiency and specificity, as it promoted chain elongation at the distal ubiquitin. It is interesting to note that Ube2S synthesizes a branched linkage with such high efficiency. As documented with linkage-specific antibodies, the accumulation of K11-linked chains during mitosis depends entirely on Ube2S (Matsumoto et al., 2010; Wickliffe et al., 2011), indicating that its linkage specificity is different from most, if not all mitotic ubiquitylation enzymes. Combined with its efficiency in synthesizing branched linkages, this observation implies that Ube2S could also branch K11-linked chains off conjugates initiated by other enzymes that interact with the APC/C. Indeed several APC/C substrates are shown to be substrates of other E3s as well (Donzelli et al., 2002; Emanuele et al., 2011; Fujii et al., 2006; Germani et al., 2000; Hsu et al., 2004; Meyer and Rape, 2011).

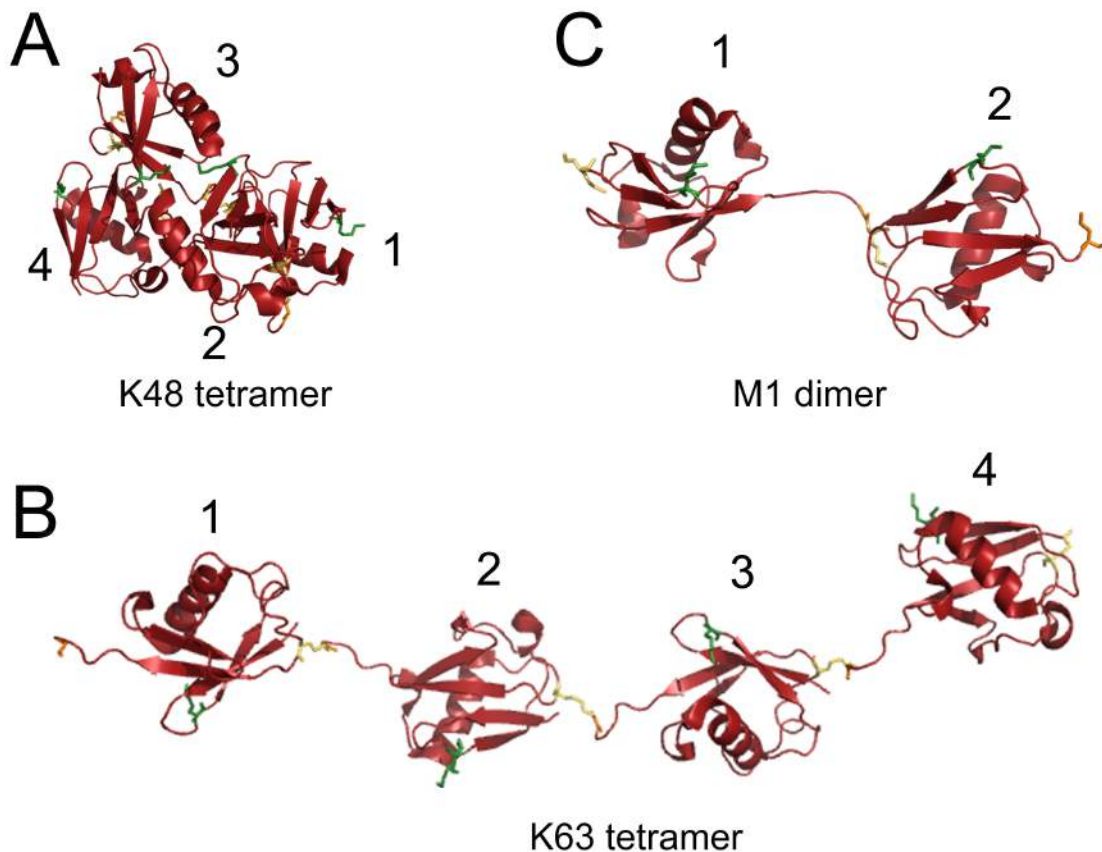


Figure 56: Conformations of differently linked ubiquitin chains. K11 is accessible in K48, K63 and M1 chains. **A.** K48-linked ubiquitin tetramers show a closed conformation. Lysine 11 residues are accessible in a closed conformation (PDB 2O6V). Position 48 in every moiety is shown in yellow. **B.** K63-linked ubiquitin tetramers show an open conformation. Lysine 11 residues are accessible in an open conformation (PDB 3HM3). K63 in every moiety is shown in yellow. **C.** M1-linked ubiquitin dimers show an open conformation. Lysine 11 residues are accessible in linear chains (PDB 2W9N). The C-terminus and M1 in every moiety is shown in yellow. Ubiquitin moieties are numbered increasingly from proximal to the very distal ubiquitin (C-terminal residues within the single moieties are orange; K11 residues are colored green).

Whether APC/C activity overlaps spatially and temporally with these other E3s needs to be analyzed in more detail. If this were the case, it raises the interesting possibility that the K11 specificity of metazoan APC/C did not arise due to a particular function of this topology, but because it allowed the formation of branched chains on as many initial ubiquitin conjugates as possible.

Mixed linkages are a general term for ubiquitin chains containing different linkages. In this study it was determined that the APC/C mainly produces K11-linked ubiquitin chains, but uses non-K11 linkages made by Ube2C to branch off K11-linked chains produced by Ube2S. Technically, therefore ubiquitin conjugates on APC/C substrates consist of mixed chains. Here it was analyzed in more detail that these particular chains are branched chains, which are technically a subcategory of mixed chains. A significant number of reports suggest the presence of mixed chains made by other E2s and E3s (Blankenship et al., 2009; Boname et al., 2010; Emmerich et al., 2013; Huang et al., 2013; Kirkpatrick et al., 2006; Newton et al., 2008; Phu et al., 2011; Ben-Saadon et al., 2006; Winborn et al., 2008). Unfortunately the topology of these conjugates was not analyzed in more detail. It can be speculated that at least some of these systems might be due to ubiquitin chain branching as well. For instance the modification of key players in the NF- κ B pathway are ubiquitylated by K63-linked chains and subsequently by M1-linked chains (Emmerich et al., 2013), raising the possibility of a combination of the two linkage types in a branched manner to enhance signaling. Additional experiments regarding these cellular processes need to be done to differentiate between mixed chains containing branches or not.

5.2. Enhanced protein degradation by branched ubiquitin chains.

To decipher the information encoded by branched chains, we generated a toolkit of E2s that allowed us to modify substrates with K11-, K48-linked or K11/K48-branched chains. Engineering Ube2G2^{CTP} to produce K48-linked ubiquitin chains with the APC/C showed that a RING E3 can be reprogrammed to form different ubiquitin topologies. Consequently the E3 and in particular the RING show no substantial restraint for a certain ubiquitin linkage. RING E3 reprogramming is consistent with a study of HECT E3s. Instead of the E2, only the C-terminal lobe of the HECT domain had to be switched out to reprogram the linkage specificity of these E3s (Wang et al., 2006). Ube2G2 is known to assemble ubiquitin chains

on its catalytic site and transfer them to the substrate *en bloc* (Li et al., 2007b). It was not fully determined if Ube2S might modify these pre-formed K48 chains on Ube2G2^{CTP} with K11-linked chains or if both E2s worked sequentially. To allow for modification with K11 and K48 ubiquitylation in a single binding event both E2s, Ube2S and Ube2G2^{CTP}, had to be bound to the APC/C at the same time. The exact binding sites and stoichiometry of Ube2S on the APC/C are not known, giving room to the assumption that multiple E2s are able to bind simultaneously to APC/C complexes via the CTP. Ube2G2^{CTP} though seems to work differently with the APC/C compared to Ube2S. While Ube2S does not seem to interact with the RING domain of APC/C in a canonical manner like Ube2C (Williamson et al., 2009a), Ube2G2^{CTP} requires its RING finger interaction sites and is inhibited by the presence of dominant negative Ube2C blocking the RING domain. Interestingly, Ube2G2^{CTP} is able to interact with the RING probably because of the raised affinity towards the APC/C due to the CTP, as Ube2G2 is inactive with the APC/C. This raises the question if RING finger interacting UBC domains would show activity with a variety of RING domains if they had additional binding motifs for the respective E3.

As a key result of this study it was shown for the same protein that K11- and K48-linked chains mediate substrate binding to the proteasome with similar efficiency, and accordingly both chain topologies trigger degradation at times when the APC/C is fully active. These findings confirm that K11-linked chains are powerful degradation signals (Jin et al., 2008; Matsumoto et al., 2010). Moreover they show that the K11 specificity of the APC/C is not essential for the turnover of anaphase substrates, while K48-linked chains are not a prerequisite for substrate targeting to the proteasome. Interestingly it was recently reported that different ubiquitin linkages show different kinetics for chain formation; the closed K48-linked chain was elongated slower than the open K63-linked chain (Kovacev et al., 2014). In this study the formation of both closed K11- and K48-linked chains seemed comparable leading to the assumption that the observed differences were caused by the conformation of the ubiquitin chain. This will need to be further tested with more precise kinetic measurements. The same report showed

slower rates for longer ubiquitin chain synthesis. If that were the case, branching would be beneficial for faster ubiquitin transfer of more ubiquitin moieties. Ube2G2^{CTP} mediated K48-linked chain formation though was not able to catalyze degradation of a weakly binding APC/C substrate or of a standard APC/C substrate under conditions of low APC/C activity. It is possible, that Ube2G2^{CTP} mediated K48-linked chain formation could not be quite as active as formation of homogenous K11-linked chains by Ube2C/Ube2S. In this particular case, inhibition by the MCC might be different regarding the engineered E2 or K11-linked chains as they do fulfill a more specific purpose under those conditions. Nevertheless the observations presented here thus support studies that found most linkages to accumulate in response to proteasome inhibition, indicative of a proteolytic role for the majority of chain topologies (Dammer et al., 2011; Peng et al., 2003; Xu et al., 2009). This finding is particularly interesting in light of the ongoing debate whether K63 chains can catalyze degradation by the proteasome similarly to K48-linked chains (Saeki et al., 2009; Thrower et al., 2000): A recent study postulated inhibition of K63 mediated proteasomal degradation by endosomal sorting complexes required for transport 0 (ESCRT0; Nathan et al., 2013). Others report preferred hydrolysis of K63 chains by DUBs (Cooper et al., 2009; Jacobson et al., 2009). On the other hand an E3 ligase making K63 chains is directly bound to the proteasome enhancing its degradation processivity (Aviram and Kornitzer, 2010; Crosas et al., 2006). Unfortunately attempts to reprogram the APC/C to make K63-linked chains by fusing Ube2N or Ube2V1 to the CTP failed suggesting that a heterodimeric E2 seems not to work in this case. However lessons learned from the debate regarding K48- and K63-linked chains were applied to the conundrum of K11- and K48-linked chains both targeting proteins to the proteasome. The ubiquitin-interacting proteins used in this study showed no apparent difference between K11- and K48-linked chains in line with similar affinities for proteasomal delivery factors determined *in vitro* (Sokratous et al., 2012). No major differences in DUB sensitivity of K11 and K48 chains were encountered, while a reported K11 specific DUB has not been shown to be involved in cell cycle regulation (Bremm et al., 2010). Additionally a

recent study presented that the DUB Rpn10 in the proteasomal lid showed no preference for a certain ubiquitin linkage (Worden et al., 2014). Nevertheless the presence of such specific proteins is still possible and needs to be further addressed in future experiments, but at the same time it seems that multiple polyubiquitin topologies mediate proteasomal degradation.

Providing a potential explanation for this apparent redundancy, it is proposed that the combination of different chain types allows formation of branched conjugates with improved signaling capacity. Branched conjugates with multiple blocks of K11-linked chains, as generated by the APC/C, increased the efficiency of substrate recognition by the proteasome, and accordingly promoted degradation in purified systems, extracts or cells even under conditions of low APC/C activity. Thus, distinct from randomly branched chains that impair degradation (Kim et al., 2007), the branched conjugates assembled by the APC/C act as particularly powerful proteolytic signals. In particular Kim and colleagues showed that branched chains were less efficiently hydrolyzed by the 26S proteasome, resulting in the enrichment of K6/K11 branches after treatment of branched chains with purified proteasome. This might not be due to branches *per se*, but because of the modification of K6, which has been reported to inhibit proteasomal processing (Shang et al., 2005). More generally they also measured that substrates being decorated with branched chains were degraded slower by the 26S proteasome. This data was acquired *in vitro* and still needs to be validated in cells showing that Ube2D would modify substrates with branched ubiquitin chains causing a slow degradation by the 26S proteasome. Another study gives further clarification regarding branched chains and the proteasome, as K48/K63 branches are reported to be processed by the proteasome (Nakasone et al., 2013). It seems that branched chains could encode different information dependent upon the linkages that were used to form these branches. Branched chains are not weaker degradation signals in general though.

Why branched chains with multiple blocks of K11 linkages facilitate proteasomal degradation requires further analysis. Here the idea is postulated that the higher signal capacity of branched chains originates from increased levels of substrate-

attached ubiquitin, which overcomes the modest affinity of effectors towards ubiquitin. Furthermore even if linkages are being mixed, the individual linkages are still read independently (Nakasone et al., 2013), which makes the presence of factors specifically recognizing the branch less likely. As longer ubiquitin chains do not provide a similar effect (Thrower et al., 2000), ubiquitin probably has to be concentrated close to the substrate, thus promoting multivalent recognition by effectors with several ubiquitin-binding domains in the same complex. Indeed, the proteasome and p97, both of which efficiently bind branched chains, contain multiple binding domains for ubiquitylated substrates (Finley, 2009; Lander et al., 2012; Richly et al., 2005). Especially the proteasome has been suggested to have other ubiquitin binding sites besides its already two postulated ubiquitin receptors (Archer et al., 2008; Finley, 2009; Lam et al., 2002). If these hypotheses were correct, it would be expected that multiple ubiquitin moieties or short chains attached to neighboring substrate lysine residues should also stimulate degradation. This is the case for cyclin B, which can be degraded under such conditions (Dimova et al., 2012). Thus branching might only be necessary when the number of ubiquitylation sites on a substrate is limited similar to dependency on Ube2S for degradation of single lysine substrates (Dimova et al., 2012). This would open up ways of regulating ubiquitin chain branching on substrates by posttranslational modifications such as acetylation limiting the number of available lysine residues (Choi et al., 2009). Moreover, attachment of the first ubiquitin to a substrate lysine is often the rate limiting step of chain formation (Pierce et al., 2009), and cleavage of the proximal ubiquitin represents the rate-limiting step of degradation (Finley, 2009). The capacity of branched chains to increase the ubiquitin density without introducing more rate limiting steps could provide an explanation for why these conjugates generate a particularly powerful proteolytic signal.

5.3. Why did branched chains evolve in metazoans?

Our discovery that human APC/C assembles branched chains might provide insights into the changes in linkage specificity that occurred between yeast and metazoan APC/C. The APC/C in *Saccharomyces cerevisiae* initiates chain formation in mitosis with Ubc4, which seems to add single ubiquitin molecules to substrates (Rodrigo-Brenni and Morgan, 2007; Stoll et al., 2011), while the metazoan APC/C initiates chain formation with Ube2C leading to the introduction of monoubiquitylations and of short chains containing K11, K48 and K63 linkages (Dimova et al., 2012; Kirkpatrick et al., 2006). Based on the reports in yeast it seems unlikely that yeast APC/C catalyzes formation of ubiquitin branches, as only single ubiquitin moieties are present after initiation. Metazoan APC/C synthesizes branched chains with Ube2C and Ube2S. While Ube2S does not have a homologue in *Saccharomyces cerevisiae*, the Ube2C homologue Ubc11 is only poorly expressed in cycling *Saccharomyces cerevisiae* cells (Chu et al., 1998). In this study it was shown that Ube2S plays an important role in prometaphase, a cell cycle stage that might not be present at all or is present in a different form in *S.cerevisiae*, which undergoes closed mitosis, and metazoans, where nuclear envelope breakdown dictates that spindle assembly occurs without the chromosomes being confined to a subcellular compartment. Interestingly Nek2A activity correlates with phosphorylation of the nuclear pore complex protein 98 (Nup98) homologue and its dispersal from the nuclear pore complex in mitosis leads to partial disassembly of the nuclear envelope (Güttinger et al., 2009; De Souza et al., 2004). At the same time Nek2A was one of the APC/C substrates that was the most sensitive to inhibition of branching by Ube2S depletion. Also possibly reflecting these differences but highly speculative is that maybe only few substrates are degraded during early mitosis in *S.cerevisiae*, whereas in metazoans several examples of APC/C substrate degradation have been reported at this cell cycle time (Amador et al., 2007; Chow et al., 2012; Gabellini et al., 2003; Hayes et al., 2006; Peart et al., 2010; Sedgwick et al., 2013; Song and Rape, 2010; Wolthuis et al., 2008). In addition

prometaphase APC/C continuously disassembles spindle checkpoint complexes, which results in a dynamic interplay between the APC/C and the checkpoint. Checkpoint disassembly is strongly promoted by a metazoan specific protein, p31^{comet}, which might point to an increased extent of checkpoint disassembly in these organisms (Foster and Morgan, 2012; Reddy et al., 2007; Uzunova et al., 2012; Varetta et al., 2011; Williamson et al., 2009a). It is therefore speculated that the increased proteolytic capacity of branched chains, formation of which required the emergence of Ube2C producing short chains and Ube2S branching off K11-linked chains, allowed the metazoan APC/C to cope with higher demands on its activity during early stages of cell division.

5.4. Concluding remarks and perspectives

In this study the APC/C was identified as an enzyme that synthesizes branched ubiquitin chains. I also discovered a critical role for such conjugates in driving efficient proteasomal degradation. Branched conjugates are synthesized during mitosis when Ube2S adds multiple K11-linked chains to mixed assemblies produced by the initiating E2s of APC/C (Figure 55). Branched chains strongly improve proteasomal substrate recognition and accordingly are required for degradation at times of limited APC/C activity. Similar branching activities for K48 and K63 specific enzymes were observed, suggesting that branched chains might frequently be employed in ubiquitin dependent signaling. Regarding the K11 branching activity of the APC/C, it will be interesting to determine if other E3s synthesizing non-K11-linked chains collaborate with the APC/C in building branched ubiquitin chains on common substrates. In future experiments other ways have to be developed to detect branched chains, i.e. raising antibodies specifically against branched chains or further improving mass spectrometry based approaches. This would allow the identification of other cellular processes regulated by ubiquitin chain branching. The presence of E4s in cells, enzymes elongating existing ubiquitin chains (Crosas et al., 2006; Huang et al., 2014;

Koegl et al., 1999; Liu et al., 2011; Shi et al., 2009), will have to be further investigated in the light of the results published in this study.

6. Abbreviations

General abbreviations

3'UTR	Three prime untranslated region
293T	Human Embryonic Kidney 293 cells with large T antigen
aa	amino acids
A	adenine in context of DNA and RNA
AMP	adenosine-5'-monophosphate
APC/C	anaphase-promoting complex/cyclosome
APS	ammonium persulfate
ATP	adenosine-5'-triphosphate
Aurora A	Aurora A kinase = serine/threonine protein kinase 6
C	cytosine in context of DNA and RNA
C-	Carboxyl-, in context of proteins
cDNA	complementary DNA
CD3	cluster of differentiation 3
Cdc	Cell-division cycle protein
Cdh1	Cdc homologue twenty 1
<i>C.elegans</i>	<i>Caenorhabditis elegans</i>
CHX	cycloheximide
CMV	cytomegalovirus
CRL	cullin-RING based Ubiquitin E3 ligase
Da	Dalton
Δ	deletion of
DBOX	destruction box of APC/C substrates (RxxL)
DMEM	Dulbecco's Modified Eagle Medium
DMSO	dimethylsulfoxide
DNA	deoxyribonucleic acid
dNTP	deoxynucleotide triphosphate
DTT	dithiothreitol
DUB	deubiquitinating enzyme
E1	ubiquitin-activating enzyme
E2	ubiquitin-conjugating enzyme
E3	ubiquitin ligase

Abbreviations

<i>E.coli</i>	<i>Escherichia coli</i>
EDTA	ethylenediaminetetraacetic acid
EGTA	ethylene glycol tetraacetic acid
Emi1	Early mitotic inhibitor 1
ER	Endoplasmic reticulum
ERAD	Endoplasmic-reticulum-associated protein degradation
FACS	Fluorescence-activated cell sorting applied in flow cytometry
FAF1	FAS-associated factor 1
FAF2	FAS-associated factor 3
FCS	fetal calve serum
Flp	flippase recombinase
FRT	flippase recognition target
G	guanine in context of DNA and RNA
G0	gap zero phase
G1	gap one phase
G2	gap two phase
GFP	green fluorescent protein
GST	Glutathione-S-transferase
HA	Human influenza hemagglutinin
HCl	hydrochloric acid
HeLa	Henrietta Lacks human cervical cancer cell line
HECT	Homologous to the E6-AP Carboxyl Terminus
HEPES	4-(2-hydroxyethyl)-1-piperazineethanesulfonic acid
HHR23A	human UV excision repair protein RAD23 homolog A
His-	Hexahistidine tagged
HURP	Hepatoma up-regulated protein
IF	Immunofluorescence
IM	Initiation motif
LB	Luria-Bertani broth
M	mitotic phase
Mad2	mitotic arrest deficient 2
MBP	maltose-binding protein
MCC	mitotic checkpoint complex
mRNA	messenger ribonucleotide acid

Abbreviations

MW	molecular weight
N-	Amino-, in context of proteins
NaCl	sodium chloride
NEBD	nuclear envelope breakdown
Nek2A	Never in mitosis A-related kinase 2
Ni-NTA	nickel nitrilotriacetic acid
NP40	Nonidet P-40
NuSAP	Nucleolar and spindle-associated protein 1
oligo	DNA or RNA oligonucleotide
ORF	open reading frame
OTU	ovarian tumor domain
p47	NSFL1 cofactor p47
p97	Transitional endoplasmic reticulum ATPase
PAGE	Polyacrylamide gel electrophoresis
PBS	phosphate buffered saline
PCR	polymerase chain reaction
qRT-PCR	real-time quantitative PCR
RING	really interesting new gene
RNA	ribonucleotide acid
RNAi	RNA interference
S	synthesis phase
S5A	26S proteasome non-ATPase regulatory subunit 4
SAC	spindle assembly checkpoint
SAKS1	SAPK substrate protein 1
<i>S.cerevisiae</i>	<i>Saccharomyces cerevisiae</i>
SCF	Skp1-Cul1-F-box
SD	standard deviation
SDS	sodium dodecyl sulfate
siRNA	small interfering RNA
TAE	Tris acetate EDTA
TEMED	Tetramethylethylenediamine
Tet	tetracycline
TEV	tobacco etch virus
Tris	tris(hydroxymethyl)aminomethane)

Abbreviations

Triton X-100	4-octylphenol polyethoxylate
thy	thymidine
U	uracile in context of RNA
Ub	ubiquitin
UBC	ubiquitin-conjugating domain
UBDX7	UBX domain-containing protein 7
Ube2C	ubiquitin-conjugating enzyme E2 C
Ube2S	ubiquitin-conjugating enzyme E2 S
ubi	ubiquitin
UPS	ubiquitin proteasome pathway
Usp37	ubiquitin-specific-processing protease 37
v/v	volume per volume
w/v	weight per volume
wt	wildtype

Units

°C	degree Celsius
g	gram
g	acceleration of gravity on earth in the context of centrifuges
h	hour
l/L	litre
m	meter
M	molar (mol/L)
min	minute
OD	optical density
pH	negative common logarithm of the proton concentration
rpm	rounds per minute
s	second
V	Volt

Abbreviations

Prefixes

M	mega-	10^6
k	kilo-	10^3
c	centi-	10^{-2}
m	milli-	10^{-3}
μ	micro-	10^{-6}
n	nano-	10^{-9}
p	pico-	10^{-12}

Code for amino acids

A	Ala	alanine
C	Cys	cysteine
D	Asp	aspartate
E	Glu	glutamate
F	Phe	phenylalanine
G	Gly	glycine
H	His	histidine
I	Ile	isoleucine
K	Lys	lysine
L	Leu	leucine
M	Met	methionine
N	Asn	asparagine
P	Pro	proline
Q	Gln	glutamine
R	Arg	arginine
S	Ser	serine
T	Thr	threonine
V	Val	valine
W	Trp	tryptophane
Y	Tyr	tyrosine
X		any amino acid

7. References

- Alexandru, G., Graumann, J., Smith, G.T., Kolawa, N.J., Fang, R., and Deshaies, R.J. (2008). UBXD7 binds multiple ubiquitin ligases and implicates p97 in HIF1alpha turnover. *Cell* *134*, 804–816.
- Amador, V., Ge, S., Santamaría, P.G., Guardavaccaro, D., and Pagano, M. (2007). APC/C(Cdc20) controls the ubiquitin-mediated degradation of p21 in prometaphase. *Mol. Cell* *27*, 462–473.
- Archer, C.T., Burdine, L., Liu, B., Ferdous, A., Johnston, S.A., and Kodadek, T. (2008). Physical and functional interactions of monoubiquitylated transactivators with the proteasome. *J. Biol. Chem.* *283*, 21789–21798.
- Aristarkhov, A., Eytan, E., Moghe, A., Admon, A., Hershko, A., and Ruderman, J.V. (1996). E2-C, a cyclin-selective ubiquitin carrier protein required for the destruction of mitotic cyclins. *Proc. Natl. Acad. Sci. U. S. A.* *93*, 4294–4299.
- Aviram, S., and Kornitzer, D. (2010). The ubiquitin ligase Hul5 promotes proteasomal processivity. *Mol. Cell. Biol.* *30*, 985–994.
- Bagola, K., von Delbrück, M., Dittmar, G., Scheffner, M., Ziv, I., Glickman, M.H., Ciechanover, A., and Sommer, T. (2013). Ubiquitin binding by a CUE domain regulates ubiquitin chain formation by ERAD E3 ligases. *Mol. Cell* *50*, 528–539.
- Bailly, E., and Bornens, M. (1992). Cell biology. Centrosome and cell division. *Nature* *355*, 300–301.
- Bailly, V., Prakash, S., and Prakash, L. (1997). Domains required for dimerization of yeast Rad6 ubiquitin-conjugating enzyme and Rad18 DNA binding protein. *Mol. Cell. Biol.* *17*, 4536–4543.
- Barford, D. (2011). Structure, function and mechanism of the anaphase promoting complex (APC/C). *Q. Rev. Biophys.* *44*, 153–190.
- Barriere, H., Nemes, C., Du, K., and Lukacs, G.L. (2007). Plasticity of polyubiquitin recognition as lysosomal targeting signals by the endosomal sorting machinery. *Mol. Biol. Cell* *18*, 3952–3965.
- Beckwith, R., Estrin, E., Worden, E.J., and Martin, A. (2013). Reconstitution of the 26S proteasome reveals functional asymmetries in its AAA+ unfoldase. *Nat. Struct. Mol. Biol.* *20*, 1164–1172.
- Bellare, P., Small, E.C., Huang, X., Wohlschlegel, J.A., Staley, J.P., and Sontheimer, E.J. (2008). A role for ubiquitin in the spliceosome assembly pathway. *Nat. Struct. Mol. Biol.* *15*, 444–451.
- Berg, J.M., Tymoczko, J.L., and Stryer (2002). *Lecture notebook for Biochemistry, fifth edition* (New York: W.H. Freeman and Co.).
- Blankenship, J.W., Varfolomeev, E., Goncharov, T., Fedorova, A.V., Kirkpatrick, D.S., Izrael-Tomasevic, A., Phu, L., Arnott, D., Aghajan, M., Zobel, K., et al. (2009). Ubiquitin binding modulates IAP antagonist-stimulated proteasomal degradation of c-IAP1 and c-IAP2(1). *Biochem. J.* *417*, 149–160.
- Boname, J.M., Thomas, M., Stagg, H.R., Xu, P., Peng, J., and Lehner, P.J. (2010). Efficient internalization of MHC I requires lysine-11 and lysine-63 mixed linkage polyubiquitin chains. *Traffic Cph. Den.* *11*, 210–220.

References

- BOOTSMA, D., BUDKE, L., and VOS, O. (1964). STUDIES ON SYNCHRONOUS DIVISION OF TISSUE CULTURE CELLS INITIATED BY EXCESS THYMIDINE. *Exp. Cell Res.* **33**, 301–309.
- Borissenko, L., and Groll, M. (2007). 20S proteasome and its inhibitors: crystallographic knowledge for drug development. *Chem. Rev.* **107**, 687–717.
- Bornens, M. (2002). Centrosome composition and microtubule anchoring mechanisms. *Curr. Opin. Cell Biol.* **14**, 25–34.
- Bossy-Wetzell, E., Schwarzenbacher, R., and Lipton, S.A. (2004). Molecular pathways to neurodegeneration. *Nat. Med.* **10 Suppl**, S2–9.
- Bremm, A., Freund, S.M.V., and Komander, D. (2010). Lys11-linked ubiquitin chains adopt compact conformations and are preferentially hydrolyzed by the deubiquitinase Cezanne. *Nat. Struct. Mol. Biol.* **17**, 939–U47.
- Carrier, L., Schlossarek, S., Willis, M.S., and Eschenhagen, T. (2010). The ubiquitin-proteasome system and nonsense-mediated mRNA decay in hypertrophic cardiomyopathy. *Cardiovasc. Res.* **85**, 330–338.
- Chandra, S., Priyadarshini, R., Madhavan, V., Tikoo, S., Hussain, M., Mudgal, R., Modi, P., Srivastava, V., and Sengupta, S. (2013). Enhancement of c-Myc degradation by BLM helicase leads to delayed tumor initiation. *J. Cell Sci.* **126**, 3782–3795.
- Chang, M., Jin, W., Chang, J.-H., Xiao, Y., Brittain, G.C., Yu, J., Zhou, X., Wang, Y.-H., Cheng, X., Li, P., et al. (2011). The ubiquitin ligase Peli1 negatively regulates T cell activation and prevents autoimmunity. *Nat. Immunol.* **12**, 1002–1009.
- Chao, W.C.H., Kulkarni, K., Zhang, Z., Kong, E.H., and Barford, D. (2012). Structure of the mitotic checkpoint complex. *Nature* **484**, 208–213.
- Chau, V., Tobias, J., Bachmair, A., Marriott, D., Ecker, D., Gonda, D., and Varshavsky, A. (1989). A Multiubiquitin Chain Is Confined to Specific Lysine in a Targeted Short-Lived Protein. *Science* **243**, 1576–1583.
- Chen, K., Chen, S., Huang, C., Cheng, H., and Zhou, R. (2013a). TCTP increases stability of hypoxia-inducible factor 1 α by interaction with and degradation of the tumour suppressor VHL. *Biol. Cell Auspices Eur. Cell Biol. Organ.* **105**, 208–218.
- Chen, Z., Barbi, J., Bu, S., Yang, H.-Y., Li, Z., Gao, Y., Jinasena, D., Fu, J., Lin, F., Chen, C., et al. (2013b). The ubiquitin ligase Stub1 negatively modulates regulatory T cell suppressive activity by promoting degradation of the transcription factor Foxp3. *Immunity* **39**, 272–285.
- Choi, E., Choe, H., Min, J., Choi, J.Y., Kim, J., and Lee, H. (2009). BubR1 acetylation at prometaphase is required for modulating APC/C activity and timing of mitosis. *EMBO J.* **28**, 2077–2089.
- Chow, C., Wong, N., Pagano, M., Lun, S.W.-M., Nakayama, K.-I., Nakayama, K., and Lo, K.-W. (2012). Regulation of APC/CCdc20 activity by RASSF1A-APC/CCdc20 circuitry. *Oncogene* **31**, 1975–1987.
- Chu, S., DeRisi, J., Eisen, M., Mulholland, J., Botstein, D., Brown, P.O., and Herskowitz, I. (1998). The transcriptional program of sporulation in budding yeast. *Science* **282**, 699–705.
- Ciechanover, A. (2005). Intracellular protein degradation: from a vague idea, through the lysosome and the ubiquitin-proteasome system, and onto human diseases and drug targeting (Nobel lecture). *Angew. Chem. Int. Ed Engl.* **44**, 5944–5967.

References

- Ciechanover, A., Heller, H., Katz-Etzion, R., and Hershko, A. (1981). Activation of the heat-stable polypeptide of the ATP-dependent proteolytic system. *Proc. Natl. Acad. Sci. U. S. A.* *78*, 761–765.
- Ciechanover, A., Elias, S., Heller, H., and Hershko, A. (1982). “Covalent affinity” purification of ubiquitin-activating enzyme. *J. Biol. Chem.* *257*, 2537–2542.
- Conze, D.B., Wu, C.-J., Thomas, J.A., Landstrom, A., and Ashwell, J.D. (2008). Lys63-linked polyubiquitination of IRAK-1 is required for interleukin-1 receptor- and toll-like receptor-mediated NF-kappaB activation. *Mol. Cell. Biol.* *28*, 3538–3547.
- Cooper, E.M., Cutcliffe, C., Kristiansen, T.Z., Pandey, A., Pickart, C.M., and Cohen, R.E. (2009). K63-specific deubiquitination by two JAMM/MPN+ complexes: BRISC-associated Brcc36 and proteasomal Poh1. *EMBO J.* *28*, 621–631.
- Crosas, B., Hanna, J., Kirkpatrick, D.S., Zhang, D.P., Tone, Y., Hathaway, N.A., Buecker, C., Leggett, D.S., Schmidt, M., King, R.W., et al. (2006). Ubiquitin chains are remodeled at the proteasome by opposing ubiquitin ligase and deubiquitinating activities. *Cell* *127*, 1401–1413.
- Dammer, E.B., Na, C.H., Xu, P., Seyfried, N.T., Duong, D.M., Cheng, D., Gearing, M., Rees, H., Lah, J.J., Levey, A.I., et al. (2011). Polyubiquitin linkage profiles in three models of proteolytic stress suggest the etiology of Alzheimer disease. *J. Biol. Chem.* *286*, 10457–10465.
- Das, R., Mariano, J., Tsai, Y.C., Kalathur, R.C., Kostova, Z., Li, J., Tarasov, S.G., McFeeters, R.L., Altieri, A.S., Ji, X., et al. (2009). Allosteric activation of E2-RING finger-mediated ubiquitylation by a structurally defined specific E2-binding region of gp78. *Mol. Cell* *34*, 674–685.
- Davies, C.C., Chakraborty, A., Diefenbacher, M.E., Skehel, M., and Behrens, A. (2013). Arginine methylation of the c-Jun coactivator RACO-1 is required for c-Jun/AP-1 activation. *EMBO J.* *32*, 1556–1567.
- Deng, L., Wang, C., Spencer, E., Yang, L., Braun, A., You, J., Slaughter, C., Pickart, C., and Chen, Z.J. (2000). Activation of the Ikbpp kinase complex by TRAF6 requires a dimeric ubiquitin-conjugating enzyme complex and a unique polyubiquitin chain. *Cell* *103*, 351–361.
- Deshais, R.J., and Joazeiro, C.A.P. (2009). RING domain E3 ubiquitin ligases. *Annu. Rev. Biochem.* *78*, 399–434.
- Dikic, I., Wakatsuki, S., and Walters, K.J. (2009). Ubiquitin-binding domains - from structures to functions. *Nat. Rev. Mol. Cell Biol.* *10*, 659–671.
- Dimova, N.V., Hathaway, N.A., Lee, B.-H., Kirkpatrick, D.S., Berkowitz, M.L., Gygi, S.P., Finley, D., and King, R.W. (2012). APC/C-mediated multiple monoubiquitylation provides an alternative degradation signal for cyclin B1. *Nat. Cell Biol.* *14*, 168–176.
- Doil, C., Mailand, N., Bekker-Jensen, S., Menard, P., Larsen, D.H., Pepperkok, R., Ellenberg, J., Panier, S., Durocher, D., Bartek, J., et al. (2009). RNF168 binds and amplifies ubiquitin conjugates on damaged chromosomes to allow accumulation of repair proteins. *Cell* *136*, 435–446.
- Donohue, T.M., Jr (2002). The ubiquitin-proteasome system and its role in ethanol-induced disorders. *Addict. Biol.* *7*, 15–28.
- Donzelli, M., Squatrito, M., Ganoth, D., Hershko, A., Pagano, M., and Draetta, G.F. (2002). Dual mode of degradation of Cdc25 A phosphatase. *EMBO J.* *21*, 4875–4884.

References

- Eddins, M.J., Carlile, C.M., Gomez, K.M., Pickart, C.M., and Wolberger, C. (2006). Mms2-Ubc13 covalently bound to ubiquitin reveals the structural basis of linkage-specific polyubiquitin chain formation. *Nat. Struct. Mol. Biol.* *13*, 915–920.
- Elbashir, S.M., Harborth, J., Lendeckel, W., Yalcin, A., Weber, K., and Tuschl, T. (2001). Duplexes of 21-nucleotide RNAs mediate RNA interference in cultured mammalian cells. *Nature* *411*, 494–498.
- Den Elzen, N., and Pines, J. (2001). Cyclin a is destroyed in prometaphase and can delay chromosome alignment and anaphase. *J. Cell Biol.* *153*, 121–135.
- Emanuele, M.J., Elia, A.E.H., Xu, Q., Thoma, C.R., Izhar, L., Leng, Y., Guo, A., Chen, Y.-N., Rush, J., Hsu, P.W.-C., et al. (2011). Global identification of modular cullin-RING ligase substrates. *Cell* *147*, 459–474.
- Emmerich, C.H., Ordureau, A., Strickson, S., Arthur, J.S.C., Pedrioli, P.G.A., Komander, D., and Cohen, P. (2013). Activation of the canonical IKK complex by K63/M1-linked hybrid ubiquitin chains. *Proc. Natl. Acad. Sci. U. S. A.* *110*, 15247–15252.
- Fang, S., Ferrone, M., Yang, C., Jensen, J.P., Tiwari, S., and Weissman, A.M. (2001). The tumor autocrine motility factor receptor, gp78, is a ubiquitin protein ligase implicated in degradation from the endoplasmic reticulum. *Proc. Natl. Acad. Sci. U. S. A.* *98*, 14422–14427.
- Fierabracci, A. (2012). Proteasome inhibitors: a new perspective for treating autoimmune diseases. *Curr. Drug Targets* *13*, 1665–1675.
- Finley, D. (2009). Recognition and Processing of Ubiquitin-Protein Conjugates by the Proteasome. In *Annual Review of Biochemistry*, (Palo Alto: Annual Reviews), pp. 477–513.
- Foley, E.A., and Kapoor, T.M. (2013). Microtubule attachment and spindle assembly checkpoint signalling at the kinetochore. *Nat. Rev. Mol. Cell Biol.* *14*, 25–37.
- Da Fonseca, P.C.A., Kong, E.H., Zhang, Z., Schreiber, A., Williams, M.A., Morris, E.P., and Barford, D. (2011). Structures of APC/C-Cdh1 with substrates identify Cdh1 and Apc10 as the D-box co-receptor. *Nature* *470*, 274–+.
- Foster, S.A., and Morgan, D.O. (2012). The APC/C Subunit Mnd2/Apc15 Promotes Cdc20 Autoubiquitination and Spindle Assembly Checkpoint Inactivation. *Mol. Cell* *47*, 921–932.
- Fry, A.M., O'Regan, L., Sabir, S.R., and Bayliss, R. (2012). Cell cycle regulation by the NEK family of protein kinases. *J. Cell Sci.* *125*, 4423–4433.
- Fujii, Y., Yada, M., Nishiyama, M., Kamura, T., Takahashi, H., Tsunematsu, R., Susaki, E., Nakagawa, T., Matsumoto, A., and Nakayama, K.I. (2006). Fbxw7 contributes to tumor suppression by targeting multiple proteins for ubiquitin-dependent degradation. *Cancer Sci.* *97*, 729–736.
- Gabellini, D., Colaluca, I.N., Vodermaier, H.C., Biamonti, G., Giacca, M., Falaschi, A., Riva, S., and Peverali, F.A. (2003). Early mitotic degradation of the homeoprotein HOXC10 is potentially linked to cell cycle progression. *EMBO J.* *22*, 3715–3724.
- Gallery, M., Blank, J.L., Lin, Y., Gutierrez, J.A., Pulido, J.C., Rappoli, D., Badola, S., Rolfe, M., and Macbeth, K.J. (2007). The JAMM motif of human deubiquitinase Poh1 is essential for cell viability. *Mol. Cancer Ther.* *6*, 262–268.

References

- Garnett, M.J., Mansfeld, J., Godwin, C., Matsusaka, T., Wu, J., Russell, P., Pines, J., and Venkitaraman, A.R. (2009). UBE2S elongates ubiquitin chains on APC/C substrates to promote mitotic exit. *Nat. Cell Biol.* *11*, 1363–U241.
- Ge, S., Skaar, J.R., and Pagano, M. (2009). APC/C- and Mad2-mediated degradation of Cdc20 during spindle checkpoint activation. *Cell Cycle Georget. Tex* *8*, 167–171.
- Geley, S., Kramer, E., Gieffers, C., Gannon, J., Peters, J.M., and Hunt, T. (2001). Anaphase-promoting complex/cyclosome-dependent proteolysis of human cyclin a starts at the beginning of mitosis and is not subject to the spindle assembly checkpoint. *J. Cell Biol.* *153*, 137–147.
- Genschik, P., Sumara, I., and Lechner, E. (2013). The emerging family of CULLIN3-RING ubiquitin ligases (CRL3s): cellular functions and disease implications. *EMBO J.* *32*, 2307–2320.
- Germani, A., Bruzzoni-Giovanelli, H., Fellous, A., Gisselbrecht, S., Varin-Blank, N., and Calvo, F. (2000). SIAH-1 interacts with alpha-tubulin and degrades the kinesin Kid by the proteasome pathway during mitosis. *Oncogene* *19*, 5997–6006.
- Glotzer, M., Murray, A.W., and Kirschner, M.W. (1991). Cyclin is degraded by the ubiquitin pathway. *Nature* *349*, 132–138.
- Gonzalez, F., Lawrence, D., Yang, B., Yee, S., Pitti, R., Marsters, S., Pham, V.C., Stephan, J.-P., Lill, J., and Ashkenazi, A. (2012). TRAF2 Sets a threshold for extrinsic apoptosis by tagging caspase-8 with a ubiquitin shutoff timer. *Mol. Cell* *48*, 888–899.
- Graham, F.L., and van der Eb, A.J. (1973). A new technique for the assay of infectivity of human adenovirus 5 DNA. *Virology* *52*, 456–467.
- Groll, M., Ditzel, L., Löwe, J., Stock, D., Bochtler, M., Bartunik, H.D., and Huber, R. (1997). Structure of 20S proteasome from yeast at 2.4 Å resolution. *Nature* *386*, 463–471.
- Guicciardi, M.E., Werneburg, N.W., Bronk, S.F., Franke, A., Yagita, H., Thomas, G., and Gores, G.J. (2014). Cellular Inhibitor of Apoptosis (cIAP)-Mediated Ubiquitination of Phosphofurin Acidic Cluster Sorting Protein 2 (PACS-2) Negatively Regulates Tumor Necrosis Factor-Related Apoptosis-Inducing Ligand (TRAIL) Cytotoxicity. *PLoS One* *9*, e92124.
- Güttinger, S., Laurell, E., and Kutay, U. (2009). Orchestrating nuclear envelope disassembly and reassembly during mitosis. *Nat. Rev. Mol. Cell Biol.* *10*, 178–191.
- Haas, A.L., and Bright, P.M. (1988). The resolution and characterization of putative ubiquitin carrier protein isozymes from rabbit reticulocytes. *J. Biol. Chem.* *263*, 13258–13267.
- Haas, A.L., and Rose, I.A. (1982). The mechanism of ubiquitin activating enzyme. A kinetic and equilibrium analysis. *J. Biol. Chem.* *257*, 10329–10337.
- Haas, A.L., Warms, J.V., Hershko, A., and Rose, I.A. (1982). Ubiquitin-activating enzyme. Mechanism and role in protein-ubiquitin conjugation. *J. Biol. Chem.* *257*, 2543–2548.
- Haas, A.L., Warms, J.V., and Rose, I.A. (1983). Ubiquitin adenylate: structure and role in ubiquitin activation. *Biochemistry (Mosc.)* *22*, 4388–4394.
- Haas, A.L., Bright, P.M., and Jackson, V.E. (1988). Functional diversity among putative E2 isozymes in the mechanism of ubiquitin-histone ligation. *J. Biol. Chem.* *263*, 13268–13275.
- Al-Hakim, A., Escribano-Diaz, C., Landry, M.-C., O'Donnell, L., Panier, S., Szilard, R.K., and Durocher, D. (2010). The ubiquitous role of ubiquitin in the DNA damage response. *DNA Repair* *9*, 1229–1240.

References

- Hamazaki, J., Sasaki, K., Kawahara, H., Hisanaga, S., Tanaka, K., and Murata, S. (2007). Rpn10-Mediated Degradation of Ubiquitinated Proteins Is Essential for Mouse Development. *Mol. Cell. Biol.* *27*, 6629–6638.
- Hames, R.S., Wattam, S.L., Yamano, H., Bacchieri, R., and Fry, A.M. (2001). APC/C-mediated destruction of the centrosomal kinase Nek2A occurs in early mitosis and depends upon a cyclin A-type D-box. *EMBO J.* *20*, 7117–7127.
- Hansen, D.V., Loktev, A.V., Ban, K.H., and Jackson, P.K. (2004). Plk1 regulates activation of the anaphase promoting complex by phosphorylating and triggering SCFbetaTrCP-dependent destruction of the APC Inhibitor Emi1. *Mol. Biol. Cell* *15*, 5623–5634.
- Hao, Y.-H., Doyle, J.M., Ramanathan, S., Gomez, T.S., Jia, D., Xu, M., Chen, Z.J., Billadeau, D.D., Rosen, M.K., and Potts, P.R. (2013). Regulation of WASH-dependent actin polymerization and protein trafficking by ubiquitination. *Cell* *152*, 1051–1064.
- Hartwell, L.H., and Weinert, T.A. (1989). Checkpoints: controls that ensure the order of cell cycle events. *Science* *246*, 629–634.
- Hayes, M.J., Kimata, Y., Wattam, S.L., Lindon, C., Mao, G., Yamano, H., and Fry, A.M. (2006). Early mitotic degradation of Nek2A depends on Cdc20-independent interaction with the APC/C. *Nat. Cell Biol.* *8*, 607–614.
- Heid, C.A., Stevens, J., Livak, K.J., and Williams, P.M. (1996). Real time quantitative PCR. *Genome Res.* *6*, 986–994.
- Hershko, A., and Ciechanover, A. (1998). The ubiquitin system. *Annu. Rev. Biochem.* *67*, 425–479.
- Hershko, A., Heller, H., Elias, S., and Ciechanover, A. (1983). Components of ubiquitin-protein ligase system. Resolution, affinity purification, and role in protein breakdown. *J. Biol. Chem.* *258*, 8206–8214.
- Herzog, F., Primorac, I., Dube, P., Lenart, P., Sander, B., Mechtler, K., Stark, H., and Peters, J.-M. (2009). Structure of the Anaphase-Promoting Complex/Cyclosome Interacting with a Mitotic Checkpoint Complex. *Science* *323*, 1477–1481.
- Hjerpe, R., Aillet, F., Lopitz-Otsoa, F., Lang, V., England, P., and Rodriguez, M.S. (2009). Efficient protection and isolation of ubiquitylated proteins using tandem ubiquitin-binding entities. *EMBO Rep.* *10*, 1250–1258.
- Hochstrasser, M. (2006). Lingering mysteries of ubiquitin-chain assembly. *Cell* *124*, 27–34.
- Hoppe, T. (2005). Multiubiquitylation by E4 enzymes: “one size” doesn’t fit all. *Trends Biochem. Sci.* *30*, 183–187.
- Hou, F., Sun, L., Zheng, H., Skaug, B., Jiang, Q.-X., and Chen, Z.J. (2011). MAVS forms functional prion-like aggregates to activate and propagate antiviral innate immune response. *Cell* *146*, 448–461.
- Hsu, J.-M., Lee, Y.-C.G., Yu, C.-T.R., and Huang, C.-Y.F. (2004). Fbx7 functions in the SCF complex regulating Cdk1-cyclin B-phosphorylated hepatoma up-regulated protein (HURP) proteolysis by a proline-rich region. *J. Biol. Chem.* *279*, 32592–32602.
- Huang, F., Zeng, X., Kim, W., Balasubramani, M., Fortian, A., Gygi, S.P., Yates, N.A., and Sorkin, A. (2013). Lysine 63-linked polyubiquitination is required for EGF receptor degradation. *Proc. Natl. Acad. Sci. U. S. A.* *110*, 15722–15727.

References

- Huang, J., Huen, M.S.Y., Kim, H., Leung, C.C.Y., Glover, J.N.M., Yu, X., and Chen, J. (2009). RAD18 transmits DNA damage signalling to elicit homologous recombination repair. *Nat. Cell Biol.* *11*, 592–603.
- Huang, J.-Y., Morley, G., Li, D., and Whitaker, M. (2007). Cdk1 phosphorylation sites on Cdc27 are required for correct chromosomal localisation and APC/C function in syncytial *Drosophila* embryos. *J. Cell Sci.* *120*, 1990–1997.
- Huang, X., Summers, M.K., Pham, V., Lill, J.R., Liu, J., Lee, G., Kirkpatrick, D.S., Jackson, P.K., Fang, G., and Dixit, V.M. (2011). Deubiquitinase USP37 is activated by CDK2 to antagonize APC(CDH1) and promote S phase entry. *Mol. Cell* *42*, 511–523.
- Huang, Y., Minaker, S., Roth, C., Huang, S., Hieter, P., Lipka, V., Wiermer, M., and Li, X. (2014). An E4 Ligase Facilitates Polyubiquitination of Plant Immune Receptor Resistance Proteins in *Arabidopsis*. *Plant Cell Online tpc.113.119057*.
- Hunt, T. (1989). Maturation promoting factor, cyclin and the control of M-phase. *Curr. Opin. Cell Biol.* *1*, 268–274.
- Ihara, Y., Morishima-Kawashima, M., and Nixon, R. (2012). The ubiquitin-proteasome system and the autophagic-lysosomal system in Alzheimer disease. *Cold Spring Harb. Perspect. Med.* *2*.
- Ikui, A.E., Yang, C.-P.H., Matsumoto, T., and Horwitz, S.B. (2005). Low concentrations of taxol cause mitotic delay followed by premature dissociation of p53CDC from Mad2 and BubR1 and abrogation of the spindle checkpoint, leading to aneuploidy. *Cell Cycle Georget. Tex* *4*, 1385–1388.
- Inobe, T., and Matouschek, A. (2014). Paradigms of protein degradation by the proteasome. *Curr. Opin. Struct. Biol.* *24C*, 156–164.
- Jacobson, A.D., Zhang, N.-Y., Xu, P., Han, K.-J., Noone, S., Peng, J., and Liu, C.-W. (2009). The lysine 48 and lysine 63 ubiquitin conjugates are processed differently by the 26 s proteasome. *J. Biol. Chem.* *284*, 35485–35494.
- Jin, J., Li, X., Gygi, S.P., and Harper, J.W. (2007). Dual E1 activation systems for ubiquitin differentially regulate E2 enzyme charging. *Nature* *447*, 1135–1138.
- Jin, L., Williamson, A., Banerjee, S., Philipp, I., and Rape, M. (2008). Mechanism of ubiquitin-chain formation by the human anaphase-promoting complex. *Cell* *133*, 653–665.
- Johansen, K.M., and Johansen, J. (2006). Regulation of chromatin structure by histone H3S10 phosphorylation. *Chromosome Res. Int. J. Mol. Supramol. Evol. Asp. Chromosome Biol.* *14*, 393–404.
- Johnson, E.S., Ma, P.C., Ota, I.M., and Varshavsky, A. (1995). A proteolytic pathway that recognizes ubiquitin as a degradation signal. *J. Biol. Chem.* *270*, 17442–17456.
- Kikuchi, R., Ohata, H., Ohoka, N., Kawabata, A., and Naito, M. (2014). APOLLON Protein Promotes Early Mitotic CYCLIN A Degradation Independent of the Spindle Assembly Checkpoint. *J. Biol. Chem.* *289*, 3457–3467.
- Kim, H.T., Kim, K.P., Lledias, F., Kisselev, A.F., Scaglione, K.M., Skowyra, D., Gygi, S.P., and Goldberg, A.L. (2007). Certain pairs of ubiquitin-conjugating enzymes (E2s) and ubiquitin-protein ligases (E3s) synthesize nondegradable forked ubiquitin chains containing all possible isopeptide linkages. *J. Biol. Chem.* *282*, 17375–17386.

References

- Kim, H.T., Kim, K.P., Uchiki, T., Gygi, S.P., and Goldberg, A.L. (2009). S5a promotes protein degradation by blocking synthesis of nondegradable forked ubiquitin chains. *EMBO J.* *28*, 1867–1877.
- Kim, I., Mi, K., and Rao, H. (2004). Multiple interactions of rad23 suggest a mechanism for ubiquitylated substrate delivery important in proteolysis. *Mol. Biol. Cell* *15*, 3357–3365.
- Kimura, Y., and Tanaka, K. (2010). Regulatory mechanisms involved in the control of ubiquitin homeostasis. *J. Biochem. (Tokyo)* *147*, 793–798.
- King, R., Peters, J., Tugendreich, S., Rolfe, M., Hieter, P., and Kirschner, M. (1995). A 20s Complex Containing Cdc27 and Cdc16 Catalyzes the Mitosis-Specific Conjugation of Ubiquitin to Cyclin-B. *Cell* *81*, 279–288.
- Kirkin, V., and Dikic, I. (2011). Ubiquitin networks in cancer. *Curr. Opin. Genet. Dev.* *21*, 21–28.
- Kirkpatrick, D.S., Hathaway, N.A., Hanna, J., Elsasser, S., Rush, J., Finley, D., King, R.W., and Gygi, S.P. (2006). Quantitative analysis of in vitro ubiquitinated cyclin B1 reveals complex chain topology. *Nat. Cell Biol.* *8*, 700–U121.
- Kleiger, G., and Mayor, T. (2014). Perilous journey: a tour of the ubiquitin-proteasome system. *Trends Cell Biol.*
- Kleiger, G., Hao, B., Mohl, D.A., and Deshaies, R.J. (2009). The acidic tail of the Cdc34 ubiquitin-conjugating enzyme functions in both binding to and catalysis with ubiquitin ligase SCFCdc4. *J. Biol. Chem.* *284*, 36012–36023.
- Klinge, S., Voigts-Hoffmann, F., Leibundgut, M., Arpagaus, S., and Ban, N. (2011). Crystal structure of the eukaryotic 60S ribosomal subunit in complex with initiation factor 6. *Science* *334*, 941–948.
- Koegl, M., Hoppe, T., Schlenker, S., Ulrich, H.D., Mayer, T.U., and Jentsch, S. (1999). A novel ubiquitination factor, E4, is involved in multiubiquitin chain assembly. *Cell* *96*, 635–644.
- Komander, D., and Rape, M. (2012). The ubiquitin code. *Annu. Rev. Biochem.* *81*, 203–229.
- Komander, D., Clague, M.J., and Urbé, S. (2009). Breaking the chains: structure and function of the deubiquitinases. *Nat. Rev. Mol. Cell Biol.* *10*, 550–563.
- Van de Kooij, B., Rooswinkel, R.W., Kok, F., Herrebout, M., de Vries, E., Paauwe, M., Janssen, G.M.C., van Veelen, P.A., and Borst, J. (2013). Polyubiquitination and proteasomal turnover controls the anti-apoptotic activity of Bcl-B. *Oncogene* *32*, 5439–5448.
- Kovacev, J., Wu, K., Spratt, D.E., Chong, R.A., Lee, C., Nayak, J., Shaw, G.S., and Pan, Z.-Q. (2014). A snapshot at ubiquitin chain elongation: Lysine 48-tetra-ubiquitin slows down ubiquitination. *J. Biol. Chem.*
- Kraft, C., Herzog, F., Gieffers, C., Mechtler, K., Hagting, A., Pines, J., and Peters, J.-M. (2003). Mitotic regulation of the human anaphase-promoting complex by phosphorylation. *EMBO J.* *22*, 6598–6609.
- Kramer, L.B., Shim, J., Previtiera, M.L., Isack, N.R., Lee, M.-C., Firestein, B.L., and Rongo, C. (2010). UEV-1 is an ubiquitin-conjugating enzyme variant that regulates glutamate receptor trafficking in *C. elegans* neurons. *PLoS One* *5*, e14291.
- Laemmli, U.K. (1970). Cleavage of structural proteins during the assembly of the head of bacteriophage T4. *Nature* *227*, 680–685.

References

- Lam, Y.A., Lawson, T.G., Velayutham, M., Zweier, J.L., and Pickart, C.M. (2002). A proteasomal ATPase subunit recognizes the polyubiquitin degradation signal. *Nature* *416*, 763–767.
- Lander, G.C., Estrin, E., Matyskiela, M.E., Bashore, C., Nogales, E., and Martin, A. (2012). Complete subunit architecture of the proteasome regulatory particle. *Nature* *482*, 186–191.
- Lara-Gonzalez, P., Westhorpe, F.G., and Taylor, S.S. (2012). The Spindle Assembly Checkpoint. *Curr. Biol.* *22*, R966–R980.
- Latres, E., Chiaur, D.S., and Pagano, M. (1999). The human F box protein beta-Trcp associates with the Cul1/Skp1 complex and regulates the stability of beta-catenin. *Oncogene* *18*, 849–854.
- Lei, C.-Q., Zhang, Y., Xia, T., Jiang, L.-Q., Zhong, B., and Shu, H.-B. (2013). FoxO1 negatively regulates cellular antiviral response by promoting degradation of IRF3. *J. Biol. Chem.* *288*, 12596–12604.
- Li, L., Zhou, Y., Sun, L., Xing, G., Tian, C., Sun, J., Zhang, L., and He, F. (2007a). NuSAP is degraded by APC/C-Cdh1 and its overexpression results in mitotic arrest dependent of its microtubules' affinity. *Cell. Signal.* *19*, 2046–2055.
- Li, W., Tu, D., Brunger, A.T., and Ye, Y. (2007b). A ubiquitin ligase transfers preformed polyubiquitin chains from a conjugating enzyme to a substrate. *Nature* *446*, 333–337.
- Li, W., Tu, D., Li, L., Wollert, T., Ghirlando, R., Brunger, A.T., and Ye, Y. (2009). Mechanistic insights into active site-associated polyubiquitination by the ubiquitin-conjugating enzyme Ube2g2. *Proc. Natl. Acad. Sci. U. S. A.* *106*, 3722–3727.
- Lin, X.-W., Xu, W.-C., Luo, J.-G., Guo, X.-J., Sun, T., Zhao, X.-L., and Fu, Z.-J. (2013). WW domain containing E3 ubiquitin protein ligase 1 (WWP1) negatively regulates TLR4-mediated TNF- α and IL-6 production by proteasomal degradation of TNF receptor associated factor 6 (TRAF6). *PLoS One* *8*, e67633.
- Linares, J.F., Duran, A., Yajima, T., Pasparakis, M., Moscat, J., and Diaz-Meco, M.T. (2013). K63 polyubiquitination and activation of mTOR by the p62-TRAF6 complex in nutrient-activated cells. *Mol. Cell* *51*, 283–296.
- Lindon, C., and Pines, J. (2004). Ordered proteolysis in anaphase inactivates Plk1 to contribute to proper mitotic exit in human cells. *J. Cell Biol.* *164*, 233–241.
- Lipkowitz, S., and Weissman, A.M. (2011). RINGs of good and evil: RING finger ubiquitin ligases at the crossroads of tumour suppression and oncogenesis. *Nat. Rev. Cancer* *11*, 629–643.
- Listovsky, T., Oren, Y.S., Yudkovsky, Y., Mahbubani, H.M., Weiss, A.M., Lebediker, M., and Brandeis, M. (2004). Mammalian Cdh1/Fzr mediates its own degradation. *Embo J.* *23*, 1619–1626.
- Liu, F., and Walters, K.J. (2010). Multitasking with ubiquitin through multivalent interactions. *Trends Biochem. Sci.* *35*, 352–360.
- Liu, C., van Dyk, D., Choe, V., Yan, J., Majumder, S., Costanzo, M., Bao, X., Boone, C., Huo, K., Winey, M., et al. (2011). Ubiquitin ligase Ufd2 is required for efficient degradation of Mps1 kinase. *J. Biol. Chem.* *286*, 43660–43667.
- Liu, J., Yan, J., Jiang, S., Wen, J., Chen, L., Zhao, Y., and Lin, A. (2012). Site-specific ubiquitination is required for relieving the transcription factor Miz1-mediated suppression on TNF- α -induced JNK activation and inflammation. *Proc. Natl. Acad. Sci. U. S. A.* *109*, 191–196.

References

- Liu, W., Shang, Y., Zeng, Y., Liu, C., Li, Y., Zhai, L., Wang, P., Lou, J., Xu, P., Ye, Y., et al. (2014). Dimeric Ube2g2 simultaneously engages donor and acceptor ubiquitins to form Lys48-linked ubiquitin chains. *EMBO J.* *33*, 46–61.
- Lucibello, F.C., Sewing, A., Brüsselbach, S., Bürger, C., and Müller, R. (1993). Deregulation of cyclins D1 and E and suppression of cdk2 and cdk4 in senescent human fibroblasts. *J. Cell Sci.* *105 (Pt 1)*, 123–133.
- Luckow, V.A., Lee, S.C., Barry, G.F., and Olins, P.O. (1993). Efficient generation of infectious recombinant baculoviruses by site-specific transposon-mediated insertion of foreign genes into a baculovirus genome propagated in *Escherichia coli*. *J. Virol.* *67*, 4566–4579.
- Ma, A., and Malynn, B.A. (2012). A20: linking a complex regulator of ubiquitylation to immunity and human disease. *Nat. Rev. Immunol.* *12*, 774–785.
- Mapelli, M., and Musacchio, A. (2007). MAD contortions: conformational dimerization boosts spindle checkpoint signaling. *Curr. Opin. Struct. Biol.* *17*, 716–725.
- Matsumoto, M.L., Wickliffe, K.E., Dong, K.C., Yu, C., Bosanac, I., Bustos, D., Phu, L., Kirkpatrick, D.S., Hymowitz, S.G., Rape, M., et al. (2010). K11-linked polyubiquitination in cell cycle control revealed by a K11 linkage-specific antibody. *Mol. Cell* *39*, 477–484.
- Matsuoka, M., Kato, J.Y., Fisher, R.P., Morgan, D.O., and Sherr, C.J. (1994). Activation of cyclin-dependent kinase 4 (cdk4) by mouse MO15-associated kinase. *Mol. Cell. Biol.* *14*, 7265–7275.
- Matyskiela, M.E., and Morgan, D.O. (2009). Analysis of activator-binding sites on the APC/C supports a cooperative substrate-binding mechanism. *Mol. Cell* *34*, 68–80.
- Maytal-Kivity, V., Reis, N., Hofmann, K., and Glickman, M.H. (2002). MPN+, a putative catalytic motif found in a subset of MPN domain proteins from eukaryotes and prokaryotes, is critical for Rpn11 function. *BMC Biochem.* *3*, 28.
- McGarry, T.J., and Kirschner, M.W. (1998). Geminin, an inhibitor of DNA replication, is degraded during mitosis. *Cell* *93*, 1043–1053.
- Metzger, M.B., Pruneda, J.N., Klevit, R.E., and Weissman, A.M. (2014). RING-type E3 ligases: master manipulators of E2 ubiquitin-conjugating enzymes and ubiquitination. *Biochim. Biophys. Acta* *1843*, 47–60.
- Meyer, H.-J., and Rape, M. (2011). Processive ubiquitin chain formation by the anaphase-promoting complex. *Semin. Cell Dev. Biol.* *22*, 544–550.
- Meyer, H., Bug, M., and Bremer, S. (2012). Emerging functions of the VCP/p97 AAA-ATPase in the ubiquitin system. *Nat. Cell Biol.* *14*, 117–123.
- Micel, L.N., Tentler, J.J., Smith, P.G., and Eckhardt, G.S. (2013). Role of ubiquitin ligases and the proteasome in oncogenesis: novel targets for anticancer therapies. *J. Clin. Oncol. Off. J. Am. Soc. Clin. Oncol.* *31*, 1231–1238.
- Mocciaro, A., and Rape, M. (2012). Emerging regulatory mechanisms in ubiquitin-dependent cell cycle control. *J. Cell Sci.* *125*, 255–263.
- Morgan, D.O. (1997). Cyclin-dependent kinases: engines, clocks, and microprocessors. *Annu. Rev. Cell Dev. Biol.* *13*, 261–291.
- Morgan, D.O. (2007). *The Cell Cycle: Principles of Control* (New Science Press).

References

- Moshe, Y., Boulaire, J., Pagano, M., and Hershko, A. (2004). Role of Polo-like kinase in the degradation of early mitotic inhibitor 1, a regulator of the anaphase promoting complex/cyclosome. *Proc. Natl. Acad. Sci. U. S. A.* *101*, 7937–7942.
- Mullis, K., Faloona, F., Scharf, S., Saiki, R., Horn, G., and Erlich, H. (1986). Specific enzymatic amplification of DNA in vitro: the polymerase chain reaction. *Cold Spring Harb. Symp. Quant. Biol.* *51 Pt 1*, 263–273.
- Murray, A.W., and Kirschner, M.W. (1989). Dominoes and clocks: the union of two views of the cell cycle. *Science* *246*, 614–621.
- Musacchio, A., and Salmon, E.D. (2007). The spindle-assembly checkpoint in space and time. *Nat. Rev. Mol. Cell Biol.* *8*, 379–393.
- Nakasone, M.A., Livnat-Levanon, N., Glickman, M.H., Cohen, R.E., and Fushman, D. (2013). Mixed-linkage ubiquitin chains send mixed messages. *Struct. Lond. Engl.* *1993 21*, 727–740.
- Narisawa-Saito, M., and Kiyono, T. (2007). Basic mechanisms of high-risk human papillomavirus-induced carcinogenesis: roles of E6 and E7 proteins. *Cancer Sci.* *98*, 1505–1511.
- Nasmyth, K. (2001). Disseminating the genome: joining, resolving, and separating sister chromatids during mitosis and meiosis. *Annu. Rev. Genet.* *35*, 673–745.
- Nasmyth, K., Peters, J.M., and Uhlmann, F. (2000). Splitting the chromosome: cutting the ties that bind sister chromatids. *Science* *288*, 1379–1385.
- Nathan, J.A., Kim, H.T., Ting, L., Gygi, S.P., and Goldberg, A.L. (2013). Why do cellular proteins linked to K63-polyubiquitin chains not associate with proteasomes? *EMBO J.* *32*, 552–565.
- Neuhoff, V., Stamm, R., and Eibl, H. (1985). Clear background and highly sensitive protein staining with Coomassie Blue dyes in polyacrylamide gels: A systematic analysis. *ELECTROPHORESIS* *6*, 427–448.
- Newton, K., Matsumoto, M.L., Wertz, I.E., Kirkpatrick, D.S., Lill, J.R., Tan, J., Dugger, D., Gordon, N., Sidhu, S.S., Fellouse, F.A., et al. (2008). Ubiquitin chain editing revealed by polyubiquitin linkage-specific antibodies. *Cell* *134*, 668–678.
- Ng, J.M.Y., Vermeulen, W., Horst, G.T.J. van der, Bergink, S., Sugasawa, K., Vrieling, H., and Hoeijmakers, J.H.J. (2003). A novel regulation mechanism of DNA repair by damage-induced and RAD23-dependent stabilization of xeroderma pigmentosum group C protein. *Genes Dev.* *17*, 1630–1645.
- Nigg, E.A. (2001). Mitotic kinases as regulators of cell division and its checkpoints. *Nat. Rev. Mol. Cell Biol.* *2*, 21–32.
- Nijholt, D.A.T., De Kimpe, L., Elfrink, H.L., Hoozemans, J.J.M., and Scheper, W. (2011). Removing protein aggregates: the role of proteolysis in neurodegeneration. *Curr. Med. Chem.* *18*, 2459–2476.
- Nishikawa, H., Ooka, S., Sato, K., Arima, K., Okamoto, J., Klevit, R.E., Fukuda, M., and Ohta, T. (2004). Mass spectrometric and mutational analyses reveal lys-6-linked polyubiquitin chains catalyzed by BRCA1-BARD1 ubiquitin ligase. *J. Biol. Chem.* *279*, 3916–3924.
- O'Regan, L., Blot, J., and Fry, A.M. (2007). Mitotic regulation by NIMA-related kinases. *Cell Div.* *2*, 25.

References

- Olsen, S.K., and Lima, C.D. (2013). Structure of a ubiquitin E1-E2 complex: insights to E1-E2 thioester transfer. *Mol. Cell* *49*, 884–896.
- Pagan, J., Seto, T., Pagano, M., and Cittadini, A. (2013). Role of the ubiquitin proteasome system in the heart. *Circ. Res.* *112*, 1046–1058.
- Peart, M.J., Poyurovsky, M.V., Kass, E.M., Urist, M., Verschuren, E.W., Summers, M.K., Jackson, P.K., and Prives, C. (2010). APC/C(Cdc20) targets E2F1 for degradation in prometaphase. *Cell Cycle Georget. Tex* *9*, 3956–3964.
- Peng, J.M., Schwartz, D., Elias, J.E., Thoreen, C.C., Cheng, D.M., Marsischky, G., Roelofs, J., Finley, D., and Gygi, S.P. (2003). A proteomics approach to understanding protein ubiquitination. *Nat. Biotechnol.* *21*, 921–926.
- Peschiarioli, A., Scialpi, F., Bernassola, F., El Sherbini, E.S., and Melino, G. (2010). The E3 ubiquitin ligase WWP1 regulates Δ Np63-dependent transcription through Lys63 linkages. *Biochem. Biophys. Res. Commun.* *402*, 425–430.
- Pestova, T.V., and Hellen, C.U.T. (2003). Translation elongation after assembly of ribosomes on the Cricket paralysis virus internal ribosomal entry site without initiation factors or initiator tRNA. *Genes Dev.* *17*, 181–186.
- Peters, J.-M. (2006). The anaphase promoting complex/cyclosome: a machine designed to destroy. *Nat. Rev. Mol. Cell Biol.* *7*, 644–656.
- Petroski, M.D., and Deshaies, R.J. (2005). Mechanism of lysine 48-linked ubiquitin-chain synthesis by the cullin-RING ubiquitin-ligase complex SCF-Cdc34. *Cell* *123*, 1107–1120.
- Pfleger, C.M., and Kirschner, M.W. (2000). The KEN box: an APC recognition signal distinct from the D box targeted by Cdh1. *Genes Dev.* *14*, 655–665.
- Phu, L., Izrael-Tomasevic, A., Matsumoto, M.L., Bustos, D., Dynek, J.N., Fedorova, A.V., Bakalarski, C.E., Arnott, D., Deshayes, K., Dixit, V.M., et al. (2011). Improved Quantitative Mass Spectrometry Methods for Characterizing Complex Ubiquitin Signals. *Mol. Cell. Proteomics MCP* *10*.
- Pickart, C.M. (2004). Back to the future with ubiquitin. *Cell* *116*, 181–190.
- Pickart, C.M., and Rose, I.A. (1985). Functional heterogeneity of ubiquitin carrier proteins. *J. Biol. Chem.* *260*, 1573–1581.
- Pierce, N.W., Kleiger, G., Shan, S., and Deshaies, R.J. (2009). Detection of sequential polyubiquitylation on a millisecond timescale. *Nature* *462*, 615–U85.
- Powell, S.R., Herrmann, J., Lerman, A., Patterson, C., and Wang, X. (2012). The ubiquitin-proteasome system and cardiovascular disease. *Prog. Mol. Biol. Transl. Sci.* *109*, 295–346.
- Primorac, I., and Musacchio, A. (2013). Panta rhei: The APC/C at steady state. *J. Cell Biol.* *201*, 177–189.
- Quinn, L.M., Herr, A., McGarry, T.J., and Richardson, H. (2001). The Drosophila Geminin homolog: roles for Geminin in limiting DNA replication, in anaphase and in neurogenesis. *Genes Dev.* *15*, 2741–2754.
- Raasi, S., Orlov, I., Fleming, K.G., and Pickart, C.M. (2004). Binding of polyubiquitin chains to ubiquitin-associated (UBA) domains of HHR23A. *J. Mol. Biol.* *341*, 1367–1379.

References

- Rape, M., and Kirschner, M.W. (2004). Autonomous regulation of the anaphase-promoting complex couples mitosis to S-phase entry. *Nature* *432*, 588–595.
- Rape, M., Reddy, S.K., and Kirschner, M.W. (2006). The processivity of multiubiquitination by the APC determines the order of substrate degradation. *Cell* *124*, 89–103.
- Reddy, S.K., Rape, M., Margansky, W.A., and Kirschner, M.W. (2007). Ubiquitination by the anaphase-promoting complex drives spindle checkpoint inactivation. *Nature* *446*, 921–925.
- Reimann, J.D.R., Freed, E., Hsu, J.Y., Kramer, E.R., Peters, J.M., and Jackson, P.K. (2001). Emi1 is a mitotic regulator that interacts with Cdc20 and inhibits the anaphase promoting complex. *Cell* *105*, 645–655.
- Richly, H., Rape, M., Braun, S., Rumpf, S., Hoege, C., and Jentsch, S. (2005). A series of ubiquitin binding factors connects CDC48/p97 to substrate multiubiquitylation and proteasomal targeting. *Cell* *120*, 73–84.
- Rieser, E., Cordier, S.M., and Walczak, H. (2013). Linear ubiquitination: a newly discovered regulator of cell signalling. *Trends Biochem. Sci.* *38*, 94–102.
- Ro, H., and Dawid, I.B. (2009). Organizer restriction through modulation of Bozozok stability by the E3 ubiquitin ligase Lnx-like. *Nat. Cell Biol.* *11*, 1121–1127.
- Rodrigo-Brenni, M.C., and Morgan, D.O. (2007). Sequential E2s drive polyubiquitin chain assembly on APC targets. *Cell* *130*, 127–139.
- Ben-Saadon, R., Zaaroor, D., Ziv, T., and Ciechanover, A. (2006). The polycomb protein Ring1B generates self atypical mixed ubiquitin chains required for its in vitro histone H2A ligase activity. *Mol. Cell* *24*, 701–711.
- Saeki, Y., Kudo, T., Sone, T., Kikuchi, Y., Yokosawa, H., Toh-e, A., and Tanaka, K. (2009). Lysine 63-linked polyubiquitin chain may serve as a targeting signal for the 26S proteasome. *EMBO J.* *28*, 359–371.
- Schneider-Poetsch, T., Ju, J., Eyler, D.E., Dang, Y., Bhat, S., Merrick, W.C., Green, R., Shen, B., and Liu, J.O. (2010). Inhibition of eukaryotic translation elongation by cycloheximide and lactimidomycin. *Nat. Chem. Biol.* *6*, 209–217.
- Schreiber, A., Stengel, F., Zhang, Z., Enchev, R.I., Kong, E.H., Morris, E.P., Robinson, C.V., da Fonseca, P.C.A., and Barford, D. (2011). Structural basis for the subunit assembly of the anaphase-promoting complex. *Nature* *470*, 227–232.
- Schulman, B.A., and Harper, J.W. (2009). Ubiquitin-like protein activation by E1 enzymes: the apex for downstream signalling pathways. *Nat. Rev. Mol. Cell Biol.* *10*, 319–331.
- Sedgwick, G.G., Hayward, D.G., Di Fiore, B., Pardo, M., Yu, L., Pines, J., and Nilsson, J. (2013). Mechanisms controlling the temporal degradation of Nek2A and Kif18A by the APC/C-Cdc20 complex. *EMBO J.* *32*, 303–314.
- Seelaar, H., Rohrer, J.D., Pijnenburg, Y.A.L., Fox, N.C., and van Swieten, J.C. (2011). Clinical, genetic and pathological heterogeneity of frontotemporal dementia: a review. *J. Neurol. Neurosurg. Psychiatry* *82*, 476–486.
- Shang, F., Deng, G., Liu, Q., Guo, W., Haas, A.L., Crosas, B., Finley, D., and Taylor, A. (2005). Lys6-modified Ubiquitin Inhibits Ubiquitin-dependent Protein Degradation. *J. Biol. Chem.* *280*, 20365–20374.

References

- Shi, D., and Grossman, S.R. (2010). Ubiquitin becomes ubiquitous in cancer: emerging roles of ubiquitin ligases and deubiquitinases in tumorigenesis and as therapeutic targets. *Cancer Biol. Ther.* *10*, 737–747.
- Shi, D., Pop, M.S., Kulikov, R., Love, I.M., Kung, A.L., Kung, A., and Grossman, S.R. (2009). CBP and p300 are cytoplasmic E4 polyubiquitin ligases for p53. *Proc. Natl. Acad. Sci. U. S. A.* *106*, 16275–16280.
- Smith, D.M., Kafri, G., Cheng, Y., Ng, D., Walz, T., and Goldberg, A.L. (2005). ATP binding to PAN or the 26S ATPases causes association with the 20S proteasome, gate opening, and translocation of unfolded proteins. *Mol. Cell* *20*, 687–698.
- Smith, M.H., Ploegh, H.L., and Weissman, J.S. (2011). Road to ruin: targeting proteins for degradation in the endoplasmic reticulum. *Science* *334*, 1086–1090.
- Sobhian, B., Shao, G., Lilli, D.R., Culhane, A.C., Moreau, L.A., Xia, B., Livingston, D.M., and Greenberg, R.A. (2007). RAP80 targets BRCA1 to specific ubiquitin structures at DNA damage sites. *Science* *316*, 1198–1202.
- Sokratous, K., Roach, L.V., Channing, D., Strachan, J., Long, J., Searle, M.S., Layfield, R., and Oldham, N.J. (2012). Probing affinity and ubiquitin linkage selectivity of ubiquitin-binding domains using mass spectrometry. *J. Am. Chem. Soc.* *134*, 6416–6424.
- Song, L., and Rape, M. (2010). Regulated degradation of spindle assembly factors by the anaphase-promoting complex. *Mol. Cell* *38*, 369–382.
- Song, E.J., Werner, S.L., Neubauer, J., Stegmeier, F., Aspden, J., Rio, D., Harper, J.W., Elledge, S.J., Kirschner, M.W., and Rape, M. (2010). The Prp19 complex and the Usp4Sart3 deubiquitinating enzyme control reversible ubiquitination at the spliceosome. *Genes Dev.* *24*, 1434–1447.
- De Souza, C.P.C., Osmani, A.H., Hashmi, S.B., and Osmani, S.A. (2004). Partial Nuclear Pore Complex Disassembly during Closed Mitosis in *Aspergillus nidulans*. *Curr. Biol.* *14*, 1973–1984.
- Spence, J., Gali, R.R., Dittmar, G., Sherman, F., Karin, M., and Finley, D. (2000). Cell cycle-regulated modification of the ribosome by a variant multiubiquitin chain. *Cell* *102*, 67–76.
- Stawiecka-Mirota, M., Pokrzywa, W., Morvan, J., Zoladek, T., Haguenaer-Tsapis, R., Urban-Grimal, D., and Morsomme, P. (2007). Targeting of Sna3p to the endosomal pathway depends on its interaction with Rsp5p and multivesicular body sorting on its ubiquitylation. *Traffic Cph. Den.* *8*, 1280–1296.
- Stegmeier, F., Rape, M., Draviam, V.M., Nalepa, G., Sowa, M.E., Ang, X.L., McDonald, E.R., 3rd, Li, M.Z., Hannon, G.J., Sorger, P.K., et al. (2007). Anaphase initiation is regulated by antagonistic ubiquitination and deubiquitination activities. *Nature* *446*, 876–881.
- Stewart, G.S., Panier, S., Townsend, K., Al-Hakim, A.K., Kolas, N.K., Miller, E.S., Nakada, S., Ylanko, J., Olivarius, S., Mendez, M., et al. (2009). The RIDDLE syndrome protein mediates a ubiquitin-dependent signaling cascade at sites of DNA damage. *Cell* *136*, 420–434.
- Stoll, K.E., Brzovic, P.S., Davis, T.N., and Klevit, R.E. (2011). The essential Ubc4/Ubc5 function in yeast is HECT E3-dependent, and RING E3-dependent pathways require only monoubiquitin transfer by Ubc4. *J. Biol. Chem.* *286*, 15165–15170.
- Stott, D.I., McLearn, J., and Marsden, H.S. (1985). A gel transfer tank for immunoblotting and its application for analysis of nuclear protein antigens. *Anal. Biochem.* *149*, 454–460.

References

- Sudakin, V., Ganoth, D., Dahan, A., Heller, H., Hershko, J., Luca, F.C., Ruderman, J.V., and Hershko, A. (1995). The cyclosome, a large complex containing cyclin-selective ubiquitin ligase activity, targets cyclins for destruction at the end of mitosis. *Mol. Biol. Cell* *6*, 185–197.
- Summers, M.K., Pan, B., Mukhyala, K., and Jackson, P.K. (2008). The unique N terminus of the UbcH10 E2 enzyme controls the threshold for APC activation and enhances checkpoint regulation of the APC. *Mol. Cell* *31*, 544–556.
- Suryadinata, R., Holien, J.K., Yang, G., Parker, M.W., Papaleo, E., and Šarčević, B. (2013). Molecular and structural insight into lysine selection on substrate and ubiquitin lysine 48 by the ubiquitin-conjugating enzyme Cdc34. *Cell Cycle Georget. Tex* *12*, 1732–1744.
- Tada, S., Li, A., Maiorano, D., Méchali, M., and Blow, J.J. (2001). Repression of origin assembly in metaphase depends on inhibition of RLF-B/Cdt1 by geminin. *Nat. Cell Biol.* *3*, 107–113.
- Tagwerker, C., Flick, K., Cui, M., Guerrero, C., Dou, Y., Auer, B., Baldi, P., Huang, L., and Kaiser, P. (2006). A Tandem Affinity Tag for Two-step Purification under Fully Denaturing Conditions Application in Ubiquitin Profiling and Protein Complex Identification Combined with in vivo Cross-Linking. *Mol. Cell. Proteomics* *5*, 737–748.
- Takizawa, C.G., and Morgan, D.O. (2000). Control of mitosis by changes in the subcellular location of cyclin-B1-Cdk1 and Cdc25C. *Curr. Opin. Cell Biol.* *12*, 658–665.
- Tang, Z., Li, B., Bharadwaj, R., Zhu, H., Ozkan, E., Hakala, K., Deisenhofer, J., and Yu, H. (2001). APC2 Cullin protein and APC11 RING protein comprise the minimal ubiquitin ligase module of the anaphase-promoting complex. *Mol. Biol. Cell* *12*, 3839–3851.
- Tauriello, D.V.F., Haegebarth, A., Kuper, I., Edelmann, M.J., Henraat, M., Canninga-van Dijk, M.R., Kessler, B.M., Clevers, H., and Maurice, M.M. (2010). Loss of the tumor suppressor CYLD enhances Wnt/beta-catenin signaling through K63-linked ubiquitination of Dvl. *Mol. Cell* *37*, 607–619.
- Thrower, J.S., Hoffman, L., Rechsteiner, M., and Pickart, C.M. (2000). Recognition of the polyubiquitin proteolytic signal. *Embo J.* *19*, 94–102.
- Tofaris, G.K., Kim, H.T., Hourez, R., Jung, J.-W., Kim, K.P., and Goldberg, A.L. (2011). Ubiquitin ligase Nedd4 promotes alpha-synuclein degradation by the endosomal-lysosomal pathway. *Proc. Natl. Acad. Sci. U. S. A.* *108*, 17004–17009.
- Uzunova, K., Dye, B.T., Schutz, H., Ladurner, R., Petzold, G., Toyoda, Y., Jarvis, M.A., Brown, N.G., Poser, I., Novatchkova, M., et al. (2012). APC15 mediates CDC20 autoubiquitylation by APC/CMCC and disassembly of the mitotic checkpoint complex. *Nat. Struct. Mol. Biol.* *19*, 1116–1123.
- Varetti, G., Guida, C., Santaguida, S., Chirolì, E., and Musacchio, A. (2011). Homeostatic control of mitotic arrest. *Mol. Cell* *44*, 710–720.
- Varghese, B., Barriere, H., Carbone, C.J., Banerjee, A., Swaminathan, G., Plotnikov, A., Xu, P., Peng, J., Goffin, V., Lukacs, G.L., et al. (2008). Polyubiquitination of prolactin receptor stimulates its internalization, postinternalization sorting, and degradation via the lysosomal pathway. *Mol. Cell Biol.* *28*, 5275–5287.
- Verma, R., Aravind, L., Oania, R., McDonald, W.H., Yates, J.R., 3rd, Koonin, E.V., and Deshaies, R.J. (2002). Role of Rpn11 metalloprotease in deubiquitination and degradation by the 26S proteasome. *Science* *298*, 611–615.
- Voet, D., and Voet, J.G. (2011). *Biochemistry* (Hoboken, NJ: John Wiley & Sons).

References

- Vu, P.K., and Sakamoto, K.M. (2000). Ubiquitin-mediated proteolysis and human disease. *Mol. Genet. Metab.* *71*, 261–266.
- Walczak, H., Iwai, K., and Dikic, I. (2012). Generation and physiological roles of linear ubiquitin chains. *BMC Biol.* *10*, 23.
- Wang, J., and Maldonado, M.A. (2006). The ubiquitin-proteasome system and its role in inflammatory and autoimmune diseases. *Cell. Mol. Immunol.* *3*, 255–261.
- Wang, M., and Pickart, C.M. (2005). Different HECT domain ubiquitin ligases employ distinct mechanisms of polyubiquitin chain synthesis. *Embo J.* *24*, 4324–4333.
- Wang, C., Deng, L., Hong, M., Akkaraju, G.R., Inoue, J., and Chen, Z.J. (2001). TAK1 is a ubiquitin-dependent kinase of MKK and IKK. *Nature* *412*, 346–351.
- Wang, L., Wang, L., Zhang, S., Qu, G., Zhang, D., Li, S., and Liu, S. (2013). Downregulation of ubiquitin E3 ligase TNF receptor-associated factor 7 leads to stabilization of p53 in breast cancer. *Oncol. Rep.* *29*, 283–287.
- Wang, M., Cheng, D., Peng, J., and Pickart, C.M. (2006). Molecular determinants of polyubiquitin linkage selection by an HECT ubiquitin ligase. *EMBO J.* *25*, 1710–1719.
- Wang, W.Y., Lim, J.H., and Li, J.-D. (2012a). Synergistic and feedback signaling mechanisms in the regulation of inflammation in respiratory infections. *Cell. Mol. Immunol.* *9*, 131–135.
- Wang, Z., Inuzuka, H., Zhong, J., Wan, L., Fukushima, H., Sarkar, F.H., and Wei, W. (2012b). Tumor suppressor functions of FBW7 in cancer development and progression. *FEBS Lett.* *586*, 1409–1418.
- Wenzel, D.M., Stoll, K.E., and Klevit, R.E. (2011a). E2s: structurally economical and functionally replete. *Biochem. J.* *433*, 31–42.
- Wenzel, D.M., Lissounov, A., Brzovic, P.S., and Klevit, R.E. (2011b). UBCH7 reactivity profile reveals parkin and HHARI to be RING/HECT hybrids. *Nature* *474*, 105–108.
- Wickliffe, K.E., Lorenz, S., Wemmer, D.E., Kuriyan, J., and Rape, M. (2011a). The mechanism of linkage-specific ubiquitin chain elongation by a single-subunit E2. *Cell* *144*, 769–781.
- Wickliffe, K.E., Williamson, A., Meyer, H.-J., Kelly, A., and Rape, M. (2011b). K11-linked ubiquitin chains as novel regulators of cell division. *Trends Cell Biol.* *21*, 656–663.
- Williamson, A., Wickliffe, K.E., Mellone, B.G., Song, L., Karpen, G.H., and Rape, M. (2009a). Identification of a physiological E2 module for the human anaphase-promoting complex. *Proc. Natl. Acad. Sci. U. S. A.* *106*, 18213–18218.
- Williamson, A., Jin, L., and Rape, M. (2009b). Preparation of synchronized human cell extracts to study ubiquitination and degradation. *Methods Mol. Biol. Clifton NJ* *545*, 301–312.
- Williamson, A., Banerjee, S., Zhu, X., Philipp, I., Iavarone, A.T., and Rape, M. (2011). Regulation of ubiquitin chain initiation to control the timing of substrate degradation. *Mol. Cell* *42*, 744–757.
- Wilson, R.C., Edmondson, S.P., Flatt, J.W., Helms, K., and Twigg, P.D. (2011). The E2-25K ubiquitin-associated (UBA) domain aids in polyubiquitin chain synthesis and linkage specificity. *Biochem. Biophys. Res. Commun.* *405*, 662–666.
- Winborn, B.J., Travis, S.M., Todi, S.V., Scaglione, K.M., Xu, P., Williams, A.J., Cohen, R.E., Peng, J., and Paulson, H.L. (2008). The deubiquitinating enzyme ataxin-3, a polyglutamine

References

- disease protein, edits Lys63 linkages in mixed linkage ubiquitin chains. *J. Biol. Chem.* **283**, 26436–26443.
- Wodarz, A., and Nusse, R. (1998). Mechanisms of Wnt Signaling in Development. *Annu. Rev. Cell Dev. Biol.* **14**, 59–88.
- Wohlschlegel, J.A., Dwyer, B.T., Dhar, S.K., Cvetic, C., Walter, J.C., and Dutta, A. (2000). Inhibition of eukaryotic DNA replication by geminin binding to Cdt1. *Science* **290**, 2309–2312.
- Wolthuis, R., Clay-Farrace, L., van Zon, W., Yekezare, M., Koop, L., Ogink, J., Medema, R., and Pines, J. (2008). Cdc20 and Cks direct the spindle checkpoint-independent destruction of cyclin A. *Mol. Cell* **30**, 290–302.
- Worden, E.J., Padovani, C., and Martin, A. (2014). Structure of the Rpn11-Rpn8 dimer reveals mechanisms of substrate deubiquitination during proteasomal degradation. *Nat. Struct. Mol. Biol.* **21**, 220–227.
- Wu, T., Merbl, Y., Huo, Y., Gallop, J.L., Tzur, A., and Kirschner, M.W. (2010). UBE2S drives elongation of K11-linked ubiquitin chains by the Anaphase-Promoting Complex. *Proc. Natl. Acad. Sci. U. S. A.* **107**, 1355–1360.
- Xia, Z.-P., Sun, L., Chen, X., Pineda, G., Jiang, X., Adhikari, A., Zeng, W., and Chen, Z.J. (2009). Direct activation of protein kinases by unanchored polyubiquitin chains. *Nature* **461**, 114–119.
- Xu, P., Duong, D.M., Seyfried, N.T., Cheng, D., Xie, Y., Robert, J., Rush, J., Hochstrasser, M., Finley, D., and Peng, J. (2009). Quantitative Proteomics Reveals the Function of Unconventional Ubiquitin Chains in Proteasomal Degradation. *Cell* **137**, 133–145.
- Xu, Z., Kohli, E., Devlin, K.I., Bold, M., Nix, J.C., and Misra, S. (2008). Interactions between the quality control ubiquitin ligase CHIP and ubiquitin conjugating enzymes. *Bmc Struct. Biol.* **8**.
- Yao, T., and Cohen, R.E. (2002). A cryptic protease couples deubiquitination and degradation by the proteasome. *Nature* **419**, 403–407.
- Ye, Y., and Rape, M. (2009). Building ubiquitin chains: E2 enzymes at work. *Nat. Rev. Mol. Cell Biol.* **10**, 755–764.
- Ye, Y., Blaser, G., Horrocks, M.H., Ruedas-Rama, M.J., Ibrahim, S., Zhukov, A.A., Orte, A., Klenerman, D., Jackson, S.E., and Komander, D. (2012). Ubiquitin chain conformation regulates recognition and activity of interacting proteins. *Nature* **492**, 266–270.
- Yeh, T.-C., and Bratton, S.B. (2013). Caspase-dependent regulation of the ubiquitin-proteasome system through direct substrate targeting. *Proc. Natl. Acad. Sci. U. S. A.* **110**, 14284–14289.
- Yerlikaya, A., and Yöntem, M. (2013). The significance of ubiquitin proteasome pathway in cancer development. *Recent Patents Anticancer Drug Discov.* **8**, 298–309.
- Yu, H.T., King, R.W., Peters, J.M., and Kirschner, M.W. (1996). Identification of a novel ubiquitin-conjugating enzyme involved in mitotic cyclin degradation. *Curr. Biol.* **6**, 455–466.
- Yuan, C., Qi, J., Zhao, X., and Gao, C. (2012). Smurf1 protein negatively regulates interferon- γ signaling through promoting STAT1 protein ubiquitination and degradation. *J. Biol. Chem.* **287**, 17006–17015.
- Zeng, W., Sun, L., Jiang, X., Chen, X., Hou, F., Adhikari, A., Xu, M., and Chen, Z.J. (2010). Reconstitution of the RIG-I pathway reveals a signaling role of unanchored polyubiquitin chains in innate immunity. *Cell* **141**, 315–330.

References

Zhang, J., Wan, L., Dai, X., Sun, Y., and Wei, W. (2014). Functional characterization of Anaphase Promoting Complex/Cyclosome (APC/C) E3 ubiquitin ligases in tumorigenesis. *Biochim. Biophys. Acta BBA - Rev. Cancer* 1845, 277–293.

Zhang, L., Fujita, T., Wu, G., Xiao, X., and Wan, Y. (2011). Phosphorylation of the anaphase-promoting complex/Cdc27 is involved in TGF-beta signaling. *J. Biol. Chem.* 286, 10041–10050.

Zieve, G.W., Turnbull, D., Mullins, J.M., and McIntosh, J.R. (1980). Production of large numbers of mitotic mammalian cells by use of the reversible microtubule inhibitor Nocodazole: Nocodazole accumulated mitotic cells. *Exp. Cell Res.* 126, 397–405.

Van Zon, W., Ogink, J., ter Riet, B., Medema, R.H., Riele, H.T., and Wolthuis, R.M.F. (2010). The APC/C recruits cyclin B1-Cdk1-Cks in prometaphase before D box recognition to control mitotic exit. *J. Cell Biol.* 190, 587–602.

Zungu, M., Schisler, J.C., Essop, M.F., McCudden, C., Patterson, C., and Willis, M.S. (2011). Regulation of AMPK by the ubiquitin proteasome system. *Am. J. Pathol.* 178, 4–11.

(2014a). Cell cycle. www.wikipedia.org

(2014b). Cyclin. www.wikipedia.org

8. (Eidesstattliche) Versicherungen und Erklärungen

(§ 5 Nr. 4 PromO)

Hiermit erkläre ich, dass keine Tatsachen vorliegen, die mich nach den gesetzlichen Bestimmungen über die Führung akademischer Grade zur Führung eines Doktorgrades unwürdig erscheinen lassen.

(§ 8 S. 2 Nr. 5 PromO)

Hiermit erkläre ich mich damit einverstanden, dass die elektronische Fassung meiner Dissertation unter Wahrung meiner Urheberrechte und des Datenschutzes einer gesonderten Überprüfung hinsichtlich der eigenständigen Anfertigung der Dissertation unterzogen werden kann.

(§ 8 S. 2 Nr. 7 PromO)

Hiermit erkläre ich eidesstattlich, dass ich die Dissertation selbständig verfasst und keine anderen als die von mir angegebenen Quellen und Hilfsmittel benutzt habe.

(§ 8 S. 2 Nr. 8 PromO)

Ich habe die Dissertation nicht bereits zur Erlangung eines akademischen Grades anderweitig eingereicht und habe auch nicht bereits diese oder eine gleichartige Doktorprüfung endgültig nicht bestanden.

(§ 8 S. 2 Nr. 9 PromO)

Hiermit erkläre ich, dass ich keine Hilfe von gewerbliche Promotionsberatern bzw. -vermittlern in Anspruch genommen habe und auch künftig nicht nehmen werde.

.....
Ort, Datum, Unterschrift